UNIVERSITY OF CALIFORNIA,
IRVINE

Evaluation the Functional Contributions of Microglia in Host Defense and Disease in a Model of Mouse Coronavirus-Induced Neurologic Disease

DISSERTATION

Submitted in partial satisfaction of the requirements for the degree of

DOCTOR OF PHILOSOPHY
In Biological Sciences

By

Yuting Cheng

Dissertation Committee:
Professor Thomas E. Lane, Chair
Professor Kim N. Green
Professor Craig M. Walsh

2022

DEDICATION

To

my family, my mother Shaofen Wang and my father Yan Cheng

for their love, encouragement, and unyielding support that made this research possible.

TABLE OF CONTENTS

LIST OF ABBREVIATIONS

AD ..... Alzheimer's disease
APC ..... antigen-presenting cell
APOE ..... Apolipoprotein E
ASC ..... antibody-secreting B cell
BBB ..... blood-brain barrier
CIS ..... clinically isolated syndrome
CNS ..... central nervous system
CSF ..... cerebral spinal fluid
CSF1R ..... colony-stimulating factor 1 receptor
CST7 ..... Cystatin F
CXCR ..... CX3C chemokine receptor
DAM ..... disease-associated molecule
DC ..... dendritic cells
DEG ..... differentially expressed gene
DMT ..... disease modifying therapy
DNA ..... deoxyribonucleic acid
EAE ..... experimental autoimmune encephalomyelitis
EMP ..... erythromyeloid progenitor
FDA ..... food and drug administration
GA ..... glatiramer acetate
GFAP ..... glial fibrillary acidic protein
GST ..... glutathione S-transferase
H&E ..... hematoxylin & eosin
HBSS ..... Hanks balanced sterile solution
HLA ..... human leukocyte antigen
i.c. ..... intracranial
Iba1 ..... ionophore calcium-binding adapter molecule 1
IFN ..... interferon
IGF1 ..... insulin like growth factor 1
IL ..... interleukin
JCV ..... John Cunningham virus
JHMV ..... John Howard Mueller strain of mouse hepatitis virus
LFB ..... luxol fast blue
Lpl ..... Lipoprotein lipase
MAP2 ..... microtubule-associated protein 2
MBP ..... myelin basic protein
MERS ..... Middle East respiratory syndrome
MHV ..... mouse hepatitis virus
MMP ..... metalloproteinases
MOG ..... myelin oligodendrocyte glycoprotein
MRI ..... Magnetic resonance imaging
MS ..... multiple sclerosis
NK ..... natural killer cells
OPC ..... precursor cell
p.i. ..... post infection

PFU ..... plaque-forming units
PLP ..... proteolipid protein
PML ..... progressive multifocal leukoencephalopathy
PPMS ..... primary progressive multiple sclerosis
RNA ..... ribonucleic acid
RPMS ..... relapsing-remitting multiple sclerosis
SARS-CoV ..... severe acute respiratory syndrome coronavirus
SEM ..... standard error of mean
SPMS ..... secondary progressive multiple sclerosis
TMEV ..... Theiler's murine encephalomyelitis virus
TNF ..... tumor necrosis factor
TREM2 ..... Myeloid Cells 2
VCAM-1 ..... vascular cell adhesion molecule-1
WNV ..... West Nile Virus

LIST OF FIGURES

LIST OF TABLES

Page

ACKNOWLEDGEMENTS

I would like to express my gratitude to my mentor Dr. Thomas E. Lane for his insight, encouragement, and mentorship. I would also like to thank my committee members Dr. Kim Green and Dr. Craig Walsh and the entire Molecular Biology and Biochemistry Department for their guidance and professional development. I'm extremely grateful to everyone in the lab for their valuable feedback and assistance. Lastly, I would like to thank my family, my mother Shaofen Wang, and my father Yan Cheng for their love, encouragement, and unyielding support that made this research possible.

Chapter 2 of this dissertation is a reprint of the material as it appears in the Journal of Virology. The co-author listed in this publication directed and supervised research which forms the basis for the dissertation. Chapter 3 of this dissertation is a reprint of the material as it appears in the Glia. The co-author listed in this publication directed and supervised research which forms the basis for the dissertation.

VITA

Yuting Cheng

EDUCATION

2020- 2022 **University of California, Irvine**
Biological Sciences
(Transferred from the University of Utah – 2020)

2017- 2019 **University of Utah**
Molecular Biology Ph.D. Program

2015- 2017 **University of Southern California**
Master of Science in Molecular Biology

2012- 2015 **Indiana University Bloomington**
Bachelor of Science in Biology

2010- 2012 **Beijing University of Civil Engineering and Architecture**
Engineering in Thermal Energy and Power Engineering

RESEARCH EXPERIENCE

2018-2022 **Dr. Thomas E. Lane's lab**
Research title: Evaluating the functional contributions of microglia to host defense, demyelination, and remyelination in a model of coronavirus-induced neurologic disease

- Examine the role of microglia in host defense and disease in response to both murine coronavirus and SARS-CoV-2 infection of the CNS
- Characterize novel anti-viral treatment in experimental models of SARS-CoV-2 infection

2015- 2017 **Dr. Pragna Patel's lab**
Thesis title: Effect of point mutations in the myelin protein, PMP22 on protein: protein interactions in Schwann cells

- Construct lentiviral vectors that express wild-type and mutant PMP22 fusion proteins
- Create stable Schwann cell lines expressing these fusion proteins
- Identify abnormal interactions of the PMP22 protein when it is mutated in patients with CMT

2013- 2015 **Dr. Scott Michael's lab**
Research title: Contributions of Linker Histones of Chromatin Dynamics

- Analysis of the degree of DNA packaging influenced by reversible post-translational modification of histones
  - ✧ Investigated mono-methylation of the core histone H3 at lysine 27 in heterochromatin by ATXR5 and ATXR6
  - ✧ Found knock-out of ATXR5/6 causes loss of H3K27mel
- Development of tools to study epitope-tagged lines and a protocol for extracting histones

- ✧ Investigated histone phosphorylation in ATXR 5/6 by developing a screen to identify mutations that affect the phosphorylation pattern of histones

2013 **Novo Nordisk (China)**

Internship Program

- Isolation of genomic and plasmid DNA
- Restriction enzyme digestion and analysis by agarose gel electrophoresis
- Electrophoretic separation of proteins

PUBLICATIONS

Hohsfield, L.A., K.I. Tsourmas, Y. Ghorbanian, A.R. Syage, S.J. Kim, **Y. Cheng**, S. Furman, M.A. Inlay, T.E. Lane and K.N. Green (2022). MAC2 is a reliable and long-lasting marker of peripheral derived myeloid cell CNS infiltrates. *Glia,* doi: 10.1002/glia.24144.

Olivarria, G.M.*, **Y. Cheng***, S. Furman*, C. Pachow, M.S. Burns, R.A. Edwards, W. Yong, L. Thompson, L. Hohsfield, C. Smith-Geater, R. Meramontes, C. Manlapaz, J. Teijaro, K.N. Green, and T.E. Lane (2021). Microglia do not restrict SARS-CoV-2 replication following infection of the central nervous system of K18-hACE2 transgenic mice. *J. Virology*, *jvi0196921. doi: 10.1128/jvi.01969-21.* *Authors contributed equally to this work.

Mangale, V.*, Syage, A. R.***,** Ekiz, H. A.*, Skinner, D. D., **Cheng, Y.**, Stone, C. L., Brown, R. M., O'Connell, R. M., Green, K. N., & Lane, T. E. (2020). Microglia influence host defense, disease, and repair following murine coronavirus infection of the central nervous system. *Glia*, *68*(11), 2345–2360. *Authors contributed equally to this work https://doi.org/10.1002/glia.23844

Marro, B. S*., Skinner, D. D***.**, **Cheng, Y.**, Grist, J. J., Dickey, L. L., Eckman, E., Stone C., Liu L., Ransohoff R. M., & Lane, T. E. (2019). Disrupted CXCR2 signaling in oligodendroglia lineage cells enhances myelin repair in a viral model of multiple sclerosis. Journal of Virology. https://doi.org/10.1128/JVI.00240-19 *Authors contributed equally to this work

Cheng, Y*., Skinner, D.D***.,** Lane, T.E. (2019) Review: Innate Immune Responses and Viral-Induced Neurologic Disease. J. Clin. Med. 8, 3. https://doi.org/10.3390/jcm8010003 *Authors contributed equally to this work

Manuscripts in preparation:

Timed ablation of microglia leads to increased demyelination and impaired remyelination in mice infected with a neurotropic murine coronavirus

TEACHING AND MENTORING

Teaching Assistant at UC Irvine

Immunology with Hematology - Grade

Exp Microbiology Lab - Set up discussion sections, answer questions, grade lab problem/lab report

Molecular Biology - Set up discussion sections, answer questions, grade weekly assignments

Teaching Assistant at IU Bloomington
Biology lab - Operated/maintained lab equipment; Assist undergraduates during their experiments

ABSTRACT OF THE DISSERTATION

Evaluating the functional contributions of microglia in host defense and disease in a model of mouse coronavirus-induced neurologic disease

By

Yuting Cheng

Doctor of Philosophy in Biological Sciences

University of California, Irvine, 2022

Professor Thomas E. Lane, Chair

An important unmet clinical need for multiple sclerosis (MS) patients is an effective method for promoting axonal sparing and remyelination that can ameliorate clinical symptoms associated with demyelination and restore motor function. Previous studies from our laboratory demonstrate an important role for microglia in restricting the severity of demyelination and promoting remyelination in a viral model of demyelination. In brief, intracranial instillation of the neuroadapted JHM strain of mouse hepatitis virus (JHMV, a member of the *Coronaviridae* family) results in an acute encephalomyelitis followed by a chronic immune-mediated demyelinating disease similar both clinically and histologically with MS. Targeted depletion of microglia via administration of PLX5622, a brain penetrant small molecule antagonist specific for colony-stimulating factor 1 receptor (CSF1R) that efficiently depletes microglia, before infection with JHMV resulted in a dramatic increase in the severity of spinal cord demyelination and markedly impaired remyelination. To better understand how microglia impact disease progression in mice persistently infected with JHMV that have established demyelination, PLX5622 was administered to mice at day 14 post-infection (p.i.) and animals remained on the drug for 14 days at which point animals were sacrificed and the severity of spinal cord

demyelination and remyelination evaluated. Our findings indicate that PLX5622-mediated ablation of microglia for 2 weeks beginning at day 14 p.i. did not lead to an increase in mortality but resulted in a significant ($p<0.05$) increase in the severity of spinal cord demyelination at day 28 p.i. when compared to control mice. Infiltration of both total and virus-specific CD4+ and CD8+ T cells into the CNS was not affected in response to PLX5622-mediated microglia ablation yet control of viral replication was impaired that correlated with muted expression of MHC class II. Finally, we observed decreased expression of mRNA transcripts encoding remyelination-associated proteins Cystatin F and Lipoprotein lipase. BulkRNAseq analysis of spinal cords indicated that targeting microglia resulted in a dramatic reduction in gene expression profiles associated with cell-mediated immune responses and phagocytosis. These findings indicate that microglia continue to impact the control of viral replication within the CNS post-acute phase of disease as well as restrict ongoing demyelination and remyelination in mice persistently infected with JHMV.

Chapter 1

Background and Introduction

1.1 Multiple Sclerosis

Multiple sclerosis (MS) is a chronic disease of the central nervous system (CNS) characterized by neuroinflammation, demyelination, and axonal loss[1]. MS was first described in 1868 by French Neurologist Jean-Martin Charcot, who related distinct symptoms to the same disease and elegantly described the multitude of glial scars, which are its namesake[2]. Globally, an estimated 2-3 million people live with MS, although this figure is likely an underestimate due to a lack of data from certain geographic areas[3].MS can occur at any age but the onset of this disease is usually between 20 to 40 years old, and women are two to three times more likely to get this disease than men[4]. Although the cause of MS is unknown, it is thought that both genetic and environmental factors contribute to the initiation of the disease[5–7]. For example, patients usually have a family history of getting MS, and white people, especially from Northern Europe, have a higher risk of developing MS than people from Asian, African, or Native American[4]. The human leukocyte antigen (HLA) class II region of the HLA-DR-2 haplotype on chromosome 6p21 was shown to be associated with MS and HLADRB1*1501 is the major susceptibility allele in MS patients from North America or European Caucasians[8–11]. Besides that, having low levels of vitamin D, low exposure to sunlight, and smokers are associated with a greater risk of MS[4].

The symptoms of MS may vary from person to person depending on the location of affected nerve fibers. Since MS is a disease of the CNS, it usually affects patients' movement such as electric-shock sensations that occur with certain neck movements, numbness or weakness in one or more limbs, and tremors. Other symptoms include vision problems, slurred speech, dizziness, tingling or pain in parts of the body, and problems with sexual, bowel, and bladder function may also happen[4].

International Advisory Committee on Clinical Trials of MS had defined four basic MS disease courses (also called types or phenotypes) in 2013: clinically isolated syndrome (CIS), relapsing-remitting (RPMS), secondary progressive (SPMS), and primary progressive (PPMS). CIS is the first episode of neurologic symptoms caused by inflammation and demyelination in the CNS[12]. During this episode, patients won't be diagnosed with MS because they may or may not go on to develop MS. A brain MRI (magnetic resonance imaging) will be suggested to take for those patients during this episode. If lesions can be seen in the MRI, which means that patients have a higher likelihood of developing MS and being diagnosed with RRMS, they may now be treated with a disease-modifying therapy (DMT) that has been approved by the U.S. Food and Drug Administration (FDA) and delay the onset of MS[12]. The DMTs are usually aimed at reducing T lymphocyte infiltration into the CNS and are aimed at preventing new lesion formation, including interferons (IFNs), Teriflunomide, Fingolimod, and monoclonal antibodies such as Natalizumab, Alemtuzumab, and Ocrelizumab[13–18]. Except for Ocrelizumab, which was recently approved for progressive MS, most of the FDA-approved DMTs are for RPMS. When patients are diagnosed with RRMS-the most common disease course, which not only means they have clearly defined attacks-also called relapses or exacerbation but also followed by periods of partial or complete recovery (remission)[12]. During the remission, all symptoms may disappear. However, during the relapsing, patients may generate new lesions on Magnetic resonance imaging (MRI) or increase in disability. Nearly 80% of patients who are diagnosed with RRMS will eventually transition to SPMS which may lead to progressive worsening of neurologic function and accumulation of disability over time[12]. Whereas approximately 15% of patients may directly accumulate disability without early relapses or remission in the PPMS course. Both the SPMS and PPMS can be further characterized as either active (with relapses and/or generating

new lesions on MRI) or not active, as well as with progression (increase disability) or without progression[12]. During the progression, accumulated cortical lesions lead to severe neurological dysfunction including loss of motor function. These symptoms are likely due to axonal degeneration, and the innate immune response, for example- microglia activation and macrophage infiltration- is associated with gray matter inflammation while T cells and B cells reside in the border of pre-existing lesions[19–22,23(p)]. Moreover, remyelination of damaged areas by oligodendrocyte precursor cells (OPCs) fails to occur which severely reduces potential recovery[24–27].

MS is considered an autoimmune disease in which activated T cells attack proteins embedded within the myelin sheath resulting in damage/destruction over time[1,5]. In addition, activated B cells also contribute to disease progression in MS patients yet the mechanisms by which these cells contribute to disease are not well-characterized[28]. Supporting an important role for activated lymphocytes in contributing to disease is that FDA-approved DMTs are primarily focused on limiting access of either T lymphocytes into the CNS e.g., Tysabri (natalizumab), or depletion of B cells via administration of CD20-specific antibodies to dampen formation of new lesions[1,5]. Natalizumab is a humanized monoclonal antibody targeting α4 subunit of the integrin α4β1 on lymphocytes that reduces leukocyte migration into the central nervous system by preventing binding to vascular cell adhesion molecule (VCAM-1). Although it has higher efficacy compared to other drugs patients take natalizumab may get potential serious adverse effects including allergic reactions, liver disorders, and more importantly, the potential of developing progressive multifocal leukoencephalopathy (PML), a rare disease that can be fatal and also is the result of an infection of oligodendrocytes in the CNS with the human polyomavirus JC (JCV)[29]. Except for the natalizumab, there are some other common drugs for

MS- interferon-β (IFN-β) and glatiramer acetate (GA) are administered by either subcutaneous or intramuscular injections with adverse effects ranging from influenza-like symptoms to injection-site reactions[30]. IFN-β reduces T cell activation and displays anti-viral effects as well as induces apoptosis of autoreactive T cells[31]. GA is a polymer of amino acids that mimic myelin basic protein presumably shifting immune responses from pro-inflammatory to anti-inflammatory[32]. When patients have a severe form of MS, they can also choose the cytotoxic agent mitoxantrone which is administered by i.v. injections. It acts through inhibition of type II topoisomerase and disrupts DNA synthesis. Some drugs, for example, FTY720 are delivered orally therefore more convenient for patients. FTY720 is the first FDA-approved oral drug for MS patients. FTY720 is a sphingosine-1-phosphate analog that binds to S1P1 expressed on lymphocytes thereby preventing their egress from lymph nodes and consequently preventing their infiltration into the CNS. Moreover, FTY720 seems to act directly on resident cells of the CNS and may reduce neurodegeneration. Teriflunomide, a pyrimidine synthesis inhibitor, reduces autoreactive T and B cells and is also administered orally. Finally, dimethyl fumarate, another oral drug for MS patients, modulates immune cell responses, however, the effector mechanisms remain undefined[33]. Most of the therapeutic strategies used to treat MS patients are trying to decrease the demyelination and neurodegeneration in the CNS, but there are currently no effective treatments to enhance remyelination and subsequently no treatment for the progressive forms of MS. Stem cell transplants offer hope in this regard and clinical investigations have begun with the intravenous injection of autologous bone-marrow-derived mesenchymal stem cells into patients with progressive MS. To date, treated patients have exhibited no serious side effects and reported improved visual acuity suggesting diminished severity of optic neuritis[34]. Besides, Oligodendrocytes- which are the myelinating cells within the

CNS are integral for maintaining axonal health and myelin integrity- also provide some thoughts for developing therapeutic treatment for MS. In MS pathology the function of mature myelinating oligodendrocytes can be dysregulated by a combination of direct infiltrating immune cell functions and released proinflammatory factors[35]. This dysregulation can ultimately lead to a failure of remyelination, which reduces the chance for remission in patients. Oligodendrocyte precursor cells (OPCs) are spread throughout the CNS and are present in MS plaques early during disease[36]. However, a failure to achieve a mature myelinating form may contribute to a lack of remyelination and a progression toward more severe symptoms. Therefore, possible therapies have looked at stimulating OPCs to a mature myelinating form within the CNS.

1.2 Preclinical model of MS

Pre-clinical animal models of MS have been invaluable in terms of understanding molecular and cellular pathways that contribute to white matter pathology as well as the development of novel therapies that limit disease progression. There are two general categories of the preclinical model of MS: autoimmune model, for example, experimental autoimmune encephalomyelitis (EAE) and viral model, including Theiler's murine encephalomyelitis virus (TMEV) and mouse hepatitis virus (MHV).

EAE model can be induced by peripheral immunization with myelin protein components[37], within this model, the type of antigenic immunization, age, sex and genetic strain of the mouse dictates the disease course, resulting in heterogeneous pathologies that share similarities to the wide spectrum of disease states that exist in MS[38] including active demyelination, oligodendrocyte, and axonal loss. All of these features are presumably mediated by myelin-specific T cells[37]. The mice model of EAE is characterized by ascending paralysis

from the tail then followed by limb and forelimb paralysis[39]. EAE can be induced with either active immunization (protein or peptide) or by passive transfer of encephalitogenic T cells with different genetic backgrounds of mice, including SJL/J, C57BL/6, and NOD. In all cases, the relevant immunogen is derived from self-CNS proteins such as myelin basic protein (MBP), proteolipid protein (PLP), or myelin oligodendrocyte glycoprotein (MOG). Different immunization protocols, animal strains, and antigens used can lead to different features. For example, inducing SJL/J mice with an immunodominant epitope of PLP (PLP 139-151) can cause a relapsing-remitting disease course[40] with the acute induction phase resulting in ascending hind limb paralysis due to white matter demyelination[38]. This is followed by a remission phase for which mice show clinical recovery for at least 2 days after peak score of acute phases. However, inducing C57BL/6 mice with immunodominant MOG (MOG35-55) peptide can cause a chronic nature[41] which is characterized by infiltration from CD4+ T Cells, CD8+ T Cells, B cells, and neutrophils leading to an eventual loss of hind limb motor movement through demyelination of the peripheral white matter in the spinal cord. Compared to the relapsing form of EAE, mice with chronic EAE disease develop increased lesion burden and more expansive axonal loss. Immunologically, chronic-EAE generates a wider and more robust cytokine and chemokine expression profile and an increased predominance of cytotoxic CD8+ T cells in CNS exhibiting MOG specificity[42]. The immune response generated following peptide immunization is primarily driven by proliferation and infiltration of pathogenic Th17 CD4+ T cells into the CNS where they act together with IFN-γ-expressing CD4+ and CD8+ T cells to induce damage[43]. Although the molecular underpinnings of disease initiation and disease course are yet to be fully unraveled, evidence indicates that Th17+ T cells can induce expression of an array of pro-inflammatory cytokines, such as GM-CSF, IL-9, IL-17 IL-21, IL-2, which can impact glial

survival[44]. The pathogenesis in EAE mediated by Th17 shares similarities to MS. For example, IL-17 mRNA and protein levels have been found to be elevated within cells found in the CSF of MS patients during relapses[45,46]. In addition, IL-17 has been detected in both CD4 and CD8 T cells via immunohistochemical analysis of active MS lesions, although a majority of acute lesions during RRMS display a Th1 type immune profile. Overall, EAE as an autoimmune model have been used in the development of several therapeutics including Fingolimod, Rituximab, and Laquinimod, and remain an important model for the development of MS therapies[47–50].

In contrast to EAE are the virus-induced models, which can result in widespread demyelination and neurological deficit. TMEV is one of the widely used viruses for inducing MS in mice[51]- which is a non-enveloped, positive-sense, single-stranded RNA virus[52]. However, different from EAE, the TMEV model can only induce inflammatory demyelination disease in mice, but only in rodents and primates. Mice infected with TMEV will generate a chronic demyelinating disease associated with virus persistence. Autoimmune responses to myelin antigens are also observed in this model, however, contribute only to lesion progression in chronically diseased animals but not initiation of the demyelination[51]. TMEV persistently infects macrophage/microglia lineage cells, oligodendrocytes, and astrocytes during the chronic phase[53], among them, depletion of macrophage can ameliorate TMEV-induced demyelination suggest that macrophages play an important role in the demyelination process.[54,55] Besides macrophages, depletion of TMEV-specific CD4+ T cells can also decrease the severity of demyelination. This result makes people think that CD4+ T cells can induce/augment demyelination in the TMEV model, however, Gerety and others showed that CD4+ Th1 cells alone cannot induce demyelination and treat TMEV infected mice with ex vivo generated induced Tregs (iTregs) in the early phase of the disease worsened clinical signs of MS but showing a protective role in the

chronic phase, as it increased IL-10 production from B cells, CD4+ T cells and dendritic cells, which may contribute to the decreased CNS inflammation[56,57]. CD8+ T cells, on the other hand, play an effector role in TMEV-induced demyelination, since CD8-deficient SJL mice showed minimal deficits with no effect on the extent of demyelination and meanwhile MHC class I molecules are up-regulated in the CNS of TMEV-infected mice[58].

1.3 MHV model of MS

MHV is used as another viral model of MS, which is an enveloped positive-sense, single-stranded ribonucleic acid (RNA) virus of the Coronaviridae family of viruses[59]. It is a member of the genus Betacoronavirus and is closely related to other coronaviruses that have caused widespread disease in humans including the Middle East respiratory syndrome (MERS) coronavirus, severe acute respiratory syndrome coronavirus (SARS-CoV), and the recently described severe acute respiratory syndrome coronavirus 2 (SARS-CoV-2), the causative agent of coronavirus disease of 2019 (COVID-19)[59,60]. Coronaviruses get their name from the spike protein projections around the spherical virion resembling the appearance of a solar corona[61(p),62]. Several strains of MHV have independent pathologies depending on the route of infection and mouse strain[59]. MHV-3 and the A59 strain induce mainly hepatitis while MHV-1 causes respiratory disease. The highly neurotropic John Howard Mueller strain of MHV (JHMV) causes encephalitis and was derived from vivarium settings in 1949 whereby mice were found to spontaneously develop hind limb paralysis[63,64]. JHMV-infected mice develop an acute encephalomyelitis characterized by widespread preclinical replication of the virus in microglia, astrocytes, and oligodendrocytes with relative sparing of neurons[65]. Within 24 hours of i.c infection, JHMV targets the ependymal layer of the lateral ventricles followed by dissemination

into the parenchyma where the virus infects oligodendrocytes, microglia, and astrocytes[66]. The virus further disseminates into the spinal cord through the cerebral spinal fluid (CSF) where it infects the glial cells of the white matter tracts[66]. The presence of virus in the glial cells and parenchyma elicits a milieu of anti-viral responses, initially consisting of components of the innate immune system and later followed by the adaptive immune system. JHMV infection results in widespread white matter tract demyelination with the presence of viral RNA for up to one-year post-infection (p.i)[67]. The spike glycoprotein and other virally encoded genes are important for neurovirulence and demyelination[68]. JHMV-induced demyelination includes pathogenic immune responses against viral antigens[69–71]. The innate immunity consists of pro-inflammatory factors such as IL-1, IL-6, IL-12, and TNF-α[72,73]. Type I interferons (IFN-α and IFN-β) provide crucial host defense against the JHMV, as mice lacking IFN-α/β show elevated viral load and higher mortality, and treatment of mice with external IFN-α/β shows a significant reduction in viral dissemination[74,75]. Innate immune cells are recruited to the CNS around 48 hours p.i and consist of macrophages, dendritic cells (DCs), neutrophils, and natural killer (NK) cells. Matrix- metalloproteinases (MMPs) along with cellular innate components such as macrophages, neutrophils, and NK cells permeate the blood-brain barrier (BBB) to allow the infiltration of adaptive immune cells into the CNS[76–78]; by day 5 p.i, Th1-polarized T lymphocytes appear in the CNS[79(p)]. CD4+ and CD8+ T lymphocytes are essential for the control of viral replication and elicit their antiviral effects by IFN-γ secretion and cytolysis[80,81]. CD8+ T cells function via cytotoxic effects on infected astrocytes and granzyme and perforin-mediated lysis of infected microglia[80,82,83]. Virus-specific CD4+ T cells support the peripheral expansion and anti-viral function of CD8+ T cells and thus are critical for controlling JHMV infection in the CNS[84,85]. CD4+ T cells limit the spread of virus by secreting IFN-γ, which controls viral

replication in oligodendrocytes and microglia[85,86]. IFN-γ induces perforin-mediated lysis of JHMV-infected astrocytes and microglia by inducing up-regulation of MHC class I[80,86]. On the other hand, oligodendrocytes are resistant to perforin-mediated lysis and clear JHMV infection by IFN-γ receptor signaling[87]. Histopathological examination of JHMV-infected spinal cord tissue from mice undergoing demyelination shows that myelin destruction and oligodendrocyte dysfunction are not due to apoptosis and loss of mature oligodendrocytes, but rather due to the presence of inflammatory infiltrates and presentation of viral antigen by antigen-presenting cells (APCs) through MHC class I and class II[88]. Infectious virus particles are cleared during the chronic phase of the disease, suggesting that infection of glial cells does not promote demyelination. However viral quasi-species are present at the later stage of the disease, which enhances inflammation and subsequently promotes chronic demyelination[89,90].

During the chronic phase, MHV persistence in white matter tracts leads to demyelination that is associated with areas of viral RNA/antigen and this can last up to one year post-infection (p.i.)[65,67,91]. Analysis of spinal cords from mice with established MHV-induced demyelination reveals that oligodendrocyte dysfunction and myelin integrity loss in the white matter tracts are correlated with the presence of inflammatory leukocytes as well as presentation of viral antigen through MHC-class I and MHC-class II and not by apoptosis and/or necrosis of mature oligodendrocytes[56,92]. Immune infiltration into the CNS diminishes in two weeks p.i., however, viral-specific T cells and macrophages persist in the CNS. Furthermore, macrophages localized within white matter areas of demyelination are shown stripping and engulfing myelin[93] and thus play an important role in demyelination[94]. Although neutralizing virus-specific antibody is considered important in suppressing viral recrudescence by limiting virus replication to oligodendrocytes[95,96], it does not appear to have a prominent role in promoting demyelination, as

neutralizing anti-MHV antibodies are not detected in early MHV rather after infectious virus has been eliminated from the CNS[97]. The scarcity of infectious viral particles present in the CNS during chronic disease suggests that demyelination is not amplified by productive infection of glial cells. Rather, the presence of viral RNA quasi-species with mutants and deletion variants in the CNS results in chronic inflammation and demyelination in persistently infected mice[67,98]. Axonopathy within the white matter tracts of the spinal cord was originally suggested to occur in conjunction with demyelination. However, axonal degeneration might take place in the absence of immune-mediated demyelination in MS patients[99]. For years, MHV was believed to induce demyelination without causing axonal loss; however, studies have shown that the MHV-A59 strain causes axonal damage within the optic nerve[100]. In addition, axonopathy was detected not only in areas of demyelination but also in areas where no myelin damage was observed in mice infected with MHV.

Sterile immunity is not achieved and the virus persists in the CNS of surviving mice in which the majority develop an immune-mediated demyelinating disease[67]. Demyelination that occurs in persistently infected mice is thought to be primarily mediated by virus-specific T cells and inflammatory macrophages that infiltrate into the CNS due to chronic secretion of pro-inflammatory chemokines and cytokines[81,101–103]. Axon damage in the white matter tracts is another hallmark of JHMV-induced disease in mice. SMI-32 staining, which stains for damaged neurofilament, has indicated that axon degeneration occurs in concord with demyelination in JHMV-infected mice[104]. However, some studies suggest that axon degeneration might precede oligodendrocyte dysfunction and demyelination[105]. JHMV-infection of mice lacking T and B cells (RAG1-/-), shows limited demyelination and extensive viral replication and adoptive transfer of JHMV-infected splenocytes into RAG1-/- mice results in demyelination[94,106]. CD4 T

cells were demonstrated to accelerate inflammation and demyelination post-JHMV infection, by trafficking macrophages into the CNS[107]. While we and others have demonstrated an important role for $CD4^+$ and $CD8^+$ T cells in contributing to JHMV-induced demyelination[69,81,83,101,108–111], the contributions of resident glial cells to host defense and/or disease progression remains to be better characterized. Nonetheless, emerging studies have demonstrated that resident cells of the CNS are actively involved in either protection and/or disease progression[112]. Indeed, microglia – the resident immune cell of the CNS - has been shown to either augment demyelination[113,114] and/or contribute to remyelination[115] depending upon the activation status. Additional studies are required to better understand how microglia contribute to these different processes.

1.4 Microglia and its function in MS preclinical model

Microglia are the resident immune cells of the CNS and constitute up to 12% of the total number of cells in rodents and 16% in humans. In mice, microglia are derived from immature, uncommitted KIT+ erythromyeloid progenitors (EMPs) in the yolk sac at embryonic day 7.5 (E7.5)-E8.0. Progenitors will start to upregulate CD45expression followed by myeloid cell markers including F4/80, CX3C chemokine receptor 1 (CXCR1), and colony-stimulating factor 1 receptor (CSF1R)[116]. Under normal conditions i.e. non-disease states, an important role for microglia is to maintain tissue homeostasis. Under homeostatic conditions, microglia exhibit a ramified morphology. Under inflammatory conditions that occur in response to infection, injury, or disease onset e.g. MS or Alzheimer's disease (AD), microglia are rapidly activated and this results in morphologic changes characterized by an amoeboid form accompanied by expression of pro-inflammatory cytokines/chemokines as well as MHC class I and MHC class II[117]. For

example, immune-mediated demyelination is associated with activated microglia characterized by increased surface expression of CD68, CD86, and MHC class II antigens accompanied by the secretion of cytokines and chemokines. Activated microglia can serve as antigen-presenting cells (APCs) that interact with virus-specific T cells that have migrated to the CNS highlighting that these cells serve various functions under neuroinflammatory conditions resulting from either infection or onset of disease by presenting antigens and either amplifying or restricting disease progression via secretion of regulatory factors that control the activation state of inflammatory immune cells.

In neurological diseases, activated microglia can contribute to both demyelination by recruiting macrophage and T cells, secrete cytokines and reactive oxygen species that can directly damage or enhance remyelination by clearing myelin debris and recruiting oligodendrocyte precursors (OPCs) to sites of white matter damage and contributing to the maturation of these cells into oligodendrocytes[118–120]. Therefore, many labs trying to figure out how microglia impact disease severity through use of pre-clinical models of human neurologic disease. One widely used method used for studying microglia function is through targeted depletion through administration of PLX5622 which is a small molecule antagonist that binds to colony stimulating factor 1 receptor (CSF1R). CSF1R is a receptor tyrosine kinase that is present on microglia and some peripheral immune cells including macrophages and dendritic cells. CSF1R regulates proliferation, differentiation, and survival of these cells when stimulated by its ligands CSF1 and IL-34[121,122]. CSF1R deficiency in adult mice does not affect viability but has few if any microglia or macrophages[123–125]. PLX5622 is used for depleting microglia in the CNS without affecting the survival and infiltration of macrophages. In EAE, M1-like microglia were more sensitive to PLX5622-mediated depletion compared to M2-like microglia[126].

Administration of PLX5622 to mice at 7 days following EAE induction resulted in a decrease in spinal cord demyelination and an increase of mature oligodendrocytes[126]. Microglia that remained after PLX5622 treatment were shifted away from inflammatory NOS2 phenotype and were more anti-inflammatory as determined by Arg1 expression [126]. Our lab has employed intracranial inoculation of susceptible C57BL/6 mice with JHMV to better understand how microglia function in response to CNS infection with a neurotropic virus. Our findings revealed that microglia depletion prior to JHMV infection resulted in an increase in mortality associated with impaired T cell-mediated control of viral replication which emphasized an important role for microglia in aiding in presentation of viral antigen to virus-specific T cells. In addition, we determined demyelination was significantly more severe compared to control mice and this was associated with impaired remyelination. Through use of single cell RNA sequencing (scRNAseq) of spinal cords, we determined that depletion of microglia resulted in an increase in transcripts encoding disease-associated molecules (DAMs) including Osteopontin, TREM2, and APOE while there was a marked reduction in transcripts encoding factors associated with remyelination including Cystatin F, Lipoprotein lipase, and Insulin growth factor-1[127]. Differential expression of these factors was associated primarily with macrophages and argues that microglia influence the spinal cord microenvironment to dampen demyelination as well as enhance remyelination. In addition, we administered PLX5622 to JHMV-infected mice beginning at day 14 p.i. which is a time in which animals are persistently infected with virus and demyelination is established. PLX5622-treated mice remained on drug for two weeks at which time animals were sacrificed to assess spinal cord demyelination and remyelination. Our rationale for performing this experiment was to determine if timed ablation of microglia affected the severity of white matter damage and repair after demyelination was established. Our findings reveal similar results when microglia

are depleted prior to JHMV infection in that demyelination was much more severe in PLX5622-treated mice compared to controls.

1.5. Summary

The thesis focuses on the functional contributions of microglia in host defense and disease in a model of coronavirus-induced neurological disease. **Chapter 2** shows how CXCR2- a chemokine receptor that is expressed on oligodendroglia- plays a role in the pathogenesis of neuroinflammatory demyelinating disease via impacting the proliferation and maturation of oligodendroglia into mature myelin-producing oligodendrocytes. Using an inducible proteolipid protein (Plp) promoter-driven Cre-loxP recombination to ablate *Cxcr2* in oligodendroglia of mice infected with JHMV, we found that genetic silencing of CXCR2 did not affect clinical disease, neuroinflammation, or demyelination, yet there was increased remyelination and this was associated with increased numbers of OPCs[128(p2)]. Collectively, our findings argue that CXCR2 signaling in oligodendroglia is dispensable with regard to contributing to neuroinflammation, but its deletion enhances remyelination in a preclinical model of the human demyelinating disease multiple sclerosis (MS) and suggests that targeting CXCR2 may offer a therapeutic avenue for enhancing remyelination in patients with demyelinating diseases. C**hapter 3** offers insight into microglia function in response to JHMV infection. In brief, these studies revealed that microglia tailor the CNS microenvironment to enhance control of coronavirus replication as well as dampen the severity of demyelination and promote remyelination. [127]. **Chapter 4** examines the role of microglia in the later state of JHMV infection and how it affects demyelination/remyelination. Ablation of microglia beginning at day 14, a time in which JHMV is persisting within the CNS and demyelination is established resulted in an

increase in the severity of demyelination. In addition, PLX5622-treated mice exhibited an increase in viral burden within the CNS that was associated with a reduction in expression of MHC class II but there was no effect on expression of MHC class I. Infiltration of total T cells, as well as virus-specific CD4+ and CD8+ T cells, was not affected arguing that CD4+ T cell-mediated control of viral replication was selectively affected. Expression of mRNA transcripts encoding remyelination-associated proteins Lipoprotein lipase and Cystatin F arguing that remyelination was also impaired in the absence of microglia. Other than that, depletion of microglia also negatively affects multiple biological process pathways, including adaptive immune response, phagocytosis, etc. Collectively, these findings support and extend findings described in Chapter 3 that microglia aid in host defense by enhancing presentation of viral antigen to virus-specific CD4+ T cells via MHC class II. Moreover, microglia restrict demyelination presumably by dampening expression of disease-associated molecules as well as promote remyelination by promoting the expression of proteins that regulate remyelination.

1.6 References

1. Steinman L. Immunology of Relapse and Remission in Multiple Sclerosis. *Annual Review of Immunology*. 2014;32(1):257-281. doi:10.1146/annurev-immunol-032713-120227

2. Pearce JMS. Historical Descriptions of Multiple Sclerosis. *ENE*. 2005;54(1):49-53. doi:10.1159/000087387

3. Understanding MS. National Multiple Sclerosis Society. Accessed March 6, 2022. https://www.nationalmssociety.org/What-is-MS/MS-FAQ-s

4. Multiple sclerosis - Symptoms and causes. Mayo Clinic. Accessed March 6, 2022. https://www.mayoclinic.org/diseases-conditions/multiple-sclerosis/symptoms-causes/syc-20350269

5. Lawrence Steinman MD. Multiple Sclerosis: A Coordinated Immunological Attack against Myelin in the Central Nervous System. *Cell*. 1996;85(3):299-302. doi:10.1016/S0092-8674(00)81107-1

6. Poser CM. The epidemiology of multiple sclerosis: A general overview. *Annals of Neurology*. 1994;36(S2):S180-S193. doi:10.1002/ana.410360805

7. Raine CS. The Dale E. McFarlin memorial lecture: The immunology of the multiple sclerosis lesion. *Annals of Neurology*. 1994;36(S1):S61-S72. doi:10.1002/ana.410360716

8. The Multiple Sclerosis Genetics Group, Haines JL, Terwedow HA, et al. Linkage of the MHC to Familial Multiple Sclerosis Suggests Genetic Heterogeneity. *Human Molecular Genetics*. 1998;7(8):1229-1234. doi:10.1093/hmg/7.8.1229

9. Olerup O, Hillert J. HLA class II-associated genetic susceptibility in multiple sclerosis: A critical evaluation. *Tissue Antigens*. 1991;38(2):1-15. doi:10.1111/j.1399-0039.1991.tb02029.x

10. Haegert DG, Michaud M, Schwab C, Tansey C, Décary F, Francis G. HLA-DRβ, -DQα, and -DQβ restriction fragment length polymorphisms in multiple sclerosis. *Journal of Neuroscience Research*. 1989;23(1):46-54. doi:10.1002/jnr.490230107

11. Fernández O, Fernández V, Alonso A, et al. DQB1*0602 allele shows a strongassociation with multiple sclerosis in patients in Malaga,Spain. *J Neurol*. 2004;251(4):440-444. doi:10.1007/s00415-004-0350-2

12. Types of MS. National Multiple Sclerosis Society. Accessed March 6, 2022. https://www.nationalmssociety.org/What-is-MS/Types-of-MS

13. Jacobs LD, Cookfair DL, Rudick RA, et al. Intramuscular interferon beta-1a for disease progression in relapsing multiple sclerosis. *Annals of Neurology*. 1996;39(3):285-294. doi:10.1002/ana.410390304

14. Confavreux C, O'Connor P, Comi G, et al. Oral teriflunomide for patients with relapsing multiple sclerosis (TOWER): a randomised, double-blind, placebo-controlled, phase 3 trial. *The Lancet Neurology*. 2014;13(3):247-256. doi:10.1016/S1474-4422(13)70308-9

15. Cohen JA, Barkhof F, Comi G, et al. Oral Fingolimod or Intramuscular Interferon for Relapsing Multiple Sclerosis. *New England Journal of Medicine*. 2010;362(5):402-415. doi:10.1056/NEJMoa0907839

16. Butzkueven H, Kappos L, Pellegrini F, et al. Efficacy and safety of natalizumab in multiple sclerosis: interim observational programme results. *J Neurol Neurosurg Psychiatry*. 2014;85(11):1190-1197. doi:10.1136/jnnp-2013-306936

17. Coles AJ, Cohen JA, Fox EJ, et al. Alemtuzumab CARE-MS II 5-year follow-up: Efficacy and safety findings. *Neurology*. 2017;89(11):1117-1126. doi:10.1212/WNL.0000000000004354

18. Frampton JE. Ocrelizumab: First Global Approval. *Drugs*. 2017;77(9):1035-1041. doi:10.1007/s40265-017-0757-6

19. Kutzelnigg A, Lucchinetti CF, Stadelmann C, et al. Cortical demyelination and diffuse white matter injury in multiple sclerosis. *Brain*. 2005;128(11):2705-2712. doi:10.1093/brain/awh641

20. Allen IV, McKeown SR. A histological, histochemical and biochemical study of the macroscopically normal white matter in multiple sclerosis. *Journal of the Neurological Sciences*. 1979;41(1):81-91. doi:10.1016/0022-510X(79)90142-4

21. Frischer JM, Bramow S, Dal-Bianco A, et al. The relation between inflammation and neurodegeneration in multiple sclerosis brains. *Brain*. 2009;132(5):1175-1189. doi:10.1093/brain/awp070

22. Booss J, Esiri MM, Tourtellotte WW, Mason DY. Immunohistological analysis of T lymphocyte subsets in the central nervous system in chronic progressive multiple sclerosis. *Journal of the Neurological Sciences*. 1983;62(1):219-232. doi:10.1016/0022-510X(83)90201-0

23. Hayashi T, Morimoto C, Burks JS, Kerr C, Hauser SL. Dual-label immunocytochemistry of the active multiple sclerosis lesion: Major histocompatibility complex and activation antigens. *Annals of Neurology*. 1988;24(4):523-531. doi:10.1002/ana.410240408

24. Wolswijk G. Chronic Stage Multiple Sclerosis Lesions Contain a Relatively Quiescent Population of Oligodendrocyte Precursor Cells. *J Neurosci*. 1998;18(2):601-609. doi:10.1523/JNEUROSCI.18-02-00601.1998

25. Prineas JW, Kwon EE, Goldenberg PZ, et al. Multiple sclerosis. Oligodendrocyte proliferation and differentiation in fresh lesions. *Lab Invest*. 1989;61(5):489-503.

26. Raine CS, Wu E. Multiple Sclerosis: Remyelination in Acute Lesions. *Journal of Neuropathology & Experimental Neurology*. 1993;52(3):199-204. doi:10.1097/00005072-199305000-00003

27. Lucchinetti C, Brück W, Parisi J, Scheithauer B, Rodriguez M, Lassmann H. Heterogeneity of multiple sclerosis lesions: Implications for the pathogenesis of demyelination. *Annals of Neurology*. 2000;47(6):707-717. doi:10.1002/1531-8249(200006)47:6<707::AID-ANA3>3.0.CO;2-Q

28. Bar-Or A, Fawaz L, Fan B, et al. Abnormal B-cell cytokine responses a trigger of T-cell–mediated disease in MS? *Annals of Neurology*. 2010;67(4):452-461. doi:10.1002/ana.21939

29. Selewski DT, Shah GV, Segal BM, Rajdev PA, Mukherji SK. Natalizumab (Tysabri). *American Journal of Neuroradiology*. 2010;31(9):1588-1590. doi:10.3174/ajnr.A2226

30. Ingwersen J, Aktas O, Hartung HP. Advances in and Algorithms for the Treatment of Relapsing-Remitting Multiple Sclerosis. *Neurotherapeutics*. 2016;13(1):47-57. doi:10.1007/s13311-015-0412-4

31. Rep MHG, Schrijver HM, van Lopik T, et al. Interferon (IFN)-β treatment enhances CD95 and interleukin 10 expression but reduces interferon-γ producing T cells in MS patients. *Journal of Neuroimmunology*. 1999;96(1):92-100. doi:10.1016/S0165-5728(98)00271-9

32. Kala M, Miravalle A, Vollmer T. Recent insights into the mechanism of action of glatiramer acetate. *Journal of Neuroimmunology*. 2011;235(1):9-17. doi:10.1016/j.jneuroim.2011.01.009

33. Sharma S, Mathur AG, Pradhan S, Singh DB, Gupta S. Fingolimod (FTY720): First approved oral therapy for multiple sclerosis. *J Pharmacol Pharmacother*. 2011;2(1):49-51. doi:10.4103/0976-500X.77118

34. Kale N. Optic neuritis as an early sign of multiple sclerosis. *Eye Brain*. 2016;8:195-202. doi:10.2147/EB.S54131

35. Greenhalgh AD, David S, Bennett FC. Immune cell regulation of glia during CNS injury and disease. *Nat Rev Neurosci*. 2020;21(3):139-152. doi:10.1038/s41583-020-0263-9

36. Wingerchuk DM, Lucchinetti CF, Noseworthy JH. Multiple Sclerosis: Current Pathophysiological Concepts. *Lab Invest*. 2001;81(3):263-281. doi:10.1038/labinvest.3780235

37. Garg N, Smith TW. An update on immunopathogenesis, diagnosis, and treatment of multiple sclerosis. *Brain and Behavior*. 2015;5(9):e00362. doi:10.1002/brb3.362

38. Stromnes IM, Goverman JM. Active induction of experimental allergic encephalomyelitis. *Nat Protoc*. 2006;1(4):1810-1819. doi:10.1038/nprot.2006.285

39. Batoulis H, Recks MS, Addicks K, Kuerten S. Experimental autoimmune encephalomyelitis – achievements and prospective advances. *APMIS*. 2011;119(12):819-830. doi:10.1111/j.1600-0463.2011.02794.x

40. Tuohy VK, Lu Z, Sobel RA, Laursen RA, Lees MB. Identification of an encephalitogenic determinant of myelin proteolipid protein for SJL mice. *The Journal of Immunology*. 1989;142(5):1523-1527.

41. Tompkins SM, Padilla J, Canto MCD, Ting JPY, Kaer LV, Miller SD. De Novo Central Nervous System Processing of Myelin Antigen Is Required for the Initiation of Experimental Autoimmune Encephalomyelitis. *The Journal of Immunology*. 2002;168(8):4173-4183. doi:10.4049/jimmunol.168.8.4173

42. Berard JL, Wolak K, Fournier S, David S. Characterization of relapsing–remitting and chronic forms of experimental autoimmune encephalomyelitis in C57BL/6 mice. *Glia*. 2010;58(4):434-445. doi:10.1002/glia.20935

43. Sonar SA, Lal G. Differentiation and Transmigration of CD4 T Cells in Neuroinflammation and Autoimmunity. *Frontiers in Immunology*. 2017;8. Accessed March 7, 2022. https://www.frontiersin.org/article/10.3389/fimmu.2017.01695

44. Mayo L, Quintana FJ, Weiner HL. The innate immune system in demyelinating disease. *Immunological Reviews*. 2012;248(1):170-187. doi:10.1111/j.1600-065X.2012.01135.x

45. Brucklacher-Waldert V, Stuerner K, Kolster M, Wolthausen J, Tolosa E. Phenotypical and functional characterization of T helper 17 cells in multiple sclerosis. *Brain*. 2009;132(12):3329-3341. doi:10.1093/brain/awp289

46. Durelli L, Conti L, Clerico M, et al. T-helper 17 cells expand in multiple sclerosis and are inhibited by interferon-β. *Annals of Neurology*. 2009;65(5):499-509. doi:10.1002/ana.21652

47. Kap YS, Driel N van, Blezer E, et al. Late B Cell Depletion with a Human Anti-Human CD20 IgG1κ Monoclonal Antibody Halts the Development of Experimental Autoimmune Encephalomyelitis in Marmosets. *The Journal of Immunology*. 2010;185(7):3990-4003. doi:10.4049/jimmunol.1001393

48. Foster CA, Foster CA, Howard LM, et al. Brain penetration of the oral immunomodulatory drug FTY720 and its phosphorylation in the central nervous system during experimental autoimmune encephalomyelitis: consequences for mode of action in multiple sclerosis. J Pharmacol Exp Ther 323: 469–475. Published online 2007. http://130.203.136.60/viewdoc/summary?doi=10.1.1.1090.7322

49. Foster CA, Mechtcheriakova D, Storch MK, et al. FTY720 Rescue Therapy in the Dark Agouti Rat Model of Experimental Autoimmune Encephalomyelitis: Expression of Central Nervous System Genes and Reversal of Blood-Brain-Barrier Damage. *Brain Pathology*. 2009;19(2):254-266. doi:10.1111/j.1750-3639.2008.00182.x

50. Wegner C, Stadelmann C, Pförtner R, et al. Laquinimod interferes with migratory capacity of T cells and reduces IL-17 levels, inflammatory demyelination and acute axonal damage in mice with experimental autoimmune encephalomyelitis. *Journal of Neuroimmunology*. 2010;227(1):133-143. doi:10.1016/j.jneuroim.2010.07.009

51. Atkins GJ, McQuaid S, Morris-Downes MM, et al. Transient virus infection and multiple sclerosis. *Reviews in Medical Virology*. 2000;10(5):291-303. doi:10.1002/1099-1654(200009/10)10:5<291::AID-RMV278>3.0.CO;2-U

52. Tsunoda I, Fujinami RS. Neuropathogenesis of Theiler's Murine Encephalomyelitis Virus Infection, An Animal Model for Multiple Sclerosis. *J Neuroimmune Pharmacol*. 2010;5(3):355-369. doi:10.1007/s11481-009-9179-x

53. Lipton HL, Twaddle G, Jelachich ML. The predominant virus antigen burden is present in macrophages in Theiler's murine encephalomyelitis virus-induced demyelinating disease. *Journal of Virology*. Published online April 1995. doi:10.1128/jvi.69.4.2525-2533.1995

54. Rodriguez M, Quddus J. Effect of cyclosporin A, silica quartz dust, and protease inhibitors on virus-induced demyelination. *Journal of Neuroimmunology*. 1986;13(2):159-174. doi:10.1016/0165-5728(86)90062-7

55. Rossi CP, Delcroix M, Huitinga I, et al. Role of macrophages during Theiler's virus infection. *Journal of Virology*. Published online April 1997. doi:10.1128/jvi.71.4.3336-3340.1997

56. Gerety SJ, Rundell MK, Canto MCD, Miller SD. Class II-restricted T cell responses in Theiler's murine encephalomyelitis virus-induced demyelinating disease. VI. Potentiation of demyelination with and characterization of an immunopathologic CD4+ T cell line specific for an immunodominant VP2 epitope. *The Journal of Immunology*. 1994;152(2):919-929.

57. Martinez NE, Karlsson F, Sato F, et al. Protective and Detrimental Roles for Regulatory T Cells in a Viral Model for Multiple Sclerosis. *Brain Pathology*. 2014;24(5):436-451. doi:10.1111/bpa.12119

58. Murray PD, Pavelko KD, Leibowitz J, Lin X, Rodriguez M. CD4+ and CD8+ T Cells Make Discrete Contributions to Demyelination and Neurologic Disease in a Viral Model of Multiple Sclerosis. *Journal of Virology*. Published online September 1, 1998. doi:10.1128/JVI.72.9.7320-7329.1998

59. Fehr AR, Perlman S. Coronaviruses: An Overview of Their Replication and Pathogenesis. In: Maier HJ, Bickerton E, Britton P, eds. *Coronaviruses: Methods and Protocols*. Methods in Molecular Biology. Springer; 2015:1-23. doi:10.1007/978-1-4939-2438-7_1

60. Dong E, Du H, Gardner L. An interactive web-based dashboard to track COVID-19 in real time. *The Lancet Infectious Diseases*. 2020;20(5):533-534. doi:10.1016/S1473-3099(20)30120-1

61. Bárcena M, Oostergetel GT, Bartelink W, et al. Cryo-electron tomography of mouse hepatitis virus: Insights into the structure of the coronavirion. *PNAS*. Accessed March 6, 2022. https://www.pnas.org/doi/abs/10.1073/pnas.0805270106

62. Neuman BW, Adair BD, Yoshioka C, et al. Supramolecular Architecture of Severe Acute Respiratory Syndrome Coronavirus Revealed by Electron Cryomicroscopy. *Journal of Virology*. Published online August 2006. doi:10.1128/JVI.00645-06

63. Cheever FS, Daniels JB, Pappenheimer AM, Bailey OT. A MURINE VIRUS (JHM) CAUSING DISSEMINATED ENCEPHALOMYELITIS WITH EXTENSIVE DESTRUCTION OF MYELIN. *J Exp Med*. 1949;90(3):181-194.

64. Bailey OT, Pappenheimer AM, Cheever FS, Daniels JB. A MURINE VIRUS (JHM) CAUSING DISSEMINATED ENCEPHALOMYELITIS WITH EXTENSIVE DESTRUCTION OF MYELIN : II. PATHOLOGY. *Journal of Experimental Medicine*. 1949;90(3):195-212. doi:10.1084/jem.90.3.195

65. Bergmann CC, Lane TE, Stohlman SA. Coronavirus infection of the central nervous system: host–virus stand-off. *Nat Rev Microbiol*. 2006;4(2):121-132. doi:10.1038/nrmicro1343

66. Wang FI, Hinton DR, Gilmore W, Trousdale MD, Fleming JO. Sequential infection of glial cells by the murine hepatitis virus JHM strain (MHV-4) leads to a characteristic distribution of demyelination. *Lab Invest*. 1992;66(6):744-754.

67. Lane TE, Buchmeier MJ. Murine coronavirus infection: a paradigm for virus-induced demyelinating disease. *Trends Microbiol*. 1997;5(1):9-14. doi:10.1016/S0966-842X(97)81768-4

68. Iacono KT, Kazi L, Weiss SR. Both Spike and Background Genes Contribute to Murine Coronavirus Neurovirulence. *Journal of Virology*. Published online July 2006. doi:10.1128/JVI.00432-06

69. Glass WG, Lane TE. Functional analysis of the CC chemokine receptor 5 (CCR5) on virus-specific CD8+ T cells following coronavirus infection of the central nervous system. *Virology*. 2003;312(2):407-414. doi:10.1016/S0042-6822(03)00237-X

70. Glass WG, Chen BP, Liu MT, Lane TE. Mouse Hepatitis Virus Infection of the Central Nervous System: Chemokine-Mediated Regulation of Host Defense and Disease. *Viral Immunology*. 2002;15(2):261-272. doi:10.1089/08828240260066215

71. Haring JS, Perlman S. Bystander CD4 T cells do not mediate demyelination in mice infected with a neurotropic coronavirus. *Journal of Neuroimmunology*. 2003;137(1):42-50. doi:10.1016/S0165-5728(03)00041-9

72. Parra B, Hinton DR, Lin MT, Cua DJ, Stohlman SA. Kinetics of Cytokine mRNA Expression in the Central Nervous System Following Lethal and Nonlethal Coronavirus-

Induced Acute Encephalomyelitis. *Virology*. 1997;233(2):260-270. doi:10.1006/viro.1997.8613

73. Pearce BD, Hobbs MV, McGraw TS, Buchmeier MJ. Cytokine induction during T-cell-mediated clearance of mouse hepatitis virus from neurons in vivo. *Journal of Virology*. Published online September 1994. doi:10.1128/jvi.68.9.5483-5495.1994

74. Ireland DDC, Stohlman SA, Hinton DR, Atkinson R, Bergmann CC. Type I Interferons Are Essential in Controlling Neurotropic Coronavirus Infection Irrespective of Functional CD8 T Cells. *Journal of Virology*. Published online January 2008. doi:10.1128/JVI.01794-07

75. Minagawa H, Takenaka A, Mohri S, Mori R. Protective effect of recombinant murine interferon beta against mouse hepatitis virus infection. *Antiviral Research*. 1987;8(2):85-95. doi:10.1016/0166-3542(87)90079-9

76. Yong VW, Zabad RK, Agrawal S, Goncalves DaSilva A, Metz LM. Elevation of matrix metalloproteinases (MMPs) in multiple sclerosis and impact of immunomodulators. *Journal of the Neurological Sciences*. 2007;259(1):79-84. doi:10.1016/j.jns.2006.11.021

77. Hosking MP, Liu L, Ransohoff RM, Lane TE. A Protective Role for ELR+ Chemokines during Acute Viral Encephalomyelitis. *PLOS Pathogens*. 2009;5(11):e1000648. doi:10.1371/journal.ppat.1000648

78. Savarin C, Stohlman SA, Atkinson R, Ransohoff RM, Bergmann CC. Monocytes Regulate T Cell Migration through the Glia Limitans during Acute Viral Encephalitis. *Journal of Virology*. Published online May 2010. doi:10.1128/JVI.00051-10

79. Marten NW, Stohlman SA, Zhou J, Bergmann CC. Kinetics of Virus-Specific CD8+-T-Cell Expansion and Trafficking following Central Nervous System Infection. *Journal of Virology*. Published online February 15, 2003. doi:10.1128/JVI.77.4.2775-2778.2003

80. Lin MT, Stohlman SA, Hinton DR. Mouse hepatitis virus is cleared from the central nervous systems of mice lacking perforin-mediated cytolysis. *Journal of Virology*. Published online January 1997. doi:10.1128/jvi.71.1.383-391.1997

81. Parra B, Hinton DR, Marten NW, et al. IFN-γ Is Required for Viral Clearance from Central Nervous System Oligodendroglia. *The Journal of Immunology*. 1999;162(3):1641-1647.

82. Ramakrishna C, Stohlman SA, Atkinson RA, Hinton DR, Bergmann CC. Differential Regulation of Primary and Secondary CD8+ T Cells in the Central Nervous System. *The Journal of Immunology*. 2004;173(10):6265-6273. doi:10.4049/jimmunol.173.10.6265

83. Bergmann CC, Parra B, Hinton DR, Ramakrishna C, Dowdell KC, Stohlman SA. Perforin and Gamma Interferon-Mediated Control of Coronavirus Central Nervous System Infection by CD8 T Cells in the Absence of CD4 T Cells. *Journal of Virology*. Published online February 15, 2004. doi:10.1128/JVI.78.4.1739-1750.2004

84. Phares TW, Stohlman SA, Hwang M, Min B, Hinton DR, Bergmann CC. CD4 T Cells Promote CD8 T Cell Immunity at the Priming and Effector Site during Viral Encephalitis. *Journal of Virology*. Published online March 1, 2012. doi:10.1128/JVI.06797-11

85. Zhou J, Hinton DR, Stohlman SA, Liu CP, Zhong L, Marten NW. Maintenance of CD8+ T Cells during Acute Viral Infection of the Central Nervous System Requires CD4+ T Cells But Not Interleukin-2. *Viral Immunology*. 2005;18(1):162-169. doi:10.1089/vim.2005.18.162

86. Bergmann CC, Parra B, Hinton DR, Chandran R, Morrison M, Stohlman SA. Perforin-Mediated Effector Function Within the Central Nervous System Requires IFN-γ-Mediated MHC Up-Regulation. *The Journal of Immunology*. 2003;170(6):3204-3213. doi:10.4049/jimmunol.170.6.3204

87. González JM, Bergmann CC, Ramakrishna C, et al. Inhibition of Interferon-γ Signaling in Oligodendroglia Delays Coronavirus Clearance without Altering Demyelination. *The American Journal of Pathology*. 2006;168(3):796-804. doi:10.2353/ajpath.2006.050496

88. Redwine JM, Buchmeier MJ, Evans CF. In Vivo Expression of Major Histocompatibility Complex Molecules on Oligodendrocytes and Neurons during Viral Infection. *The American Journal of Pathology*. 2001;159(4):1219-1224. doi:10.1016/S0002-9440(10)62507-2

89. Adami C, Pooley J, Glomb J, et al. Evolution of Mouse Hepatitis Virus (MHV) during Chronic Infection: Quasispecies Nature of the Persisting MHV RNA. *Virology*. 1995;209(2):337-346. doi:10.1006/viro.1995.1265

90. Fleming JO, Adami C, Pooley J, et al. Mutations Associated with Viral Sequences Isolated from Mice Persistently Infected with MHV-JHM. In: Talbot PJ, Levy GA, eds. *Corona- and Related Viruses: Current Concepts in Molecular Biology and Pathogenesis*. Advances in Experimental Medicine and Biology. Springer US; 1995:591-597. doi:10.1007/978-1-4615-1899-0_94

91. Hosking MP, Lane TE. The Biology of Persistent Infection: Inflammation and Demyelination Following Murine Coronavirus Infection of the Central Nervous System. *Current Immunology Reviews*. 2009;5(4):267-276. doi:10.2174/157339509789504005

92. Barac-Latas V, Suchanek G, Breitschopf H, Stuehler A, Wege H, Lassmann H. Patterns of oligodendrocyte pathology in coronavirus-induced subacute demyelinating encephalomyelitis in the lewis rat. *Glia*. 1997;19(1):1-12. doi:10.1002/(SICI)1098-1136(199701)19:1<1::AID-GLIA1>3.0.CO;2-5

93. Sarma JD, Kenyon LC, Hingley ST, Shindler KS. Mechanisms of Primary Axonal Damage in a Viral Model of Multiple Sclerosis. *J Neurosci*. 2009;29(33):10272-10280. doi:10.1523/JNEUROSCI.1975-09.2009

94. Wu GF, Perlman S. Macrophage Infiltration, but Not Apoptosis, Is Correlated with Immune-Mediated Demyelination following Murine Infection with a Neurotropic

Coronavirus. *Journal of Virology*. Published online October 1, 1999. doi:10.1128/JVI.73.10.8771-8780.1999

95. Lin MT, Hinton DR, Marten NW, Bergmann CC, Stohlman SA. Antibody Prevents Virus Reactivation Within the Central Nervous System. *The Journal of Immunology*. 1999;162(12):7358-7368.

96. Ramakrishna C, Stohlman SA, Atkinson RD, Shlomchik MJ, Bergmann CC. Mechanisms of Central Nervous System Viral Persistence: the Critical Role of Antibody and B Cells. *The Journal of Immunology*. 2002;168(3):1204-1211. doi:10.4049/jimmunol.168.3.1204

97. Weiner LP. Pathogenesis of Demyelination Induced by a Mouse Hepatitis. *Archives of Neurology*. 1973;28(5):298-303. doi:10.1001/archneur.1973.00490230034003

98. Perlman S, Wheeler DL. Neurotropic Coronavirus Infections. In: Reiss CS, ed. *Neurotropic Viral Infections: Volume 1: Neurotropic RNA Viruses*. Springer International Publishing; 2016:115-148. doi:10.1007/978-3-319-33133-1_5

99. Garbern JY, Yool DA, Moore GJ, et al. Patients lacking the major CNS myelin protein, proteolipid protein 1, develop length-dependent axonal degeneration in the absence of demyelination and inflammation. *Brain*. 2002;125(3):551-561. doi:10.1093/brain/awf043

100. Shindler KS, Kenyon LC, Dutt M, Hingley ST, Sarma JD. Experimental Optic Neuritis Induced by a Demyelinating Strain of Mouse Hepatitis Virus. *Journal of Virology*. Published online September 2008. doi:10.1128/JVI.00920-08

101. Marten NW, Stohlman SA, Bergmann CC. MHV Infection of the CNS: Mechanisms of Immune-Mediated Control. *Viral Immunology*. 2001;14(1):1-18. doi:10.1089/08828240151061329

102. Krasemann S, Madore C, Cialic R, et al. The TREM2-APOE Pathway Drives the Transcriptional Phenotype of Dysfunctional Microglia in Neurodegenerative Diseases. *Immunity*. 2017;47(3):566-581.e9. doi:10.1016/j.immuni.2017.08.008

103. Chabas D, Baranzini SE, Mitchell D, et al. The Influence of the Proinflammatory Cytokine, Osteopontin, on Autoimmune Demyelinating Disease. *Science*. 2001;294(5547):1731-1735. doi:10.1126/science.1062960

104. Dandekar AA, Wu GF, Pewe L, Perlman S. Axonal Damage Is T Cell Mediated and Occurs Concomitantly with Demyelination in Mice Infected with a Neurotropic Coronavirus. *Journal of Virology*. Published online July 1, 2001. doi:10.1128/JVI.75.13.6115-6120.2001

105. Sarma JD, Fu L, Hingley ST, Lavi E. Mouse Hepatitis Virus Type-2 Infection in Mice: An Experimental Model System of Acute Meningitis and Hepatitis. *Experimental and Molecular Pathology*. 2001;71(1):1-12. doi:10.1006/exmp.2001.2378

106. Pewe L, Perlman S. Cutting Edge: CD8 T Cell-Mediated Demyelination Is IFN-γ Dependent in Mice Infected with a Neurotropic Coronavirus. *The Journal of Immunology*. 2002;168(4):1547-1551. doi:10.4049/jimmunol.168.4.1547

107. Lane TE, Liu MT, Chen BP, et al. A Central Role for CD4+ T Cells and RANTES in Virus-Induced Central Nervous System Inflammation and Demyelination. *Journal of Virology*. Published online February 1, 2000. doi:10.1128/JVI.74.3.1415-1424.2000

108. Glass WG, Hickey MJ, Hardison JL, Liu MT, Manning JE, Lane TE. Antibody Targeting of the CC Chemokine Ligand 5 Results in Diminished Leukocyte Infiltration into the Central Nervous System and Reduced Neurologic Disease in a Viral Model of Multiple Sclerosis. *The Journal of Immunology*. 2004;172(7):4018-4025. doi:10.4049/jimmunol.172.7.4018

109. Glass WG, Lane TE. Functional Expression of Chemokine Receptor CCR5 on CD4+ T Cells during Virus-Induced Central Nervous System Disease. *Journal of Virology*. Published online January 1, 2003. doi:10.1128/JVI.77.1.191-198.2003

110. Liu MT, Chen BP, Oertel P, et al. Cutting Edge: The T Cell Chemoattractant IFN-Inducible Protein 10 Is Essential in Host Defense Against Viral-Induced Neurologic Disease. *The Journal of Immunology*. 2000;165(5):2327-2330. doi:10.4049/jimmunol.165.5.2327

111. Liu MT, Armstrong D, Hamilton TA, Lane TE. Expression of Mig (Monokine Induced by Interferon-γ) Is Important in T Lymphocyte Recruitment and Host Defense Following Viral Infection of the Central Nervous System. *The Journal of Immunology*. 2001;166(3):1790-1795. doi:10.4049/jimmunol.166.3.1790

112. Benarroch EE. Microglia: Multiple roles in surveillance, circuit shaping, and response to injury. *Neurology*. 2013;81(12):1079-1088. doi:10.1212/WNL.0b013e3182a4a577

113. Trapp BD, Peterson J, Ransohoff RM, Rudick R, Mörk S, Bö L. Axonal Transection in the Lesions of Multiple Sclerosis. *New England Journal of Medicine*. 1998;338(5):278-285. doi:10.1056/NEJM199801293380502

114. Henderson APD, Barnett MH, Parratt JDE, Prineas JW. Multiple sclerosis: Distribution of inflammatory cells in newly forming lesions. *Annals of Neurology*. 2009;66(6):739-753. doi:10.1002/ana.21800

115. Miron VE, Boyd A, Zhao JW, et al. M2 microglia and macrophages drive oligodendrocyte differentiation during CNS remyelination. *Nat Neurosci*. 2013;16(9):1211-1218. doi:10.1038/nn.3469

116. Kierdorf K, Erny D, Goldmann T, et al. Microglia emerge from erythromyeloid precursors via Pu.1- and Irf8-dependent pathways. *Nat Neurosci*. 2013;16(3):273-280. doi:10.1038/nn.3318

117. Yin J, Valin KL, Dixon ML, Leavenworth JW. The Role of Microglia and Macrophages in CNS Homeostasis, Autoimmunity, and Cancer. *Journal of Immunology Research*. 2017;2017:e5150678. doi:10.1155/2017/5150678

118. Franklin RJM, Ffrench-Constant C. Remyelination in the CNS: from biology to therapy. *Nat Rev Neurosci*. 2008;9(11):839-855. doi:10.1038/nrn2480

119. Kotter MR, Zhao C, van Rooijen N, Franklin RJM. Macrophage-depletion induced impairment of experimental CNS remyelination is associated with a reduced oligodendrocyte progenitor cell response and altered growth factor expression. *Neurobiol Dis*. 2005;18(1):166-175. doi:10.1016/j.nbd.2004.09.019

120. Lampron A, Larochelle A, Laflamme N, et al. Inefficient clearance of myelin debris by microglia impairs remyelinating processes. *J Exp Med*. 2015;212(4):481-495. doi:10.1084/jem.20141656

121. Patel S, Player MR. Colony-Stimulating Factor-1 Receptor Inhibitors for the Treatment of Cancer and Inflammatory Disease. *Current Topics in Medicinal Chemistry*. 2009;9(7):599-610. doi:10.2174/156802609789007327

122. Elmore MRP, Najafi AR, Koike MA, et al. Colony-Stimulating Factor 1 Receptor Signaling Is Necessary for Microglia Viability, Unmasking a Microglia Progenitor Cell in the Adult Brain. *Neuron*. 2014;82(2):380-397. doi:10.1016/j.neuron.2014.02.040

123. Dai XM, Ryan GR, Hapel AJ, et al. Targeted disruption of the mouse colony-stimulating factor 1 receptor gene results in osteopetrosis, mononuclear phagocyte deficiency, increased primitive progenitor cell frequencies, and reproductive defects. *Blood*. 2002;99(1):111-120. doi:10.1182/blood.V99.1.111

124. Erblich B, Zhu L, Etgen AM, Dobrenis K, Pollard JW. Absence of Colony Stimulation Factor-1 Receptor Results in Loss of Microglia, Disrupted Brain Development and Olfactory Deficits. *PLOS ONE*. 2011;6(10):e26317. doi:10.1371/journal.pone.0026317

125. Li J, Chen K, Zhu L, Pollard JW. Conditional deletion of the colony stimulating factor-1 receptor (c-fms proto-oncogene) in mice. *genesis*. 2006;44(7):328-335. doi:10.1002/dvg.20219

126. Nissen JC, Thompson KK, West BL, Tsirka SE. Csf1R inhibition attenuates experimental autoimmune encephalomyelitis and promotes recovery. *Exp Neurol*. 2018;307:24-36. doi:10.1016/j.expneurol.2018.05.021

127. Mangale V, Syage AR, Ekiz HA, et al. Microglia influence host defense, disease, and repair following murine coronavirus infection of the central nervous system. *Glia*. 2020;68(11):2345-2360. doi:10.1002/glia.23844

128. Marro BS, Skinner DD, Cheng Y, et al. Disrupted CXCR2 Signaling in Oligodendroglia Lineage Cells Enhances Myelin Repair in a Viral Model of Multiple Sclerosis. *Journal of Virology*. Published online June 26, 2019. doi:10.1128/JVI.00240-19

Chapter 2

DISRUPTED CXCR2 SIGNALING IN OLIGODENDROGLIA LINEAGE CELLS ENHANCES MYELIN REPAIR IN A VIRAL MODEL OF MULTIPLE SCLEROSIS

Disrupted CXCR2 Signaling in Oligodendroglia Lineage Cells Enhances Myelin Repair in a Viral Model of Multiple Sclerosis

Brett S. Marro,[a] Dominic D. Skinner,[b] Yuting Cheng,[b] Jonathan J. Grist,[b] Laura L. Dickey,[b] Emily Eckman,[b] Colleen Stone,[b] Liping Liu,[d] Richard M. Ransohoff,[e]* Thomas E. Lane[b],[c]

[a]Department of Molecular Biology & Biochemistry, University of California, Irvine, Irvine, California, USA

[b]Division of Microbiology & Immunology, Department of Pathology, University of Utah School of Medicine, Salt Lake City, Utah, USA

[c]Immunology, Inflammation & Infectious Disease Initiative, University of Utah, Salt Lake City, Utah, USA

[d]Lerner Research Institute, Cleveland Clinic, Cleveland, Ohio, USA

[e]Department of Cell Biology, Harvard University School of Medicine, Boston, Massachusetts, USA

ABSTRACT

CXCR2 is a chemokine receptor expressed on oligodendroglia that has been implicated in the pathogenesis of neuroinflammatory demyelinating diseases as well as enhancement of the migration, proliferation, and myelin production by oligodendroglia. Using an inducible proteolipid protein (*Plp*) promoter-driven Cre-*loxP* recombination system, we were able to assess how timed ablation of *Cxcr2* in oligodendroglia affected disease following intracranial infection with the neurotropic JHM strain of mouse hepatitis virus (JHMV). Generation of *Plp-Cre-ER(T)::Cxcr2*$^{flox/flox}$ transgenic mice (termed *Cxcr2*-CKO mice) allows for *Cxcr2* to be silenced in oligodendrocytes in adult mice following treatment with tamoxifen. Ablation of oligodendroglia *Cxcr2* did not influence clinical severity in response to intracranial infection with JHMV. Infiltration of activated T cells or myeloid cells into the central nervous system (CNS) was not affected, nor was the ability to control viral infection. In addition, the severity of demyelination was similar between tamoxifen-treated mice and vehicle- treated controls. Notably, deletion of *Cxcr2* resulted in increased remyelination, as assessed by *g*-ratio (the ratio of the inner axonal diameter to the total outer fiber diameter) calculation, compared to that in vehicle-treated control mice. Collectively, our findings argue that CXCR2 signaling in oligodendroglia is dispensable with regard to contributing to neuroinflammation, but its deletion enhances remyelination in a preclinical model of the human demyelinating disease multiple sclerosis (MS).

IMPORTANCE

Signaling through the chemokine receptor CXCR2 in oligodendroglia is important for developmental myelination in rodents, while chemical inhibition or non-specific genetic deletion of CXCR2 appears to augment myelin repair in animal models of the human demyelinating

disease multiple sclerosis (MS). To better understand the biology of CXCR2 signaling on oligodendroglia, we generated transgenic mice in which *Cxcr2* is selectively ablated in oligodendroglia upon treatment with tamoxifen. Using a viral model of neuroinflammation and demyelination, we demonstrate that genetic silencing of CXCR2 on oligodendroglia did not affect clinical disease, neuroinflammation, or demyelination, yet there was increased remyelination. These findings support and extend previous findings suggesting that targeting CXCR2 may offer a therapeutic avenue for enhancing remyelination in patients with demyelinating diseases.

KEYWORDS

chemokine receptors, demyelination, oligodendrocyte, remyelination, virus

INTRODUCTION

Multiple sclerosis (MS) is a chronic inflammatory neurodegenerative disease characterized by multifocal regions of central nervous system (CNS) neuroinflammation, demyelination, and axonal loss that ultimately results in extensive neurologic disability (1). Preclinical animal models of MS indicate that CNS infiltration of neutrophils, monocyte/macrophages, and inflammatory T cells, including those that are autoreactive to specific proteins embedded in the myelin sheath, is important in disease initiation and maintaining demyelination. Through the use of mouse models of MS, chemokines and chemokine receptors have been implicated as being important in attracting targeted populations of activated immune cells into the CNS and have been considered relevant targets for clinical intervention for MS patients (2–11). CXCR2 is a receptor for ELR-positive CXC chemokines, e.g., CXCL1 and CXCL2, and is expressed on polymorphonuclear neutrophils (PMN) as well as glia (12–16). CXCR2 signaling on neutrophils promotes demyelination in models of experimental autoimmune encephalomyelitis (EAE), cuprizone-induced demyelination, as well as virus-induced demyelination (8, 17–19). However, CXCR2 has additional roles that extend beyond influencing neutrophil activity, as it is expressed on immature oligodendrocyte progenitor cells (OPCs) as well as mature myelinating oligodendrocytes (20). *In vitro* studies have demonstrated that signaling through CXCR2 influences OPC proliferation and differentiation (21), whereas in vivo studies argue that CXCR2 controls the positional migration of OPCs within the spinal cord and regulates OPC numbers to ensure the structural integrity of the white matter during CNS development (22). Indeed, mice devoid of CXCR2 exhibit a paucity of OPCs and structural misalignments that persist into adulthood of the mouse, resulting in reduced numbers of mature oligodendrocytes and total myelin within the white matter (23).

Moreover, either genetic deletion or antibody- mediated targeting of CXCR2 increases myelin synthesis in demyelinated cerebellum slice cultures (24). The concept of CXCR2 signaling on oligodendroglia regulating myelin synthesis is further supported by a recent report by Liu and colleagues (25) that demonstrated that targeted ablation of CXCR2 on oligodendroglia enhanced remyelination following toxin-induced demyelination. Collectively, these findings argue that CXCR2 signaling on oligodendroglia ultimately contributes to maintaining myelin integrity and axonal protection both under homeostatic conditions and following demyelination.

Intracranial (i.c.) inoculation of susceptible mice with the neurotropic JHM strain of mouse hepatitis virus (JHMV) results in an acute encephalomyelitis characterized by widespread viral replication in glial cells with relative sparing of neurons (26, 27). CNS-infiltrating $CD4^+$ and $CD8^+$ T cells control viral replication through the secretion of gamma interferon (IFN-γ) and cytolytic activity, yet sterile immunity is not acquired and virus persists in white matter tracts, resulting in an immune-mediated demyelinating disease with clinical and histologic similarities to the human demyelinating disease MS (28, 29). Previous studies employing the JHMV model have demonstrated important roles for select chemokines in participating in host defense as well as demyelination by attracting targeted populations of leukocytes into the CNS (30–36). More recently, we have shown that treatment of JHMV-infected mice with blocking antibody specific for CXCR2 led to an increase in clinical disease associated with more severe demyelination (37). Examination of spinal cords revealed that the increase in white matter damage in anti-CXCR2-treated mice was associated with oligodendroglia apoptosis, arguing for a protective role for CXCR2 signaling in a model of virus-induced demyelination (37). Nonetheless, other resident cells as well as inflammatory cells express CXCR2, making it difficult to assign a specific role for CXCR2 signaling on oligodendroglia in contributing to either protection or disease

progression. The present study was undertaken to better understand how selective deletion of *Cxcr2* within oligodendroglia lineage cells in adult mice influences host defense and disease in response to JHMV infection of the CNS.

RESULTS

Generation and characterization of Cxcr2-CKO mice. We sought to ablate *Cxcr2* signaling within oligodendrocytes and their progenitors to assess the impact on disease and repair in an animal model of neuroinflammation and demyelination. A *Plp-Cre-ER(T)::Cxcr2*$^{flox/flox}$ mouse line (referred to as *Cxcr2*-CKO) that utilizes Cre recombinase to ablate *Cxcr2* in a selective and inducible manner was employed (17, 38–41). The proteolipid protein (PLP) regulatory element promotes expression of Cre-ER(T) (42) and has previously been shown to accurately reflect endogenous PLP expression spatially and temporally in oligodendroglia (42). To aid in visualizing cells actively expressing Cre recombinase, *Cxcr2*-CKO mice were crossed to a Cre-inducible *Rosa26*-tdTomato reporter line on the C57BL/6 mouse background (**Figure. 1A**). Ablation of *Cxcr2* was confirmed within oligodendrocyte lineage cells following *ex vivo* culture of oligodendroglia generated from the brains of postnatal day 1 (P1) *Cxcr2*-CKO mice. Addition of (Z)-4- hydroxytamoxifen (4-OHT; 100 nM) induced Cre-mediated recombination at the *Cxcr2* locus, as detected by PCR using primers that specifically generate an amplicon following excision of exon 2 of *Cxcr2* (**Figure. 1B**). 4-OHT induced expression of tdTomato red in the majority of cultured cells from the brains of P1 *Cxcr2*-CKO mice at day 6 post treatment, with the tdTomato red being distributed throughout the cell body and the cell morphology resembling oligodendrocytes (**Figure. 1C**). Immunocytochemical staining revealed >90% of cultured oligodendroglia expressing the late-stage O1 surface marker, in contrast to vehicle-treated cultures (**Figure. 1D**).

Tamoxifen treatment results in enriched tdTomato red expression in spinal cord oligodendroglia. To determine the cellular specificity of Cre activity *in vivo*, 4-week-old *Cxcr2*-CKO mice were treated with 1 mg tamoxifen by intraperitoneal (i.p.) administration twice daily

for 5 days, and the targeting of *Cxcr2* was subsequently determined (43, 44). Recombination at the *Cxcr2* locus was detected by PCR in the brain and spinal cord of *Cxcr2*-CKO mice but not in the spleen, liver, or kidney (**Figure. 2A**). In response to tamoxifen treatment, there was a dramatic increase in tdTomato expression that was distributed throughout the cell body as well as processes. To identify cells expressing tdTomato within the CNS in response to tamoxifen treatment, immunohistochemical staining for defined cellular markers of the CNS was performed. In addition to oligodendroglia, we focused our attention on neurons (45, 46) and macrophages/ microglia (45, 47), as these cells have been reported to express CXCR2. Expression of CXCR2 by astrocytes has not been reported, and we did not concentrate on this population of cells (48, 49). We found that the majority of tdTomato-positive cells in tamoxifen-treated *Cxcr2*-CKO mice were oligodendroglia, as defined by staining either oligodendrocyte transcription factor 2 (Olig2) (50, 51) or glutathione S-transferase π (GST-π), a marker of mature oligodendrocytes (52, 53). In tamoxifen-treated mice, ~82% of tdTomato-positive cells (cells in which the tdTomato signal was distributed throughout the cell body) expressed nuclear-specific markers (Olig2, 42.1% ± 7.7%; GST-π, 39.9% ± 7.9%) (**Figure. 2B, C, and F**). MAP2-positive neurons accounted for <4% of tdTomato-positive cells (3.3% ± 0.8%) in tamoxifen-treated *Cxcr2*-CKO mice (**Figure. 2D and F**). Similarly, very few IBA1-positive macrophages/microglia expressed tdTomato (2.6% ± 0.3%) (**Figure. 2E and F**). We have previously demonstrated that neutrophils require CXCR2 to traffic and accumulate within the CNS in response to JHMV infection (54). Tamoxifen treatment did not modulate CXCR2 expression in neutrophils, as no differences were observed in surface expression of CXCR2 on splenic neutrophils obtained from tamoxifen-treated *Cxcr2*-CKO mice and vehicle-treated mice, as deter- mined by flow cytometry (**Figure. 2G**). These results demonstrate that tamoxifen-

induced targeting of *Cxcr2* is highly specific to oligodendrocyte lineage cells. It is important to note that we did not perform CXCR2 immunohistochemical staining in experimental tissues, as we have previously reported that there are no validated CXCR2-specific antibodies, as we routinely detected nonspecific CXCR2 staining in experimental *Cxcr2*$^{-/-}$ mice (24). The remaining tdTomato-positive cells present within the spinal cords of tamoxifen-treated mice (∼12%) most likely represent oligodendroglia cellular processes extending from the cell bodies in which neither Olig2 or GST-π is detected. No defects in myelin formation/synthesis following *Cxcr2* ablation in oligodendroglia. We next evaluated whether tamoxifen-mediated targeting of *Cxcr2* in oligodendroglia in adult mice affected myelin integrity, as previous studies have indicated that adult *Cxcr2*$^{-/-}$ animals have deficient myelin formation (22, 23). *Cxcr2*-CKO mice were treated twice daily with either 1 mg tamoxifen or vehicle, followed by resting for 2 weeks, at which point the spinal cords were removed to evaluate spinal cord myelin. Similar to the findings of Liu et al. (25), we did not detect any differences in either the size or behavior in tamoxifen-treated *Cxcr2*-CKO mice compared to their vehicle-treated littermates. Assessment of spinal cord myelin via toluidine blue staining revealed no overt differences between tamoxifen-treated *Cxcr2*-CKO mice and vehicle-treated control *Cxcr2*-CKO mice (**Figure. 3A and B**). As an additional test of myelin integrity, electron microscopy (EM) analysis of spinal cord sections was performed. Assessment of the *g* ratio, the ratio of the inner axonal diameter to the total outer fiber diameter, is commonly employed as a structural index of myelin. We did not detect any changes in qualitative differences in myelin thickness between naive tamoxifen-treated *Cxcr2*-CKO mice and vehicle-treated *Cxcr2*-CKO mice (**Figure. 3C and D**); subsequent calculation of the g ratios between experimental groups confirmed that targeting of CXCR2 in oligodendroglia in adult mice did not alter myelin integrity (**Figure. 3E and F**). In all experimental groups, the *g*

ratios averaged ~0.8, indicating normal myelinated axons in the spinal cord (**Figure. 3E and F**) (55–57). These findings argue that inducible deletion of CXCR2 in oligodendroglia lineage cells in young (4-week-old) mice does not affect the myelin content in a nondisease state.

***Cxcr2* ablation within oligodendrocytes does not impair antiviral responses.**

Intracranial (i.c.) instillation of the neuroadapted JHM strain of mouse hepatitis virus (JHMV) results in an acute encephalomyelitis followed by a chronic demyelinating disease characterized by viral persistence in white matter tracts accompanied by immune-mediated demyelination (26). Tamoxifen- or vehicle-treated *Cxcr2*-CKO mice were infected i.c. with JHMV (250 PFU), and clinical disease was monitored. Vehicle- treated *Cxcr2*-CKO mice had worse ($P < 0.05$) clinical disease at 12 days post infection (p.i.) than control mice, but otherwise, no overt differences in morbidity or mortality were observed in the experimental mice out to day 28 p.i. (**Figure. 4A**). Examination of the viral titers in the brains at days 5, 7, and 10 p.i. showed similar levels of virus present between tamoxifen- and vehicle-treated mice (**Figure. 4B**). Although the titers were higher ($P < 0.05$) in tamoxifen-treated animals at day 7 p.i. than in the controls, we do not believe that this reflects an overall difference in the control of viral replication, as there were no differences in viral titers between experimental groups at the other time points examined. By day 21 p.i., virus was not detected (ND) in the brains of experimental mice (**Figure. 4B**). There were no differences in viral titers in the spinal cords of experimental mice at days 5, 7, and 10 p.i. (**Figure. 4B**). Collectively, these findings indicate that *Cxcr2* targeting did not compromise the control of viral replication within the CNS. Moreover, similar frequencies of $CD4^+$ and $CD8^+$ T cells specific for the immunodominant viral epitopes M133-144 and S510-518, respectively, as determined by tetramer staining, were detected within the brains of the experimental mice at day 7, further supporting that targeting of *Cxcr2* within oligodendroglia did not impact the generation

of a protective antiviral immune response (**Figure. 4C**). There were no differences in either total T cell subsets, neutrophils ($CD11b^{+}$ $Ly6G^{+}$), or macrophages ($CD45^{hi}$ $F4/80^{hi}$) at day 7 p.i. between vehicle- and tamoxifen-treated mice (**Figure. 4D**). The comparable acute inflammatory response to JHMV between vehicle- and tamoxifen-treated *Cxcr2*-CKO mice was further supported by the observation of no significant differences in expression of proinflammatory cytokine and chemokine genes (a detailed inventory of the probes is provided in Materials and Methods) within the brain at day 7 p.i. (**Figure. 4E**). Collectively, these findings indicate that selectively targeting *Cxcr2* within oligodendroglia does not mute neuroinflammation or impair control of JHMV replication within the CNS.

***Cxcr2* ablation does not affect the severity of demyelination.** JHMV infection of mice results in persistent CNS infection and a chronic immune-mediated demyelinating disease. Evaluation of demyelination in JHMV-infected *Cxcr2*-CKO mice indicated that there were no significant differences in the severity of demyelination between vehicle- and tamoxifen-treated *Cxcr2*-CKO mice at days 21 (**Figure. 5A to C**) and 28 (**Figure. 5E to G**) p.i. Evaluation of immune cell infiltration into the spinal cords of tamoxifen- and vehicle- treated mice by flow cytometry at either day 21 p.i. (**Figure. 5D**) or day 28 p.i. (**Figure. 5H**) revealed no difference in $CD4^{+}$ or $CD8^{+}$ T cell as well as macrophage ($CD45^{lo}$ $F4/80^{+}$) infiltration. Furthermore, examination of demyelination within the brains of JHMV- infected *Cxcr2*-CKO mice treated with either vehicle or tamoxifen revealed no differences in the severity of demyelination (data not shown). These findings argue that tamoxifen-mediated targeting of *Cxcr2* within oligodendroglia does not alter immune cell infiltration into the spinal cords of JHMV-infected mice or influence the severity of white matter damage. Remyelination is enhanced upon silencing of CXCR2 in oligodendroglia. Previous work has indicated that targeting of CXCR2 signaling

through either administration of receptor-specific small molecules (58) or genetic targeting (25) results in increased remyelination. To determine whether remyelination was occurring following tamoxifen-mediated silencing of *Cxcr2* signaling, JHMV-infected *Cxcr2*-CKO mice were sacrificed at day 28 p.i., and EM analysis of spinal cord sections was performed to calculate *g* ratios. High-magnification (X1,200) images of the spinal cord lateral white matter columns concentrated within thoracic vertebrae 6 to 10 of tamoxifen-treated and vehicle-treated control *Cxcr2*-CKO mice were used to evaluate axons. Representative EM images from JHMV-infected mice treated with vehicle depict axons with very little to no myelin sheath (**Figure. 6A**). Remyelinated axons in tamoxifen-treated JHMV- infected *Cxcr2*-CKO mice were identified by thin myelin sheaths, in contrast to the thicker myelin sheath detected on a normal myelinated axon (**Figure. 6B**). In vehicle-treated *Cxcr2*-CKO mice, there was an overall increase of demyelinated axons and fewer remyelinated axons compared to tamoxifen-treated *Cxcr2*-CKO mice. To more accurately quantitate these differences, we quantified both the g ratio and the myelin thickness in infected mice. Tamoxifen-induced ablation of *Cxcr2* on oligodendroglia resulted in a g ratio (0.78 ± 0.006, $n = 5$ mice) significantly ($P < 0.05$) lower than that in control mice (0.87 ± 0.006, $n = 4$ mice) (**Figure. 6C and D**). In addition, there was a corresponding significant ($P < 0.01$) increase in myelin thickness in tamoxifen-treated *Cxcr2*-CKO mice compared to vehicle-treated mice (**Figure. 6E and F**). Collectively, these findings indicate that selective ablation of *Cxcr2* in oligodendroglia enhances remyelination following JHMV-induced demyelination.

Small-molecule targeting of CXCR2 has been shown to enhance the maturation of cultured oligodendrocyte progenitor cells (OPCs) to mature myelin-producing oligodendroglia (58). To better understand how tamoxifen-mediated targeting of *Cxcr2* within oligodendroglia

led to an increase in remyelination, we stained for NG2, a marker associated with OPCs, and GST-π, which is normally associated with mature myelin-producing oligodendrocytes in the spinal cords of experimental mice. There was a significant ($P < 0.01$) decrease in NG2-positive cells in the spinal cords of tamoxifen- treated mice compared to the vehicle controls (**Figure. 7A to C**). Conversely, we detected an increase in the numbers of GST-π-positive cells in tamoxifen-treated mice compared to the controls (**Figure. 7D to F**). These findings argue that targeted ablation of *Cxcr2* within oligodendrocytes increases the numbers of mature oligodendrocytes and that this correlates with a diminished pool of OPCs and, correspondingly, an increase in remyelination.

DISCUSSION

Chemokine signaling networks that are associated with chronic CNS diseases, such as MS, or persistent viral infections are thought to amplify disease severity by attracting targeted populations of leukocytes into the CNS (59). One chemokine pathway that is emerging as important in chronic CNS disease involves the CXCR2 receptor and its cognate ELR-positive chemokine ligands CXCL1, -2, and -3 and CXCL5, -6, -7, and -8. CXCR2 is highly expressed on circulating neutrophils, enabling these cells to rapidly migrate to the blood-brain barrier (BBB) in response to CNS-derived ELR-ligand expression, whereby these cells participate in degrading components of the BBB. Evidence for a proinflammatory role of neutrophils in chronic neurologic disease is supported by the work of Segal and colleagues (8), who have shown that genetic silencing or antibody- mediated blockade of CXCR2 in mice following PLP-induced EAE results in reduced clinical disease and relapses as a result of limiting BBB permeability. Within the context of acute viral infection of the CNS, we have previously reported that antibody-mediated neutralization of CXCR2 during JHMV infection enhances disease (54). This outcome was a result of reduced neutrophil and monocyte trafficking, as these cells are critical in permeabilizing the BBB, which subsequently allows the penetration of virus-specific T cells in the parenchyma to combat viral replication.

In addition to being expressed on circulating myeloid cells, CXCR2 is also expressed on neurons (45, 46), cerebral endothelial cells (60, 61), as well as resident glia, including microglia (45, 47) and oligodendrocytes (13, 14, 22, 25, 62, 63). Further, addition of IFN-γ to cultured OPCs derived from mouse neural progenitor cells results in apoptosis, while inclusion of the CXCL1 protein blocks OPC apoptotic death (14). CXCR2 also influences OPC proliferation and differentiation (21) as well as controls the migration of spinal cord OPCs during development

(22). Ablation of Cxcr2 results in a paucity of OPC numbers and structural misalignments that persist into adulthood in the mouse and manifest as reduced numbers of mature oligodendrocytes and total myelin within the white matter (23).

The functional role of CXCR2 signaling in mouse models of demyelination within the CNS is enigmatic. Some findings suggest that the CXCR2 signaling axis downregulates myelin production by oligodendrocytes (64), while we have reported that CXCR2 signaling is a survival mechanism for OPCs needed to halt the apoptosis induced by cytotoxic factors secreted during an inflammatory response (14, 37, 63, 65). With regards to CXCR2 signaling and survival, these studies were performed using either antibody targeting of CXCR2 or germ line Cxcr2-/- mice, and this opens the possibility of CXCR2 signaling on other cell types, either resident or immune cells, in augmenting experimental outcomes. Previously, members of our group (24) used bone marrow chimeric mice to partition the contribution of CXCR2 expression on either hematopoietic or CNS-derived cells. Adoptive transfer of hematopoietic cells derived from the bone marrow of *Cxcr2*$^{+/+}$ mice into *Cxcr2*$^{-/-}$ mice enabled the study of both EAE- and cuprizone-mediated demyelination and demonstrated increased oligodendrocyte differentiation in both models of demyelination, suggesting that CXCR2 may be an inhibitory signaling cue for myelin repair (24). CXCR2 antagonism via neutralizing antibodies enhanced oligodendrocyte differentiation and clinical recovery during EAE, further supporting a detrimental role for CXCR2 signaling within the CNS in mouse models of chronic inflammatory demyelinating disease (58). Conversely, inducible overproduction of CXCL1 by astrocytes reduced EAE clinical disease, although it was unclear whether increased levels of CXCL1 directly affected oligodendrocyte biology or modulated immune cell recruitment into the CNS (65). We have recently shown that induced expression of CXCL1 resulted in increased demyelination mediated

by neutrophils in both JHMV and EAE models of neurologic disease (18, 19). In addition, previous work from our laboratories employing antibody-mediated targeting of CXCR2 shows that blocking signaling in JHMV-infected mice increases the severity of demyelination, arguing for a protective role for CXCR2 in a model of virus-induced demyelination, as previously discussed (37). However, whether this is a direct effect of blocking CXCR2 signaling on oligodendroglia and/or other CNS resident cells is un- known. Given the various resident cell types within the CNS that express CXCR2 as well as inflammatory myeloid cells expressing CXCR2, it is difficult to accurately assign a specific role for CXCR2 in protecting spinal cord oligodendroglia from apoptosis using an antibody-mediated targeting approach. It may be possible that anti-CXCR2 treatment of JHMV-infected mice altered the signaling responses on other CXCR2-positive resident cells and/or infiltrating immune cells and that this contributed to the increased clinical disease severity associated with more severe demyelination and oligodendrocyte death.

Our present study used a more incisive genetic model to further our understanding of how CXCR2 signaling on oligodendrocytes affects neurologic disease in a preclinical animal model of MS. Using this genetic approach, our findings indicate that targeted deletion of *Cxcr2* occurs in oligodendrocytes both in vitro and in vivo. In addition, our previous work indicates that CXCR2 expression on neutrophils is important in host defense by allowing these cells to participate in increasing the permeability of the blood-brain barrier, allowing access of virus-specific T cells into the CNS to control virus replication. However, tamoxifen treatment did not diminish CXCR2 expression on neutrophils, as determined by flow cytometry. In addition, we have previously reported that antibody targeting of CXCR2 during acute JHMV-induced disease

limits neutrophil migration to the CNS, resulting in increased mortality correlating with impaired T cell access to CNS and increased viral titers (54).

Targeting of CXCR2 in *Cxcr2*-CKO mice was selective to oligodendroglia and did not affect myelin thickness in adult naive animals. These findings allowed us to move forward and assess how silencing of *Cxcr2* on oligodendrocytes influences neuroinflammation, demyelination, and remyelination in response to intracerebral inoculation with the neurotropic virus JHMV. Targeting of CXCR2 signaling on oligodendroglia did not dampen the accumulation of either myeloid cells or lymphocytes; the infiltration of virus-specific T cells was not affected, and this correlated with the ability to efficiently control viral replication within the CNS. We also determined that expression of proinflammatory genes within the CNS was not impacted in response to tamoxifen-mediated silencing of *Cxcr2* on oligodendrocytes, further supporting the notion that chemokine signaling through CXCR2 oligodendrocytes does not influence neuroinflammation. Sterile immunity is not acquired in JHMV-infected mice, and persistent virus is enriched within glial cells present within white matter tracts, resulting in an immune-mediated demyelinating disease mediated by activated T lymphocytes as well as microglia and macrophages (28). We did not detect differences in the severity of demyelination in tamoxifen-treated JHMV-infected *Cxcr2*-CKO mice from that in the controls, and these results are consistent with our findings that selective ablation of *Cxcr2* in oligodendrocytes does not impact neuroinflammation.

We observed increased numbers of mature GST-π oligodendrocytes along with reduced numbers of NG2-positive cells representing OPCs in the spinal cords of *Cxcr2*-CKO mice treated with tamoxifen compared to the vehicle-treated controls. Through EM analysis of the spinal cords of the experimental mice, we determined that an increase in the remyelination of

axons occurred following targeting of CXCR2 and that this correlated with an increased myelin thickness compared to that in control animals. Collectively, these findings support the concept that targeted ablation of CXCR2 on oligodendroglia in adult mice may enhance the maturation of OPCs into myelin-producing oligodendrocytes (25, 58).

Previously, members of our group (25) generated mice in which *Cxcr2* was selectively ablated in oligodendrocytes. Similar to the findings for the animals that we report here, *Cxcr2* was silenced within oligodendroglia in adult mice upon tamoxifen treatment (25). Employing toxin models of demyelination, the authors clearly showed enhanced remyelination in animals in which CXCR2 signaling in oligodendrocytes was inhibited, arguing for an important role for this chemokine receptor in influencing oligodendrocyte biology. Our findings would suggest that the influence of CXCR2 signaling on oligodendroglia is not model dependent, as remyelination is observed in both toxin and viral models of demyelination. Our findings are consistent with those of Kerstetter et al. (58), who showed that treatment of mice with MOG35–55-induced EAE with small-molecule antagonists specific for CXCR2 resulted in improved motor skills that correlated with diminished white matter damage associated with enhanced remyelination, arguing that CXCR2 may be a relevant therapeutic target for the treatment of demyelinating diseases. We would not argue with this conclusion but suggest that the small-molecule antagonists employed in this study may be targeting other cell types, e.g., resident glia and/or inflammatory cells, including neutrophils, resulting in improved clinical and histologic outcomes.

MATERIALS AND METHODS

Mice and tamoxifen treatment. *Plp-Cre-ER(T)::Cxcr2*$^{floc/floc}$ mice were crossed to mice of the reporter strain B6.Cg-Gt*(ROSA)26Sor*$^{tm9(CAG\text{-}tdTomato)Hze}$*/J* (stock number 007909; The Jackson Laboratory) to generate *Plp-Cre-ER(T)::Cxcr2*$^{floc/floc}$*::R26-stop-Td*$^{+/-}$ (*Cxcr2*-CKO) mice. Tamoxifen was prepared by resuspending it at 10 mg/ml in prewarmed sesame seed oil. Four-week-old *Cxcr2*-CKO mice received either 1 mg/ml tamoxifen or vehicle (control) twice daily for 5 days via intraperitoneal (i.p.) injection, rested for 2 weeks, and subsequently infected intracranially with JHMV (43, 44).

Viral infection. Age-matched 5- to 6-week-old *Cxcr2*-CKO mice were infected i.c. with 250 PFU of JHMV in 30 µl of sterile Hanks balanced salt solution (HBSS); sham-infected animals received 30 µl HBSS via i.c. injection (56, 66). For viral titer analysis, one half of each brain or whole spinal cord was homogenized and used in a plaque assay as previously described (19, 67). Clinical disease severity was assessed using a previously described scoring system (19, 67). All animal experiments were approved by the University of Utah Institutional Animal Care and Use Committee per protocol no.16-09008.

Primary oligodendrocyte cultures. Cortices from postnatal day 1 *Cxcr2*-CKO mice were dissected and processed according to previously published protocols (68). In brief, following removal of the meninges, cortical tissue was minced with a razor and placed in prewarmed Dulbecco modified Eagle medium (DMEM) containing papain in order to completely dissociate the tissue. Following further aspiration through a Pasteur pipette, single-cell suspensions were added to poly-D-lysine-coated culture flasks and grown for 9 days in DMEM supplemented with

10% fetal bovine serum. Th flasks were then transferred to an orbital shaker in a 5% CO2 tissue culture incubator and shaken for approximately 16 h at 220 rpm in order to remove loosely adherent oligodendroglia. Medium containing OPCs was transferred to 10-cm dishes for 30 min to remove strongly adherent astroglial contaminants. Oligodendroglia were transferred to a 1- ml conical tube and centrifuged at 300 X g for 5 min. The cells were counted and plated onto Matrigel-coated Nunc Lab-Tek II chamber slides (Thermo Fisher Scientific, Waltham, MA) at 50,000 OPCs per chamber in N2 medium supplemented with 3,3=,5-triiodo-L-thyronine sodium salt hydrate (T3; Sigma, St. Louis, MO). After 2 days, fresh medium supplemented with (Z)-4-hydroxytamoxifen (4-OHT; Sigma, St. Louis, MO) at 100 nM was used to induce Cre-mediated recombination. Cells were cultured for an additional 6 days.

Cell isolation and flow cytometry. Flow cytometry was performed to identify inflammatory cells entering the CNS using established protocols (67, 69). In brief, single-cell suspensions were generated from tissue samples by grinding with frosted microscope slides. Immune cells were enriched via a 2-step Percoll cushion (90% and 63%), and the cells at the interface of the two Percoll layers were collected. Before staining with fluorescent antibodies, isolated cells were incubated with anti-CD16/32 Fc block (BD Biosciences, San Jose, CA) at a 1:200 dilution. Immunophenotyping was performed using commercially available antibodies specific for the following cell surface markers: F4/80 (Serotec, Raleigh, NC), CD4, CD8, Ly6G, and CD11b (BD Biosciences, San Jose, CA), and Ly6C (eBioscience, San Diego, CA). The indicated flow cytometric gating strategies were employed for following inflammatory cells isolated from the CNS: neutrophils (CD45hi CD11b^{+} Ly6G^{+}), monocytes (CD45^{hi} CD11b^{+} Ly6C^{+} Ly6G^{-}), macrophages (CD45^{hi} CD11b^{+} F4/80^{+}), and microglia (CD45^{lo} CD11b^{+} F4/80^{lo}).

Allophycocyanin (APC)-conjugated rat anti- mouse CD4 and a phycoerythrin (PE)-conjugated tetramer specific for the CD4 immunodominant epitope present within the JHMV matrix (M) glycoprotein spanning amino acids 133 to 147 (the M133–147 tetramer) were used to determine total and virus-specific $CD4^+$ cells, respectively (19, 56); APC- conjugated rat anti-mouse CD8a and a PE-conjugated tetramer specific for the CD8 immunodominant epitope present in the spike (S) glycoprotein spanning amino acids 510 to 518 (S510 –518) were used to identify total and virus-specific $CD8^+$ cells, respectively (19, 56). Samples were analyzed using a BD LSR Fortessa X-20 flow cytometer and analyzed with FlowJo software (Tree Star Inc.).

PCR array and semiquantitative RT-qPCR. Proinflammatory gene expression was determined using a mouse cytokine and chemokine RT2 Profiler PCR array (Qiagen Inc., Valencia, CA), which included the following genes: chemokine genes *Ccl1, Ccl11, Ccl12, Ccl17, Ccl19, Ccl2, Ccl20, Ccl22, Ccl24, Ccl3, Ccl4, Ccl5, Ccl7, Cx3cl1, Cxcl1, Cxcl10, Cxcl11, Cxcl12, Cxcl13, Cxcl16, Cxcl3, Cxcl5, Cxcl9, Pf4, Ppbp,* and *Xcl1*; interleukin/ cytokine genes *Il10, Il11, Il12a, Il12b, Il13, Il15, Il16, Il17a, Il17f, Il18, Il1a, Il1b, Il1rn, Il2, Il21, Il22, Il23a, Il24, Il27, Il3, Il4, Il5, Il6, Il7, Il9, Adipoq (Acrp30), Ctf1, Hc, Mif, Spp1, Tgfb2, Ccl19, Il10, Il11, Il12a, Il12b, Il13, Il18, Il2, Il22, Il23a, Il24, Il4, Il6,* and *Tgfb2;* interferon genes *Ifna2* and *Ifng*; growth factor genes *Bmp2, Bmp4, Bmp6, Bmp7, Cntf, Csf1, Csf2, Csf3, Gpi1, Lif, Mstn, Nodal, Osm, Thpo*, and *Vegfa;* and TNF receptor superfamily member genes *Cd40lg, Cd70, Fasl, Lta, Ltb, Tnf, Tnfrsf11b, Tnfsf10, Tnfsf11,* and *Tnfsf13b*. For reverse transcription-quantitative PCR (RT-qPCR) analysis, total cDNA from the brains of JHMV-infected mice at day 7 p.i. was generated via SuperScript III reverse transcriptase (Life Technologies, Carlsbad, CA) after homogenization in the TRIzol reagent (Life Technologies, Carlsbad, CA).

Histology. Mice were euthanized at defined times points according to approved IACUC protocol no.16-09008, and the length of the spinal cord extending from thoracic vertebrae 6 to 10 was cryoprotected in 30% sucrose, cut into 1-mm transverse blocks, processed so as to preserve the craniocaudal orientation, and subsequently embedded in OCT (VWR, Radnor, PA, USA). Eight-micrometer-thick coronal sections were cut, sections were stained with hematoxylin/eosin (H&E) in combination with Luxol fast blue (LFB), and between 4 and 8 sections per mouse were analyzed. Areas of total white matter and demyelinated white matter were determined with ImageJ software, and demyelination was scored as the percentage of total demyelination from the spinal cord sections analyzed (55, 67, 70).

Quantitative immunocytochemistry. For cultured oligodendroglia, cells were fixed for 20 min in 4% paraformaldehyde before being blocked with species-appropriate serum. Cells were then stained with mouse anti-O1 (1:50 dilution; eBioscience, San Diego, CA) overnight at 4°C, followed by a secondary stain with fluorescently labeled secondary antibodies. Control sections were incubated with an appropriate secondary antibody in the absence of primary antibody. Cell morphology and the presence of nuclei were criteria for determining cells dual positive for tdTomato and O1. TdTomato red expression in O1-positive oligodendrocyte cultures was quantified by random selection of 10 imaging sections (X20 magnification) from three independently isolated oligodendrocyte-enriched cultures. The slides were deidentified and read independently by two investigators.

Quantitative immunohistochemistry. Spinal cords (ranging from thoracic vertebrae 6 to 10) were removed from experimental mice at defined times p.i. and processed as described above. For immunohistochemical analysis, 8-μm sections were desiccated at room temperature for 2 h before beginning the staining process. The slides were then washed in phosphate-buffered saline (PBS) and blocked with species-appropriate serum for 1 h at room temperature. Rabbit anti-GST-π (1:1,000 dilution; MBL Life Science, Woburn, MA), rabbit anti-Olig2 (1:500 dilution; Millipore Corp., Temecula, CA), rabbit anti-NG2 (1:200 dilution; Millipore Corp., Temecula, CA), mouse anti-MAP2 (1:200 dilution; Sigma-Aldrich, St. Louis, MO), and rabbit anti-IBA1 (1:500 dilution; Wako Chemicals, Inc., Richmond, VA) were used to stain the slides overnight at 4°C, the slides were subsequently washed in PBS, and appropriate secondary fluorescently conjugated antibodies were used for detection of targeted antigens. Control sections were incubated with appropriate secondary antibody in the absence of primary antibody. Quantitative analysis of NG2- and GST-π-positive cells was performed by analyzing spinal cords from *Cxcr2*-CKO mice treated with tamoxifen (n = 4) from two independent experiments and performed in a blind fashion, and the results were read by two investigators. Coronal spinal cord sections (ranging from 4 to 10 sections per mouse) were used to count cells positive for either NG2 or GST-π in each experimental group. Microscopy was performed on a Nikon A1 confocal laser microscope (University of Utah Cell Imaging Core Facility). To phenotype tdTomato-positive cells, spinal cords from tamoxifen-treated mice (n = 5) were used to detect cells dual positive for tdTomato and cellular markers for neurons (MAP2), macrophage/microglia (IBA1), or oligodendroglia (Olig2 and GST-TI). Coronal spinal cord sections (ranging from 2 to 5 sections per mouse) were used to count dual-positive cells.

EM. For electron microscopy (EM) analysis of spinal cords (ranging from thoracic vertebrae 6 to 10), experimental mice were sacrificed and underwent cardiac perfusion with 0.1 M cacodylate buffer containing 2% paraformaldehyde–2.5% glutaraldehyde. Serial ultrathin sections of spinal cords embedded in Epon epoxy resin were stained with uranyl acetate-lead citrate and analyzed as previously described (36, 55, 56, 71). Images at X1,200 magnification were analyzed for the *g* ratio and myelin sheath thickness. In adult animals, there is a relationship between axon circumference and total myelin sheath thickness (number of lamellae), expressed by the *g* ratio (axon diameter/total fiber diameter); in remyelination, this relationship changes such that myelin sheaths are abnormally thin for the axons that they surround (72). An abnormally thin myelin sheath relative to the axonal diameter was used as the criterion for oligodendrocyte remyelination. The absence of a myelin sheath was used as the criterion for demyelination. Analysis was performed in ventral and lateral white matter columns of spinal cords isolated from experimental mice. For vehicle-treated mice, a total of 297 axons were counted (n = 4 mice) from a total of 25 randomly selected fields, and for tamoxifen-treated mice, a total of 493 axons were counted (n = 5 mice) from a total of 34 randomly selected fields. EM images were analyzed using ImageJ software.

Statistics. For RT-qPCR quantification, the fold change in expression was determined by normalizing the expression of each sample to that of β-actin and then quantifying the fold change in expression relative to that in naive mice. A log-rank (Mantel-Cox) test was used for survival curve analysis. Comparisons of two groups were analyzed by two-tailed Student's t tests unless otherwise indicated. Data are reported as the mean ± standard error of the mean (SEM), with a P value of <0.05 being considered significant.

ACKNOWLEDGMENTS

T.E.L. was supported by funding from the National Institutes of Health (NIH; grant R01 NS041249), the National Multiple Sclerosis Society (NMSS) Collaborative Research Center (grant CA-1607-25040), The Ray and Tye Noorda Foundation, and The McCarthey Family Foundation. B.S.M. was supported by NIH training grant 5T3232A1007319. L.L.D. was supported by postdoctoral fellowship FG20105A1 from the NMSS. R.M.R. and L.L. were supported by NIHR grant R01-NS32151.

We gratefully acknowledge Thomas Fielder and the UC Irvine transgenic core facility for assistance in generating the transgenic animals used for these studies. We also thank Sarah Winn for excellent technical assistance.

We declare no competing financial interests.

REFERENCES

1. Steinman L. 2014. Immunology of relapse and remission in multiple sclerosis. Annu Rev Immunol 32:257–281. https://doi.org/10.1146/ annurev-immunol-032713-120227.

2. Holman DW, Klein RS, Ransohoff RM. 2011. The blood-brain barrier, chemokines and multiple sclerosis. Biochim Biophys Acta 1812:220 –230. https://doi.org/10.1016/j.bbadis.2010.07.019.

3. Engelhardt B, Ransohoff RM. 2012. Capture, crawl, cross: the T cell code to breach the blood-brain barriers. Trends Immunol 33:579 –589. https:// doi.org/10.1016/j.it.2012.07.004.

4. Izikson L, Klein RS, Charo IF, Weiner HL, Luster AD. 2000. Resistance to experimental autoimmune encephalomyelitis in mice lacking the Cc chemokine receptor (Ccr2). J Exp Med 192:1075–1080. https://doi.org/ 10.1084/jem.192.7.1075.

5. Ransohoff RM, Hamilton TA, Tani M, Stoler MH, Shick HE, Major JA, Estes ML, Thomas DM, Tuohy VK. 1993. Astrocyte expression of mRNA encod- ing cytokines IP-10 and JE/MCP-1 in experimental autoimmune en- cephalomyelitis. FASEB J 7:592– 600. https://doi.org/10.1096/fasebj.7.6.8472896.

6. Karpus WJ, Lukacs NW, McRae BL, Strieter RM, Kunkel SL, Miller SD. 1995. An important role for the chemokine macrophage inflammatory protein-1 alpha in the pathogenesis of the T cell-mediated autoimmune disease, experimental autoimmune encephalomyelitis. J Immunol 155:5003–5010.

7. Fife BT, Huffnagle GB, Kuziel WA, Karpus WJ. 2000. CC chemokine receptor 2 is critical for induction of experimental autoimmune encephalomyelitis. J Exp Med 192:899 –905. https://doi.org/10.1084/jem.192.6.899.

8. Carlson T, Kroenke M, Rao P, Lane TE, Segal B. 2008. The Th17-ELR+ CXC chemokine pathway is essential for the development of central nervous system autoimmune disease. J Exp Med 205:811– 823. https://doi.org/ 10.1084/jem.20072404.

9. Kleinewietfeld M, Puentes F, Borsellino G, Battistini L, Rotzschke O, Falk K. 2005. CCR6 expression defines regulatory effector/memory-like cells within the CD25+CD4+ T-cell subset. Blood 105:2877–2886. https://doi.org/10.1182/blood-2004-07-2505.

10. Reboldi A, Coisne C, Baumjohann D, Benvenuto F, Bottinelli D, Lira S, Uccelli A, Lanzavecchia A, Engelhardt B, Sallusto F. 2009. C-C chemokine receptor 6-regulated entry of TH-17 cells into the CNS through the choroid plexus is required for the initiation of EAE. Nat Immunol 10: 514 –523. https://doi.org/10.1038/ni.1716.

11. Horuk R. 2009. Chemokine receptor antagonists: overcoming developmental hurdles. Nat Rev Drug Discov 8:23–33. https://doi.org/10.1038/ nrd2734.

12. Witko-Sarsat V, Rieu P, Descamps-Latscha B, Lesavre P, Halbwachs- Mecarelli L. 2000.

Neutrophils: molecules, functions and pathophysiological aspects. Lab Invest 80:617– 653. https://doi.org/10.1038/labinvest.3780067.

13. Omari KM, John G, Lango R, Raine CS. 2006. Role for CXCR2 and CXCL1 on glia in multiple sclerosis. Glia 53:24 –31. https://doi.org/10.1002/glia.20246.

14. Tirotta E, Ransohoff RM, Lane TE. 2011. CXCR2 signaling protects oligodendrocyte progenitor cells from IFN-gamma/CXCL10-mediated apoptosis. Glia 59:1518 –1528. https://doi.org/10.1002/glia.21195.

15. Horuk R, Martin AW, Wang Z, Schweitzer L, Gerassimides A, Guo H, Lu Z, Hesselgesser J, Perez HD, Kim J, Parker J, Hadley TJ, Peiper SC. 1997. Expression of chemokine receptors by subsets of neurons in the central nervous system. J Immunol 158:2882–2890.

16. Flynn G, Maru S, Loughlin J, Romero IA, Male D. 2003. Regulation of chemokine receptor expression in human microglia and astrocytes. J Neuroimmune 136:84 –93. https://doi.org/10.1016/S0165-5728(03)00009-2.

17. Liu L, Li M, Spangler LC, Spear C, Veenstra M, Darnall L, Chang C, Cotleur AC, Ransohoff RM. 2013. Functional defect of peripheral neutrophils in mice with induced deletion of CXCR2. Genesis 51:587–595. https://doi.org/10.1002/dvg.22401.

18. Grist JJ, Marro BS, Skinner DD, Syage AR, Worne C, Doty DJ, Fujinami RS, Lane TE. 2018. Induced CNS expression of CXCL1 augments neurologic disease in a murine model of multiple sclerosis via enhanced neutrophil recruitment. Eur J Immunol 48:1199 –1210. https://doi.org/10.1002/eji.201747442.

19. Marro BS, Grist JJ, Lane TE. 2016. Inducible expression of CXCL1 within the central nervous system amplifies viral-induced demyelination. J Immunol 196:1855–1864. https://doi.org/10.4049/jimmunol.1501802.

20. Robinson S, Tani M, Strieter RM, Ransohoff RN, Miller RH. 1998. The chemokine growth-regulated oncogene-alpha promotes spinal cord oligodendrocyte precursor proliferation. J Neurosci 18:10457–10463. https://doi.org/10.1523/JNEUROSCI.18-24-10457.1998.

21. Filipovic R, Zecevic N. 2008. The effect of CXCL1 on human fetal oligodendrocyte progenitor cells. Glia 56:1–15. https://doi.org/10.1002/glia.20582.

22. Tsai HH, Frost E, To V, Robinson S, Ffrench-Constant C, Geertman R, Ransohoff RM, Miller RH. 2002. The chemokine receptor CXCR2 controls positioning of oligodendrocyte precursors in developing spinal cord by arresting their migration. Cell 110:373–383. https://doi.org/10.1016/ S0092-8674(02)00838-3.

23. Padovani-Claudio DA, Liu LP, Ransohoff RM, Miller RH. 2006. Alterations in the oligodendrocyte lineage, myelin, and white matter in adult mice lacking the chemokine receptor CXCR2. Glia 54:471– 483. https://doi.org/ 10.1002/glia.20383.

24. Liu L, Darnall L, Hu T, Choi K, Lane TE, Ransohoff RM. 2010. Myelin repair is accelerated by inactivating CXCR2 on nonhematopoietic cells. J Neu- rosci 30:9074 –9083. https://doi.org/10.1523/JNEUROSCI.1238-10.2010.

25. Liu L, Spangler LC, Prager B, Benson B, Hu B, Shi S, Love A, Zhang C, Yu M, Cotleur AC, Ransohoff RM. 2015. Spatiotemporal ablation of CXCR2 on oligodendrocyte lineage cells: role in myelin repair. Neurol Neuroimmunol Neuroinflamm 2: e174. https://doi.org/10.1212/NXI.0000000000000174.

26. Bergmann CC, Lane TE, Stohlman SA. 2006. Coronavirus infection of the central nervous system: host-virus stand-off. Nat Rev Microbiol 4:121–132. https://doi.org/10.1038/nrmicro1343.

27. Skinner D, Marro BS, Lane TE. 2018. Chemokine CXCL10 and coronavirus- induced neurologic disease. Viral Immunol 32:25–37. https://doi.org/10.1089/vim.2018.0073.

28. Hosking MP, Lane TE. 2009. The biology of persistent infection: inflammation and demyelination following murine coronavirus infection of the central nervous system. Curr Immunol Rev 5:267–276. https://doi.org/10.2174/157339509789504005.

29. Lane TE, Buchmeier MJ. 1997. Murine coronavirus infection: a paradigm for virus-induced demyelinating disease. Trends Microbiol 5:9 –14. https://doi.org/10.1016/S0966-842X(97)81768-4.

30. Glass WG, Chen BP, Liu MT, Lane TE. 2002. Mouse hepatitis virus infection of the central nervous system: chemokine-mediated regulation of host defense and disease. Viral Immunol 15:261–272. https://doi.org/10.1089/08828240260066215.

31. Glass WG, Lane TE. 2003. Functional analysis of the CC chemokine receptor 5 (CCR5) on virus-specific CD8+ T cells following coronavirus infection of the central nervous system. Virology 312:407– 414. https:// doi.org/10.1016/S0042-6822(03)00237-X.

32. Glass WG, Liu MT, Kuziel WA, Lane TE. 2001. Reduced macrophage infiltration and demyelination in mice lacking the chemokine receptor CCR5 following infection with a neurotropic coronavirus. Virology 288: 8 –17. https://doi.org/10.1006/viro.2001.1050.

33. Held KS, Chen BP, Kuziel WA, Rollins BJ, Lane TE. 2004. Differential roles of CCL2 and CCR2 in host defense to coronavirus infection. Virology 329:251–260. https://doi.org/10.1016/j.virol.2004.09.006.

34. Hosking MP, Lane TE. 2010. The role of chemokines during viral infection of the CNS. PLoS Pathog 6: e1000937. https://doi.org/10.1371/journal.ppat.1000937.

35. Liu MT, Chen BP, Oertel P, Buchmeier MJ, Armstrong D, Hamilton TA, Lane TE. 2000. The T cell chemoattractant IFN-inducible protein 10 is essential in host defense against viral-

induced neurologic disease. J Immunol 165:2327–2330. https://doi.org/10.4049/jimmunol.165.5.2327.

36. Liu MT, Keirstead HS, Lane TE. 2001. Neutralization of the chemokine CXCL10 reduces inflammatory cell invasion and demyelination and im- proves neurological function in a viral model of multiple sclerosis. J Immunol 167:4091– 4097. https://doi.org/10.4049/jimmunol.167.7.4091.

37. Hosking MP, Tirotta E, Ransohoff RM, Lane TE. 2010. CXCR2 signaling protects oligodendrocytes and restricts demyelination in a mouse model of viral-induced demyelination. PLoS One 5: e11340. https://doi.org/10.1371/journal.pone.0011340.

38. Feil R, Brocard J, Mascrez B, LeMeur M, Metzger D, Chambon P. 1996. Ligand-activated site-specific recombination in mice. Proc Natl Acad Sci U S A 93:10887–10890. https://doi.org/10.1073/pnas.93.20.10887.

39. Feil R, Wagner J, Metzger D, Chambon P. 1997. Regulation of Cre recombinase activity by mutated estrogen receptor ligand-binding do-mains. Biochem Biophys Res Commun 237:752–757. https://doi.org/10.1006/bbrc.1997.7124.

40. Metzger D, Clifford J, Chiba H, Chambon P. 1995. Conditional site- specific recombination in mammalian cells using a ligand-dependent chimeric Cre recombinase. Proc Natl Acad Sci U S A 92:6991– 6995. https://doi.org/10.1073/pnas.92.15.6991.

41. Zhang Y, Riesterer C, Ayrall AM, Sablitzky F, Littlewood TD, Reth M. 1996. Inducible site-directed recombination in mouse embryonic stem cells. Nucleic Acids Res 24:543–548. https://doi.org/10.1093/nar/24.4.543.

42. distinguishes two populations of NG2-positive cells throughout neonatal cortical development. J Neurosci 22:876 – 885. https://doi.org/ 10.1523/JNEUROSCI.22-03-00876.2002.

43. Feil S, Valtcheva N, Feil R. 2009. Inducible Cre mice. Methods Mol Biol 530:343–363. https://doi.org/10.1007/978-1-59745-471-1_18.

44. Leone DP, Genoud S, Atanasoski S, Grausenburger R, Berger P, Metzger D, Macklin WB, Chambon P, Suter U. 2003. Tamoxifen-inducible glia- specific Cre mice for somatic mutagenesis in oligodendrocytes and Schwann cells. Mol Cell Neurosci 22:430 – 440. https://doi.org/10.1016/ S1044-7431(03)00029-0.

45. Lin YF, Liu TT, Hu CH, Chen CC, Wang JY. 2018. Expressions of chemokines and their receptors in the brain after heat stroke-induced cortical damage. J Neuroimmunol 318:15–20. https://doi.org/10.1016/j.jneuroim.2018.01.014.

46. Xu J, Zhu MD, Zhang X, Tian H, Zhang JH, Wu XB, Gao YJ. 2014. NFkappaB-mediated CXCL1 production in spinal cord astrocytes contributes to the maintenance of bone cancer

pain in mice. J Neuroinflammation 11:38. https://doi.org/10.1186/1742-2094-11-38.

47. Ryu JK, Cho T, Choi HB, Jantaratnotai N, McLarnon JG. 2015. Pharmaco- logical antagonism of interleukin-8 receptor CXCR2 inhibits inflammatory reactivity and is neuroprotective in an animal model of Alzheimer's disease. J Neuroinflammation 12:144. https://doi.org/10.1186/s12974-015-0339-z.

48. Zhang Y, Chen K, Sloan SA, Bennett ML, Scholze AR, O'Keeffe S, Phatnani HP, Guarnieri P, Caneda C, Ruderisch N, Deng S, Liddelow SA, Zhang C, Daneman R, Maniatis T, Barres BA, Wu JQ. 2014. An RNA-sequencing transcriptome and splicing database of glia, neurons, and vascular cells of the cerebral cortex. J Neurosci 34:11929 –11947. https://doi.org/10.1523/JNEUROSCI.1860-14.2014.

49. Zhang Y, Sloan SA, Clarke LE, Caneda C, Plaza CA, Blumenthal PD, Vogel H, Steinberg GK, Edwards MSB, Li G, Duncan JA, III, Cheshier SH, Shuer LM, Chang EF, Grant GA, Gephart MGH, Barres BS. 2016. Purification and characterization of progenitor and mature human astrocytes reveals transcriptional and functional differences with mouse. Neuron 89:37–53. https://doi.org/10.1016/j.neuron.2015.11.013.

50. Ehrlich M, Mozafari S, Glatza M, Starost L, Velychko S, Hallmann AL, Cui QL, Schambach A, Kim KP, Bachelin C, Marteyn A, Hargus G, Johnson RM, Antel J, Sterneckert J, Zaehres H, Scholer HR, Baron-Van Evercooren A, Kuhlmann T. 2017. Rapid and efficient generation of oligodendrocytes from human induced pluripotent stem cells using transcription factors. Proc Natl Acad Sci U S A 114: E2243–E2252. https://doi.org/10.1073/pnas.1614412114.

51. Mitew S, Hay CM, Peckham H, Xiao J, Koenning M, Emery B. 2014. Mechanisms regulating the development of oligodendrocytes and central nervous system myelin. Neuroscience 276:29 – 47. https://doi.org/10.1016/j.neuroscience.2013.11.029.

52. Doerflinger NH, Macklin WB, Popko B. 2003. Inducible site-specific re- combination in myelinating cells. Genesis 35:63–72. https://doi.org/10.1002/gene.10154.

53. Tansey FA, Cammer W. 1991. A pi form of glutathione-S-transferase is a myelin- and oligodendrocyte-associated enzyme in mouse brain. J Neurochem 57:95–102. https://doi.org/10.1111/j.1471-4159.1991.tb02104.x.

54. Hosking MP, Liu L, Ransohoff RM, Lane TE. 2009. A protective role for ELR+ chemokines during acute viral encephalomyelitis. PLoS Pathog 5: e1000648. https://doi.org/10.1371/journal.ppat.1000648.

55. Blanc CA, Grist JJ, Rosen H, Sears-Kraxberger I, Steward O, Lane TE. 2015. Sphingosine-1-phosphate receptor antagonism enhances proliferation and migration of engrafted neural progenitor cells in a model of viral- induced demyelination. Am J Pathol 185:2819 –2832. https://doi.org/10.1016/j.ajpath.2015.06.009.

56. Chen L, Coleman R, Leang R, Tran H, Kopf A, Walsh CM, Sears-Kraxberger I, Steward O,

Macklin WB, Loring JF, Lane TE. 2014. Human neural precursor cells promote neurologic recovery in a viral model of multiple sclerosis. Stem Cell Rep 2:825– 837. https://doi.org/10.1016/j.stemcr.2014.04.005.

57. Mei F, Lehmann-Horn K, Shen Y-A, Rankin KA, Stebbins KJ, Lorrain DS, Pekarek K, Sagan SA, Xiao L, Teuscher C, von Budingen HC, Wess J, Lawrence JJ, Green AJ, Fancy SP, Zamvil SS, Chan JR. 2016. Accelerated remyelination during inflammatory demyelination prevents axonal loss and improves functional recovery. Elife 5: e18246. https://doi.org/10.7554/eLife.18246.

58. Kerstetter AE, Padovani-Claudio DA, Bai L, Miller RH. 2009. Inhibition of CXCR2 signaling promotes recovery in models of multiple sclerosis. Exp Neurol 220:44 –56. https://doi.org/10.1016/j.expneurol.2009.07.010.

59. Charo IF, Ransohoff RM. 2006. The many roles of chemokines and chemokine receptors in inflammation. N Engl J Med 354:610 – 621. https://doi.org/10.1056/NEJMra052723.

60. Wu F, Zhao Y, Jiao T, Shi D, Zhu X, Zhang M, Shi M, Zhou H. 2015. CXCR2 is essential for cerebral endothelial activation and leukocyte recruitment during neuroinflammation. J Neuroinflammation 12:98. https://doi.org/ 10.1186/s12974-015-0316-6.

61. Zhang R, Zhang Z, Wang L, Wang Y, Gousev A, Zhang L, Ho KL, Morshead C, Chopp M. 2004. Activated neural stem cells contribute to stroke- induced neurogenesis and neuroblast migration toward the infarct boundary in adult rats. J Cereb Blood Flow Metab 24:441– 448. https:// doi.org/10.1097/00004647-200404000-00009.

62. Omari KM, John GR, Sealfon SC, Raine CS. 2005. CXC chemokine receptors on human oligodendrocytes: implications for multiple sclerosis. Brain 128:1003–1015. https://doi.org/10.1093/brain/awh479.

63. Tirotta E, Kirby LA, Hatch MN, Lane TE. 2012. IFN-gamma-induced apoptosis of human embryonic stem cell derived oligodendrocyte progenitor cells is restricted by CXCR2 signaling. Stem Cell Res 9:208 –217. https:// doi.org/10.1016/j.scr.2012.06.005.

64. Liu L, Belkadi A, Darnall L, Hu T, Drescher C, Cotleur AC, Padovani- Claudio D, He T, Choi K, Lane TE, Miller RH, Ransohoff RM. 2010. CXCR2-positive neutrophils are essential for cuprizone-induced demyelination: relevance to multiple sclerosis. Nat Neurosci 13:319 –326. https://doi.org/10.1038/nn.2491.

65. Omari KM, Lutz SE, Santambrogio L, Lira SA, Raine CS. 2009. Neuroprotection and remyelination after autoimmune demyelination in mice that inducibly overexpress CXCL1. Am J Pathol 174:164 –176. https://doi.org/ 10.2353/ajpath.2009.080350.

66. Carbajal KS, Schaumburg C, Strieter R, Kane J, Lane TE. 2010. Migration of engrafted neural stem cells is mediated by CXCL12 signaling through CXCR4 in a viral model of multiple sclerosis. Proc Natl Acad Sci U S A 107:11068 –11073.

https://doi.org/10.1073/pnas.1006375107.

67. Blanc CA, Rosen H, Lane TE. 2014. FTY720 (fingolimod) modulates the severity of viral-induced encephalomyelitis and demyelination. J Neuro- inflammation 11:138. https://doi.org/10.1186/s12974-014-0138-y.

68. O'Meara RW, Ryan SD, Colognato H, Kothary R. 2011. Derivation of enriched oligodendrocyte cultures and oligodendrocyte/neuron myelinating co-cultures from post-natal murine tissues. J Vis Exp 2011:3324. https://doi.org/10.3791/3324.

69. Lane TE, Liu MT, Chen BP, Asensio VC, Samawi RM, Paoletti AD, Campbell IL, Kunkel SL, Fox HS, Buchmeier MJ. 2000. A central role for CD4(+) T cells and RANTES in virus-induced central nervous system inflammation and demyelination. J Virol 74:1415–1424. https://doi.org/10.1128/jvi.74.3.1415-1424.2000.

70. Dickey LL, Worne CL, Glover JL, Lane TE, O'Connell RM. 2016. MicroRNA- 155 enhances T cell trafficking and antiviral effector function in a model of coronavirus-induced neurologic disease. J Neuroinflammation 13:240. https://doi.org/10.1186/s12974-016-0699-z.

71. Totoiu MO, Nistor GI, Lane TE, Keirstead HS. 2004. Remyelination, axonal sparing, and locomotor recovery following transplantation of glial- committed progenitor cells into the MHV model of multiple sclerosis. Exp Neurol 187:254 –265. https://doi.org/10.1016/j.expneurol.2004.01.028.

72. Smith KJ, Bostock H, Hall SM. 1982. Saltatory conduction precedes remyelination in axons demyelinated with lysophosphatidyl choline. J Neurol Sci 54:13–31. https://doi.org/10.1016/0022-510X(82)90215-5.

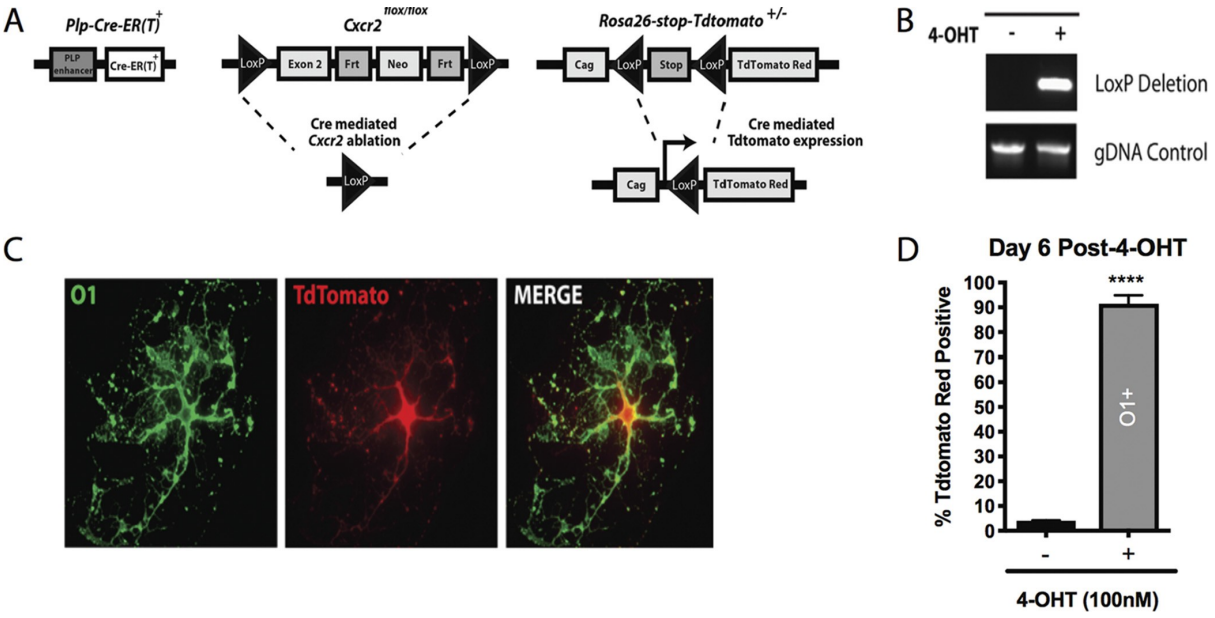

Figure 1 Cre-mediated recombination is detected *in vitro*. (A) Schematic diagram showing the genetic strategy used to generate tamoxifen-inducible knockout of *Cxcr2* within oligodendroglia. (B) Cre-mediated recombination at the *Cxcr2* locus was detected by PCR from oligodendroglia-enriched cultures derived from postnatal day 1 (P1) *Cxcr2*-CKO mice following addition of 100 nM (*Z*)-4-hydroxytamoxifen (4-OHT). gDNA, genomic DNA. (C) Representative immunofluorescent staining for O1 (a marker for mature oligodendrocytes) from cultured oligodendroglia following 6 days of treatment with 4-OHT, showing a morphology characteristic of mature oligodendrocytes and colocalization of O1 (green) and tdTomato red. (D) Treatment of cultured oligodendroglia with 4-OHT resulted in expression of tdTomato in >90% of O1-positive oligodendrocytes (****, $P < 0.0001$; 91.4% ± 2.02%) derived from P1 *Cxcr2*-CKO mice, in contrast to vehicle treatment (3.92% ± 0.14%); data are presented as the average + SEM and represent those from 3 independent experiments

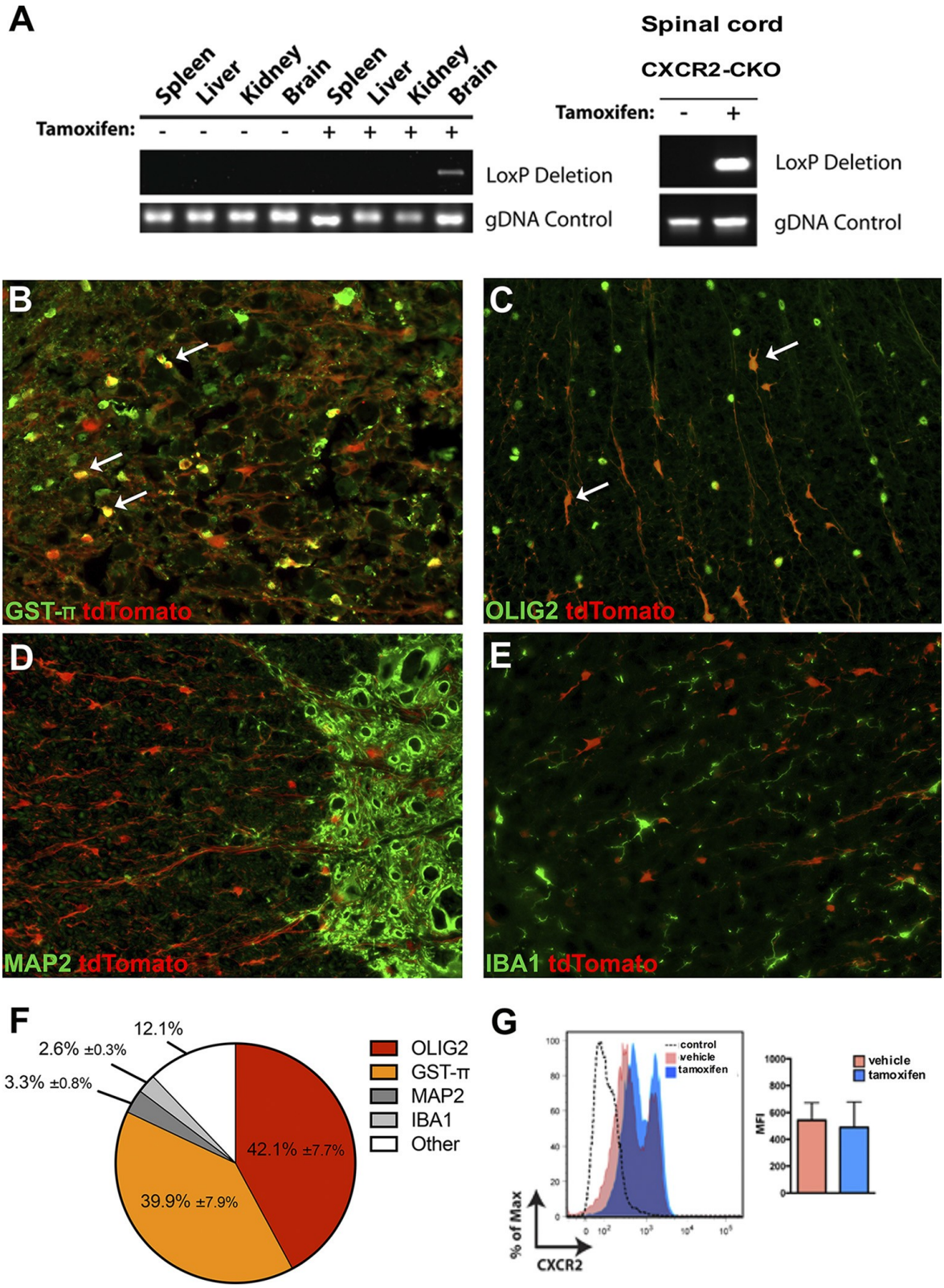
A
Spleen
Liver
Kidney
Brain
Spleen
Liver
Kidney
Brain
Tamoxifen: - - - - + + + +
LoxP Deletion
gDNA Control
Spinal cord
CXCR2-CKO
Tamoxifen: - +
LoxP Deletion
gDNA Control
B
GST-π tdTomato
C
OLIG2 tdTomato
D
MAP2 tdTomato
E
IBA1 tdTomato
F
12.1%
2.6% ±0.3%
3.3% ±0.8%
42.1% ±7.7%
39.9% ±7.9%
OLIG2
GST-π
MAP2
IBA1
Other
G
control
vehicle
tamoxifen
% of Max
CXCR2
MFI
vehicle
tamoxifen

Figure 2 *Cxcr2* is ablated in vivo following tamoxifen treatment. (A) Detection of Cre-mediated recombination at the *Cxcr2* locus in the brain and spinal cord of *Cxcr2*-CKO mice 2 weeks following tamoxifen treatment. (B to E) Phenotyping of tdTomato-positive cells was performed via immunofluorescent staining for defined cell-specific markers. Representative staining of spinal cords from tamoxifen-treated (n = 5) *Cxcr2*-CKO mice for oligodendroglia via GST-π (B), Olig2 (C), neurons (MAP2) (D), and macrophage/microglia (IBA1) (E). Magnifications, X20. Arrows in panels B and C represent dual-positive cells. (F) Quantification of dual-positive cells in the spinal cords of tamoxifen-treated mice; the data were derived from 2 independent experiments, with the data presented as the average ± SEM. (G) The surface expression of CXCR2 on neutrophils was not affected in tamoxifen-treated *Cxcr2*-CKO mice (n = 2), in contrast to the vehicle- treated controls (n = 2); the data are presented as the average ± SEM. MFI, mean fluorescence intensity.

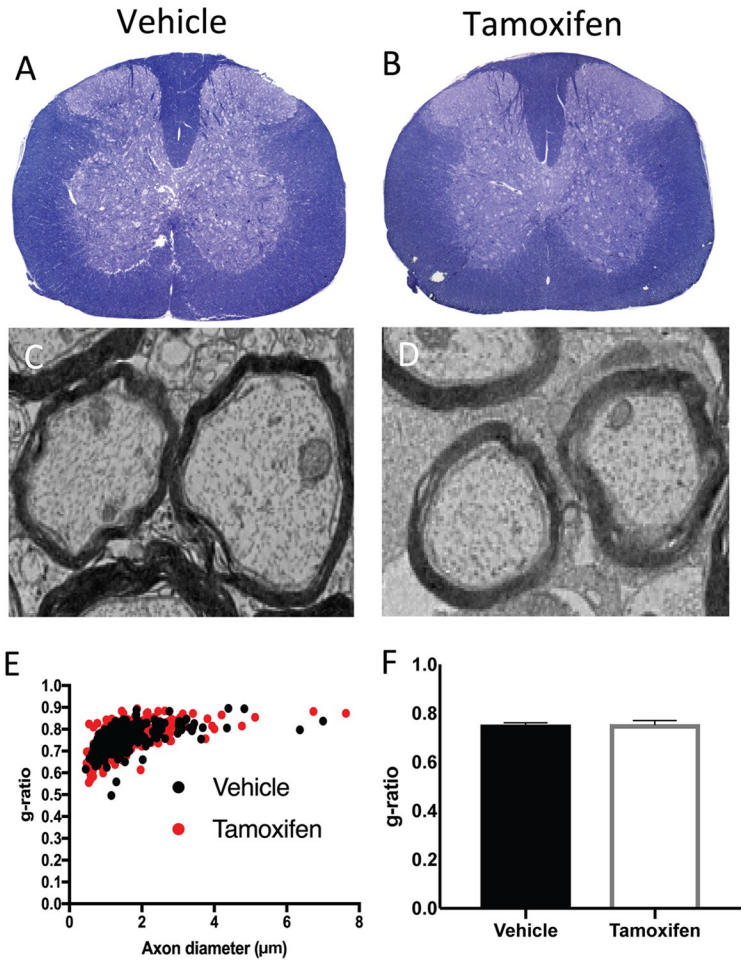

Figure 3 Myelin integrity and ultrastructure are not affected following tamoxifen-treatment of naive *Cxcr2*-CKO mice. *Cxcr2*-CKO mice were treated with either vehicle or tamoxifen for 1 week and sacrificed 2 weeks later to evaluate myelin integrity. (A and B) Representative spinal cord semithin sections stained with toluidine blue demonstrate no visible differences in myelin between vehicle-treated (A) and tamoxifen-treated (B) mice. (C and D) Representative EM images showing myelinated axons within the spinal cords of vehicle-treated (C) and tamoxifen-treated (D) *Cxcr2*-CKO mice. Analysis was performed in the ventral and lateral white matter tracts. Magnifications, X1,200. (E) Scatter plot depicting the g ratios of individual axons as a function of the axonal diameter. (F) Calculation of the *g* ratios of vehicle-treated (n = 3, 0.75 ± 0.004, 222 axons) and tamoxifen- treated (n = 3, 0.75 ± 0.004, 298 axons) *Cxcr2*-CKO mice. The data were derived from two independent experiments with 2 to 4 mice per group and are presented as the mean ± SEM.

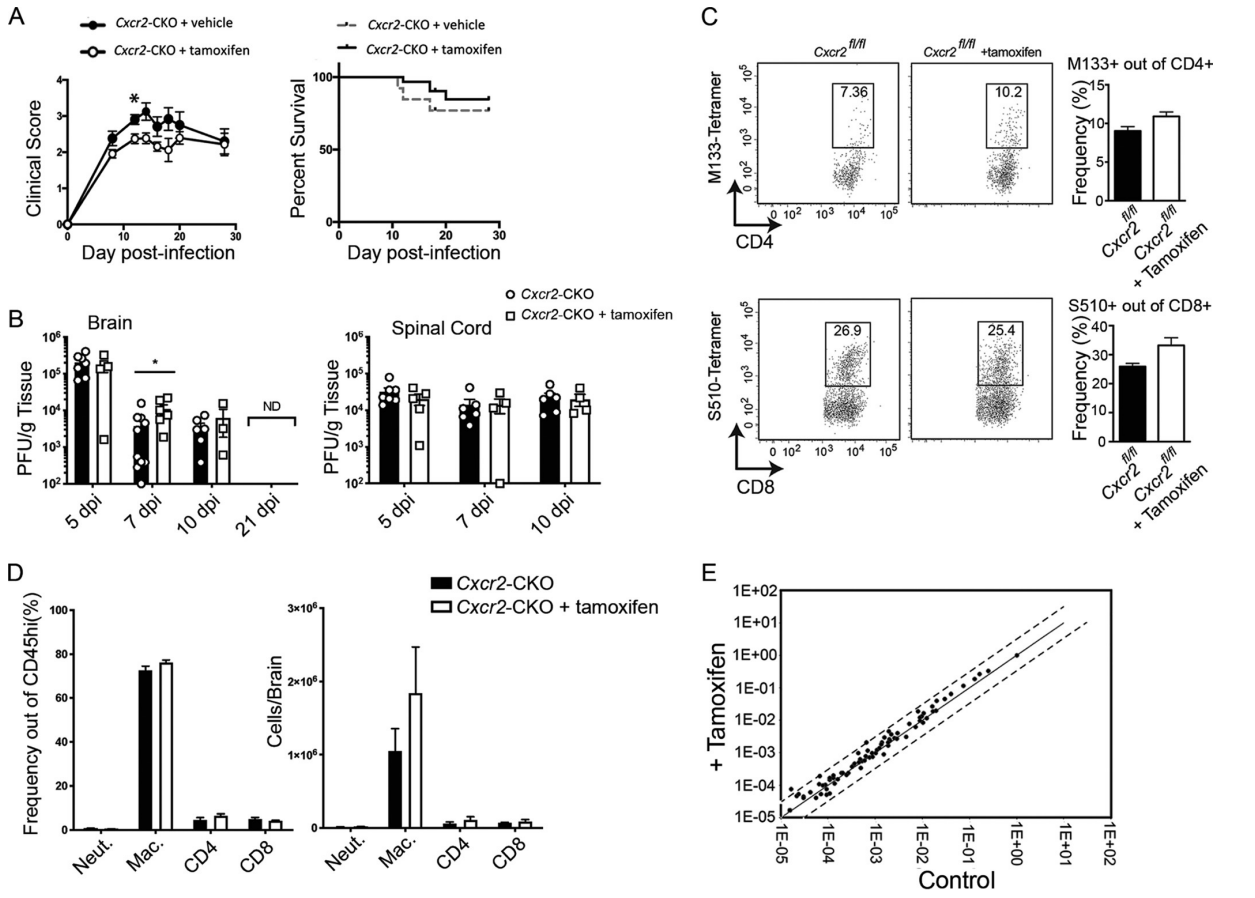

Figure 4 Tamoxifen-treated *Cxcr2*-CKO mice are susceptible to JHMV-induced neuroinflammation. *Cxcr2*-CKO mice were treated with either tamoxifen (n = 22) or vehicle (n = 10), rested for 2 weeks, and infected i.c. with 250 PFU of JHMV. The data are representative of those from 3 independent experiments. (A) Clinical disease developed in both groups, and vehicle-treated Cxcr2-CKO mice had worse ($P < 0.05$) disease at 12 days p.i. than control mice, but otherwise, there were no statistically significant differences in disease severity or mortality out to day 28 p.i. between the experimental groups. (B) Viral titers in the brains and spinal cords of tamoxifen- and vehicle-treated mice at days 5, 7, and 10 p.i. *, $P < 0.05$. By day 21 p.i., virus was not detected (ND) in the brains of experimental mice. dpi, day post infection. (C) No differences in the frequencies of virus-specific $CD4^+$ and $CD8^+$ T cells were detected, as determined by tetramer staining at day 7 p.i. (D) At day 7 p.i., similar numbers of neutrophils (Neut.), macrophages (Mac.), and T cells were detected in the brains of JHMV-infected *Cxcr2*-CKO mice treated with either vehicle or tamoxifen. Day 7 p.i. flow cytometric data were derived from 2 independent experiments with a minimum of 3 mice per group for each experiment. (E) RNA analysis revealed no changes in proinflammatory gene expression within the brains of the experimental groups at day 7 p.i. The data represent the average for 2 mice per group

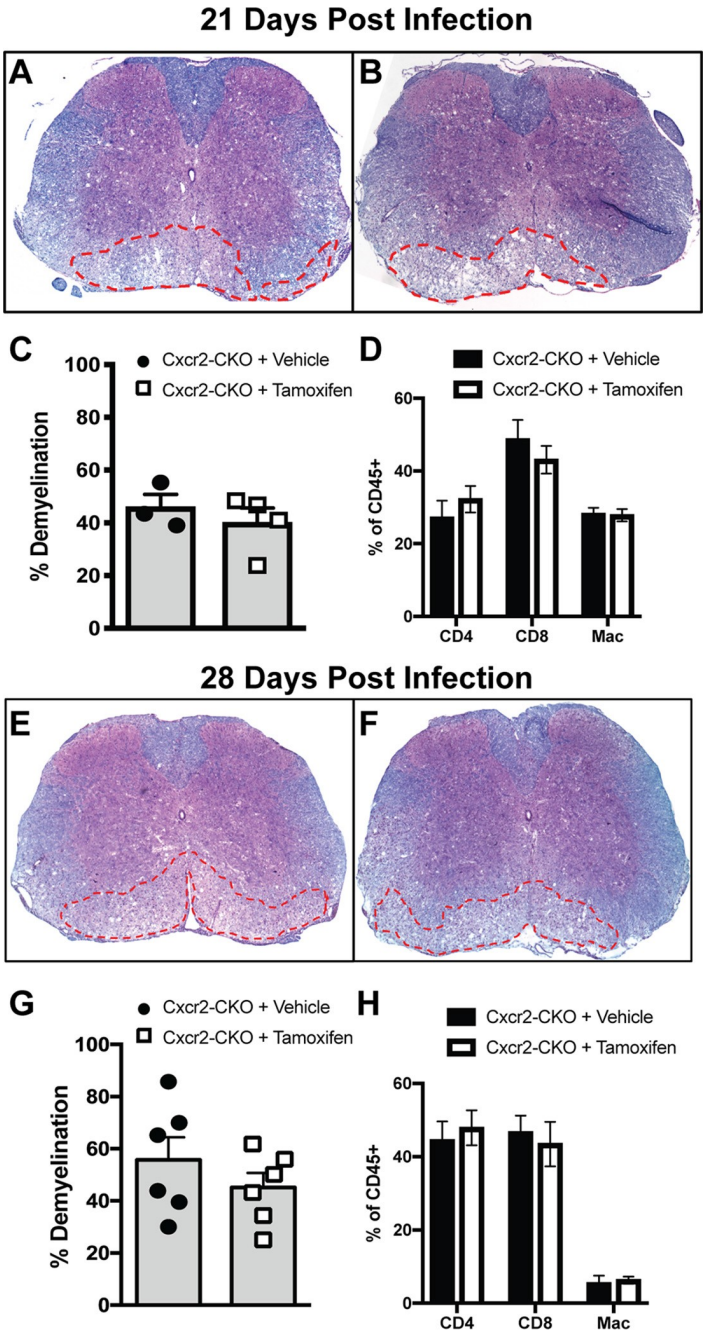

Figure 5 Demyelination is not affected following *Cxcr2* ablation. JHMV-infected *Cxcr2*-CKO mice were treated with vehicle or tamoxifen and sacrificed at days 21 and 28 p.i., and spinal cords were removed to assess the severity of demyelination. Representative spinal cords from either vehicle-treated (A, E) or tamoxifen-treated (B, F) mice were collected at day 21 p.i. (A and B) or day 28 p.i. (E and F) and stained with Luxol fast blue (LFB). Quantification of the severity of demyelination revealed no differences at either day 21 p.i. (C) or day 28 p.i. (G). Flow cytometric data revealed no differences in spinal cord infiltration of T cells ($CD4^+$ and $CD8^+$ subsets) or macrophages ($CD45^{hi}$ $F4/80^+$) at either day 21 p.i. (D) or day 28 p.i. (H). The data were derived from two independent experiments with 2 to 3 mice per group and are presented as the mean ± SEM

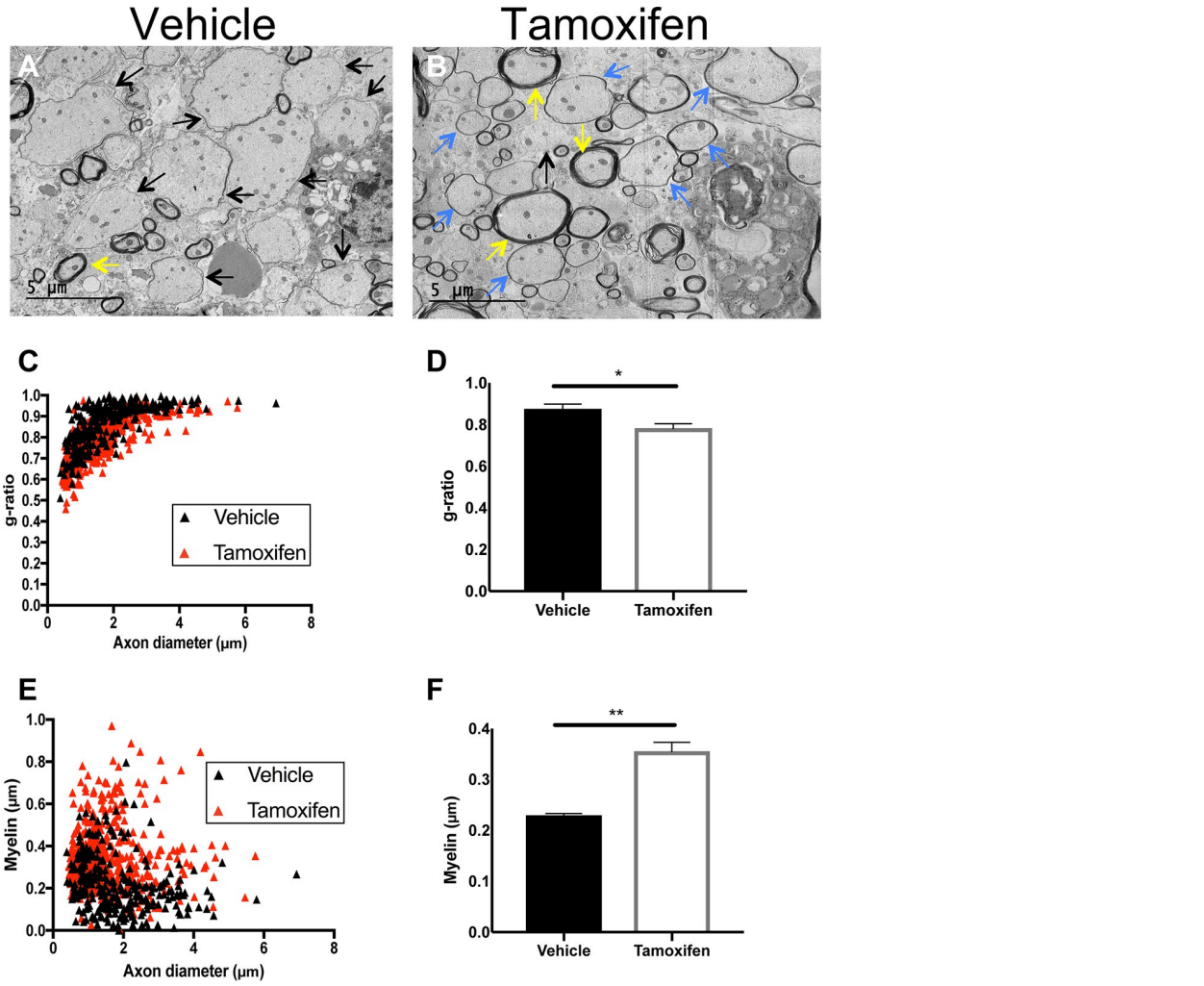

Figure 6 Remyelination is increased following *Cxcr2* ablation in oligodendroglia. Spinal cords were removed at day 28 p.i. from JHMV-infected mice treated with either vehicle control or tamoxifen. (A and B) Representative EM images from vehicle-treated mice depict demyelinated axons (black arrows) (A), whereas in tamoxifen-treated mice, remyelinated axons (blue arrows) were present (B). Normal myelinated axons (yellow arrows) are also shown. Magnifications, X1,200. Analysis was performed in ventral and lateral white matter columns of spinal cords isolated from experimental mice. (C) Scatter plot depicting the g ratios of individual axons from vehicle- and tamoxifen-treated mice as a function of axonal diameter. (D) Calculation of the *g* ratio of vehicle-treated *Cxcr2*-CKO mice (0.87 ± 0.006, n = 4 mice; 297 axons randomly selected from a total of 25 fields) and tamoxifen-treated *Cxcr2*-CKO mice (0.78 ± 0.006, n = 5 mice; 493 axons randomly selected from a total of 34 fields) indicates a significant ($P < 0.05$) reduction in the g ratios in tamoxifen-treated mice compared to the vehicle-treated controls. (E) Scatter plot depicting the myelin thickness of individual axons from vehicle- and tamoxifen-treated mice as a function of axon diameter. (F) Quantification of myelin thickness in vehicle-treated mice (0.23 µm ± 0.008 µm) and tamoxifen-treated mice (0.35 µm ± 0.007 µm) indicated a significant ($P < 0.01$) increase in myelin thickness in tamoxifen-treated mice compared to the vehicle-treated controls. The results are derived from two independent experiments, and the data in panels D and F are presented as the mean ± SEM.

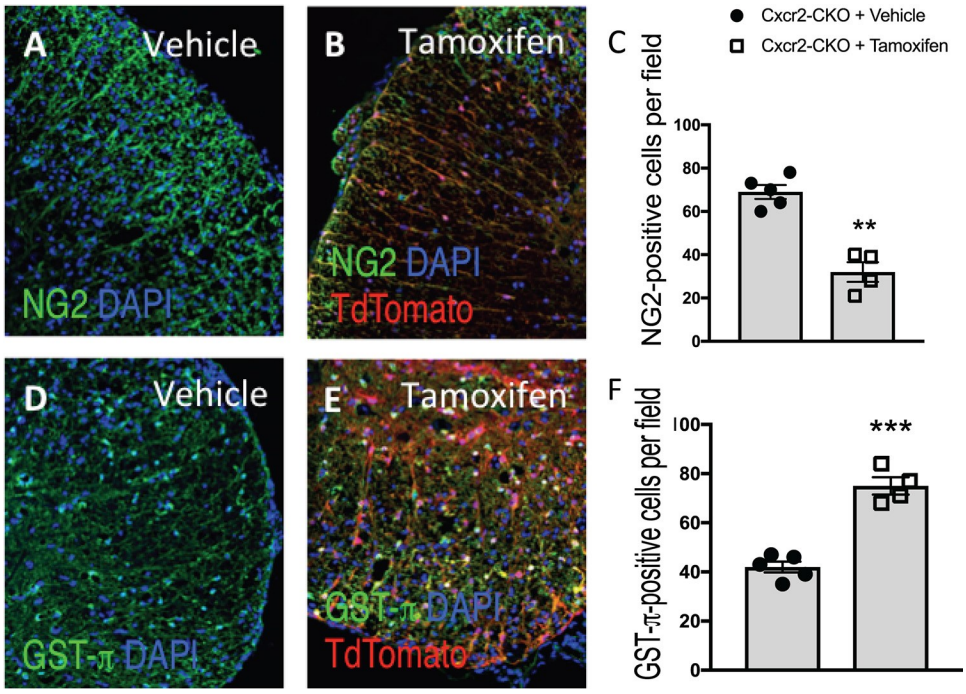

Figure 7 *Cxcr2* ablation increases the numbers of mature oligodendrocytes in JHMV-infected mice. JHMV-infected *Cxcr2*-CKO mice were treated with vehicle or tamoxifen, and at day 28 p.i. the animals were sacrificed and the spinal cords were removed. Representative NG2 (A, B) and GST-π (D, E) staining in control ($n = 5$) and tamoxifen-treated ($n = 4$) mice is shown. Quantification reveals reduced numbers of NG2-positive cells in tamoxifen-treated mice (C) and increased numbers of dual-positive GST-π-positive cells in tamoxifen-treated mice (F) compared to vehicle- treated mice. Data represent those from 2 independent experiments, and significance was measured using an unpaired 2-tailed Student's *t* test. **, $P < 0.01$; ***, $P < 0.001$. DAPI, 4=,6-diamidino-2-phenylindole.

Chapter 3

MICROGLIA INFLUENCE HOST DEFENSE, DISEASE, AND REPAIR FOLLOWING MURINE CORONAVIRUS INFECTION OF THE CENTRAL NERVOUS SYSTEM

Microglia influence host defense, disease, and repair following murine coronavirus infection of the central nervous system

Vrushali Mangale[1] Amber R. Syage[2] H. Atakan Ekiz[1] Dominic D. Skinner[1] Yuting Cheng[2] Colleen L. Stone[1] R. Marshall Brown[1] Ryan M. O'Connell[1] Kim N. Green[2] Thomas E. Lane[2]

[1]Division of Microbiology & Immunology, Department of Pathology, University of Utah School of Medicine, Salt Lake City, Utah

[2]Department of Neurobiology & Behavior, School of Biological Sciences, University of California, Irvine, California

Correspondence

Thomas E. Lane, Department of Neurobiology & Behavior, 2205 McGaugh Hall, University of California, Irvine, CA 92697. Email: tlane@uci.edu

Funding information

National Institute of Neurological Disorders and Stroke, Grant/Award Numbers: R01NS041249, R01NS091939; National Institutes of Health, Grant/Award Number: R01AG047956; National Multiple Sclerosis Society, Grant/Award Number: CA-1607-25040

Vrushali Mangale, Amber R. Syage, and H. Atakan Ekiz equally contributed to this work

ABSTRACT

The present study examines functional contributions of microglia in host defense, demyelination, and remyelination following infection of susceptible mice with a neurotropic coronavirus. Treatment with PLX5622, an inhibitor of colony stimulating factor 1 receptor (CSF1R) that efficiently depletes microglia, prior to infection of the central nervous system (CNS) with the neurotropic JHM strain of mouse hepatitis virus (JHMV) resulted in increased mortality compared with control mice that correlated with impaired control of viral replication. Single cell RNA sequencing (scRNASeq) of CD45+ cells isolated from the CNS revealed that PLX5622 treatment resulted in muted CD4+ T cell activation profile that was associated with decreased expression of transcripts encoding MHC class II and CD86 in macrophages but not dendritic cells. Evaluation of spinal cord demyelination revealed a marked increase in white matter damage in PLX5622-treated mice that corresponded with elevated expression of transcripts encoding disease-associated proteins Osteopontin (*Spp1*), Apolipoprotein E (*Apoe*), and Triggering receptor expressed on myeloid cells 2 (Trem2) that were enriched within macrophages. In addition, PLX5622 treatment dampened expression of Cystatin F (*Cst7*), Insulin growth factor 1 (*Igf1*), and lipoprotein lipase (*Lpl*) within macrophage populations which have been implicated in promoting repair of damaged nerve tissue and this was associated with impaired remyelination. Collectively, these findings argue that microglia tailor the CNS microenvironment to enhance control of coronavirus replication as well as dampen the severity of demyelination and influence repair.

Main points

- Microglia augment host defense in response to CNS infection by the neurotropic coronavirus JHMV.
- A role for microglia in restricting demyelination and promoting remyelination in JHMV-infected mice also is demonstrated.

KEY WORDS

coronavirus, demyelination, host defense, microglia, remyelination

INTRODUCTION

Intracranial inoculation of C57BL/6 mice with the neurotropic JHM strain of mouse hepatitis virus (JHMV), a member of the Coronaviridae family, leads to an acute encephalomyelitis in which virus infects and replicates within glial cells with relative sparing of neurons (Bergmann, Lane, & Stohlman, 2006; Lane & Hosking, 2010; Templeton & Perlman, 2007; Weiss & Leibowitz, 2011). Expression of type I interferon (IFN-I) is critical in helping control viral replication as mice lac- king IFN-I receptor exhibit increased mortality associated with enhanced viral replication (Ireland, Stohlman, Hinton, Atkinson, & Bergmann, 2008). In addition, localized expression of T cell chemotactic chemokines including CCL5, CXCL9, and CXCL10 within the CNS contribute to host defense by attracting virus-specific CD4+ and CD8+ T cells into the CNS that further control viral replication through secretion of interferon-γ (IFN-γ) and cytolytic activity (Bergmann et al., 2004; Glass et al., 2004; Glass & Lane, 2003a; Glass & Lane, 2003b; Liu et al., 2000; Liu, Armstrong, Hamilton, & Lane, 2001; Marten, Stohlman, & Bergmann, 2001; Parra et al., 1999). Antibody-secreting cells (ASCs) are also capable of responding to CXCL9 and CXCL10 and aid in host defense (Phares, Marques, Stohlman, Hinton, & Bergmann, 2011; Phares, Stohlman, Hinton, & Bergmann, 2013). Nonetheless, sterile immunity is not achieved and the majority of animals that survive the acute stage of disease develop immune-mediated demyelination in which both virus-specific T cells and macrophages amplify the severity of white matter damage associ- ated with hind-limb paralysis (Bergmann et al., 2006; Hosking & Lane, 2009; Hosking & Lane, 2010; Templeton & Perlman, 2007).

While the functional roles of T cells and B cells in both host defense and disease in JHMV-infected mice have been extensively studied, there is increasing interest in better understanding how resi- dent cells of the CNS contribute to these events. Microglia are consid-

ered the resident immune cells of the CNS and aid in a diverse array of functions including maintaining CNS homeostasis as well as con- tributing to various disease-associated conditions (Hammond, Robinton, & Stevens, 2018; Salter & Stevens, 2017; Tejera & Heneka, 2019; Wolf, Boddeke, & Kettenmann, 2017). Moreover, microglia are immunologically competent and capable of rapidly responding to infection and/or damage via specific expression of sur- face receptors culminating in morphologic changes accompanied by secretion of proinflammatory cytokines/chemokines that function in amplifying neuroinflammation. Recently, the functional role of microglia in contributing to host defense in response to CNS infection with neurotropic viruses has been examined. These studies have been greatly aided by findings demonstrating that mice lacking colony stimulating factor 1 receptor (CSF1R−/−) lack microglia emphasizing the importance of this signaling pathway in microglia development (Ginhoux et al., 2010). Subsequent studies by Green and colleagues (Elmore et al., 2014) showed that blocking CSF1R signaling in adult mice through administration of CSF1R antagonists is also important in survival of microglia in adult mice. Recent studies have employed treatment of mice with PLX5622, a brain penetrant and selective antagonist of the CSF1R that results in a dramatic reduction in microglia, to better understand functional roles of these cells in pre- clinical models of neurodegenerative disease (Acharya et al., 2016; Dagher et al., 2015; Elmore et al., 2014; Spangenberg et al., 2019). In addition, PLX5622-mediated targeting of microglia results in increased susceptibility to West Nile virus (WNV) (Funk & Klein, 2019; Seitz, Clarke, & Tyler, 2018), Japanese encephalitis virus (JEV) (Seitz et al., 2018), Theiler's murine encephalomyelitis virus (TMEV) (Sanchez et al., 2019a; Waltl et al., 2018), and JHMV (Wheeler, Sariol, Meyerholz, & Perlman, 2018) arguing for a protective role for microglia against acute viral-induced encephalitis.

The current study was undertaken to evaluate how microglia tai- lor the immunological landscape in response to JHMV infection within the brain and spinal cord at different stages of infection with regard to pathways associated with both host defense and neuropathology. We believe microglia will be critical in aiding in host defense through regulating a number of different pathways including antigen presentation and T cell activation as well as augmenting demyelination. To address this, we used a comprehensive set of analytical approaches including single cell RNA sequencing (scRNAseq), flow cytometry, and histopathological techniques to assess disease outcome in JHMV- infected mice treated with PLX5622 at defined times post infection. Our findings emphasize an important role for microglia in aiding in host defense in response to JHMV infection of the CNS as well as influencing both the severity of spinal cord demyelination and remyelination in a model of murine coronavirus-induced neurologic disease.

MATERIALS AND METHODS

Mice and viral infection. Five-week-old C57BL/6 male mice were purchased from The Jackson Laboratory. Mice were infected intracranially (i.c.) with 250 plaque forming units (PFU) of JHMV strain J2.2v-1 in 30 µl of sterile Hanks balanced sterile solution (HBSS) and animals were euthanized at days 3, 7, 12, and 21 post infection (p.i.). Clinical disease in JHMV-infected mice was evaluated using a previously described scale (Lane et al., 2000). To determine viral titers within brains, experimental animals were sacrificed at defined times p.i., brains isolated, homogenized and plaque assay were performed on the DBT astrocytoma cell line as described previously (Hirano, Murakami, Fujiwara, & Matsumoto, 1978). All animal studies were reviewed and approved by the University of Utah Animal Care and Use Committee.

PLX5622 treatment. AIN-76A (Research Diets, NJ) rodent chow formulated with CSF1R inhibitor-PLX5622 at a dose of 1,200 mg/kg of chow was kindly pro- vided by Plexxikon, Inc (Berkeley, CA). Mice were fed with either PLX5622 chow or control chow 7 days prior to viral infection and chow was continued until the mice were sacrificed to harvest tissues at defined times p.i.

Cell isolation and flow cytometry. Flow cytometry was performed to identify inflammatory cells entering the CNS using established protocols (Blanc, Rosen, & Lane, 2014; Chen et al., 2014). In brief, single cell suspensions were generated from tissue samples by grinding with frosted microscope slides. Immune cells were enriched via a two-step Percoll cushion (90 and 63%) and cells were collected at the interface of the two Percoll layers. Before staining with fluorescent antibodies, isolated cells were incubated with anti-CD16/32 Fc block (BD

Biosciences, San Jose, CA) at a 1:200 dilution. Immunophenotyping was performed using commercially available antibodies specific for the following cell surface markers: CD4, CD8, CD11b (BD Biosciences, San Jose, CA), and CD45 (eBioscience, San Diego, CA). The following flow cytometric gating strategies were employed for inflammatory cells isolated from the CNS: macrophages (CD45hiCD11b+) and microglia (CD45lo CD11b+). APC-conjugated rat anti-mouse CD4 and a PE-conjugated tetramer specific for the CD4 immunodominant epitope present within the JHMV matrix (M) glycoprotein spanning amino acids 133–147 (M133-147 tetramer) to determine total and virus-specific CD4+ cells, respectively (Chen et al., 2014; Marro, Grist, & Lane, 2016a); APC-conjugated rat anti-mouse CD8a and a PE- conjugated tetramer specific for the CD8 immunodominant epitope present in the spike (S) glycoprotein spanning amino acids 510-518 (S510-518) to identify total and virus-specific CD8+ cells, respectively (Chen et al., 2014; Marro et al., 2016a). Data were collected using a BD LSR Fortessa X-20 flow cytometer and analyzed with FlowJo software (Tree Star Inc.).

scRNASeq. Immune cells were isolated as described above from brain (day 7 p.i.) and spinal cord (day 14 p.i.) and stained with DAPI and APC conjugated anti-CD45 for 20 min on ice in 1× PBS containing 0.5% bovine serum albumin (BSA). Live CD45+ cells were enriched through the use of BD FACS Aria flow sorter (University of Utah Health Science Center) and washed once with 0.04% BSA. Samples were then processed for single cell RNA sequencing via the 10× Genomics plat- form performed at the Huntsman Cancer Institute High Throughput Genomics Shared Resource Core Facility (https://uofuhealth.utah.edu/huntsman/ shared-resources/gba/). RNA sequencing was per- formed via Agilent Hiseq next generation sequencer. Sequencing data was processed using the 10X Genomics Cell Ranger pipeline and analyzed using the Seurat R

package. Gene expression signatures defining cell clusters were analyzed from PLX5622-treated and controls at day 7 p.i. (brains) and day 14 p.i. (spinal cords). Cells from each aggregated sample data set were clustered into corresponding immune cell populations by a shared nearest neighbor modularity optimization- based clustering algorithm using the Seurat package. The resulting clusters were defined using an immune-cell scoring algorithm (https:// aekiz.shinyapps.io/CIPR/) (Ekiz et al., 2019) that compares the gene signatures of each cluster in the experimental data set with the micro- array data available in the Immunological Genome (ImmGen) Project Database. Expression levels and distribution of population-specific immune cell markers were then analyzed to further refine the identified clusters and expose any subpopulations that should be separated as independent clusters. Once the clusters were established and identified, plots were generated using Seurat, ggpubr, and fgsea R packages.

Histology. Mice were euthanized at defined times points according to IACUC- approved guidelines and the length of spinal cord extending from thoracic vertebrate 6–10 was cryoprotected in 30% sucrose, cut into 1-mm transverse blocks and processed to preserve the craniocaudal orientation and subsequently embedded in O.C.T. (VWR, Radnor, PA). Eight micron (μm)-thick coronal sections were cut and sections were stained with hematoxylin/eosin (H&E) in combination with luxol fast blue (LFB) and between 4 and 8 sections/mouse analyzed. Areas of total white matter and demyelinated white matter were determined with ImageJ Software and demyelination was scored as a percentage of total demyelination from spinal cord sections analyzed (Blanc et al., 2015; Blanc, et al., 2014; Dickey, Worne, Glover, Lane, & O'Connell, 2016; Marro, Grist, & Lane, 2016b).

Electron microscopy and g-ratio analysis. For electron microscopy (EM) analysis of spinal cords, mice were sacrificed and underwent cardiac perfusion with 0.1 M cacodylate buffer containing 2% paraformaldehyde/2% glutaraldehyde. Serial ultrathin sections of spinal cords embedded in Epon epoxy resin were stained with uranyl acetate-lead citrate and analyzed as previously described (Liu, Keirstead, & Lane, 2001). Images at ×1200 magnification were analyzed for g-ratio using ImageJ software. In adult animals there is a relationship between axon circumference and myelin sheath thickness (number of lamellae) expressed by the g-ratio (axon diameter/total fiber diameter); in remyelination this relationship changes such that myelin sheaths are abnormally thin for the axons they surround (Smith, Bostock, & Hall, 1982). An abnormally thin myelin sheath, relative to axonal diameter, was used as the criterion for oligodendrocyte remyelination. Absence of a myelin sheath was used as the criterion for demyelination. For most axons, two measurements were conducted with a minimum of 400 axons analyzed per experimental group. In all cases, slides were blinded and read independently by two investigators.

Statistical analysis. GraphPad Prism was used to perform statistical analyses. Data for each experiment is presented as mean ± SEM. For flow cytometry analysis unpaired Student's t test was used to determine significance and a p value of $<.05$ was considered statistically significant. Wilcoxon test was used for analyzing gene expression in scRNASeq clusters and the resulting p values were corrected for multiple comparisons by Holm-Sidak method and a p value of $<.05$ was considered statistically significant.

RESULTS

PLX5622 treatment increases susceptibility to JHMV-induced neurologic disease.

To evaluate the contribution of microglia to disease progression in JHMV-infected mice, the CSF1R inhibitor PLX5622 was administered as previous studies have reported this pharmacologic approach effectively depletes >90% of microglia (Acharya et al., 2016; Najafi et al., 2018). Mice were treated with PLX5622 (1,200 mg/kg) 7 days prior to infection and continued on the drug for the duration of the experiment. Treatment with PLX5622 resulted in an overall increase in mortality with ~25% of PLX5622-treated mice surviving to day 21 p.i. whereas ~75% of control-chow treated mice survived to this time (**Figure 1a**). The increase in mortality in PLX5622-treated mice correlated with increased viral titers within the brains and spinal cords at days 3, 7, and 12 p.i. compared with control animals; however, by day 21 p.i. viral titers were not detected (ND) in experimental groups (**Figure 1b**). We confirmed efficient microglia ($CD45^{lo}CD11b+$) depletion in PLX5622-treated mice within the brain at day 7 p.i. (**Figure 1c**) and spinal cord at day 14 p.i. (**Figure 1d**) using flow cytometry. PLX5622 treatment did not affect numbers of macrophages ($CD45^{hi}CD11b+$) within brains and spinal cords of experimental mice (**Figure 1c and d**). These findings support earlier work indicating that PLX5622-targeting of microglia impacts efficient immune-mediated control of viral replication following infection with neurotropic viruses (Funk & Klein, 2019; Sanchez et al., 2019b; Seitz et al., 2018; Waltl et al., 2018; Wheeler et al., 2018).

PLX5622 treatment and immune cell infiltration into the brains of JHMV-infected mice during acute disease

Our findings reveal that PLX5622 treatment of mice increases susceptibility to JHMV-induced neurologic disease associated with impaired ability to control viral replication. In order to better understand the effects of PLX5622 treatment on influencing the immune cell composition of the CNS we used 10× Genomics scRNAseq technology. Experimental mice were fed either control chow or chow containing PLX5622 for 7 days prior to infection and remained on chow until sacrificed at either day 7 p.i. or 14 p.i., at which point, live CD45+ cells were sorted from the brains or spinal cords, respectively. The respective tissues were found appropriate to study host defense and disease pathogenesis. The immune response to JHMV infection peaks around day 7 p.i. in the brain and ensuing spinal cord demyelination is present at day 14 p.i. We aggregated data from 4,806 cells taken from control-treated (n = 6) and 3,868 cells from PLX5622-treated (n = 6) mice brain tissue at day 7 p.i. and performed unsupervised clustering analysis based on similarity of gene expression signatures using Seurat single cell genomics R package (Ekiz et al., 2019) (**Table 1**). This approach revealed 16 distinct cell clusters representative of both lymphoid and myeloid linages at day 7 p.i. (**Figure 2a**). To better understand the overlapping expression of marker genes and identification of cell clusters, we employed a recently described algorithm that com- pares the gene expression signatures of cell clusters with publicly available ImmGen database (Ekiz et al., 2019). As previously described (Ekiz et al., 2019), this algorithm calculates an aggregate identity score for each scRNAseq cell cluster as a measure of molecular similarity to the ImmGen subsets. Through combinations of these two approaches, we identified three CD8+ T cell subsets [naïve, effector (Eff.), and memory (Mem.)], two macrophage subsets (Mac 1 and Mac 2), four dendritic cell (DC) subsets (plasmacytoid, NADPH [*Nox2*], XCR1 [*Xcr1*], CCL22 [*Ccl22*]), and single subsets of CD4+ T cells, regulatory T cells (Treg), natural killer (NK) cells, B cells, microglia, neutrophils (neuts),

and monocytes at day 7 p.i. (**Figure 2a**). In order to verify the algorithm-assisted identification of cell clusters, we examined expression of known cellular markers in our data set; expression of these markers corresponded with the respective identities of the distinct clusters (**Figure 2b and c**). Our initial preliminary analyses focusing on samples separately are in agreement with the results of this aggregated approach.

We next analyzed differences in CD45+ cells between PLX5622-treated and control mice at day 7 p.i. following JHMV infection. When data from the cellular genotypes were plotted side-by- side, treatment-dependent dynamics within the tissues started to emerge (**Figure 3a and b**). Importantly, we were able to show that PLX5622 treatment resulted in decreased expression of microglia- associated transcripts *Tmem119, P2ry12,* and *Sparc* compared with control mice (**Figure 3c**). Expression of IFN-α is critical in effective control of JHMV replication within the CNS (Athmer et al., 2018; Ireland et al., 2008; Vijay et al., 2017). We examined IFN-α responses by both macrophages and DCs in order to gain better insight into potential mechanisms by which PLX5622 treatment led to impaired control of viral replication. When the global expression signatures of macrophages and DCs were examined, IFN-α response genes were found to be significantly enriched within the brains of PLX5622-treated mice compared with controls arguing that targeting microglia did not diminish IFN-I responses (**Figure 3d and e**).

PLX5622-treatment alters infiltration and activation phenotype of T cells during acute disease

Control of JHMV replication within the CNS is associated with infiltration of activated virus-specific CD4+ and CD8+ T cells (Marten et al., 2001; Pearce, Hobbs, McGraw, & Buchmeier, 1994; Williamson & Stohlman, 1990). At day 7 p.i., PLX5622 treatment did not

significantly alter CD4+ T cell infiltration yet there was an increase in CD8+ T cells ($p < .05$) compared with control mice as determined by flow cytometric analysis (Figure S1a). There were no differences in virus-specific CD4+ and CD8+ T cells specific for immunodominant epitopes present within the Matrix (M) (Figure S1b) and Spike (S) glycoproteins (Figure S1c) as determined by tetramer staining (Blanc, et al., 2014; Marro et al., 2016b).

Evaluation of defined factors associated with T cell activation at day 7 p.i. revealed reduced expression of the Th1-associated tran- scription factor Tbet (*Tbx21*) ($p < .01$) and this was associated with reduced ($p < .05$) expression of Tnf transcripts, but not Ifng transcripts, in PLX5622-treated mice compared to control mice **(Figure 4a**). We also determined reduced expression of activation markers CD69 (*Cd69*) and CD44 (*Cd44*, $p < .05$) in CD4+ T cells from the brains of PLX5622-treated mice compared to control mice at day 7 p.i. (**Figure 4a**). In addition, the CD4+ T cells subset from PLX5622-treated mice also expressed reduced transcripts for *Il2ra* ($p < .05$) and *Il2rb* ($p < .01$) that encode for components of the IL-2 receptor when compared to control-treated mice (**Figure 4a**). Previous work from Bergmann and colleagues (Phares et al., 2013) identified that IL-21 derived from CD4+ T cells is important in enhancing anti- viral effector functions by CD8+ T cells following JHMV infection. Comparison of *Il21* transcript levels in CD4+ T cells between PLX5622-treated mice compared to control mice indicated no significant difference at day 7 p.i. (**Figure 4c**). In contrast, CD8+ T cells isolated from brains of PLX5622-treated mice expressed increased transcripts specific for perforin (*Prf1*, $p < .0001$), granzyme B (*Gzmb*, $p < .001$) and programmed cell death 1, PD-1 (Pdcd1, $p < .0001$) (**Figure 4b**). There was no difference in expression of *Ifng* transcripts between experimental groups (**Figure 4b**).

Correlating with muted CD4+ T cell activation was the demonstration of a reduction ($p < .0001$) in transcripts associated with MHC class II as well as the co-stimulatory molecule CD86 in macrophages in PLX5622-treated mice compared controls (**Figure 4d**). Flow cytometric staining for MHC class II on cells isolated from the brains of PLX5622 and control mice at day 7 p.i. confirmed expression was reduced ($p < .001$) on macrophages obtained from PLX5622-treated mice compared to controls (**Figure 4f**). Additionally, MHC class II expression on remaining microglia within the brains of PLX5622-treated mice was also reduced ($p < .001$) compared to expression on microglia from control mice (**Figure 4f**). Dampened expression of MHC class II in PLX5622-treated mice was further confirmed through immunofluorescent staining in combination with Iba1 (**Figure 4g**). Expression of MHC class I-associated transcripts was increased ($p < .0001$) in macrophages isolated from the brains of PLX5622-treated mice compared with control animals in macro- phages which was consistent with apparent increased CD8+ T cell activation (**Figure 4d**). With regard to dendritic cells at day 7 p.i., we did not detect changes in expression of transcripts associated with either MHC Class II or MHC Class I (**Figure 4e**) between PLX5622-treated mice and controls.

PLX5622 treatment and immune cell infiltration into spinal cords of JHMV-infected mice during immune-mediated demyelination

We next performed scRNAseq on CD45+ cells enriched from the spinal cords of JHMV-infected mice treated with either PLX5622 or control at day 14 p.i. Using the same approach as described above using aggregated data from 2,725 cells taken from control-treated ($n = 6$) and 4,891 cells from PLX5622-treated ($n = 6$) mice (Table 1), we detected 18 cell clusters within spinal cords of experimental mice rep- resenting lymphoid and myeloid populations (**Figure 5a**).

In brief, this included 3 DC subsets (plasmacytoid, NADPH [*Nox2*], XCR1 [*Xcr1*]), five macrophage subsets (CD40 [*Cd40*], [Interferon-induced proteins with Tetratricopeptide repeats IFIT (*Ifit1,Ifit2,Ifit3*)], Mac 1, Mac 2, and Mac 3), three populations of microglia that included Galectin+ microglia and Insulin growth factor 1-positive (*Igf1*+) microglia, two populations of CD8+ T cells [effector (Eff.) and effector cycling (Eff. Cyc.)], and single populations of neuts, Tregs, CD4+ T cells and B cells. Expression of known cellular markers in our data set corresponded with respective identities of clusters (**Figure 5b and c**). Consistent with our spinal cord flow data (Figure 1d), PLX5622 treatment led to a reduction in microglia with a trend toward an increase in macrophage populations (**Figure 5d and e**). The presence of *Ifit*-positive macrophages argues for a role in contributing to anti-viral immune responses (Diamond & Farzan, 2013). Further, we also detected the presence of Galectin-positive microglia although there were no differences in frequency between experimental populations (**Figure 5d and e**). Finally, we did find a reduced frequency of *Igf*-1-positive microglia within the spinal cords of PLX5622-treated mice compared to controls (**Figure 5d and e**).

CSF1R antagonism increases the severity of demyelination in JHMV-infected mice

CNS inflammatory T cells augment demyelination in JHMV-infected mice presumably through recognition of viral antigens resulting in secretion of cytokines for example, IFN-γ that activate both resident CNS cells and inflammatory macrophages/myeloid cells to secrete proinflammatory cytokines/chemokines as well as molecules damaging to oligodendrocyte function (Hosking & Lane, 2009; Templeton & Perlman, 2007). By day 14 p.i., we detected no difference in CD4+ T cells in the spinal cords of PLX5622-treated mice versus controls, though there was an increase ($p < .05$) in CD8+ T cells (Figure S2a) as well as virus-specific CD4+

(Figure S2b) and CD8+ T cells (Figure S2c) compared with controls. Similar to what we observed at day 7 p.i., we detected reduced expression of Cd69 transcripts ($p < .01$), *Il2rb* transcripts ($p < .0001$), and *Tbx21* ($p < .0001$) in CD4+ T cells isolated from spinal cords of PLX5622-treated mice compared to controls (**Figure 6a**). There were no differences in expression of Cd44 or cytokines *Ifng* and *Tnf* within CD4+ T cells between experimental groups of mice (**Figure 6a**). However, *Il21* transcript levels were significantly ($p < .0001$) reduced in CD4+ T cells isolated from PLX5622-treated mice compared to control mice at this time (**Figure 6c**). In addition, there was no difference in transcript levels for *Gzmb* or *Ifng* in CD8+ T cells isolated from spinal cords of PLX5622-treated mice compared with controls (**Figure 6b**). However, expression of both *Pdcd1* ($p < .01$) and *Prf1* ($p < .05$) were reduced in CD8+ T cells from PLX5622-treated mice versus controls (**Figure 6b**). PLX5622-treatment resulted in reduced expression of *Cd86* ($p < .0001$), *H2_Aa* ($p < .0001$), *H2_Ab1* ($p < .001$), and *H2_DMb1* ($p < .0001$) in spinal cord macrophages compared with control mice (**Figure 6d**). In contrast, expression of MHC class I- associated transcripts *H2_K1* ($p < .0001$), *H2_M3* ($p < .05$) remained elevated in spinal cord macrophages isolated from PLX5622-treated mice compared to controls yet there was no difference expression of *H2_Q7* transcripts (**Figure 6d**).

We next assessed how PLX5622 treatment affected the severity of demyelination in JHMV-infected mice. Using Luxol Fast Blue (LFB) staining of spinal cords from experimental mice, we determined that PLX5622 treatment resulted in an increase in the severity of demyelination at days 14 ($p < .01$) and 21 p.i. ($p < .05$) compared with control mice (**Figure 7a and b**). These findings indicate that targeting microglia via PLX5622 treatment results in increased demyelination arguing these cells exert a protective role in limiting the severity of white matter pathology in JHMV-infected mice. We also looked at expression of several genes

associated with immune-mediated demyelinating dis- eases. Through scRNAseq analysis of CD45 + -enriched cells from the spinal cords of JHMV-infected mice treated with either PLX5622 or control chow, we consistently observed a dramatic increase in transcripts encoding for molecules associated with demyelination including Apoliprotein E (*Apoe*) (Krasemann et al., 2017), Osteopontin (*Spp1*) (Chabas et al., 2001), and Triggering receptor expressed on myeloid cells (*Trem2*) (Krasemann et al., 2017; Ulrich & Holtzman, 2016) in macrophage clusters within the spinal cords of PLX5622-treated mice compared to controls (**Figure 7c**). In addition, transcripts encoding proteins associated with remyelination including *Cst7* (Cystatin F), *Igf1* (insulin growth factor 1), and *Lpl* (Lipoprotein lipase) were decreased in spinal cord macrophages within the spinal cords of PLX5622-treated mice compared to controls (**Figure 7f**) (Bruce et al., 2018; Durose et al., 2019; Hlavica et al., 2017; Ma et al., 2011; Shimizu et al., 2017; Wlodarczyk et al., 2017; Ye, Li, Richards, DiAugustine, & D'Ercole, 2002). This suggests that microglia may have a role in suppressing expression of molecules associated with demyelination and even promoting expression of those related to remyelination in macrophages. To determine whether remyelination was impacted in response to PLX5622 treatment, EM analysis of spinal cord sections was performed. Assessment of the g-ratio, the ratio of the inner axonal diameter to the total outer fiber diameter, is commonly employed as a structural index of remyelination; lower ratios indicate more extensive myelination (Liu, Keirstead, & Lane, 2001; Moore et al., 2013). High magnification (×1,200) images of the spinal cord ventral funiculus of PLX5622-treated and control mice were used to evaluate myelinated and demyelinated axons. PLX5622 treatment resulted in a significant ($p < .05$) decrease in remyelination as determined by calculating g-ratio's (0.87 ± 0.004, minimum of 400 axons counted/mouse) compared with

control treated mice (0.79 ± 0.003, minimum of 400 axons counted/mouse) (**Figure 7d**) as well as measuring myelin thickness (**Figure 7e**).

DISCUSSION

Viral infection of the central nervous system (CNS) presents unique challenges to the immune system with regard to controlling and eliminating the invading pathogen. The CNS is composed of a variety of highly specialized cells, many of which have limited renewal capacity, that represent potential targets of infection by numerous different viruses (Klein et al., 2019). A significant hurdle encountered by infiltrating antigen-specific lymphocytes is the elimination of virus from infected cells while limiting the damage that may have long-term detrimental consequences to the host. Therefore, characterizing the mechanisms involved in how viral infection of the CNS is controlled is an important question. It is becoming increasingly clear that CNS resident cells are critical in host defense through either secretion of anti-viral cytokines for example, type I interferon (IFN-I) and/or presentation of antigen within the context of either MHC Classes I or II. Recently, an important role for microglia in aiding in host defense in response to CNS viral infection has been identified (Funk & Klein, 2019; Sanchez et al., 2019a; Seitz et al., 2018; Waltl et al., 2018; Wheeler et al., 2018). Perlman and colleagues (Wheeler et al., 2018) have shown that microglia are required for optimal host defense in response to JHMV infection of the CNS. Targeted depletion of microglia through administration of PLX5622 revealed a role in limiting mortality that was associated with impaired control of JHMV replication. The increase in susceptibility to disease did not appear to be due to altered expression of IFN-I but more likely a reflection of impaired antigen-presentation due to muted MHC Class II expression by macrophages infiltrating the CNS of PLX5622-treated mice and this likely resulted in dampened T cell responses (Wheeler et al., 2018). We believe the increase in expression of IFN-I response genes in PLX5622-treated mice most likely reflects the overall increase in viral titers within the brains. Similarly, microglia depletion led to increased mortality

in mice infected with WNV associated with diminished activation of APCs and limited reactivation of virus-specific T cells that led to reduced viral clearance (Funk & Klein, 2019; Seitz et al., 2018). These findings clearly implicate microglia in enhancing optimal host responses following CNS viral infection, in part, by influencing antigen-presentation that affects virus- specific T cell responses.

We undertook the present study to better understand how microglia contribute to host defense as well as demyelination and repair following JHMV infection of the CNS using sophisticated molecular, cellular, and histologic approaches. Employing PLX5622 to deplete microglia, we found increased mortality associated with impaired control of CNS viral replication. CSF1R antagonism led to a selective decrease in microglia with sparing of macrophages as well dendritic cells indicating that resident APCs within the CNS were not affected. To better understand the functional contributions of microglia in aiding in host defense, we performed scRNAseq on CD45+ cells enriched from the brains of PLX5622 and control mice at day 7 p.i. Using a verified and unbiased bioinformatics approach (Ekiz et al., 2019), we were able to reliably identify clusters of cells associated with innate immune responses for example, microglia, monocytes, macrophages, NK cells, and neutrophils as well as adaptive responses including T cell subsets and dendritic cells (**Figure 2a-c**). Moreover, this approach revealed the heterogeneity of both the innate and adaptive immune cell response by infiltrating cells as well as resident microglia with the identification of different subsets of DCs, macrophages, and T cells. These findings emphasize the complexity of both the innate and adaptive immune responses that occur in response to viral infection of the CNS and raises interesting questions with regard to functional roles for these populations of cells in either defense and/or disease progression. Employing scRNAseq demonstrated that PLX5622-mediated depletion of microglia

did not dramatically alter the presence of the majority of immune cells identified including neutrophils, monocytes, DC and macrophage subsets, as well as Tregs and naïve and memory CD8+ T cells, not to say that these populations are not transcriptionally different. This approach did indicate that PLX5622-treatment resulted in increased effector CD8+ T cells, CD4+ T cells and, interestingly, B cells. These findings would argue that microglia may not impact either directly or indirectly the synthesis/secretion of proinflammatory cytokines/chemokines by other resident CNS cells for example, astrocytes and/or inflammatory macrophages. Nonetheless, the use of scRNAseq to assess gene expression profiles of CD45+ cells has yielded a tremendous amount of data that we will continue to examine with the goals of elucidating mechanisms not tied to current dogma associated with both anti-viral host defense mechanisms in response to viral infection of the CNS and viral-induced demyelination.

Expression of IFN-I is critical in host defense in response to JHMV infection of the CNS (Athmer et al., 2018; Ireland et al., 2008; Vijay et al., 2017). PLX5622-mediated targeting of microglia did not affect IFN-I signaling as GSEA analysis revealed IFN-α response genes were significantly enriched in both macrophages and dendritic cells within the brains of PLX5622-treated mice at days 7 compared with controls (**Figure 3d and e**). These findings may reflect the increase in viral titers within the CNS of PLX5622-treated mice at these times but also argue that microglia are not solely responsible for production of IFN-I. We detected altered T cell responses within the CNS following PLX5622 treatment as determined by both flow cytometry and scRNASeq. There were increased numbers of total CD8+ T cells ($p < .05$) as well as virus-specific CD8+ T cells within the brains of JHMV-infected mice treated with PLX5622 compared to controls at day 7 p.i. We also found a trend towards increased total CD4+ T cells and virus-specific CD4+ T cells in PLX5622-treated mice compared to controls although these differences

were not significant. In terms of T cell activation, we detected differential responses in T cell subsets at day 7 p.i. In CD4+ T cells, there was a reduction in transcripts associated with Th1-polarized activation for example, T-bet (Tbx21) in PLX5622-treated mice compared to controls although there were no differences in *Ifng* transcripts in CD4+ T cells in experimental groups. PLX5622-treatment also resulted in reduced expression of CD4+ T cell surface activation markers including CD44, CD69, and components of IL-2 receptor in PLX5622-treated mice compared with controls whereas there was an overall increased activation phenotype associated with CD8+ T cells compared with controls. A role for CD4+ T cell-derived IL-21 has previously been shown to enhance antiviral CD8+ T cell responses following JHMV infection of the CNS (Phares, DiSano, et al., 2013). While expression of Il21 transcripts in CD4+ T cells was not affected at day 7 p.i. in PLX5622-treated mice, expression was significantly reduced by day 14 p.i. This reduction in *Il21* expression in CD4+ T cells in PLX5622-treated mice may have impacted virus-specific CD8+ T cell function and partially explain mechanisms associated with impaired control of JHMV replication within the CNS. In addition, the muted activation phenotype by CD4+ T cells was associated with reduced expression of MHC class II by macrophages, but not DCs, at day 7 p.i. in PLX5622-treated mice, demonstrating a selective effect in response to microglia depletion. This selective effect of reduced MHC class II expression by macrophages in PLX5622-treated mice was further emphasized in that expression of MHC class I transcripts was increased in macrophages, but not DCs, compared with control mice. Identifying the mechanisms by which microglia augment expression of MHC class II on macrophages will be a focus of ongoing studies.

Our results examining immune cell infiltration and activation in spinal cords of experimental mice at day 14 p.i. through scRNAseq were intriguing as we observed differences

in both macrophage and microglial populations compared with the brain at day 7 p.i., regardless of the experimental groups. First, there were both *Ifit* + and CD40+ macrophages present within the spinal cords of both PLX5622 and control mice, suggesting these cells may be responsible for host defense in response to viral infection (Diamond & Farzan, 2013). It is important to note that both populations of cells were present at a low frequency and there were no dramatic differences between experimental groups, although *CD40*+ macrophages were present at a much higher frequency compared to *Ifit* + macrophages. Furthermore, there was a small population of Galectin+ microglia in spinal cords in control mice yet not in PLX5622-treated mice and previous studies argue for a role for certain isoforms of Galectin in potentially contributing to demyelination in patients with multiple sclerosis (MS) (de Jong et al., 2018) while other isoforms are considered important in driving oligodendrocyte differentiation associated with remyelination (Thomas & Pasquini, 2018). Our findings that spinal cord demyelination was significantly increased in PLX5622-treated mice supports an emerging role for microglia in restricting the severity of white matter and this is consistent with a recent study from our group indicating that microglia influence the severity of demyelination in JHMV- infected mice (Brown et al., 2019). While we are currently exploring the molecular and cellular mechanisms by which microglia may modulate the CNS microenvironment in mice persistently infected with JHMV, evidence presented in the current study indicates that PLX5622 treatment resulted in increased expression of transcripts encoding for Osteopontin, APOE, and TREM2 all of which have been implicated in contributing to demyelination (Chabas et al., 2001; Krasemann et al., 2017; Ulrich & Holtzman, 2016). Interestingly, expression of all three transcripts were enriched within macrophage populations suggesting a specific effect by which microglia may suppress expression and limit myelin damage.

Emerging studies have pointed to a protective role for microglia in limiting neuropathology and promoting repair (Baaklini, Rawji, Dun- can, Ho, & Plemel, 2019; Lee, Hamanaka, Lo, & Arai, 2019; Lloyd & Miron, 2019). In support of this concept are recent studies from Miron and colleagues (Lloyd & Miron, 2019) showing an important role for microglia in enhancing remyelination in a toxin-model of demyelination that is aided by microglial death and subsequent microglial repopulation; here, in this study, the absence of microglia prevents their further death and repopulation and is associated with increased white matter damage. Although mechanisms by which microglia may support remyelination have not been completely defined, it is though that these cells aid in clearance of myelin debris and/or secrete growth factors/cytokines that influence maturation of oligodendrocyte progenitor cells (OPCs) into mature myelin-producing oligodendrocytes. What is also clear is that microglia are heterogenous in terms of transcriptome and protein expression which is likely regulated during disease and this would influence the role of these cells in enhancing or muting disease progression and potential repair. In support of a protective role for microglia in restricting neuropathology and promoting repair is our data demonstrating that PLX5622 treatment of JHMV-infected mice results in an increase in white matter damage associated with impaired remyelination (**Figure 7a, b, d, and e**). In addition, scRNASeq also shows reduced expression of genes encoding proteins previously associated with remyelination including Cystatin F (Durose et al., 2019; Ma et al., 2011; Shimizu et al., 2017), Insulin growth factor 1 (IGF1) (Hlavica et al., 2017; Wlodarczyk et al., 2017; Ye et al., 2002) and Lipoprotein lipase (Bruce et al., 2018) within macrophages isolated from the spinal cords of PLX5622-treated mice (Figure 7f). These findings further support the notion that microglia may either directly or indirectly influence remyelination within the spinal cord by contributing to controlling expression of genes encoding proteins that

regulate OPC maturation. We are currently pursuing the functional contributions of Cystatin F, IGF1, and Lipoprotein lipase in contributing to remyelination in JHMV-infected mice.

We would caution that although demyelination was worsened and remyelination was impaired when microglia are depleted, this may reflect the model employed that is, targeted depletion of microglia prior to JHMV infection of the CNS which may lead to increased neuropathology through altered macrophage biology and/or resident cells of the CNS including astrocytes and oligodendrocytes. We are currently determining if microglia depletion in mice persistently infected with JHMV in which demyelination is established affects either neuro-pathology and/or viral recrudescence as this is a more clinically-relevant question. Similarly, we are also determining if there is efficient repopulation of microglia in mice persistently infected with JHMV upon removal of PLX5622 treatment. Another important area we are pursuing relates to whether depletion of microglia in mice with established demyelination impacts remyelination.

ACKNOWLEDGMENTS

T. E. L. was supported by funding from the National Institutes of Health (NIH) R01NS041249, R01NS091939, National Multiple Sclerosis Society (NMSS) Collaborative Research Center Grant CA- 1607-25040 and The Ray and Tye Noorda Foundation. R. M. O. was supported by NIH R01AG047956 and NMSS CA-1607-25040.

CONFLICT OF INTEREST

The authors declare no competing financial interests.

DATA AVAILABILITY STATEMENT

The data that support the findings of this study are available from the corresponding author upon reasonable request.

ORCID

Kim N. Green https://orcid.org/0000-0002-6049-6744

Thomas E. Lane https://orcid.org/0000-0003-0392-0825

REFERENCES

1. Acharya, M. M., Green, K. N., Allen, B. D., Najafi, A. R., Syage, A., Minasyan, H., … Limoli, C. L. (2016). Elimination of microglia improves cognitive function following cranial irradiation. Scientific Reports, 6, 31545.

2. Athmer, J., Fehr, A. R., Grunewald, M. E., Qu, W., Wheeler, D. L., Graepel, K. W., … Perlman, S. (2018). Selective packaging in murine coronavirus promotes virulence by limiting type I interferon responses. MBio, 9, e00272-18. https://doi.org/10.1128/mBio.00272-18

3. Baaklini, C. S., Rawji, K. S., Duncan, G. J., Ho, M. F. S., & Plemel, J. R. (2019). Central nervous system remyelination: Roles of glia and innate immune cells. Frontiers in Molecular Neuroscience, 12, 225.

4. Bergmann, C. C., Lane, T. E., & Stohlman, S. A. (2006). Coronavirus infection of the central nervous system: Host-virus stand-off. Nature Reviews Microbiology, 4, 121–132.

5. Bergmann, C. C., Parra, B., Hinton, D. R., Ramakrishna, C., Dowdell, K. C., & Stohlman, S. A. (2004). Perforin and gamma interferon-mediated control of coronavirus central nervous system infection by CD8 T cells in the absence of CD4 T cells. Journal of Virology, 78, 1739–1750.

6. Blanc, C. A., Grist, J. J., Rosen, H., Sears-Kraxberger, I., Steward, O., & Lane, T. E. (2015). Sphingosine-1-phosphate receptor antagonism enhances proliferation and migration of engrafted neural progenitor cells in a model of viral-induced demyelination. The American Journal of Pathology, 185, 2819–2832.

7. Blanc, C. A., Rosen, H., & Lane, T. E. (2014). FTY720 (fingolimod) modu- lates the severity of viral-induced encephalomyelitis and demyelination. Journal of Neuroinflammation, 11, 138.

8. Brown, D. G., Soto, R., Yandamuri, S., Stone, C., Dickey, L., Gomes- Neto, J. C., … Round, J. L. (2019). The microbiota protects from viral- induced neurologic damage through microglia-intrinsic TLR signaling. eLife, 8, e47117. https://doi.org/10.7554/eLife.47117

9. Bruce, K. D., Gorkhali, S., Given, K., Coates, A. M., Boyle, K. E., Macklin, W. B., & Eckel, R. H. (2018). Lipoprotein lipase is a feature of alternatively-activated microglia and may facilitate lipid uptake in the CNS during demyelination. Frontiers in Molecular Neuroscience, 11, 57.

10. Chabas, D., Baranzini, S. E., Mitchell, D., Bernard, C. C., Rittling, S. R., Denhardt, D. T., … Steinman, L. (2001). The influence of the proinflammatory cytokine, osteopontin, on autoimmune demyelinating disease. Science, 294, 1731–1735.

11. Chen, L., Coleman, R., Leang, R., Tran, H., Kopf, A., Walsh, C. M., …Lane, T. E. (2014). Human neural precursor cells promote neurologic recovery in a viral model of multiple sclerosis. Stem Cell Reports, 2, 825–837.

12. Dagher, N. N., Najafi, A. R., Kayala, K. M., Elmore, M. R., White, T. E., Medeiros, R., … Green, K. N. (2015). Colony-stimulating factor 1 receptor inhibition prevents microglial plaque association and improves cognition in 3xTg-AD mice. Journal of Neuroinflammation, 12, 139.

13. de Jong, C., Stancic, M., Pinxterhuis, T. H., van Horssen, J., van Dam, A. M., Gabius, H. J., & Baron, W. (2018). Galectin-4, a negative regulator of oligodendrocyte differentiation, is persistently present in axons and microglia/macrophages in multiple sclerosis lesions. Journal of Neuro- pathology and Experimental Neurology, 77, 1024–1038.

14. Diamond, M. S., & Farzan, M. (2013). The broad-spectrum antiviral func- tions of IFIT and IFITM proteins. Nature Reviews. Immunology, 13, 46–57.

15. Dickey, L. L., Worne, C. L., Glover, J. L., Lane, T. E., & O'Connell, R. M. (2016). MicroRNA-155 enhances T cell trafficking and antiviral effec- tor function in a model of coronavirus-induced neurologic disease. Journal of Neuroinflammation, 13, 240.

16. Durose, W. W., Shimizu, T., Li, J., Abe, M., Sakimura, K., Chetsawang, B., … Ikenaka, K. (2019). Cathepsin C modulates myelin oligodendrocyte glycoprotein-induced experimental autoimmune encephalomyelitis. Journal of Neurochemistry, 148, 413–425.

17. Ekiz, H. A., Huffaker, T. B., Grossmann, A. H., Stephens, W. Z., Williams, M. A., Round, J. L., & O'Connell, R. M. (2019). MicroRNA-155 coordinates the immunological landscape within murine melanoma and correlates with immunity in human cancers. JCI Insight, 4, 126543. https://doi.org/10.1172/jci.insight.126543

18. Elmore, M. R., Najafi, A. R., Koike, M. A., Dagher, N. N., Spangenberg, E. E., Rice, R. A., … Green, K. N. (2014). Colony-stimulating factor 1 receptor signaling is necessary for microglia viability, unmasking a microglia pro- genitor cell in the adult brain. Neuron, 82, 380–397.

19. Funk, K. E., & Klein, R. S. (2019). CSF1R antagonism limits local restimulation of antiviral CD8(+) T cells during viral encephalitis. Journal of Neuroinflammation, 16, 22.

20. Ginhoux, F., Greter, M., Leboeuf, M., Nandi, S., See, P., Gokhan, S., … Merad, M. (2010). Fate mapping analysis reveals that adult microglia derive from primitive macrophages. Science, 330, 841–845.

21. Glass, W. G., Hickey, M. J., Hardison, J. L., Liu, M. T., Manning, J. E., & Lane, T. E. (2004). Antibody targeting of the CC chemokine ligand 5 results in diminished leukocyte infiltration into the central nervous system and reduced neurologic disease in a viral model of multiple sclerosis. Journal of Immunology, 172, 4018–4025.

22. Glass, W. G., & Lane, T. E. (2003a). Functional analysis of the CC chemokine receptor 5 (CCR5) on virus-specific CD8+ T cells following coronavirus infection of the central nervous

system. Virology, 312, 407–414.

23. Glass, W. G., & Lane, T. E. (2003b). Functional expression of chemokine receptor CCR5 on CD4(+) T cells during virus-induced central nervous system disease. Journal of Virology, 77, 191–198.

24. Hammond, T. R., Robinton, D., & Stevens, B. (2018). Microglia and the brain: Complementary Partners in Development and Disease. Annual Review of Cell and Developmental Biology, 34, 523–544.

25. Hirano, N., Murakami, T., Fujiwara, K., & Matsumoto, M. (1978). Utility of mouse cell line DBT for propagation and assay of mouse hepatitis virus. The Japanese Journal of Experimental Medicine, 48, 71–75.

26. Hlavica, M., Delparente, A., Good, A., Good, N., Plattner, P. S., Seyedsadr, M. S., … Ineichen, B. V. (2017). Intrathecal insulin-like growth factor 1 but not insulin enhances myelin repair in young and aged rats. Neuroscience Letters, 648, 41–46.

27. Hosking, M. P., & Lane, T. E. (2009). The biology of persistent infection: Inflammation and demyelination following murine coronavirus infection of the central nervous system. Current Immunology Reviews, 5, 267–276.

28. Hosking, M. P., & Lane, T. E. (2010). The role of chemokines during viral infection of the CNS. PLoS Pathogens, 6, e1000937.

29. Ireland, D. D., Stohlman, S. A., Hinton, D. R., Atkinson, R., & Bergmann, C. C. (2008). Type I interferons are essential in controlling neurotropic coronavirus infection irrespective of functional CD8 T cells. Journal of Virology, 82, 300–310.

30. Klein, R. S., Garber, C., Funk, K. E., Salimi, H., Soung, A., Kanmogne, M., … Cain, M. (2019). Neuroinflammation during RNA viral infections. Annual Review of Immunology, 37, 73–95.

31. Krasemann, S., Madore, C., Cialic, R., Baufeld, C., Calcagno, N., El Fatimy, R., … Butovsky, O. (2017). The TREM2-APOE pathway drives the transcriptional phenotype of dysfunctional microglia in neurodegenerative diseases. Immunity, 47(566–581), e9.

32. Lane, T. E., & Hosking, M. P. (2010). The pathogenesis of murine coronavirus infection of the central nervous system. Critical Reviews in Immu- nology, 30, 119–130.

33. Lane, T. E., Liu, M. T., Chen, B. P., Asensio, V. C., Samawi, R. M., Paoletti, A. D., … Buchmeier, M. J. (2000). A central role for CD4(+) T cells and RANTES in virus-induced central nervous system inflammation and demyelination. Journal of Virology, 74, 1415–1424.

34. Lee, J., Hamanaka, G., Lo, E. H., & Arai, K. (2019). Heterogeneity of microglia and their differential roles in white matter pathology. CNS Neuroscience & Therapeutics, 25, 1290–

1298.

35. Liu, M. T., Armstrong, D., Hamilton, T. A., & Lane, T. E. (2001). Expression of Mig (monokine induced by interferon-gamma) is important in T lymphocyte recruitment and host defense following viral infection of the central nervous system. Journal of Immunology, 166, 1790–1795.

36. Liu, M. T., Chen, B. P., Oertel, P., Buchmeier, M. J., Armstrong, D., Hamilton, T. A., & Lane, T. E. (2000). The T cell chemoattractant IFN- inducible protein 10 is essential in host defense against viral-induced neurologic disease. Journal of Immunology, 165, 2327–2330.

37. Liu, M. T., Keirstead, H. S., & Lane, T. E. (2001). Neutralization of the chemokine CXCL10 reduces inflammatory cell invasion and demyelination and improves neurological function in a viral model of multiple sclerosis. Journal of Immunology, 167, 4091–4097.

38. Lloyd, A. F., & Miron, V. E. (2019). The pro-remyelination properties of microglia in the central nervous system. Nature Reviews. Neurology, 15, 447–458.

39. Ma, J., Tanaka, K. F., Shimizu, T., Bernard, C. C., Kakita, A., Takahashi, H., … Ikenaka, K. (2011). Microglial cystatin F expression is a sensitive indicator for ongoing demyelination with concurrent remyelination. Journal of Neuroscience Research, 89, 639–649.

40. Marro, B. S., Grist, J. J., & Lane, T. E. (2016a). Inducible expression of CXCL1 within the central nervous system amplifies viral-induced demyelination. Journal of Immunology, 196, 1855–1864. https://doi. org/10.4049/jimmunol.1501802

41. Marten, N. W., Stohlman, S. A., & Bergmann, C. C. (2001). MHV infection of the CNS: Mechanisms of immune-mediated control. Viral Immunology, 14, 1–18.

42. Moore, S., Khalaj, A. J., Yoon, J., Patel, R., Hannsun, G., Yoo, T., … Tiwari- Woodruff, S. K. (2013). Therapeutic laquinimod treatment decreases inflammation, initiates axon remyelination, and improves motor deficit in a mouse model of multiple sclerosis. Brain and Behavior: A Cognitive Neuroscience Perspective, 3, 664–682.

43. Najafi, A. R., Crapser, J., Jiang, S., Ng, W., Mortazavi, A., West, B. L., & Green, K. N. (2018). A limited capacity for microglial repopulation in the adult brain. GLIA, 66, 2385–2396.

44. Parra, B., Hinton, D. R., Marten, N. W., Bergmann, C. C., Lin, M. T., Yang, C. S., & Stohlman, S. A. (1999). IFN-gamma is required for viral clearance from central nervous system oligodendroglia. Journal of Immunology, 162, 1641–1647.

45. Pearce, B. D., Hobbs, M. V., McGraw, T. S., & Buchmeier, M. J. (1994). Cytokine induction during T-cell-mediated clearance of mouse hepatitis virus from neurons in vivo. Journal of Virology, 68, 5483–5495.

46. Phares, T. W., DiSano, K. D., Hinton, D. R., Hwang, M., Zajac, A. J., Stohlman, S. A., &

Bergmann, C. C. (2013). IL-21 optimizes T cell and humoral responses in the central nervous system during viral encephalitis. Journal of Neuroimmunology, 263, 43–54.

47. Phares, T. W., Marques, C. P., Stohlman, S. A., Hinton, D. R., & Bergmann, C. C. (2011). Factors supporting intrathecal humoral responses following viral encephalomyelitis. Journal of Virology, 85, 2589–2598.

48. Phares, T. W., Stohlman, S. A., Hinton, D. R., & Bergmann, C. C. (2013). Astrocyte-derived CXCL10 drives accumulation of antibody-secreting cells in the central nervous system during viral encephalomyelitis. Journal of Virology, 87, 3382–3392.

49. Salter, M. W., & Stevens, B. (2017). Microglia emerge as central players in brain disease. Nature Medicine, 23, 1018–1027.

50. Sanchez, J. M. S., DePaula-Silva, A. B., Doty, D. J., Truong, A., Libbey, J. E., & Fujinami, R. S. (2019a). Microglial cell depletion is fatal with low level picornavirus infection of the central nervous system. Journal of Neurovirology, 25, 415–421.

51. Seitz, S., Clarke, P., & Tyler, K. L. (2018). Pharmacologic depletion of microglia increases viral load in the brain and enhances mortality in murine models of Flavivirus-induced encephalitis. Journal of Virology, 92, e00525-18. https://doi.org/10.1128/JVI.00525-18

52. Shimizu, T., Wisessmith, W., Li, J., Abe, M., Sakimura, K., Chetsawang, B., … Ikenaka, K. (2017). The balance between cathepsin C and cystatin F controls remyelination in the brain of Plp1-overexpressing mouse, a chronic demyelinating disease model. GLIA, 65, 917–930.

53. Smith, K. J., Bostock, H., & Hall, S. M. (1982). Saltatory conduction pre- cedes remyelination in axons demyelinated with lysophosphatidyl choline. Journal of the Neurological Sciences, 54, 13–31.

54. Spangenberg, E., Severson, P. L., Hohsfield, L. A., Crapser, J., Zhang, J., Burton, E. A., … Green, K. N. (2019). Sustained microglial depletion with CSF1R inhibitor impairs parenchymal plaque development in an Alzheimer's disease model. Nature Communications, 10, 3758.

55. Tejera, D., & Heneka, M. T. (2019). Microglia in Neurodegenerative Disorders. Methods in Molecular Biology, 2034, 57–67.

56. Templeton, S. P., & Perlman, S. (2007). Pathogenesis of acute and chronic central nervous system infection with variants of mouse hepatitis virus, strain JHM. Immunologic Research, 39, 160–172.

57. Thomas, L., & Pasquini, L. A. (2018). Galectin-3-mediated glial crosstalk drives oligodendrocyte differentiation and (re)myelination. Frontiers in Cellular Neuroscience, 12, 297.

58. Ulrich, J. D., & Holtzman, D. M. (2016). TREM2 function in Alzheimer's dis- ease and neurodegeneration. ACS Chemical Neuroscience, 7, 420–427.

59. Vijay, R., Fehr, A. R., Janowski, A. M., Athmer, J., Wheeler, D. L., Grunewald, M., … Perlman, S. (2017). Virus-induced inflammasome activation is suppressed by prostaglandin D2/DP1 signaling. Proceedings of the National Academy of Sciences of the United States of America, 114, E5444–E5453.

60. Waltl, I., Kaufer, C., Gerhauser, I., Chhatbar, C., Ghita, L., Kalinke, U., & Loscher, W. (2018). Microglia have a protective role in viral encephalitis-induced seizure development and hippocampal damage. Brain, Behavior, and Immunity, 74, 186–204.

61. Weiss, S. R., & Leibowitz, J. L. (2011). Coronavirus pathogenesis. Advances in Virus Research, 81, 85–164.

62. Wheeler, D. L., Sariol, A., Meyerholz, D. K., & Perlman, S. (2018). Microglia are required for protection against lethal coronavirus encephalitis in mice. The Journal of Clinical Investigation, 128, 931–943.

63. Williamson, J. S., & Stohlman, S. A. (1990). Effective clearance of mouse hepatitis virus from the central nervous system requires both CD4+ and CD8+ T cells. Journal of Virology, 64, 4589–4592.

64. Wlodarczyk, A., Holtman, I. R., Krueger, M., Yogev, N., Bruttger, J., Khorooshi, R., … Owens, T. (2017). A novel microglial subset plays a key role in myelinogenesis in developing brain. The EMBO Journal, 36, 3292–3308.

65. Wolf, S. A., Boddeke, H. W., & Kettenmann, H. (2017). Microglia in physiology and disease. Annual Review of Physiology, 79, 619–643.

66. Ye, P., Li, L., Richards, R. G., DiAugustine, R. P., & D'Ercole, A. J. (2002). Myelination is altered in insulin-like growth factor-I null mutant mice. The Journal of Neuroscience, 22, 6041–6051.

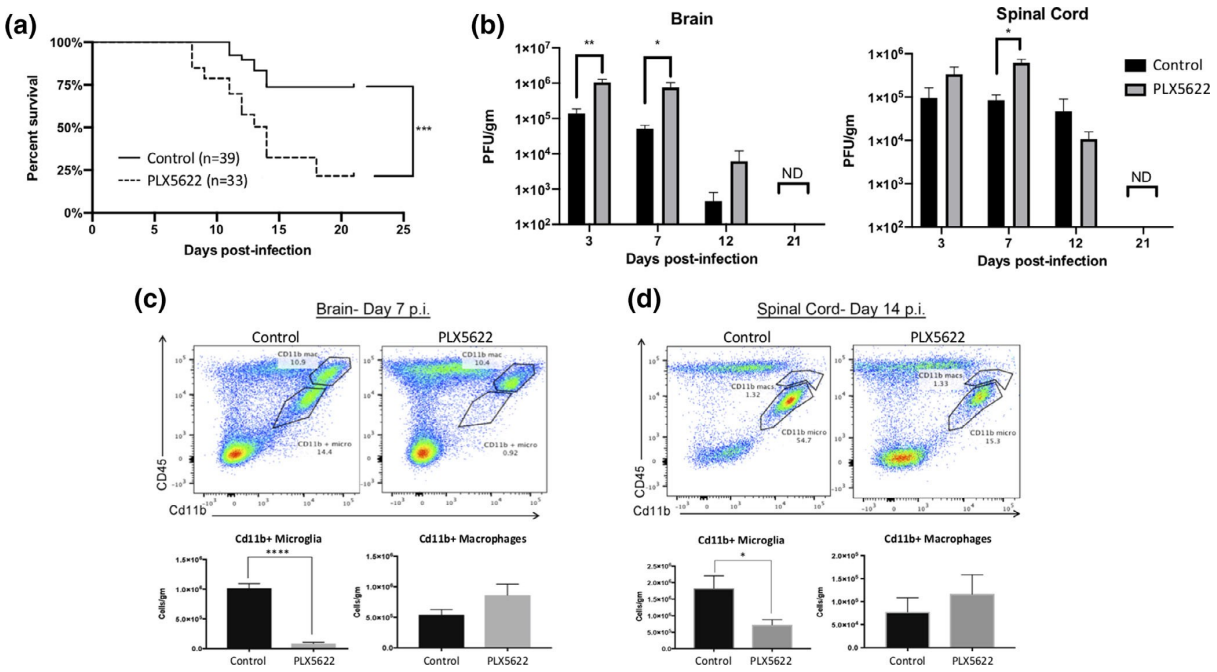

Figure 1 PLX5622 treatment increases susceptibility to JHMV-induced neurologic disease. Mice were fed either PLX5622 or control chow for 7 days prior to i.c. infection with JHMV (250 PFU) and subsequently remained specific chow for the duration of the experiment. PLX5622 treatment led to (a) increased mortality compared to control mice that was associated with an (b) impaired ability to control viral replication within the brains and spinal cords at days 3, 7, and 12 p.i. compared with control mice. Representative flow cytometric data from JHMV-infected mice treated with either PLX5622 or control chow and gating on microglia ($CD45^{lo}CD11b+$ cells) or macrophages ($CD45^{hi}$ CD11b+ cells) in (c) brains at day 7 p.i., and (d) spinal cords at day 14 p.i. PLX5622-treatment resulted in reduced numbers of microglia in brains and spinal cords compared with control mice. Data are derived from a minimum of three independent experiments with a minimum of 3 mice/time points. Data in B, C, and D are presented as average ± SEM. ND, not detected; *$p < .05$, ****$p < .0001$

Time point	Day 7 p.i.	Day 7 p.i.	Day 14 p.i.	Day 14 p.i.
Diet	Control chow	PLX5622	Control chow	PLX5622
Tissue	Brain	Brain	Spinal cord	Spinal cord
Pooled N	6	6	7	5
Cell number	4,806	3,868	2,725	4,891
Reads/cell	54,593	61,984	111,721	41,498

Table 1 Overview of experimental conditions showing treatment, sacrifice time points, tissue collected, and total number of CD45+ cells isolated as well as reads/cell following scRNAseq analysis

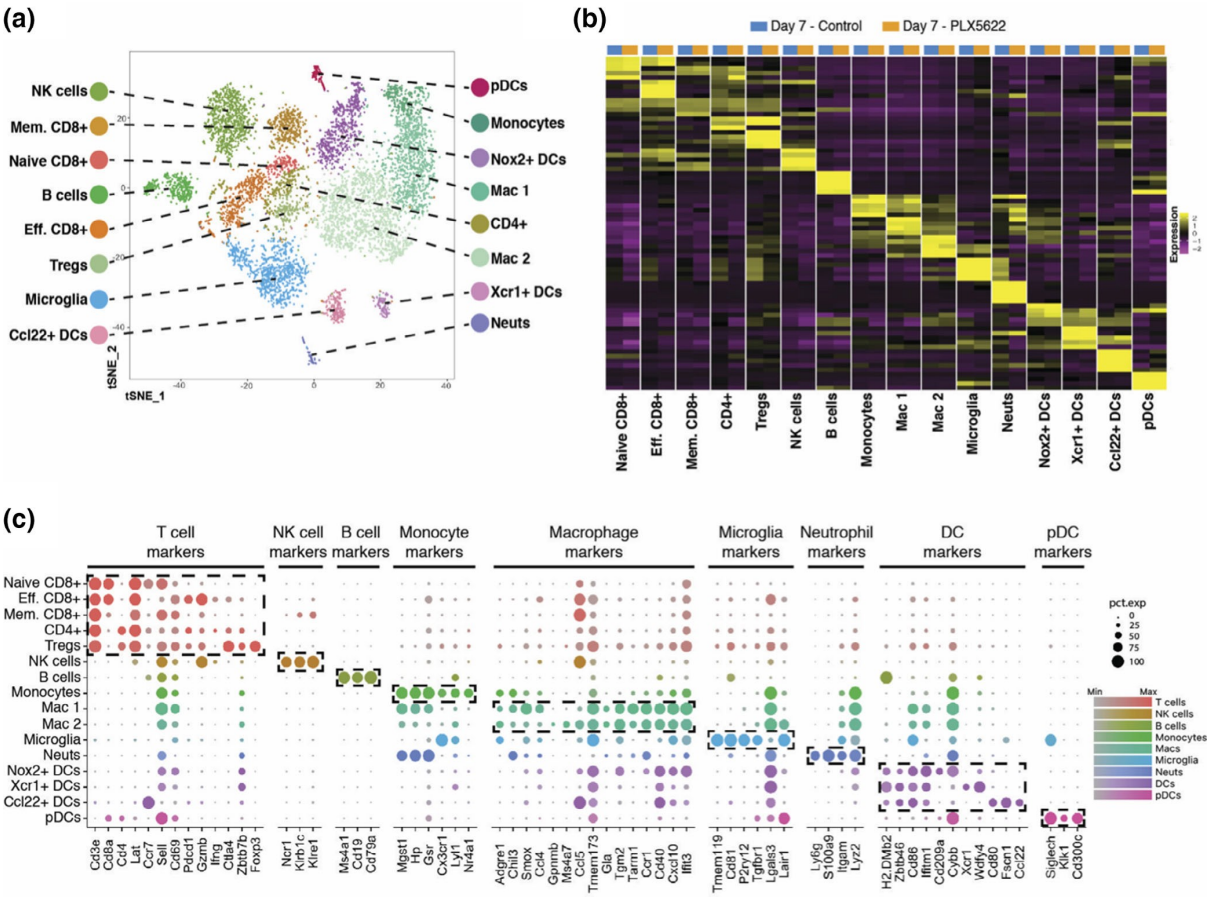

Figure 2 scRNAseq of CD45+ cells isolated from brains of JHMV-infected mice treated with PLX5622 at day 7 p.i. (a) T-distributed stochastic neighbor embedding (t-SNE) plot of scRNASeq data revealing 16 distinct cell clusters (aggregate data from PLX5622 and control treated animals at 7 days p.i). (b) Heat map showing the top five differentially expressed genes within each cluster. Columns represent the different clusters, with sub-columns displaying both control-treated (blue) and PLX5622-treated (orange) groups, and rows specify genes. (c) Dot plot presenting expression of selected genes within the 16 cell clusters. Size of the dot is representative of the frequency of cells within a cluster expressing the gene of interest, while the degree of color intensity is indicative of the level of expression of the gene. The dashed boxes highlight commonly and uniquely expressed genes of clusters within overarching cell types

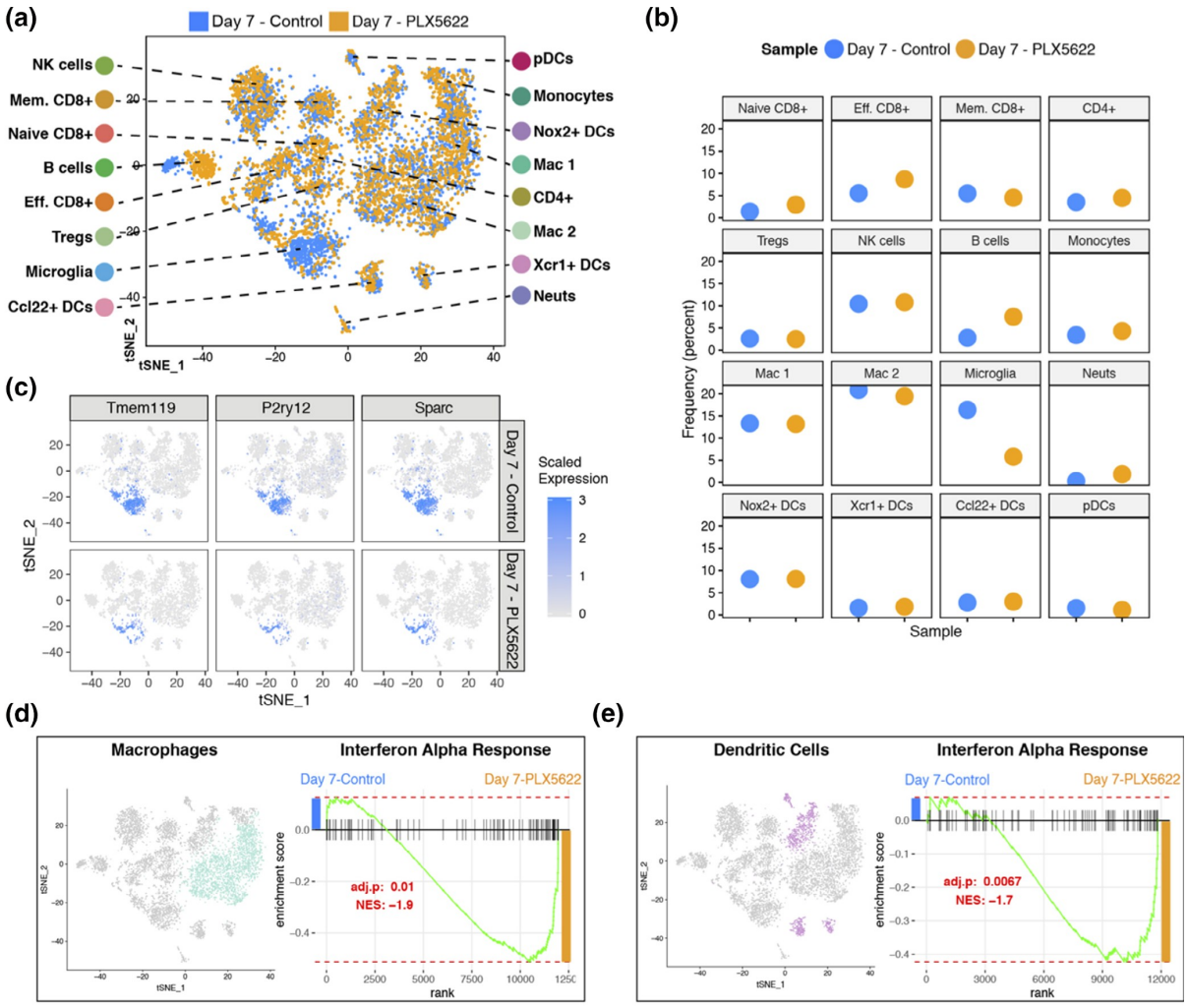

Figure 3 PLX5622 treatment and immune cell infiltration into the CNS at day 7 p.i. (a) t-SNE plot showing the immune landscape in brains of control-(blue) and PLX5622-(orange) treated animals at 7 days p.i. (b) Frequency of cell clusters in brains of control- and PLX5622-treated animals at 7 days post JHMV infection. (c) t-SNE plot showing decreased expression of microglia-associated transcripts Tmem119, P2ry12, and Sparc in PLX5622 mice compared with controls. Gene set enrichment analysis (GSEA) for IFN-α responses in combined (d) macrophage (teal) and (e) dendritic cell (purple) populations isolated at day 7 from brains of JHMV-infected mice treated with either PLX5622 or control chow, represented in t-SNE plots. Area under the curve represents enrichment of response genes. Responses to IFN-α were enriched in both macrophages and dendritic cells isolated from brains of PLX5622 mice compared with control animals at day 7 p.i. Normalized enrichment scores and *p* values are shown.

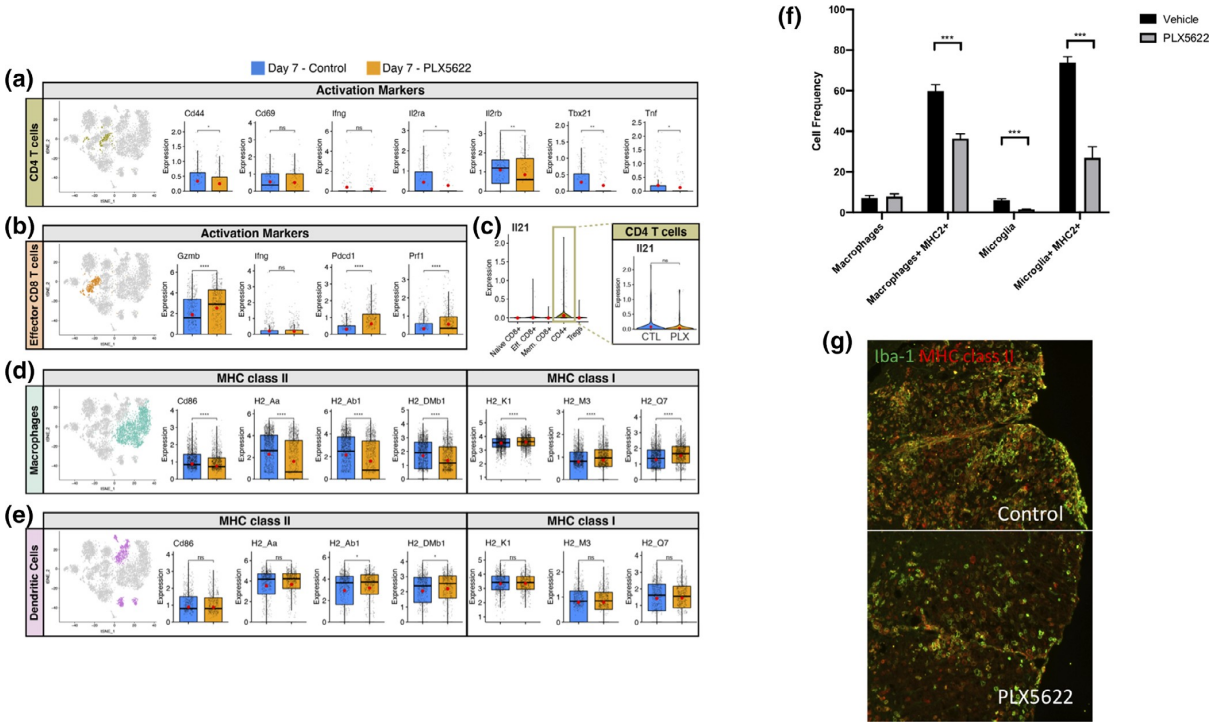

Figure 4 Altered T cell activation profiles in PLX5622-treated mice at day 7 p.i. t-SNE plot from brains of JHMV-infected mice treated with PLX5622 or control at day 7 p.i. showing (a) CD4+ T cells from either PLX5622-treated or control mice and box plots comparing expression of transcripts encoding for activation markers *Cd44* (CD44), *Cd69* (CD69), *Il2ra* (IL-2 receptor subunit alpha) *Il2rb* (IL-2 receptor subunit beta), *Tbx21* (Transcription factor T-bet) *Ifng* (interferon gamma), and *Tnf* (tumor necrosis factor alpha). (b) CD8+ T cells comparing the expression levels of transcripts encoding effector and activation markers in CD8+ T cells *Prf1* (Perforin), *Pdcd1* (Programmed cell death 1, PD1), *Gzmb* (Granzyme B), and *Ifng*. (c) Violin plots depicting expression of *Il21* transcripts within T cell populations isolated from the brains of experimental mice; there was no significant (ns) difference in expression of *Il21* in CD4+ T cells from control or PLX5622-treated mice. Expression of MHC class II-associated genes (*H2-Aa, H2-Ab1*, and *H-2DMb1*) and co-stimulatory molecule Cd86, as well as MHC class I-associated genes (*H2-K1, H2-M3, and H2-Q7*), are shown in (d) macrophages and (e) dendritic cells from experimental mice. In these plots, each dot represents a single cell. Normalized expression values were used and random noise was added to show the distribution of data points. The box plots show interquartile range and the median value (bold horizontal bar). Average expression value per sample is indicated by the red dots. Wilcoxon's test was used for statistical analysis. (f) MHC class II expression on macrophages (CD11b + $CD45^{high}$) and microglia (CD11b + $CD45^{lo}$) isolated from the brains of JHMV- infected mice treated with either PLX5622 or control at day 7 p.i. as determined by flow cytometric analysis. Data presented as average + SEM. (b) Representative immunofluorescent staining for MHC class II on spinal cords isolated from infected mice treated with either PLX5622 or control at day 7 p.i. ns, not significant; *$p < .05$; **$p < .01$ ***$p \leq .001$, ****$p \leq .0001$

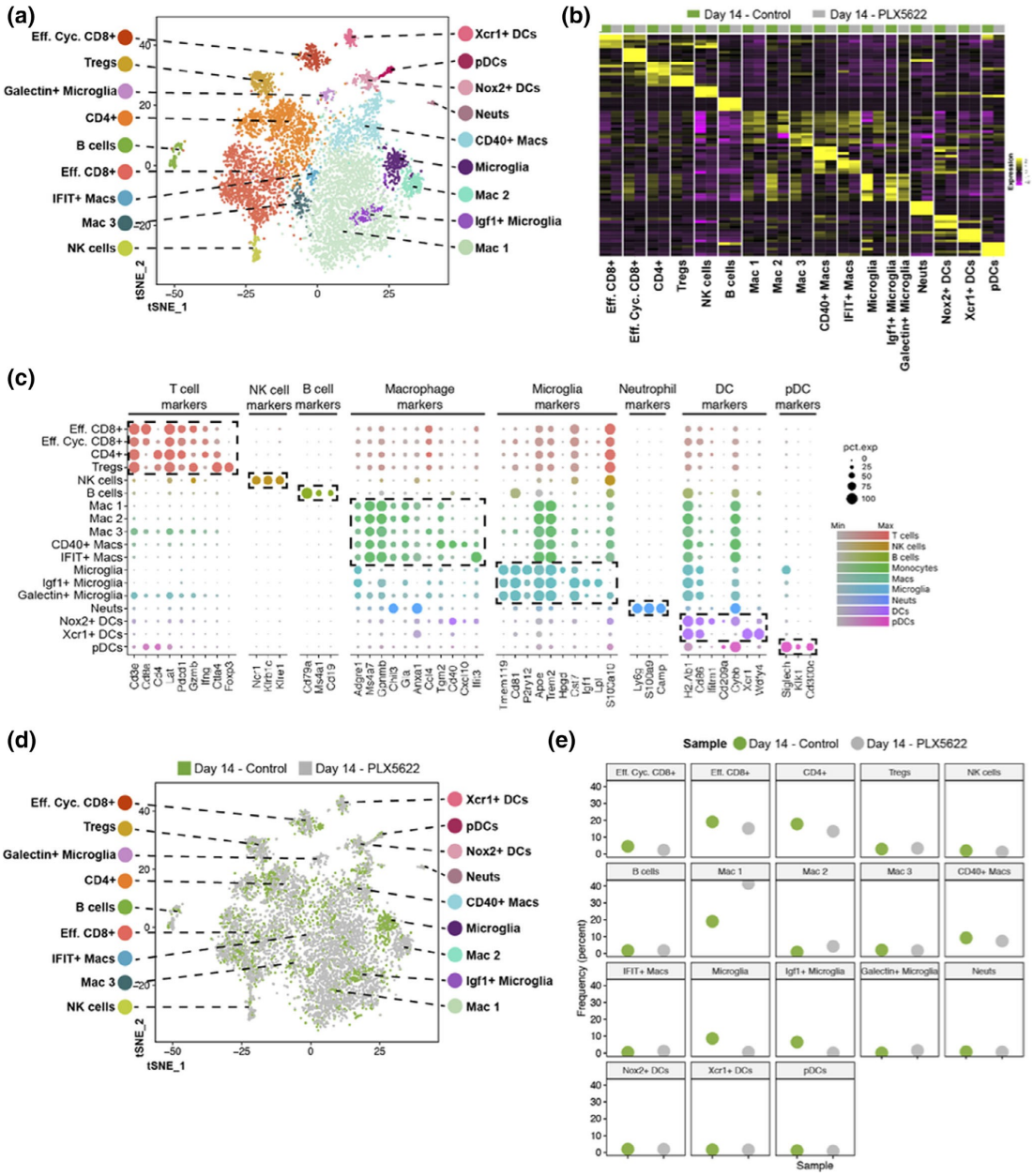

Figure 5 scRNAseq of CD45+ cells isolated from spinal cords of JHMV-infected mice treated with PLX5622 at day 14 p.i. (a) t-SNE plots of scRNASeq data revealing 18 distinct cell clusters. Aggregate data are from spinal cords isolated from PLX5622- and control-treated animals at 14 days p.i. (b) Heat map showing the top five differentially expressed genes within each cluster. Columns represent the different clusters, with sub-columns displaying both control-treated (green) and PLX5622-treated (gray) groups, and rows specify genes. (c) Dot plot presenting expression of selected genes within the 18 cell clusters. Size of the dot is representative of the frequency of cells within a cluster expressing the gene of interest, while the degree of color intensity is indicative of the level of expression of the gene. The dashed boxes highlight commonly and uniquely expressed genes of clusters within overarching cell types. (d) t-SNE plot showing the immune landscape in spinal cords of control-(green) and PLX5622-(gray) treated animals at day14 p.i. (e) Frequency of cell clusters in spinal cords of control- and PLX5622-treated animals at day 14 p.i.

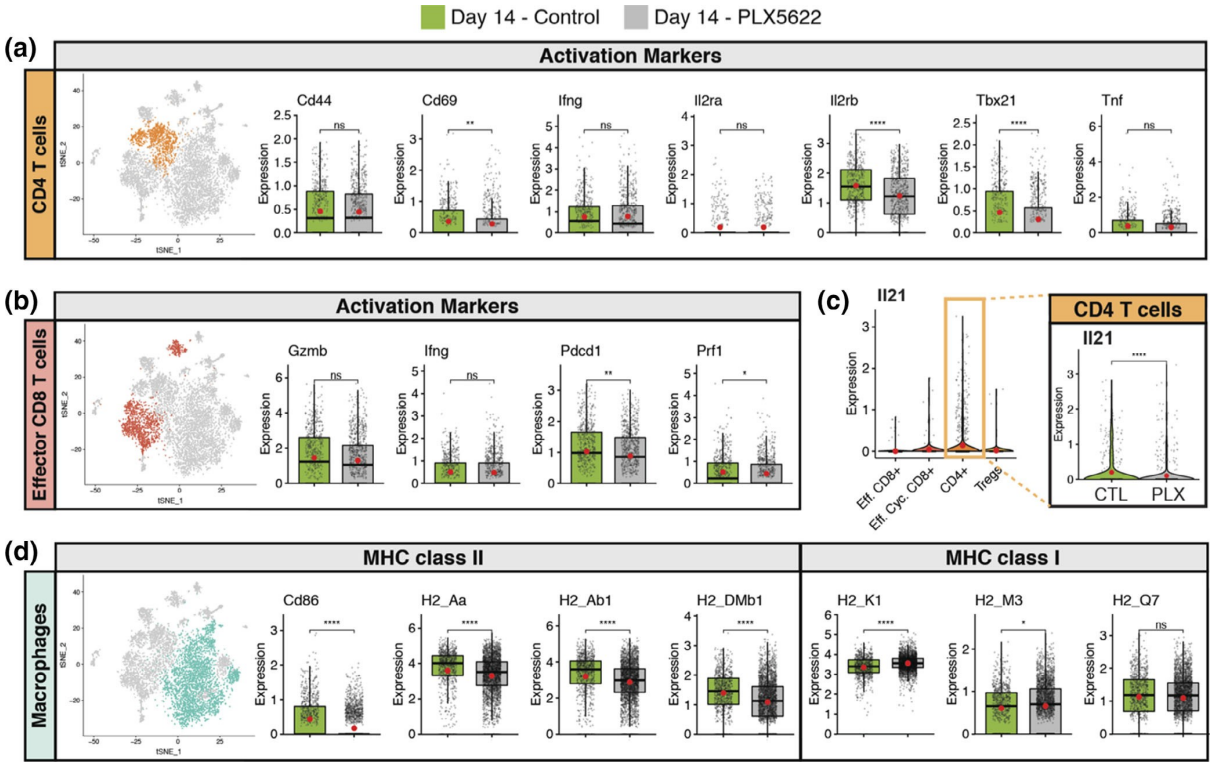

Figure 6 Muted activation profiles of spinal cord CD4+ T cells isolated from PLX5622-treated mice at day 14 p.i. JHMV-infected mice treated with either control chow or PLX5622 were sacrificed at day 14 p.i. and CD45+ cells sorted from spinal cords to evaluate mRNA expression profiles via scRNASeq. (a) CD4+ T cells from spinal cords of mice treated with PLX5622-treated or control mice, comparing expression of transcripts encoding for activation markers Cd44, Cd69, Il2ra, Il2rb, Tbx21, Ifng, and Tnf. (b) Expression levels of transcripts encoding effector and activation markers in CD8+ T cells *Prf1, Pdcd1, Gzmb*, and *Ifng*. (c) Violin plots depicting expression of *Il21* transcripts within T cell populations isolated from the spinal cords of experimental mice; expression is reduced ($p < .0001$) in CD4+ T cells from PLX5622-treated mice compared to controls. (d) Expression of MHC class II-associated genes (*H2-Aa, H2-Ab1*, and *H-2DMb1*) and co-stimulatory molecule *Cd86*, as well as MHC class I-associated genes (*H2-K1, H2-M3*, and *H2-Q7*), are shown in macrophages from experimental mice. In these plots, each dot represents a single cell. Normalized expression values were used and random noise was added to show the distribution of data points. The box plot shows interquartile range and the median value (bold horizontal bar). Average expression per sample is represented by the red dot. Wilcoxon test was used for statistical analysis. ns, not significant; *$p \leq .05$; ** $p \leq .01$; ****$p \leq .0001$

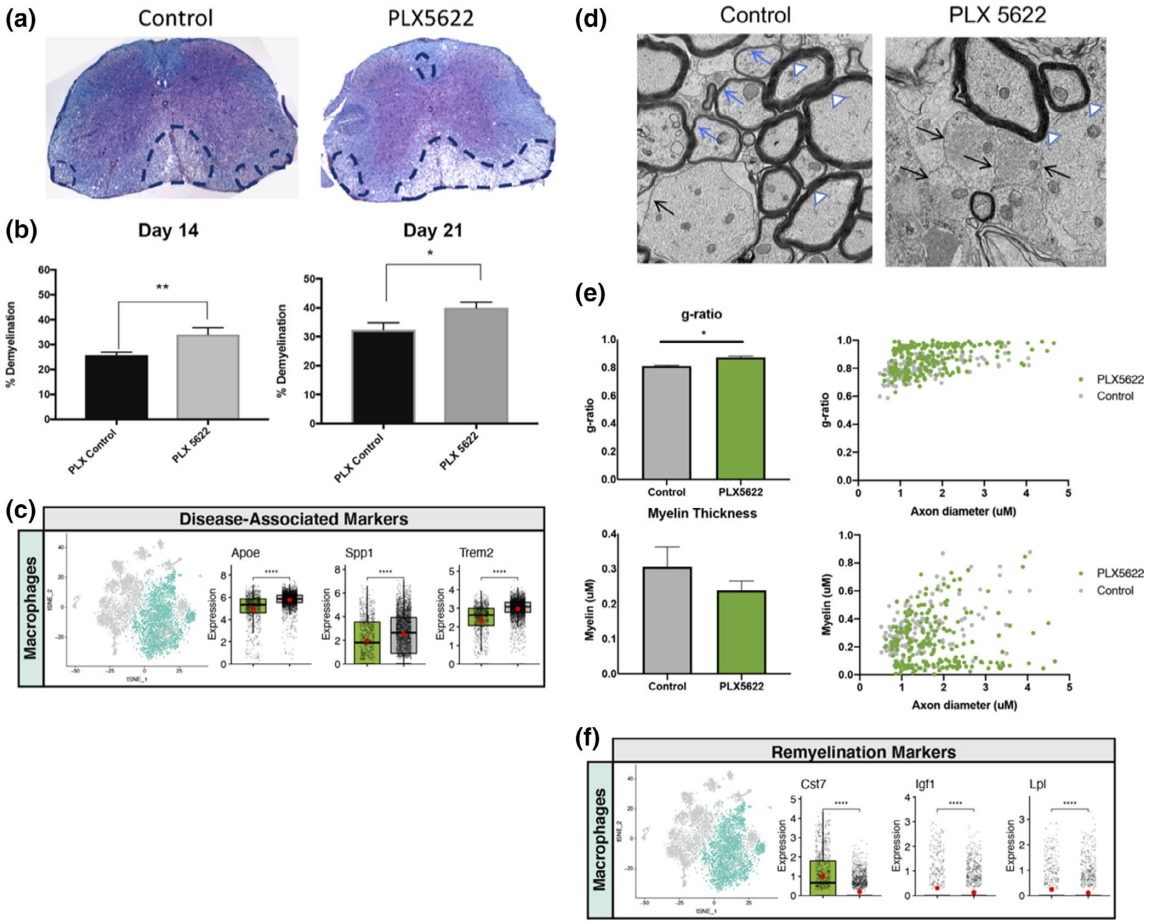

Figure 7 The severity of spinal cord demyelination is increased in PLX5622-treated mice compared with control mice. (a) Representative images of H&E/LFB-stained spinal cord sections showing an increase in severity of demyelination (dashed black lines) in JHMV-infected mice treated with PLX5622 compared with control treated mice at day 14 p.i. (b) Quantification of spinal cord demyelination reveals a significant increase after PLX5622 treatment compared with control-treated animals (minimum of 12 mice/experimental group) at days 14 and 21 p.i. (c) t- SNE plots showing increased expression of transcripts encoding disease-associated factors APOE (*Apoe*), Osteopontin (*Spp1*), and TREM2 (*Trem2*) in spinal cords of PLX5622-treated mice compared with controls at day 14 p.i. Normalized expression values were used, and random noise was added to show the distribution of data points. The box plots show interquartile range and the median value (bold horizontal bar). (d) Representative EM images (×1,200) from spinal cords from control and PLX5622-treated mice showing normal myelinated axons (white arrowheads), demyelinated axons (black arrows), and remyelinated axons (blue arrows) at day 21 p.i. (e) Calculation of *g*-ratio of control and PLX5622; scatter plot depicting individual *g*-ratio's from lateral white matter columns of control (gray) and PLX5622 (green) treated mice as a function of axon diameter. Data in panels b and e are presented as mean ± SEM. Average expression value per sample is indicated by the red points. Wilcoxon's test was used for statistical comparisons. (f) t-SNE plots showing decreased expression of transcripts encoding remyelination- associated markers Cystatin F (*Cst7*), Insulin growth factor 1 (*Igf1*), and Lipoprotein lipase (*Lpl*) in spinal cords of PLX5622-treated mice compared with controls at day 14 p.i. *$p < .05$, $p < .01$, ***$p < .001$, ****$p < .000$

Chapter 4

Timed ablation of microglia leads to increased demyelination and impaired remyelination in mice infected with a neurotropic murine coronavirus

ABSTRACT

Previous studies from our laboratory have demonstrated that ablation of microglia via administration of PLX5622, a small molecule antagonist specific for colony stimulating factor 1 receptor (CSF1R), to C57BL/6 mice prior to infection with the neurotropic JHM strain of mouse hepatitis virus (JHMV) results in increased mortality associated with impaired T cell-mediated control of viral replication combined with an increase in the severity of demyelination and impaired remyelination arguing for a protective role for microglia in response to the infection of the CNS with a neurotropic virus. To better understand how microglia impact disease progression in mice persistently infected with JHMV that have established demyelination, PLX5622 was administered to mice at day 14 post-infection (p.i.) and animals remained on drug for 14 days at which point animals were sacrificed and the severity of spinal cord demyelination and remyelination evaluated. Our findings indicate that PLX5622-mediated ablation of microglia for 2 weeks beginning at day 14 p.i. did not lead to an increase in mortality but resulted in a significant ($p<0.05$) increase in the severity of spinal cord demyelination at day 28 p.i. when compared to control mice. Infiltration of both total and virus-specific CD4+ and CD8+ T cells into the CNS was not affected in response to PLX5622-mediated microglia ablation yet control of viral replication was impaired that correlated with muted expression of MHC class II. Finally, we observed decreased expression of mRNA transcripts encoding remyelination-associated proteins Cystatin F and Lipoprotein lipase. BulkRNAseq analysis of spinal cords indicated that targeting microglia resulted in a dramatic reduction in gene expression profiles associated with cell-mediated immune responses and phagocytosis. These findings indicate that microglia continue to impact control of viral replication within the CNS post-acute phase of disease as well as restrict ongoing demyelination and remyelination in mice persistently infected with JHMV.

INTRODUCTION

Intracranial inoculation of susceptible C57BL/6 mice with the neuroadapted JHM strain of mouse hepatitis virus (JHMV, a member of the *Coronaviridae* family) results in an acute encephalomyelitis characterized by wide-spread replication of virus in astrocytes, oligodendroglia, and microglia with relative sparing of neurons. Innate immune responses characterized by the expression of type I interferons as well as other inflammatory cytokines and chemokines are critical with regards to controlling viral replication as well as attracting cellular components of the innate immune response[1]. This is highlighted by inflammatory neutrophils expressing the chemokine receptor CXCR2 that are attracted to the CNS of JHMV-infected mice by responding to the chemokine CXCL1[2]. Inflammatory neutrophils were important in host defense by secreting MMPs (matrix metalloproteinase) that increase the permeability of the blood-brain-barrier (BBB) which subsequently allows access of virus-specific CD4+ and CD8+ T cells that control viral replication via expression of anti-viral cytokines including IFN-γ as well as cytolytic activity[2(p2),3,4].

While inflammatory T cells are efficient in controlling viral replication and reducing viral titers, sterile immunity is not achieved and virus persists primarily in spinal cord white matter tracts[5]. Persistent viral infection within glial cells leads to expression of both T cell and monocyte/macrophage chemokine gene expression[6,7] resulting in chronic infiltration of these activated cells resulting in immune-mediated demyelination[8–10]. We and others have demonstrated an important role for $CD4^+$ and $CD8^+$ T cells in contributing to JHMV-induced demyelination[9,11–17], yet the contributions of glial cells to disease progression remain to be better characterized. Emerging studies have demonstrated that resident cells of the CNS are actively involved in either protection and/or disease progression[18]. Microglia are the resident immune

cells of the CNS. In mice, microglia derived from immature, uncommitted KIT+ erythromyeloid progenitors (EMPs) in the yolk sac at embryonic day 7.5 (E7.5)-E8.0. When derived, these progenitors will start to upregulate CD45 followed by myeloid cell markers, such as F4/80, CX3C chemokine receptor 1 (CXCR1), and colony-stimulating factor 1 receptor (CSF1R)[19]. Under non-inflamed disease states, microglia function to maintain tissue homeostasis and exhibit a ramified morphology. Under inflammatory conditions that occur in response to infection, injury, or disease onset e.g. MS or Alzheimer's disease (AD), microglia are rapidly activated and this results in morphologic changes associated with an amoeboid form and expression of pro-inflammatory cytokines/chemokines[20].

Immune-mediated demyelination is associated with activated microglia that are characterized by increased surface expression of CD68, CD86, and MHC class II antigens accompanied by the secretion of cytokines and chemokines. Accordingly, activated microglia can serve as antigen-presenting cells (APCs) to recruit activated antigen-sensitized T cells to the CNS. Therefore, activated microglia serve various functions under neuroinflammatory conditions resulting from either infection or onset of disease by presenting antigens and either amplifying or restricting disease progression via secretion of regulatory factors that control the activation state of inflammatory immune cells. Pharmacologic depletion of microglia via administration of PLX5622, a small molecule antagonist specific for colony stimulating factor 1 receptor (CSF1R), results in >95% ablation of microglia in recipient mice[21]. We have reported that PLX5622-mediated depletion of microglia prior to JHMV infection results in increased morbidity/mortality that is associated with impaired control of viral replication that was associated with muted anti-viral CD4+ T cell responses[22]. Moreover, microglia depletion resulted in a significant increase in the severity of demyelination accompanied by a reduction in

remyelination arguing that microglia augment both host defense as well as restrict myelin damage and influence repair[22]. Single cell RNA sequencing (scRNAseq) revealed that PLX5622-mediated reduction of microglia led to increased expression of transcripts of disease associated molecules (DAMs) including Osteopontin (*Spp1*), APOE (*Apoe*), and TREM2 (*Trem2*) while transcripts encoding remyelination factors such as Lipoprotein lipase (*Lpl*), Insulin growth factor alpha (*Igf1*) and Cystatin F (*Cst7*) are reduced when compared to control mice[22]. The current studies were undertaken to examine if PLX5622-mediated ablation of microglia following the onset of JHMV-induced demyelination affected the severity of immune cell infiltration into the CNS as well as demyelination and remyelination. Our results indicate that time ablation of microglia phenocopied our earlier studies in terms of an overall significant ($p<0.5$) increase in the severity of demyelination as well as impaired control of viral replication associated with decreased expression of MHC class II, and negatively impact remyelination efficiency with decreased expression of *Lpl* and *Cst7* in the spinal cord. These findings argue that microglia can restrict the severity of demyelination in mice persistently infected with JHMV as well as influence remyelination.

METHODS AND MATERIALS

Mice, viral infection, and PLX5622 treatment. C57BL/6 mice (male and female mice, 6-8 weeks of age) were purchased from the Jackson Laboratory. Mice were inoculated via intracranial (i.c.) infection with between 750-1000 plaque-forming units (PFU) of JHMV-CV34 in 30μL of sterile Hanks balanced sterile solution (HBSS). Inoculations were performed under deep anesthesia through an intraperitoneal injection of a mixture of ketamine and xylazine. AIN-76A (Research Diets, NJ) rodent chow formulated with CSF1R inhibitor-PLX5622 at a dose of 1200mg/kg was provided by Plexxikon, Inc (Berkeley, CA). Mice were continuously fed with either PLX5622 chow or control chow from day 14 p.i. until the mice were sacrificed to harvest brains and spinal cords at day 21 and 28 p.i. Clinical disease in JHMV-infected mice was evaluated using a previously described scale[23,24]. Vial titers within brains and spinal cords at defined days p.i. were determined by plaque assay on DBT astrocytoma cell line as described previously[25]. All experiments were performed following animal protocols approved by the University of California, Irvine Institutional Animal Care and Use Committee.

Cell isolation and flow cytometry. Flow cytometry was performed by using established protocols[26(p720),27]. In brief, single cell suspensions were generated from tissue samples by grinding and immune cells were enriched via a 2-step Percoll gradient (90% and 63%) and cells were collected at the interface of the two Percoll layers. Isolated cells were incubated with anti-CD16/32 Fc block (BD Biosciences, San Jose, CA) at a 1:200 dilution before staining with fluorescent antibodies. Immune cells were identified by staining with following cell surface markers: CD4, CD8 (eBioscience), CD11b (Abcam) and CD45 (BD Pharmingen). APC-conjugated rat anti-mouse CD4 and a PE-conjugated tetramer specific for the CD4

immunodominant epitope present within the JHMV matrix (M) glycoprotein spanning amino acids 133-147 (M133-147 tetramer) to determine total and virus-specific $CD4^+$ cells, respectively[27,28]; APC-conjugated rat anti-mouse CD8a and a PE-conjugated tetramer specific for the CD8 immunodominant epitope present in the spike (S) glycoprotein spanning amino acids 510-518 (S510-518) to identify total and virus-specific $CD8^+$ cells, respectively[27,28]. Data were collected using an ACEA NovoCyte 2060 flow cytometer and analyzed with FlowJo software (Tree Star Inc.).

Histology and immunohistochemical staining. Experimental mice were euthanized at defined time points p.i. and tissues were harvested according to IACUC-approved guidelines. Tissues were collected and placed in 4% PFA for fixation and subsequent histological analysis. Following fixation, the 24-48hr brains were cryoprotected in 30% sucrose, embedded in O.C.T., and sliced via Cryostat in 10µm sagittal sections. Sliced tissues were stained with hematoxylin/eosin (H&E) in combination with luxol fast blue (LFB) to assess demyelination within the spinal cords of experimental mice. Areas of total white matter and demyelinated white matter were determined with ImageJ software and demyelination was scored as percentage of total demyelination from spinal cord sections analyzed[26,28–30]. For immunohistochemical staining, slides were rinsed with PBS to remove residual O.C.T., and antigen retrieval (incubation with 10mM sodium Citrate at 95ºC for 15min) was performed if required for specific antigens at which point samples were incubated with 5% normal goat serum and 0.1% Triton-X, followed by overnight incubation at 4 ºC with primary antibodies. Several primary antibodies were used, including Iba1 (1:500 Wako), Mac2/ Galactin-3 (1:500, CL8942AP Cedarlane), GFAP (1:1000 Abcam), MHC I (1:200 Abcam), and MHC II (1:200 Abcam). On the second day,

slides were treated with appropriate secondary antibodies (1:1000 goat anti-rat/rabbit Invitrogen, 1:1000 goat anti-chicken, Abcam) following PBS rinsing. Slides were then mounted with DAPI Fluoromount-G (SouthernBiotech). High-resolution fluorescent images were obtained using Revolve-D75.

qPCR analysis. RNA from mice spinal cords was extracted via the RNeasy Mini Kit (Qiagen, 74106) using the "Purification of Total RNA, Including Small RNAs, from Animal Tissues" protocol. TRIzol was substituted for QIAzol, and Buffer RW1 was substituted for Buffer RWT. cDNA was made by following the "First Strand cDNA Synthesis" standard protocol provided by New England Biolabs with their AMV Reverse Transcriptase (New England Biolabs, M0277L). Random hexamers (Invitrogen, N8080127) were used for the reactions. qPCRs were performed using the Bio-Rad iQ5 and iTaq™ Universal SYBR® Green Supermix (Bio-Rad, 1725120). Reactions were 10µL, and the machine was set to run for 1 cycle (95℃ for 3 minutes), followed by 40 cycles (95℃ for 10 seconds, then 55℃ for 30 seconds). The following primer sequences were used:

Gene target	**Forward Sequence**	**Reverse Sequence**
GAPDH	AACTTTGGCATTGTGGAAGG	GGATGCAGGGATGATGTTCT
JHMV	TCAACCCCGAAACAAACAACC	GGCTGTTAGTGTATGGTAATCCTCA
Trem2	CTACCAGTGTCAGAGTCTCCGA	CCTCGAAACTCGATGACTCCTC
ApoE	GAACCGCTTCTGGGATTACCTG	GCCTTTACTTCCGTCATAGTGTC
Spp1	GCTTGGCTTATGGACTGAGGTC	CCTTAGACTCACCGCTCTTCATG
Igf1	GTGGATGCTCTTCAGTTCGTGTG	TCCAGTCTCCTCAGATCACAGC
Lpl	GCGTAGCAGGAAGTCTGACCAA	AGCGTCATCAGGAGAAAGGCGA
Cst7	AAGGAGTCCCATGTCAGCAAAGC	GTCTTCCTGCATGTAGTTCGGC

Ct values for each sample were normalized to an internal control (GAPDH), yielding the dCt values.

Electron microscopy and g-ratio analysis. For EM analysis of spinal cords, mice were sacrificed and underwent cardiac perfusion with 0.1 M cacodylate buffer containing 2% paraformaldehyde/2% glutaraldehyde. Serial ultrathin sections of spinal cords embedded in Epon epoxy resin were stained with uranyl acetate-lead citrate and analyzed as previously described[22]. Images at 1200X magnification were analyzed for *g*-ratio using Image J software. In adult animals there is a relationship between axon circumference and myelin sheath thickness (number of lamellae) expressed by the g-ratio (axon diameter/total fiber diameter); in remyelination this relationship changes such that myelin sheaths are abnormally thin for the axons they surround[31]. An abnormally thin myelin sheath, relative to axonal diameter, was used as the criterion for oligodendrocyte remyelination. Absence of a myelin sheath was used as the criterion for demyelination. For most axons, two measurements were conducted with a minimum of 400 axons analyzed per experimental group.

RNA sequencing. Whole transcriptome RNAseq libraries were produced from spinal cords of control and PLX5622 treated mice sacrificed at day 28 p.i.. RNA was isolated with a RNeasy Mini Kit (Qiagen, Valencia, USA) according to the manufacturer's instructions. Library preparation, RNA sequencing, and read mapping analysis were performed by Novagene Co.

Statistical analysis. GraphPad Prism was used to perform statistical analyses. Data for each experiment is presented as mean±standard error of mean (SEM). For flow cytometry analysis

unpaired Student's *t* test was used to determine significance and a *p* value of < 0.05 was considered statistically significant.

RESULTS

Timed ablation of microglia in JHMV-infected mice leads to impaired control of viral replication.

To evaluate the contribution of microglia to demyelination following onset of JHMV-induced demyelination, JHMV-infected mice were fed formulated chow containing either PLX5622 (1,200 mg/kg) or control chow beginning at day 14 p.i. and mice were kept on either PLX5622 or control chow until sacrificed at days 21 and 28 p.i. at which point brains and spinal cords were collected to assess viral burden and neuropathology. Notably, there were no differences in either clinical disease severity or survival (**Figure 1A and B**) between PLX5622 and control chow-treated mice; however, targeting microglia resulted in higher viral titers within the brains at days 21 and 28 p.i. compared to control mice as determined by plaque assay (**Figure 1C**). Using flow cytometry, we confirmed efficient microglia ($CD45^{lo}CD11b+$) depletion in PLX5622-treated mice within the brain at days 21 p.i. ($p<0.05$) and 28 p.i. ($p<0.005$) (**Figure 2A and B**). PLX5622 treatment did not affect numbers of macrophages ($CD45^{hi}CD11b+$) within brains of experimental mice (**Figure 2A and B**). PLX5622-treatment also reduced microglia numbers within the spinal cords while not affecting macrophages a day 21 p.i. (**Figure 2C**). Immunohistochemical staining for microglia and inflammatory monocyte/macrophages via Iba1 and Mac2 expression, respectively[32] confirmed that PLX5622 did result in reduced staining for Iba1-positive microglia within the spinal cords of mice whereas inflammatory Mac2-positive monocyte/macrophages were not affected (**Figure 2D**).

T cell infiltration into the CNS of PLX5622-treated is not altered.

Virus-specific CD4+ and CD8+ cells are required to control viral replication during acute disease via secretion of anti-viral cytokines. We have previously showed that PLX5622-mediated reduction of microglia within the CNS of mice prior to JHMV infection results in an impaired ability to control viral replication that was associated with a selective decrease in expression of MHC class II on inflammatory monocyte/macrophages and this correlated with muted CD4+ T cell activation[22]. Virus-specific CD4+ T cells enhance anti-viral activity of virus-specific CD8+ T cells arguing that the impaired control of viral replication in PLX5622-treated mice during acute disease was due, in part, to dampened anti-viral T cell effector responses[22]. Initiating PLX5622 treatment at day 14 in JHMV-infected mice did not affect infiltration of total CD4+ or CD8+ T cells into the brain compared to control mice at days 21 and 28 p.i. (**Figure 3A**). Moreover, there were no differences in virus-specific CD4+ and CD8+ T cells in brains at days 21 and 28 p.i. (**Figure 3B**). Expression of MHC class II was reduced within the spinal cords of PLX5622-treated mice compared to controls while MHC class I expression was unaffected as determined by immunohistochemical (**Figure 3C-E**). These findings indicate that microglia continue to support the control of coronavirus replication within the CNS past the acute stage of disease and this is dependent upon continued activation of virus-specific CD4+ T cells via MHC class II expression on inflammatory cells from the periphery which are presumably monocyte/macrophages.

Microglia restrict the severity of demyelination in mice persistently with JHMV.

Previous studies from our laboratory as well as Perlman and colleagues[22,33]have indicated that depletion of microglia prior to JHMV infection results in an increase in the severity of demyelination as well as limiting remyelination arguing that microglia function to limit white

matter damage and promote myelin repair. In order to determine if depletion of microglia in mice persistently infected with JHMV with established demyelination affects the severity of demyelination, JHMV-infected mice were fed either PLX5622-formulated chow or control chow beginning at day 14 p.i. and were subsequently sacrificed at days 21 and 28 p.i. to assess the severity of spinal cord demyelination by luxol fast blue (LFB) staining of the spinal cord. PLX5622-mediated ablation of microglia starting at day 14 did not affect the severity of spinal cord demyelination at day 21 p.i between experimental groups; however, by day 28 p.i. demyelination was significantly ($p<0.05$) increased in PLX5622-treated mice when compared to control mice (**Figure 4A-C**). To further evaluate the severity of demyelination in experimental groups of mice, EM analysis of spinal cord sections was performed. Assessment of the *g*-ratio, the ratio of the inner axonal diameter to the total outer fiber diameter, is commonly employed as a structural index of both demyelination and remyelination with lower ratios indicating myelination[22,34]. Preliminary analysis of spinal cords revealed calculation of g-ratio's indicated no difference in spinal cord myelination between PLX5622-treated mice compared to control animals arguing that in mice persistently infected with JHMV microglia do not impact remyelination but do help restrict the severity of white matter damage (**Figure 4D-F**).

Targeting microglia impacts expression of immune response pathways. Next generation RNA sequencing was performed on spinal cords from experimental mice at day 28 p.i. in order to try and identify how ablation of microglia affected specific gene pathways associated with host defense, demyelination, and repair. Using this approach, we were able to identify differentially expressed genes (DEGs) between JHMV-infected PLX5622-treated and control mice. We determined ~95% (13,532 genes) of DEGs were common between the two

experimental groups with PLX5622-treated mice having 515 unique DEGs and control having 253 suggesting microglia depletion affected gene expression (**Figure 5A**). PLX5622 treatment resulted in impaired expression of microglia-associated genes including *Tmem119*, *P2ry12*, *Cx3cr1,* and *Csfr1* (**Figure 5B**). Heat map analysis further emphasizes the overall impact of microglia ablation on DEGs within the spinal cords of JHMV-infected mice (**Figure 5C**). Moreover, PLX5622-mediated targeting of microglia resulted in a dramatic reduction in immunology-related pathways that can impact the control of viral replication as well as potentially contribute to demyelination and remyelination (**Figure 6**).

DISCUSSION

In this study, we demonstrate that microglia continue to restrict the severity of demyelination as well as contribute to remyelination in mice persistently infected with demyelination. Ablation of microglia in JHMV-infected mice beginning at 2 weeks p.i. which represents a time in which replicating virus is controlled and demyelination is established resulted in an increase in the severity of demyelination as well as dampened control of viral replication. In addition, our data suggest that remyelination is also impaired. These findings complement earlier studies from our laboratory[22] and Perlman and colleagues[35] that demonstrated that targeted ablation of microglia prior to JHMV infection resulted in decreased survival, impaired control of viral replication, increased demyelination, and impaired remyelination. The current study was performed to assess whether microglia continue to function in a protective manner in animals persistently infected with JHMV with established demyelination. Our findings indicate that microglia continue to protect against demyelination and aid in remyelination as well as control viral replication. These results also demonstrate the lack of redundancy of macrophages and microglia in the demyelinated CNS. These results are consistent with others describing distinct functions for microglia and macrophages in CNS pathologies[36–38]. In one EAE study, macrophages were associated with demyelination, while microglia were anti-inflammatory and required for debris removal[36].

The mechanisms by which microglia aid in controlling appear to be through regulating expression of MHC class II on monocyte/macrophages that are infected with virus. This is most likely mediated directly via secretion of cytokines that selectively influence MHC class II expression but not expression of MHC class I. In addition, inflammatory virus-specific T cells

secrete IFN-γ that could also activate microglia to express cytokines/chemokines that impact expression of MHC class II on monocyte/macrophages.

Our findings that spinal cord demyelination was significantly increased in PLX5622-treated mice persistently infected with JHMV support a role for microglia in restricting the severity of white matter[22,35,39]. We are continuing to explore the molecular and cellular mechanisms by which microglia modulate the CNS microenvironment that influence demyelination. We found that depletion of microglia does not affect mRNA expression of DAMs that we identified in our previous study[22] including Osteopontin (*Spp1*), *ApoE*, and *Trem2*. However, the expression of molecules associated with remyelination including Cystatin F (*Cst7*) and Lipoprotein lipase (*Lpl*) were negatively affected after depletion of microglia which consistent with our previous study[22], but the mRNA expression of Insulin growth factor 1 (*Igf1*) was not affect in the PLX5622-treated mice spinal cords compare to the controls. Emerging studies have pointed to a protective role for microglia in limiting neuropathology and promoting repair[40–42]. In support of this concept are recent studies from Miron and colleagues[42] showing an important role for microglia in enhancing remyelination in a toxin-model of demyelination that is aided by microglial death and subsequent microglial repopulation. Although mechanisms by which microglia may support remyelination have not been completely defined, it is thought that these cells aid in clearance of myelin debris and/or secrete growth factors/cytokines that influence maturation of oligodendrocyte progenitor cells (OPCs) into mature myelin-producing oligodendrocytes.

To summarize, our data, in conjunction with previous reports[22], indicate distinct roles for microglia in mice infected with a neurotropic coronavirus on not only facilitating control of viral replication and enhancing remyelination and limiting demyelination but also modulating the immunological landscape by altering transcriptomes of multiple biological process pathways.

REFERENCES

1. Ireland DDC, Stohlman SA, Hinton DR, Atkinson R, Bergmann CC. Type I Interferons Are Essential in Controlling Neurotropic Coronavirus Infection Irrespective of Functional CD8 T Cells. *Journal of Virology*. Published online January 2008. doi:10.1128/JVI.01794-07

2. Hosking MP, Tirotta E, Ransohoff RM, Lane TE. CXCR2 Signaling Protects Oligodendrocytes and Restricts Demyelination in a Mouse Model of Viral-Induced Demyelination. *PLOS ONE*. 2010;5(6):e11340. doi:10.1371/journal.pone.0011340

3. Marro BS, Skinner DD, Cheng Y, et al. Disrupted CXCR2 Signaling in Oligodendroglia Lineage Cells Enhances Myelin Repair in a Viral Model of Multiple Sclerosis. *Journal of Virology*. Published online June 26, 2019. doi:10.1128/JVI.00240-19

4. Zlokovic BV. Remodeling after stroke. *Nat Med*. 2006;12(4):390-391. doi:10.1038/nm0406-390

5. Bergmann CC, Lane TE, Stohlman SA. Coronavirus infection of the central nervous system: host–virus stand-off. *Nat Rev Microbiol*. 2006;4(2):121-132. doi:10.1038/nrmicro1343

6. Lane TE, Asensio VC, Yu N, Paoletti AD, Campbell IL, Buchmeier MJ. Dynamic Regulation of α- and β-Chemokine Expression in the Central Nervous System During Mouse Hepatitis Virus-Induced Demyelinating Disease. *The Journal of Immunology*. 1998;160(2):970-978.

7. Syage AR, Ekiz HA, Skinner DD, Stone C, O'Connell RM, Lane TE. Single-Cell RNA Sequencing Reveals the Diversity of the Immunological Landscape following Central Nervous System Infection by a Murine Coronavirus. Gallagher T, ed. *J Virol*. 2020;94(24):e01295-20. doi:10.1128/JVI.01295-20

8. Lane TE, Liu MT, Chen BP, et al. A Central Role for CD4+ T Cells and RANTES in Virus-Induced Central Nervous System Inflammation and Demyelination. *Journal of Virology*. Published online February 1, 2000. doi:10.1128/JVI.74.3.1415-1424.2000

9. Glass WG, Hickey MJ, Hardison JL, Liu MT, Manning JE, Lane TE. Antibody Targeting of the CC Chemokine Ligand 5 Results in Diminished Leukocyte Infiltration into the Central Nervous System and Reduced Neurologic Disease in a Viral Model of Multiple Sclerosis. *The Journal of Immunology*. 2004;172(7):4018-4025. doi:10.4049/jimmunol.172.7.4018

10. Liu MT, Keirstead HS, Lane TE. Neutralization of the Chemokine CXCL10 Reduces Inflammatory Cell Invasion and Demyelination and Improves Neurological Function in a Viral Model of Multiple Sclerosis. *The Journal of Immunology*. 2001;167(7):4091-4097. doi:10.4049/jimmunol.167.7.4091

11. Iacono KT, Kazi L, Weiss SR. Both Spike and Background Genes Contribute to Murine Coronavirus Neurovirulence. *Journal of Virology*. Published online July 2006. doi:10.1128/JVI.00432-06

12. Parra B, Hinton DR, Marten NW, et al. IFN-γ Is Required for Viral Clearance from Central Nervous System Oligodendroglia. *The Journal of Immunology*. 1999;162(3):1641-1647.

13. Bergmann CC, Parra B, Hinton DR, Ramakrishna C, Dowdell KC, Stohlman SA. Perforin and Gamma Interferon-Mediated Control of Coronavirus Central Nervous System Infection by CD8 T Cells in the Absence of CD4 T Cells. *Journal of Virology*. Published online February 15, 2004. doi:10.1128/JVI.78.4.1739-1750.2004

14. Marten NW, Stohlman SA, Bergmann CC. MHV Infection of the CNS: Mechanisms of Immune-Mediated Control. *Viral Immunology*. 2001;14(1):1-18. doi:10.1089/08828240151061329

15. Glass WG, Lane TE. Functional Expression of Chemokine Receptor CCR5 on CD4+ T Cells during Virus-Induced Central Nervous System Disease. *Journal of Virology*. Published online January 1, 2003. doi:10.1128/JVI.77.1.191-198.2003

16. Liu MT, Chen BP, Oertel P, et al. Cutting Edge: The T Cell Chemoattractant IFN-Inducible Protein 10 Is Essential in Host Defense Against Viral-Induced Neurologic Disease. *The Journal of Immunology*. 2000;165(5):2327-2330. doi:10.4049/jimmunol.165.5.2327

17. Liu MT, Armstrong D, Hamilton TA, Lane TE. Expression of Mig (Monokine Induced by Interferon-γ) Is Important in T Lymphocyte Recruitment and Host Defense Following Viral Infection of the Central Nervous System. *The Journal of Immunology*. 2001;166(3):1790-1795. doi:10.4049/jimmunol.166.3.1790

18. Benarroch EE. Microglia: Multiple roles in surveillance, circuit shaping, and response to injury. *Neurology*. 2013;81(12):1079-1088. doi:10.1212/WNL.0b013e3182a4a577

19. Prinz M, Priller J. Microglia and brain macrophages in the molecular age: from origin to neuropsychiatric disease. *Nat Rev Neurosci*. 2014;15(5):300-312. doi:10.1038/nrn3722

20. Yin J, Valin KL, Dixon ML, Leavenworth JW. The Role of Microglia and Macrophages in CNS Homeostasis, Autoimmunity, and Cancer. *Journal of Immunology Research*. 2017;2017:e5150678. doi:10.1155/2017/5150678

21. Dagher NN, Najafi AR, Kayala KMN, et al. Colony-stimulating factor 1 receptor inhibition prevents microglial plaque association and improves cognition in 3xTg-AD mice. *J Neuroinflammation*. 2015;12(1):139. doi:10.1186/s12974-015-0366-9

22. Mangale V, Syage AR, Ekiz HA, et al. Microglia influence host defense, disease, and repair following murine coronavirus infection of the central nervous system. *Glia*. 2020;68(11):2345-2360. doi:10.1002/glia.23844

23. Houtman JJ, Fleming JO. Dissociation of demyelination and viral clearance in congenitally immunodeficient mice infected with murine coronavirus JHM. *Journal of Neurovirology*. 1996;2(2):101-110. doi:10.3109/13550289609146543

24. Lane TE, Fox HS, Buchmeier MJ. Inhibition of nitric oxide synthase-2 reduces the severity of mouse hepatitis virus-induced demyelination: implications for NOS2/NO regulation of chemokine expression and inflammation. *Journal of Neurovirology*. 1999;5(1):48-54. doi:10.3109/13550289909029745

25. Hirano N, Murakami T, Fujiwara K, Matsumoto M. Utility of mouse cell line DBT for propagation and assay of mouse hepatitis virus. *Jpn J Exp Med*. 1978;48(1):71-75.

26. Blanc CA, Rosen H, Lane TE. FTY720 (fingolimod) modulates the severity of viral-induced encephalomyelitis and demyelination. *Journal of Neuroinflammation*. 2014;11(1):138. doi:10.1186/s12974-014-0138-y

27. Chen L, Coleman R, Leang R, et al. Human Neural Precursor Cells Promote Neurologic Recovery in a Viral Model of Multiple Sclerosis. *Stem Cell Reports*. 2014;2(6):825-837. doi:10.1016/j.stemcr.2014.04.005

28. Marro BS, Grist JJ, Lane TE. Inducible Expression of CXCL1 within the Central Nervous System Amplifies Viral-Induced Demyelination. *The Journal of Immunology*. 2016;196(4):1855-1864. doi:10.4049/jimmunol.1501802

29. Blanc CA, Grist JJ, Rosen H, Sears-Kraxberger I, Steward O, Lane TE. Sphingosine-1-Phosphate Receptor Antagonism Enhances Proliferation and Migration of Engrafted Neural Progenitor Cells in a Model of Viral-Induced Demyelination. *The American Journal of Pathology*. 2015;185(10):2819-2832. doi:10.1016/j.ajpath.2015.06.009

30. Dickey LL, Worne CL, Glover JL, Lane TE, O'Connell RM. MicroRNA-155 enhances T cell trafficking and antiviral effector function in a model of coronavirus-induced neurologic disease. *Journal of Neuroinflammation*. 2016;13(1):240. doi:10.1186/s12974-016-0699-z

31. Smith KJ, Bostock H, Hall SM. Saltatory conduction precedes remyelination in axons demyelinated with lysophosphatidyl choline. *J Neurol Sci*. 1982;54(1):13-31. doi:10.1016/0022-510x(82)90215-5

32. Hohsfield LA, Tsourmas KI, Ghorbanian Y, et al. MAC2 is a long-lasting marker of peripheral cell infiltrates into the mouse CNS after bone marrow transplantation and coronavirus infection. *Glia*. 2022;70(5):875-891. doi:10.1002/glia.24144

33. Wheeler DL, Sariol A, Meyerholz DK, Perlman S. Microglia are required for protection against lethal coronavirus encephalitis in mice. *J Clin Invest*. 2018;128(3):931-943. doi:10.1172/JCI97229

34. Moore S, Khalaj AJ, Yoon J, et al. Therapeutic laquinimod treatment decreases inflammation, initiates axon remyelination, and improves motor deficit in a mouse model of multiple sclerosis. *Brain Behav*. 2013;3(6):664-682. doi:10.1002/brb3.174

35. Microglia depletion exacerbates demyelination and impairs remyelination in a neurotropic coronavirus infection. PNAS. Accessed April 18, 2022. https://www.pnas.org/doi/abs/10.1073/pnas.2007814117

36. Yamasaki R, Lu H, Butovsky O, et al. Differential roles of microglia and monocytes in the inflamed central nervous system. *J Exp Med*. 2014;211(8):1533-1549. doi:10.1084/jem.20132477

37. London A, Cohen M, Schwartz M. Microglia and monocyte-derived macrophages: functionally distinct populations that act in concert in CNS plasticity and repair. *Front Cell Neurosci*. 2013;7:34. doi:10.3389/fncel.2013.00034

38. Kronenberg G, Uhlemann R, Richter N, et al. Distinguishing features of microglia- and monocyte-derived macrophages after stroke. *Acta Neuropathol*. 2018;135(4):551-568. doi:10.1007/s00401-017-1795-6

39. Brown DG, Soto R, Yandamuri S, et al. The microbiota protects from viral-induced neurologic damage through microglia-intrinsic TLR signaling. *eLife*. 8:e47117. doi:10.7554/eLife.47117

40. Baaklini CS, Rawji KS, Duncan GJ, Ho MFS, Plemel JR. Central Nervous System Remyelination: Roles of Glia and Innate Immune Cells. *Frontiers in Molecular Neuroscience*. 2019;12. Accessed April 18, 2022. https://www.frontiersin.org/article/10.3389/fnmol.2019.00225

41. Lee J, Hamanaka G, Lo EH, Arai K. Heterogeneity of microglia and their differential roles in white matter pathology. *CNS Neuroscience & Therapeutics*. 2019;25(12):1290-1298. doi:10.1111/cns.13266

42. Lloyd AF, Miron VE. The pro-remyelination properties of microglia in the central nervous system. *Nat Rev Neurol*. 2019;15(8):447-458. doi:10.1038/s41582-019-0184-2

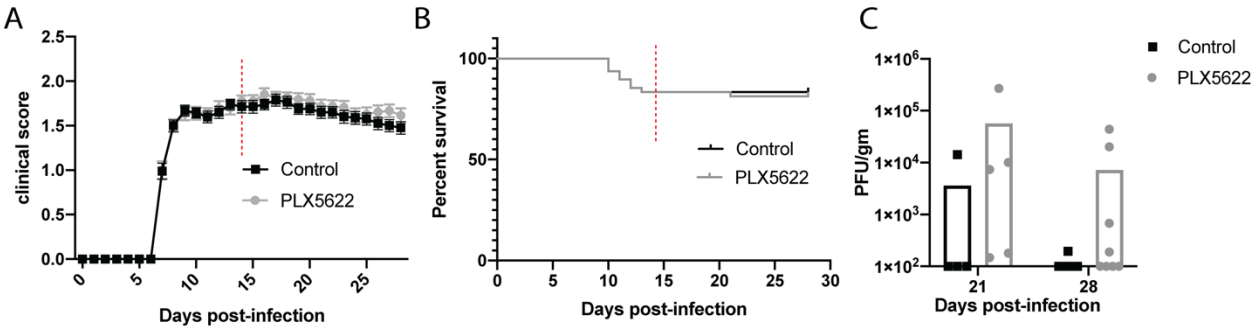

Figure 1 Treatment of JHMV-infected mice with PLX5622 beginning at day 14 p.i. does not affect clinical disease or survival. JHMV-infected mice were fed either PLX5622 or control chow beginning at day 14 p.i. with JHMV (750-1000 PFU) through day 28 p.i. PLX5622 treatment does not affect either (**A**) clinical disease (n=44 per group) or (**B**) survival (n=44 per group) compared to control mice. The red dash line indicates the time point that we begin PLX5622 treatment. (**C**) PLX5622-treatment led to an increase of viral titers within the brains at days 21 and 28 p.i. (control n=4 at day 21 p.i., n=9 at day 28 p.i.; PLX5622 n=5 at day 21p.i., n=9 at day 28 p.i.) compared to control mice as determined by plaque assay.

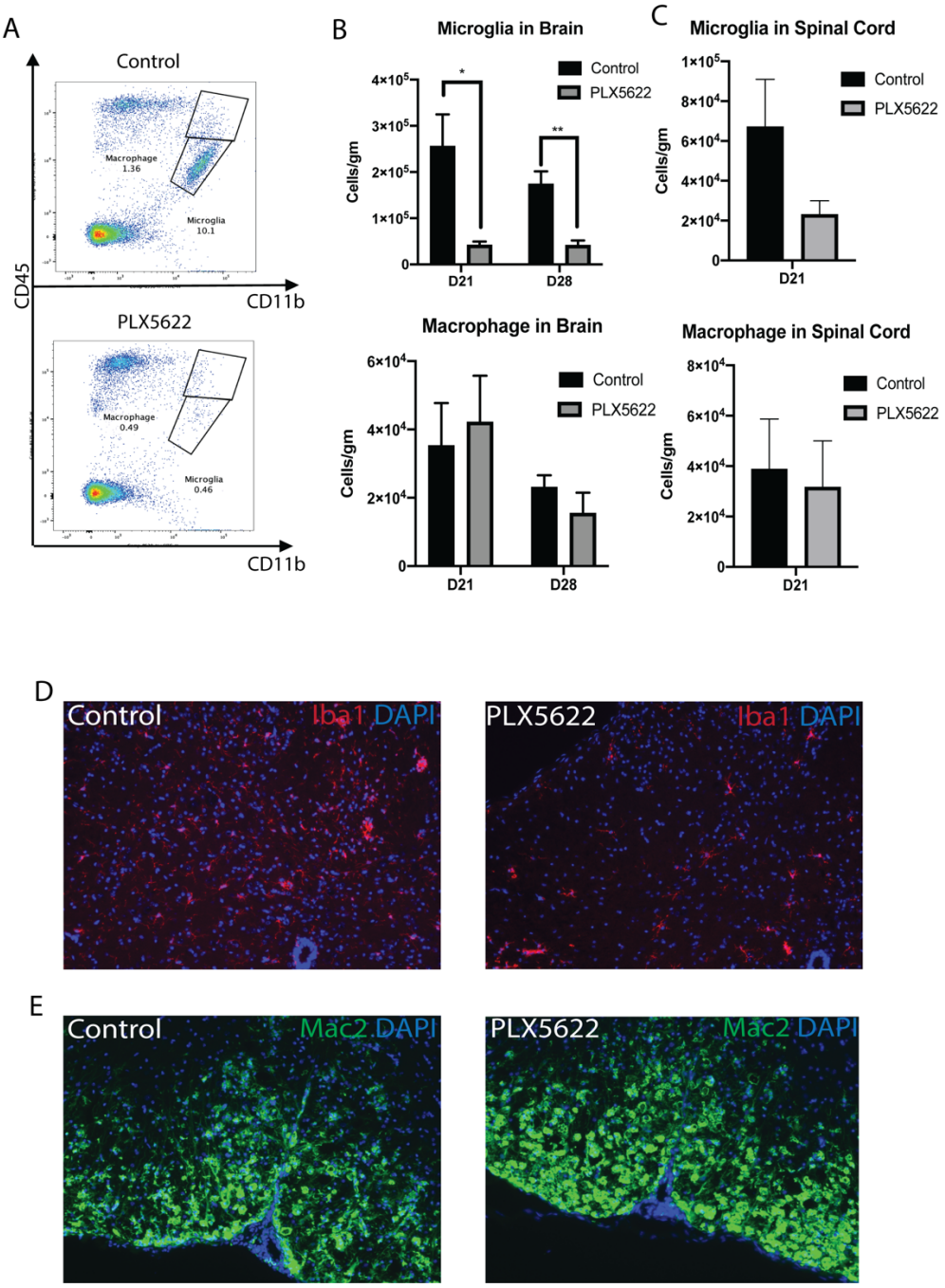

Figure 2 PLX5622 selectively targets microglia in mice persistently infected with JHMV. (**A**) Representative flow cytometric data from JHMV-infected mice treated with either PLX5622 or control chow and gating on microglia ($CD45^{lo}CD11b^{+}$ cells) or macrophages ($CD45^{hi}$ $CD11b^{+}$ cells) quantified in (**B**) brains at day 21 and 28 p.i. (n=6 per group at day 21 p.i.; n=4 per group at day 28 p.i.) and (**C**) spinal cords at day 21 p.i. (n=5 per group). PLX5622-treatment resulted in reduced numbers of microglia in brains at day 21 p.i. ($p<0.05$) and day 28 p.i. ($p<0.005$) compared to control mice. Immunohistochemistry data also indicate that (**D**) microglia (Iba1) have been depleted but (**E**) macrophages (Mac2) have not been affected at day 28 p.i. in the brain. Data in *B* and *C* are presented as average $\pm$ SEM.

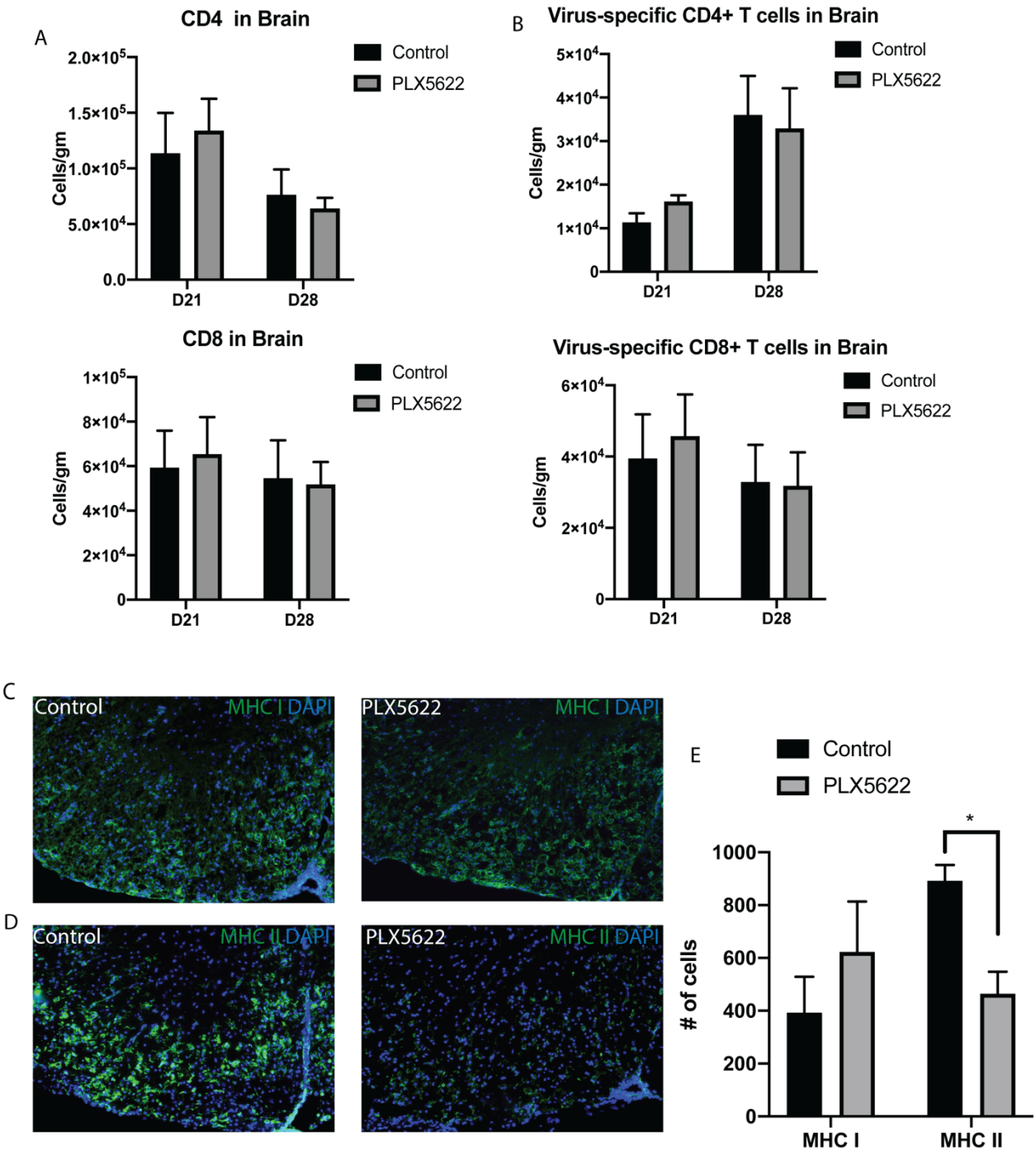

Figure 3 PLX5622 treatment does not affect T cell infiltration but reduces MHC class II expression. (**A**) Infiltration of CD4+ T cells and CD8+ T cells and (**B**) virus-specific CD4+ T cells and virus-specific CD8+ T cells from either PLX5622-treated or control mice brains were detected by flow cytometry (n=6 per group at day 21 p.i.; n=4 per group at day 28 p.i.). Immunohistochemistry data of (**C**) MHC class I and (**D**) MHC class II shows that (**E**) there was a decrease of MHC class II expression from PLX5622-treated mice compared to the controls. Data in *A*, *B,* and *E* are presented as average ± SEM.

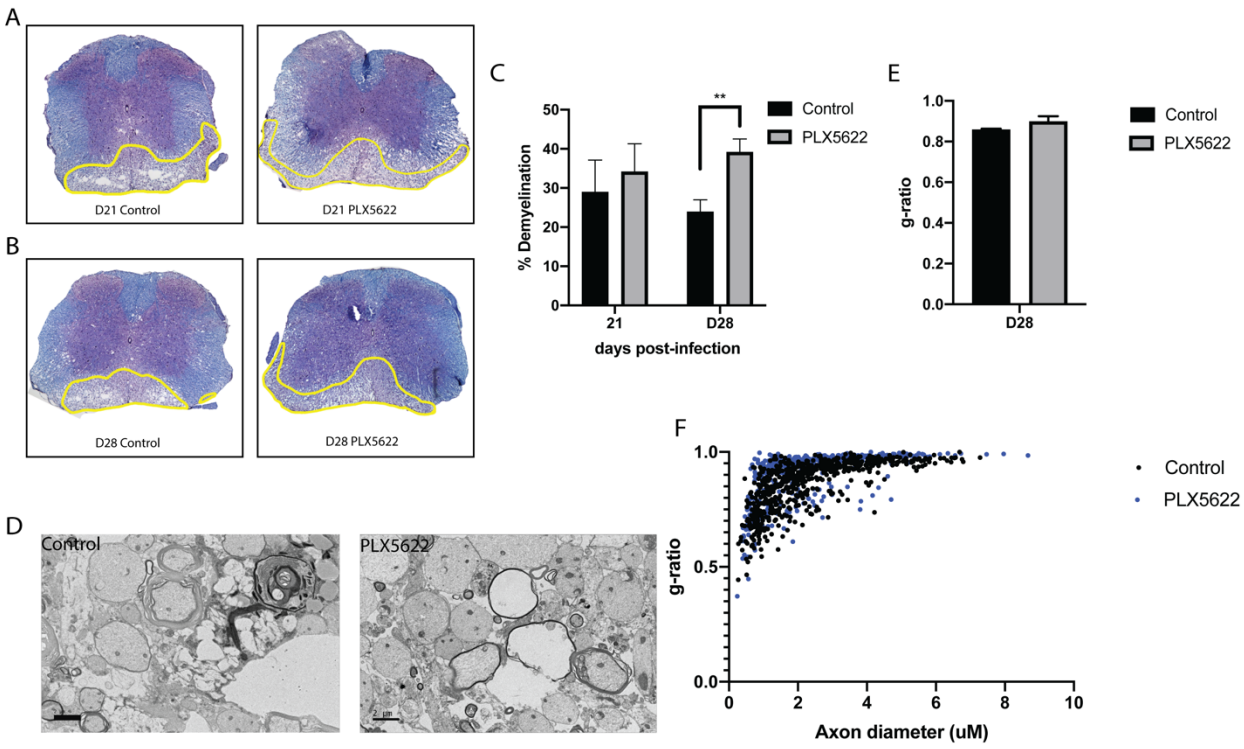

Figure 4 The severity of spinal cord demyelination is increased in PLX5622-treated mice compared to control mice. JHMV-infected mice treated with either control chow or PLX5622 from day 14 p.i. were sacrificed at day 21 or 28 p.i. and spinal cords were removed to evaluate the severity of demyelination. Representative images of H&E/LFB-stained spinal cord sections showing an increase in severity of demyelination (yellow line) in JHMV-infected mice treated with PLX5622 compared to control treated mice at day (**A**) 21 p.i. and (**B**) 28 p.i.. (**C**) Quantification of spinal cord demyelination (control n=4 at day 21 p.i., n=9 at day 28 p.i.; PLX5622 n=5 at day 21p.i., n=12 at day 28 p.i.) reveals a significant ($p<0.005$) increase after PLX5622 treatment compared to control-treated animals at 28 p.i.. (**D**) Representative EM images with magnification x1200 from control and PLX5622 mice spinal cord. (**E**) Calculation of g-ratio of control and PLX5622, scatter plot (**F**) depicting individual g-ratio's from lateral and ventral white matter columns of control and PLX5622 treated mice as a function of axon diameter. Data in *C* and *E* are presented as average $\pm$ SEM.

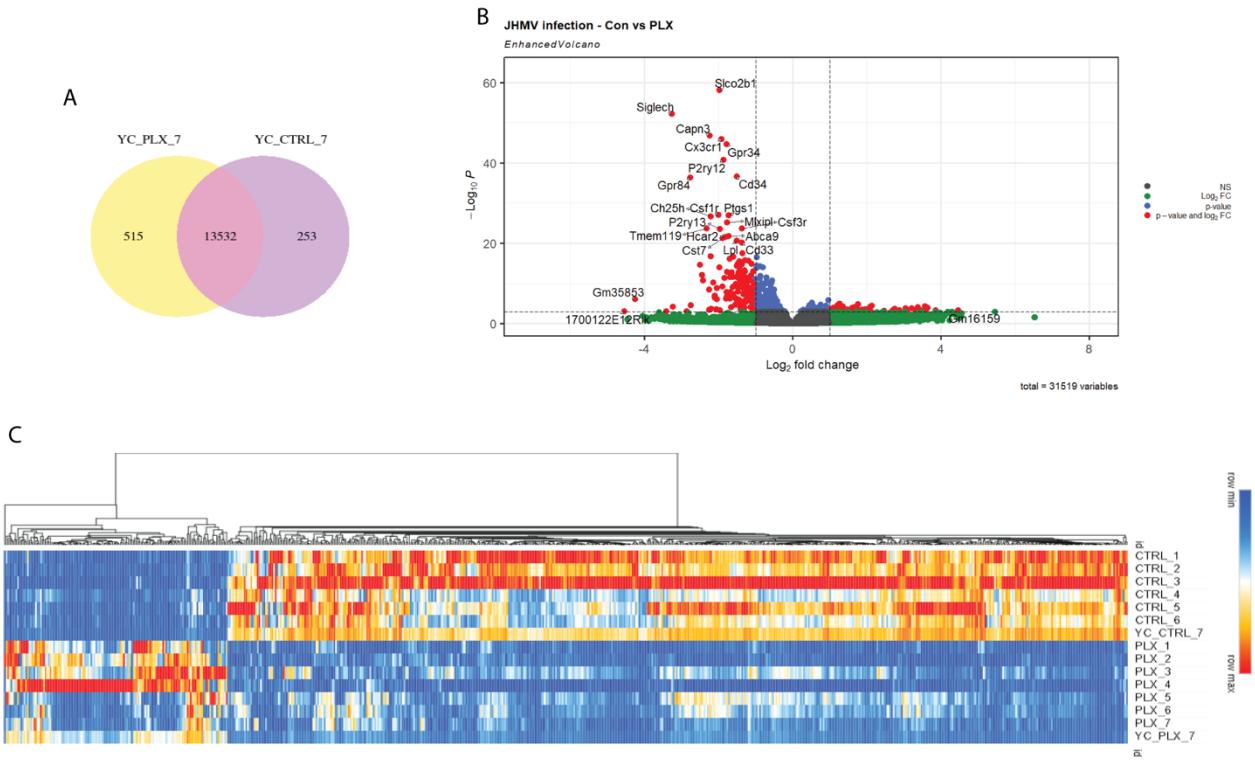

Figure 5 Targeting microglia impacts immune response related gene expression. RNA sequencing was performed on spinal cords from experimental mice at day 28 p.i.. (**A**) The correlation of DEGs between control and PLX5622 treated mice. (**B**) Volcano graph of DEGs between control and PLX5622 treated mice. (**C**) Heat map analysis.

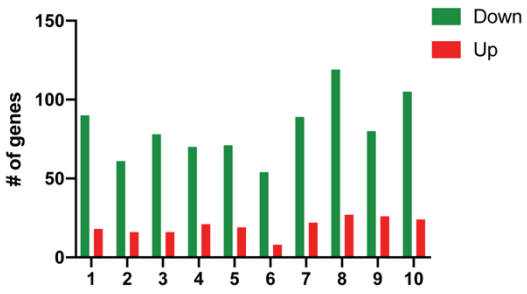

1	adaptive immune response
2	adaptive immune response based on somatic recombination of immune receptors built from immunoglobulin superfamily domains
3	leukocyte mediated immunity
4	leukocyte migration
5	leukocyte proliferation
6	phagocytosis
7	positive regulation of cytokine production
8	positive regulation of immune response
9	regulation of immune effector process
10	regulation of leukocyte activation

Figure 6 Targeting microglia impacts expression of immune response pathways. JHMV-infected mice treated with either control chow or PLX5622 from day 14 p.i. were sacrificed at day 28 p.i. and spinal cords were removed for RNA sequencing. Above are the top 10 biological process pathways that have been affected after PLX5622 treatment compare to controls.

CHAPTER 5

Summary

5.1. Summary and Significance

Cxcr2 signaling in oligodendrocytes contributes to the remyelination in the viral model of Multiple Sclerosis. Several excellent rodent models of MS have been developed that have greatly increased our understanding of molecular and cellular mechanisms contributing to both demyelination as well as remyelination. Infection of susceptible mice with the neurotropic JHM strain of mouse hepatitis virus (JHMV) represents a well-accepted model of viral-induced neurologic disease that shares many clinical and histopathological similarities with MS. Intracranial (i.c.) infection of susceptible strains of mice such as C57BL/6 with JHMV results in an acute encephalomyelitis that is accompanied by gray matter involvement with infection of oligodendrocytes, astrocytes, and microglia[2]. In response to JHMV infection of the CNS, there is a rapid synthesis of mRNA transcripts encoding proinflammatory cytokines and chemokines.

Chemokines are expressed early in response to JHMV infection of the CNS and have important functional roles in host defense during acute disease. Expression of CXCL1 serves to attract neutrophils to the CNS by signaling through the receptor CXCR2 expressed on the neutrophil cell surface. The importance of attracting neutrophils is highlighted by the demonstration that blocking the migration of these cells via treatment with neutralizing anti-CXCR2 results in increased mortality and impaired ability to control viral replication[3]. In addition, CXCR2 is also expressed on neurons[4,5], cerebral endothelial cells[6(p2),7], as well as resident glia, including microglia[4,8] and oligodendrocytes[9(p2),10–14]. *Cxcr2* expression on oligodendroglia offers an interesting target for studying possible remyelination strategies. CXCR2 has been shown to be important in myelination during development as well as remyelination in response to immune-mediated demyelination. During development, CXCR2 signaling is involved in the positional migration of OPCs, and ablating Cxcr2 leads to deficits in

myelin production and oligodendrocyte numbers[15]. Additionally, OPCs taken from Cxcr2 knockout mice have reduced ability to differentiate into mature oligodendrocytes *in vitro*[15]. Furthermore, in MS patient samples CXCR2 expression was found on both proliferating and mature oligodendrocytes within active lesion areas[9,16]. CXCR2 expressing oligodendrocytes were also found closely associated with CXCL1 positive astrocytes, highlighting a role for this pathway during MS disease. In pre-clinical demyelinating models of disease, CXCR2 has also been shown to play a role in oligodendrocyte survival and maturation. In the JHMV model, CXCR2 signaling is important in protecting oligodendroglia from apoptosis. Indeed, anti-CXCR2 treatment increased white mature damage and disease severity without affecting infiltrating immune cells during the chronic phase of disease[10(p2),10,14]. Additionally, CXCR2 signaling is protective in vitro against IFN-γ induced apoptosis of mouse and human OPCs[10(p2),14]. This is important in the context of JHMV infection as IFN-γ is primarily secreted to help control viral replication but can also damage infected cells such as oligodendrocytes. However, the numbers of earlier studies used either global genetic knockout of *Cxcr2* or anti-CXCR2 treatment, which target broadly all cell types that express this chemokine pathway making it hard to target the effects to a certain cell type.

Because multiple cell types express CXCR2 and we know that CXCR2 function is important for the recruitment of neutrophils which can augment demyelination, it is important to develop cell-specific strategies to better understand how the CXCR2 signaling pathway affects oligodendroglia biology, demyelination, and remyelination. Recent studies by Ransohoff and colleagues using a transgenic mouse in which *Cxcr2* was selectively ablated in oligodendroglia found that silencing *Cxcr2* in both the cuprizone and LPC models of toxin-induced demyelination stimulated remyelination[12].

Therefore, our laboratory developed a transgenic mouse model in which *Cxcr2* is conditionally ablated within oligodendroglia in adult mice following tamoxifen treatment. In addition, upon tamoxifen-induced ablation of *Cxcr2*, tdTomato expression is activated making it possible to identify fluorescently labeled cells. Using this mouse model, we found that silencing *Cxcr2* on oligodendroglia did not affect infiltrating immune cells, viral load, or clinical disease. Importantly, *Cxcr2* silencing also did not affect the severity of demyelination between tamoxifen or control treated mice nor did it affect the production of myelin in naïve mice. However, we did find that silencing CXCR2 signaling resulted in an increase in mature oligodendrocytes and enhanced spinal cord remyelination following JHMV induced demyelination. This is an important step in discerning cell type specific function of CXCR2 signaling pathway in models of disease and repair.

Functional contribution of microglia in demyelination and remyelination in viral model of Multiple Sclerosis. Resident glial cells clearly aid in host defense in response to microbial infection through various effector functions including secretion of IFN-I as well as proinflammatory cytokines/chemokines that assist in attracting cellular components of both the innate and adaptive immune response. However, more refined roles for resident glia in host defense in response to microbial infection are being discovered. As indicated above, production of IFN-I by activated microglia relies, in part, on prostaglandin D2 signaling via D-prostanoid receptor 1 (DP1)[17]. However, defining discrete functional roles of microglia in terms of host defense in response to JHMV infection is challenging in the face of infiltrating myeloid cells that may have overlapping functions. In the face of these challenges, Perlman and colleagues[18] provided an important study that further emphasizes that microglia are an active participant

involved in an effective host response following JHMV infection of the CNS. Through use of an inhibitor of colony stimulating factor 1 receptor (CSF1R) that depletes microglia, yet only has a minimal effect on macrophages, it was determined that microglia play a critical role in both the early innate as well as virus-specific T cell responses. As early as day 4 post-infection, there is a dramatic increase in gene expression within microglia with the majority of genes being associated with IFN signaling and activation of IFN-regulatory factors. Depletion of microglia resulted in a dramatic increase in mortality that correlated with impaired ability to control viral replication within the CNS. In addition, microglia depletion led to increased infiltration of monocyte/macrophages into the CNS—although these cells had a less mature phenotype characterized by reduced MHC class II and elevated Ly6C expression. In addition, there was an overall increase in numbers of virus-specific CD8+ T cells yet there was an overall reduction in frequency and numbers of IFN-γ-producing CD4+ T cells and this likely contributed to the increase in viral titers within the CNS. Collectively, these findings illustrate important and previously unappreciated roles for microglia in contributing to protection from viral encephalomyelitis.

To examine the functional role of microglia in either host defense and/or disease in response to JHMV infection of the CNS, we administered the CSF1R inhibitor PLX5622 to deplete microglia 7 days prior to infection. We found that elimination of microglia resulted in similar results described by Perlman and colleagues[19] in that there was reduced survival accompanied by impaired control of viral replication that was associated with muted CD4+ anti-viral T cell responses and decreased expression of MHC class II on antigen-presenting monocytes/macrophages[20]. In addition, increased spinal cord demyelination was associated with increased expression of DAMs including Osteopontin, TREM2, and APOE by inflammatory

monocyte/macrophages while the reduction in remyelination correlated with reduced expression of Lipoprotein lipase, Cystatin F, and Insulin Growth Factor 1. Collectively, these findings support previous studies that microglia enhance host defense in response to infection with a neurotropic murine coronavirus as well as modulate the CNS environment to alter expression of genes involved with both demyelination and remyelination.

We also determined whether targeted ablation of microglia in mice persistently infected with JHMV that had established demyelination either improved white matter damage or further increased the severity of demyelination. Administration of PLX5622 to JHMV-infected mice at day 14 resulted in increased spinal cord demyelination associated with an increase in viral burden which correlated with a reduction in the expression of MHC class II on inflammatory myeloid cells. We also determined via qPCR that expression of remyelination-associated factors Lipoprotein lipase and Cystatin F were decreased in PLX5622-treated mice compared to controls. These findings argue that in mice persistently infected with JHMV, microglia continue to function in aiding in the control of viral replication as well as limiting the severity of white matter damage. Furthermore, we performed bulkRNA sequencing of spinal cords obtained from JHMV-infected mice fed with either PLX5622 or control chow and found that depletion of microglia impact expression of immune response related genes and negatively affect multiple biological process pathways.

5.2 Future direction.

Our laboratory will continue to explore mechanisms by which microglia tailor the CNS microenvironment to promote effective control of viral replication through increased expression of MHC class II as well as other potential important anti-viral effector mechanisms. Similarly,

we are interested in how microglia impact both demyelination and remyelination through regulating expression of DAMs as well as remyelination-associated molecules. To this end, we will assess remyelination through electron microscopic evaluation of spinal cords from experimental mice in order to calculate *g*-ratio. Furthermore, we will employ CyTOF to better understand the cellular landscape that exists in PLX5622-treated or control mice.

5.3 References

1. Tsunoda I, Fujinami RS. Neuropathogenesis of Theiler's Murine Encephalomyelitis Virus Infection, An Animal Model for Multiple Sclerosis. *J Neuroimmune Pharmacol*. 2010;5(3):355-369. doi:10.1007/s11481-009-9179-x

2. Bergmann CC, Lane TE, Stohlman SA. Coronavirus infection of the central nervous system: host–virus stand-off. *Nat Rev Microbiol*. 2006;4(2):121-132. doi:10.1038/nrmicro1343

3. Hosking MP, Liu L, Ransohoff RM, Lane TE. A Protective Role for ELR+ Chemokines during Acute Viral Encephalomyelitis. *PLOS Pathogens*. 2009;5(11):e1000648. doi:10.1371/journal.ppat.1000648

4. Lin YF, Liu TT, Hu CH, Chen CC, Wang JY. Expressions of chemokines and their receptors in the brain after heat stroke-induced cortical damage. *Journal of Neuroimmunology*. 2018;318:15-20. doi:10.1016/j.jneuroim.2018.01.014

5. Xu J, Zhu MD, Zhang X, et al. NFκB-mediated CXCL1 production in spinal cord astrocytes contributes to the maintenance of bone cancer pain in mice. *J Neuroinflammation*. 2014;11(1):38. doi:10.1186/1742-2094-11-38

6. Wu F, Zhao Y, Jiao T, et al. CXCR2 is essential for cerebral endothelial activation and leukocyte recruitment during neuroinflammation. *J Neuroinflammation*. 2015;12(1):98. doi:10.1186/s12974-015-0316-6

7. Zhang R, Zhang Z, Wang L, et al. Activated neural stem cells contribute to stroke-induced neurogenesis and neuroblast migration toward the infarct boundary in adult rats. *J Cereb Blood Flow Metab*. 2004;24(4):441-448. doi:10.1097/00004647-200404000-00009

8. Ryu JK, Cho T, Choi HB, Jantaratnotai N, McLarnon JG. Pharmacological antagonism of interleukin-8 receptor CXCR2 inhibits inflammatory reactivity and is neuroprotective in an animal model of Alzheimer's disease. *J Neuroinflammation*. 2015;12:144. doi:10.1186/s12974-015-0339-z

9. Omari KM, John G, Lango R, Raine CS. Role for CXCR2 and CXCL1 on glia in multiple sclerosis. *Glia*. 2006;53(1):24-31. doi:10.1002/glia.20246

10. Tirotta E, Ransohoff RM, Lane TE. CXCR2 signaling protects oligodendrocyte progenitor cells from IFN-γ/CXCL10-mediated apoptosis. *Glia*. 2011;59(10):1518-1528. doi:10.1002/glia.21195

11. Tsai HH, Frost E, To V, et al. The chemokine receptor CXCR2 controls positioning of oligodendrocyte precursors in developing spinal cord by arresting their migration. *Cell*. 2002;110(3):373-383. doi:10.1016/s0092-8674(02)00838-3

12. Liu L, Spangler LC, Prager B, et al. Spatiotemporal ablation of CXCR2 on oligodendrocyte lineage cells: Role in myelin repair. *Neurol Neuroimmunol Neuroinflamm*. 2015;2(6):e174. doi:10.1212/NXI.0000000000000174

13. Omari KM, John GR, Sealfon SC, Raine CS. CXC chemokine receptors on human oligodendrocytes: implications for multiple sclerosis. *Brain*. 2005;128(5):1003-1015. doi:10.1093/brain/awh479

14. Tirotta E, Kirby LA, Hatch MN, Lane TE. IFN-γ-induced apoptosis of human embryonic stem cell derived oligodendrocyte progenitor cells is restricted by CXCR2 signaling. *Stem Cell Res*. 2012;9(3):208-217. doi:10.1016/j.scr.2012.06.005

15. Padovani-Claudio DA, Liu L, Ransohoff RM, Miller RH. Alterations in the oligodendrocyte lineage, myelin, and white matter in adult mice lacking the chemokine receptor CXCR2. *Glia*. 2006;54(5):471-483. doi:10.1002/glia.20383

16. Filipovic R, Jakovcevski I, Zecevic N. GRO-alpha and CXCR2 in the human fetal brain and multiple sclerosis lesions. *Dev Neurosci*. 2003;25(2-4):279-290. doi:10.1159/000072275

17. Vijay R, Fehr AR, Janowski AM, et al. Virus-induced inflammasome activation is suppressed by prostaglandin D2/DP1 signaling. *Proc Natl Acad Sci U S A*. 2017;114(27):E5444-E5453. doi:10.1073/pnas.1704099114

18. Wheeler DL, Sariol A, Meyerholz DK, Perlman S. Microglia are required for protection against lethal coronavirus encephalitis in mice. *J Clin Invest*. 2018;128(3):931-943. doi:10.1172/JCI97229

19. Microglia depletion exacerbates demyelination and impairs remyelination in a neurotropic coronavirus infection. PNAS. Accessed April 18, 2022. https://www.pnas.org/doi/abs/10.1073/pnas.2007814117

20. Mangale V, Syage AR, Ekiz HA, et al. Microglia influence host defense, disease, and repair following murine coronavirus infection of the central nervous system. *Glia*. 2020;68(11):2345-2360. doi:10.1002/glia.23844

APPENDIX

INNATE IMMUNE RESPONSES AND VIRAL-INDUCED NEUROLOGIC DISEASE

Journal of Clinical Medicine

Review

Innate Immune Responses and Viral-Induced Neurologic Disease

Yuting Cheng †, Dominic D. Skinner † and Thomas E. Lane †,*

Division of Microbiology & Immunology, Department of Pathology, University of Utah School of Medicine, Salt Lake City, UT 84112, USA; yuting.cheng@path.utah.edu (Y.C.); dominic.skinner@path.utah.edu (D.D.S.)

* Correspondence: tom.lane@path.utah.edu; Tel.: +1-801-585-5554

† All authors contributed equally to this work.

ABSTRACT

Multiple sclerosis (MS) is a disease of the central nervous system (CNS) characterized by chronic neuroinflammation, axonal damage, and demyelination. Cellular components of the adaptive immune response are viewed as important in initiating formation of demyelinating lesions in MS patients. This notion is supported by preclinical animal models, genome-wide association studies (GWAS), as well as approved disease modifying therapies (DMTs) that suppress clinical relapse and are designed to impede infiltration of activated lymphocytes into the CNS. Nonetheless, emerging evidence demonstrates that the innate immune response e.g., neutrophils can amplify white matter damage through a variety of different mechanisms. Indeed, using a model of coronavirus-induced neurologic disease, we have demonstrated that sustained neutrophil infiltration into the CNS of infected animals correlates with increased demyelination. This brief review highlights recent evidence arguing that targeting the innate immune response may offer new therapeutic avenues for treatment of demyelinating disease including MS.

Keywords

virus; innate immunity; neutrophils; demyelination; remyelination

INTRODUCTION

Multiple sclerosis (MS) is a chronic inflammatory neurodegenerative disease characterized by multifocal regions of central nervous system (CNS) neuroinflammation, demyelination, and axonal loss that ultimately results in extensive neurologic disability [1]. Multifocal demyelinating lesions eventually lead to various clinical symptoms such as impaired motor skills, cognitive decline, behavioral deficits, and vision loss [1–3]. Inflammatory T cells reactive to proteins embedded within the myelin sheath are considered important in lesion formation. This notion is supported by preclinical animal models of MS, genome-wide association studies (GWAS) studies and the mechanisms-of-action of FDA-approved disease-modifying therapies that mute clinical relapse by impeding infiltration of activated T cells into the CNS [1,4]. In addition, the success of anti-CD20 therapies in reducing new lesion formation argues for an important role for B cells in contributing to disease [5]. With this in mind, new areas of investigation are focusing on identifying how oligodendrocytes may contribute to disease [6] as well as developing strategies that promote maturation of oligodendrocyte progenitor cells (OPCs) into mature myelin-producing oligodendroglia. Trapp and colleagues [7] have demonstrated OPCs are spread throughout the CNS and appear in high density within some subacute lesions during early stages of MS. Subsequent to OPC maturation, there is limited remyelination leading to the formation of shadow plaques, in which patches of remyelinated white matter are composed of disproportionally thin myelin sheaths surrounding axons [7–13]. Nonetheless, as disease progresses, there is ultimately remyelination failure that is reflective of an inability of OPCs to mature into myelin-producing oligodendrocytes.

Available evidence indicates that the cause of MS is multifactorial and includes the genetic background of the individual as well as potential environmental influences [4,14–16].

Although viruses such as herpes simplex virus type-1 (HSV-1), measles, human T cell leukemia virus type-1 (HTLV-1), human coronaviruses, human herpesvirus-6 (HHV-6), human endogenous retroviruses (HERV), and Epstein Bar Virus (EBV) have been suggested to be associated etiologically with MS, no clear causal relationship between MS and viral infection has been firmly established [17–27]. The development of animal models in which the clinical and histopathology is similar to that observed in the majority of patients is imperative in order to better understand the underlying pathological mechanisms contributing to MS.

JHMV-Induced Neurologic Disease

Several excellent rodent models of MS have been developed which meet the necessary criteria. The neurotropic JHM strain of mouse hepatitis virus (JHMV) and Theiler's murine encephalomyelitis virus (TMEV) are two well-accepted models of viral-induced neurologic disease which mimic clinical and histopathological characteristics of MS. TMEV infection of the CNS of susceptible SJL mice results in a persistent infection associated with an immune-mediated chronic demyelinating disease [28]. Herein, we focus on the JHMV model of neurologic disease and cellular contributors to demyelination in persistently infected mice. Intracranial (i.c.) infection of susceptible strains of mice such as C57BL/6 with JHMV results in an acute encephalomyelitis that is accompanied by gray matter involvement with infection of oligodendrocytes, astrocytes, and microglia [29]. With regards to viral infection of the CNS, it is critical for the immune system to rapidly respond to control viral replication and subsequent spread in order to limit neuropathology and long-term damage. Pattern recognition receptors (PPRs) including Toll-like receptors (TLRs) and RIG-I are expressed within the CNS and provide important sentinel functions that aid in initiating innate immune responses following viral infection. Myd88 is an adapter protein that provides a critical role in transmitting signals

provided by TLRs that leads to expression of type I IFN (IFN-I) in addition to proinflammatory genes. The importance of Myd88 in host defense following JHMV infection is emphasized in a recent report indicating that infection of Myd88$^{-/-}$ mice increased mortality associated with failure to control viral replication and enhanced neuropathology [30]. Interestingly, CD4+ T cell responses—but not CD8+ T cell responses—were impacted as evidenced by reduced CD4+ T cell recruitment to the CNS and muted IFN-γ expression [30].

Secretion of Proinflammatory Cytokines/Chemokines in Response to JHMV Infection of the CNS

In response to JHMV infection of the CNS, there is a rapid synthesis of mRNA transcripts encoding proinflammatory cytokines and chemokines. In situ hybridization has revealed that astrocytes and microglia are responsible for secreting cytokines and chemokines following JHMV infection [31,32], although it is likely that other resident CNS cells e.g., neurons, macrophages, ependymal cells, etc. are also capable of secreting these molecules. The rapid secretion of cytokines and chemokines serves to help control viral replication as well as mobilize and attract cellular components of the innate immune response. Among the cytokines expressed following JHMV infection is IFN-I. In addition to a role in controlling viral replication within the CNS, IFN-I also enhances expression of cytokines and chemokines as well as increasing expression of MHC and costimulatory molecules. Previous studies have highlighted the importance of IFN-I in host defense against neurotropic viruses including West Nile, Sindbis, and vesicular stomatitis virus [33–35]. Within the context of CNS infection by JHMV, Bergmann and colleagues [36] clearly demonstrated that type I IFNs are critical in controlling viral replication. Intracranial infection of IFN-I-receptor knock-out mice resulted in increased

mortality and impaired ability to control infection that was associated with increased viral replication in glial cells as well as infecting and replicating in defined populations of neurons. Moreover, expression of IFN-I-stimulated genes was impaired, accompanied with reduced expression of MHC class I. Nonetheless, trafficking and accumulation of virus-specific CD8+ T cells was not affected in the absence of IFN-I signaling arguing that IFN-I is not required for T cell survival as has been shown to occur in response to LCMV infection [37]. These findings elegantly demonstrate that IFN-I is responsible for early control of viral replication and tropism that subsequently allows for more effective T cell-mediated protection. More recently, Perlman and colleagues [38] showed that microglia/macrophage activation and production of IFN-I is dependent upon prostaglandin D2 signaling via D-prostanoid receptor 1 (DP1). Additionally, prostaglandin signaling is required for limiting excessive inflammasome activation and increasing survival.

Chemokine Signaling Promotes Immune Cell Infiltration into the CNS

Chemokines are also expressed early in response to JHMV infection of the CNS and have important functional roles in host defense during acute disease. Expression of CXCL1 serves to attract neutrophils to the CNS by signaling through the receptor CXCR2 expressed on the neutrophil cell surface. The importance of attracting neutrophils is highlighted by the demonstration that blocking the migration of these cells via treatment with neutralizing anti-CXCR2 results in increased mortality and impaired ability to control viral replication. Neutrophils contribute to defense through release of matrix metalloprotease 9 (MMP9) which helps increase the permeability of the blood–brain barrier (BBB) ultimately leading to increased infiltration of virus-specific T cells into the CNS [39]. The effect of anti-CXCR2 treatment was

specific for neutrophils as T cell migration is not impacted following administration of this antibody [39].

We have shown that the T cell chemoattractant chemokine interferon-inducible protein 10 kDa (IP-10)/CXCL10 is rapidly expressed in response to JHMV infection and is strictly colocalized with viral RNA within the CNS [31]. Among the cell types responsible for CXCL10 expression, astrocytes were the primary cellular source as demonstrated through both in vitro and in vivo experiments [31]. Although not defined, we believe that expression of CXCL10 is in response to early expression of IFN-I as this cytokine has previously been shown to induce CXCL10 expression [40]. In addition to CXCL10, another T cell chemoattractant chemokine, CXCL9, is also expressed early in response to JHMV infection of the CNS [41]. Both CXCL9 and CXCL10 function by binding and signaling through the chemokine receptor CXCR3 which is expressed upon the surface of natural killer (NK) cells, activated CD4+ and CD8+ T cells, and antibody secreting cells (ASCs). We previously employed a recombinant strain of mouse hepatitis virus A59 (MHV-A59) that expressed CXCL10 from gene 4 of the viral genome to evaluate how CXCL10 shapes the innate immune response [42]. In brief, infection of the CNS of $RAG1^{-/-}$ mice (lacking functional T and B lymphocytes) with the CXCL10-expressing recombinant virus resulted in protection from disease associated with increased infiltration of NK cells into the CNS. Protection was mediated, in part, by secretion of IFN-γ which contributes to controlling viral replication within the CNS. However, the key functional role for both CXCL9 and CXCL10 is to attract virus-specific T cells (both CD4+ and CD8+ subsets) into the CNS by signaling through CXCR3. Through use of neutralizing antibodies specific for either CXCL9, CXCL10, or CXCR3 or employment of mice deficient in CXCL10, we demonstrated increased mortality accompanied by impaired ability to control replication within the CNS if

these signaling pathways are disrupted [41,43–45]. The function of CXCL10 appears limited to the recruitment of activated T cells as antiviral effector functions e.g., proliferation, secretion of IFN-γ, and cytolytic activity remained intact [45]. In addition to recruiting activated T cells into the CNS, CXCL10 performs a similar function to attract ASCs into the perivascular space as well as parenchyma and this also aids in host defense by controlling viral replication [46]. Upon entry into the CNS, virus-specific T cells combat JHMV spread within the CNS through either secretion of IFN-γ or cytolytic activity [47,48]. CD4+ T cells are critical in not only directly controlling JHMV replication via secreting IFN-γ but also through providing support to CD8+ T cells. Studies by Hwang et al. [49] revealed that depletion of CD4+ T cells prior to infection did not significantly impact either the peripheral expansion, IFN-γ secretion, or recruitment of virus-specific CD8+ T cells into the CNS. Nonetheless, findings derived from this work revealed that CD4+ T cells are essential to prolong primary CD8+ T-cell function in the CNS as well as influencing memory CD8+ T cells for recall responses.

Microglial Involvement in JHMV Disease Progression

Resident glial cells clearly aid in host defense in response to microbial infection through various effector functions including secretion of IFN-I as well as proinflammatory cytokines/chemokines that assist in attracting cellular components of both the innate and adaptive immune response. However, more refined roles for resident glia in host defense in response to microbial infection are being discovered. As indicated above, production of IFN-I by activated microglia relies, in part, on prostaglandin D2 signaling via D-prostanoid receptor 1 (DP1) [38]. However, defining discrete functional roles of microglia in terms of host defense in response to JHMV infection is challenging in the face of infiltrating myeloid cells that may have

overlapping functions. In the face of these challenges, Perlman and colleagues [50] provided an important study that further emphasizes that microglia are an active participant involved in an effective host response following JHMV infection of the CNS. Through use of an inhibitor of colony stimulating factor 1 receptor (CSF1R) that depletes microglia, yet only has a minimal effect on macrophages, it was determined that microglia play a critical role in both the early innate as well as virus-specific T cell responses. As early as day 4 post infection, there is a dramatic increase in gene expression within microglia with the majority of genes being associated with IFN signaling and activation of IFN-regulatory factors. Depletion of microglia resulted in a dramatic increase in mortality that correlated with impaired ability to control viral replication within the CNS. In addition, microglia depletion led to increased infiltration of monocyte/macrophages into the CNS—although these cells had a less mature phenotype characterized by reduced MHC class II and elevated Ly6C expression. In addition, there was an overall increase in numbers of virus-specific CD8+ T cells yet there was an overall reduction in frequency and numbers of IFN-γ-producing CD4+ T cells and this likely contributed to the increase in viral titers within the CNS. Collectively, these findings illustrate important and previously unappreciated roles for microglia in contributing to protection from viral encephalomyelitis.

JHMV-Induced Demyelination

Although virus replication within the CNS is controlled by infiltrating virus-specific T cells, sterile immunity is not achieved and JHMV persists primarily in white matter tracts. JHMV persistence results in a chronic demyelinating disease in which loci of demyelination are associated with areas of viral RNA/antigen [51]. Clinically, mice develop loss of tail tone and a partial-to-complete hind-limb paralysis. Due to similarities in both clinical and histologic disease

with the human demyelinating disease multiple sclerosis (MS), the JHMV model is considered a relevant animal model for studying mechanisms contributing to demyelination as well as remyelination [52–54]. A recent report detailed the genes and pathways associated with JHMV-induced demyelinating disease in the spinal cord. Through use of high-throughput sequencing of the host transcriptome, Weiss and colleagues [55] demonstrated that demyelination is accompanied by numerous transcriptional changes indicative of immune infiltration as well as changes in the cytokine production. Furthermore, these findings also supported a Th1-driven response that is associated with JHMV persistence and demyelination.

Virally-encoded genes, notably for the spike glycoprotein, are important in JHMV neurovirulence and demyelination [56,57]. However, JHMV-induced demyelination involves immunopathologic responses directed against viral antigens expressed in infected tissues [58–62]. Inflammatory T cells and macrophages are considered important contributors to white matter damage in JHMV-infected mice. The importance of the immune system in driving demyelination in JHMV-infected mice is further emphasized by the demonstration that infection of RAG1-/- mice does not result in demyelination even though viral replication in resident glial cells, including oligodendroglia, is unrestricted. Adoptive transfer of either splenocytes derived from JHMV-immunized mice or virus-specific T cells results in spinal cord demyelination, further emphasizing the importance of T cells in driving disease. Secretion of IFN-γ by infiltrating T cells contributes to demyelination in JHMV-infected mice presumably through activating resident glia as well as inflammatory macrophages. The importance of both T cells and macrophages in contributing to demyelination in JHMV-infected mice is further highlighted by experiments in which targeting chemokines e.g., CXCL10 or CCL5 that attract activated T cells and macrophages limits the severity of white matter damage [63,64].

Neutrophils and JHMV-Induced Demyelination

While T cells and macrophages clearly are critical in contributing to demyelination in JHMV-infected mice, emerging evidence supports a role for other cell types that participate in white matter damage. For example, microglia have been argued to be important in demyelination through secretion of proinflammatory cytokines/chemokines as well as directed phagocytizing of the myelin sheath [65,66]. Emerging studies demonstrate an important role for neutrophils in experimental models of demyelination [67–70] and other models of CNS injury [71–75]. Neutrophil involvement has also been implicated in a number of systemic autoimmune diseases including systemic lupus erythematosus, rheumatoid arthritis, and anti-neutrophil cytoplasm antibody-associated systemic vasculitis [76]. Notably, neutrophils are a hallmark pathological feature of neuromyelitis optica (NMO) which is triggered by autoantibodies directed against the water channel aquaporin 4 expressed on astrocytes [77]. NMO lesions show accumulation of neutrophils in human patients while animal studies modeling NMO have found reduced neuroinflammation and myelin loss following treatment with neutrophil protease inhibitors [78,79]. Increasing evidence supports a role for neutrophil and/or neutrophil-derived molecules in amplifying the severity of white matter damage in human demyelinating diseases including MS [80–85]. Neutrophils are transient phagocytes that function as part of the innate immune system to respond to sites of injury and infection. Among the first responders following microbial infection, neutrophils enter into the bloodstream and follow chemotactic gradients to sites of injury within the CNS. CXCR2 binds the ELR+ family of chemokines including CXCL1 and CXCL2. Inflammatory events stimulate the release of granulocyte colony-stimulating factor (G-CSF) which in turn upregulates CXCL1, CXCL2, and

CXCR2 while downregulating the CXCL12–CXCR4 axis that serves to retain neutrophils within the bone marrow. Circulating neutrophils must first attach to the vasculature before gaining entry into the CNS. Endothelial cells increase expression of transmembrane proteins including adhesion molecules (ICAM1 and VCAM1) and the neutrophil chemoattractants CXCL1 and CXCL2. These molecules attract and anchor neutrophils to the vasculature and this contributes to increasing the permeability of the BBB. Upon entry into the CNS, neutrophils continue to migrate to sites of infection/injury by responding to specific chemokine signals. Neutrophils have a potent antimicrobial arsenal including the release of reactive oxygen and nitrogen species that are toxic to many microbial pathogens. However, secretion of these molecules can lead to bystander damage instigating injury to surrounding host tissue. Indeed, preclinical mouse models of demyelination e.g., EAE and toxin models have demonstrated that neutrophils increase the severity of neuropathology and demyelination [86–88]. A better understanding of how neutrophils influence clinical disease and demyelination in preclinical models of MS is necessary to determine if these cells are relevant therapeutic targets.

Neutrophils in MS Patients

In MS patients, neutrophils are normally not detected in MS lesions and this most likely reflects their transient nature. Nonetheless, numerous studies have correlated neutrophil-associated factors with clinical disease in MS patients [83,85,89–91]. Higher levels of the neutrophil chemoattractant CXCL8 have been detected in the cerebrospinal fluid (CSF) of MS patients compared to healthy individuals. Additionally, CXCL8 levels measured through ELISA of CSF were higher in MS patients during relapsing episodes [92]. G-CSF, an important regulator for neutrophil trafficking from the bone marrow, was found to be upregulated in acute

MS lesions taken from autopsy tissue [91]. Circulating neutrophils also exhibit a more primed state in MS patients characterized by higher expression of TLR-2, enhanced degranulation and oxidative burst, along with reduced apoptosis [83]. Neutrophil protease activity is also increased in MS patients experiencing a relapse compared to patients in remission or healthy controls. Moreover, relapsing MS patients showed increased plasma levels of CXCL5 during lesion formation. Expression levels of CXCL1, CXCL5, and neutrophil elastase also correlated with measures of MS lesion burden [85]. Collectively, these findings argue that neutrophils may contribute to disease progression in MS patients.

Neutrophil Involvement in Preclinical Models of Demyelination

Supporting this notion is the demonstration that neutrophils have been shown to modulate demyelination in various preclinical models of MS. Liu and colleagues [86] found using the cuprizone toxin model of demyelination that $Cxcr2^{-/-}$ mice were resistant to demyelination. Furthermore, neutrophils were both necessary and sufficient in contributing to demyelination arguing CNS infiltration increased neurotoxic and inflammatory mechanisms which exacerbated toxin-induced demyelination. Further evidence for a role for neutrophils in augmenting demyelination is provided by Segal and colleagues [93] who demonstrated that $Cxcr2^{-/-}$ mice are relatively resistant to EAE and this correlated with reduced infiltration of neutrophils into CNS; however, transfer of CXCR2+ neutrophils into Cxcr2-/- mice immunized with encephalitogenic myelin peptides resulted in increased clinical disease and demyelination supporting the notion that neutrophils contribute to disease in EAE. Stoolman et al. [88] have expanded on these findings to show that enriched expression of CXCL2 within the brainstem attracts neutrophils that substantially contribute to the pathogenesis of EAE. Similarly, mice in which neutrophils

lack suppressor of cytokine signaling 3 (SOCS3) exhibit an increase in susceptibility to the atypical EAE and this correlates with preferential recruitment of neutrophils into the cerebellum and brainstem [94]. The site of neutrophil recruitment may be critical in terms of amplifying histopathology as neutrophil accumulation within the brain, and to a limited extent in the spinal cord, contribute to tissue injury [87]. Collectively, these findings indicate that neutrophils can affect the severity of clinical disease and neuroinflammation in EAE.

In addition to EAE, TMEV infection of the CNS results in a rapid mobilization of neutrophils and monocytes that are recruited to the CNS. These cells are detected in the hippocampus of infected mice which is coincident with pathology. Targeted depletion of neutrophils/monocytes resulted in hippocampal neuroprotection and improved cognitive function [72]. Although the signaling mechanisms by neutrophils infiltrate into the CNS of TMEV-infected mice are not defined, the neutrophil chemoattractant chemokines CXCL1 and CXCL2 are secreted by astrocytes in response to infection suggesting these chemokines may function in attracting neutrophils into the CNS [95,96].

JHMV infection of the CNS results in the secretion of the ELR+ chemokines CXCL1, CXCL2, and CXCL5 at early times postinfection with virus [39,97]. Although we and others have determined that astrocytes express CXCL1 [31,97–100], it does not exclude the possibility that other resident CNS cells as microglia, neurons, and inflammatory immune cells are also capable of expressing CXCL1 as well as CXCL2 and CXCL5. These chemokines bind and signal through CXCR2 pathway to rapidly recruit neutrophils to the BBB. This also contributes to host defense by increasing BBB permeability via release of MMPs which subsequently enhances infiltration of virus-specific T cells [39]. Although neutrophils have been shown to contribute to clinical disease and white matter damage in EAE as well as toxin models of

demyelination [86–88,93,94], the function of these cells in models of viral-induced demyelination have not been as well-characterized. To address this issue, we recently generated transgenic mice where targeted expression of CXCL1 in astrocytes is induced upon treatment with doxycycline (Dox) (**Figure 1A and B**) [101]. Treatment of JHMV-infected CXCL1 transgenic mice with Dox resulted in increased expression of CXCL1 mRNA transcripts and protein within the brain and spinal cords when compared to Dox-treated control mice (**Figure 1C**) [101]. Surprisingly, Dox-induced overexpression of CXCL1 within the CNS of transgenic mice did not influence expression of other proinflammatory cytokines/chemokines nor were there differences in inflammatory T cells into the CNS and control of viral replication within the CNS was not affected. Rather, there was a selective increase in neutrophil accumulation in the CNS and this was associated with an increase in clinical disease and demyelination (**Figure 2A–C**). Blocking neutrophil accumulation within the CNS of Dox-treated CXCL1 mice resulted in a significant reduction in demyelination further supporting a role for neutrophils in contributing to white matter disease (**Figure 2D**). Moreover, our lab has recently demonstrated similar results using this transgenic mouse model in the EAE model of demyelination. We observed that induced expression of CXCL1 in CXCL1-dg mice correlated with increased disease severity associated with neutrophil infiltration into the CNS and enhanced white matter damage. Blocking of neutrophil infiltration into the CNS ameliorated the severity of demyelination [102]. Importantly, we are now seeking to define the mechanisms by which CNS infiltrating neutrophils participate in white damage with a particular focus on secretion of reactive oxygen/nitrogen intermediates, neutrophil extracellular traps (NETs) as well as potentially activating resident glial cells and/or inflammatory monocytes/ macrophages [103,104] (**Figure 3**).

Possible Neutrophil Mechanisms of Action in Demyelination

Reactive oxygen and nitrogen species have been shown to be toxic to oligodendroglia and Reactive oxygen and nitrogen species have been shown to be toxic to oligodendroglia and suggested to be involved in the pathogenesis of demyelination [108,109]. An additional neutrophil suggested to be involved in the pathogenesis of demyelination [108,109]. An additional neutrophil killing mechanism is the release of neutrophil extracellular traps (NETs). NET release is characterized killing mechanism is the release of neutrophil extracellular traps (NETs). NET release is characterized by the neutrophil releasing DNA structures to ensnare foreign pathogens through chromatin by the neutrophil releasing DNA structures to ensnare foreign pathogens through chromatin decondensation. NETs can occupy 3–5 times the space as condensed chromatin. Different models of decondensation. NETs can occupy 3–5 times the space as condensed chromatin. Different models of NETosis have been previously described including suicidal NETosis which occurs in a 2–4-h timeframe NETosis have been previously described including suicidal NETosis which occurs in a 2–4-h and vital NETosis in which nuclear or mitochondrial DNA is released within minutes to an hour timeframe and vital NETosis in which nuclear or mitochondrial DNA is released within minutes to following activation [110–112]. DNA is intrinsically toxic to microbes disrupting their membranes. an hour following activation [110–112]. DNA is intrinsically toxic to microbes disrupting their Additionally, numerous neutrophil proteins also adhere to the expunged DNA including elastase membranes. Additionally, numerous neutrophil proteins also adhere to the expunged DNA and myeloperoxidase, which have their own antimicrobial effects. Viruses specifically have been including elastase and myeloperoxidase, which have their own antimicrobial effects. Viruses investigated in relation to NET formation. Influenza, dengue, and human immunodeficiency

virus specifically have been investigated in relation to NET formation. Influenza, dengue, and human 1 have all been shown to stimulate NET formation from circulating neutrophils. NETs have also immunodeficiency virus 1 have all been shown to stimulate NET formation from circulating been linked to a number of autoimmune diseases including psoriasis, rheumatoid arthritis, and neutrophils. NETs have also been linked to a number of autoimmune diseases including psoriasis, systemic lupus erythematosus. However, little is known about NETs in relation to models of MS. rheumatoid arthritis, and systemic lupus erythematosus. However, little is known about NETs in Patient studies have shown higher circulating levels of NETs in serum from relapsing remitting MS relation to models of MS. Patient studies have shown higher circulating levels of NETs in serum from patients compared to healthy controls, which has been suggested to aggravate tissue injuries [83]. relapsing remitting MS patients compared to healthy controls, which has been suggested to aggravate Interestingly, a follow-up study by Sospedra and colleagues [113] found higher circulating NETs in tissue injuries [83]. Interestingly, a follow-up study by Sospedra and colleagues [113] found higher male relapsing remitting MS patients compared to women suggesting an underlying sex-specific circulating NETs in male relapsing remitting MS patients compared to women suggesting a difference in pathogeneses. While current MS therapies focus on limiting infiltration of activated T underlying sex-specific difference in pathogeneses. While current MS therapies focus on limiting cells into the CNS, the heterogeneous cellular nature of MS lesions argues that other cell types may be infiltration of activated T cells into the CNS, the heterogeneous cellular nature of MS lesions argues contributing to disease. As indicated above, neutrophils have been suggested to potentially participate that other cell types may be contributing to disease. As indicated above, neutrophils have been in disease progression MS patients arguing that focusing on these cells may offer new

therapeutic suggested to potentially participate in disease progression MS patients arguing that focusing on these options for managing disease. Targeting neutrophil infiltration into the CNS through, for example, cells may offer new therapeutic options for managing disease. Targeting neutrophil infiltration into specific small molecule inhibitors that block chemokine receptor e.g., CXCR2 function may provide the CNS through, for example, specific small molecule inhibitors that block chemokine receptor e.g., additional benefits when combined with existing disease modifying agents that limit the infiltration of CXCR2 function may provide additional benefits when combined with existing disease modifying circulating leukocytes. However, muting neutrophil recruitment to the CNS may have disadvantages agents that limit the infiltration of circulating leukocytes. However, muting neutrophil recruitment as these cells are important in host defense against different neurotropic viruses and this approach to the CNS may have disadvantages as these cells are important in host defense against different may impact effective host responses. neurotropic viruses and this approach may impact effective host responses.

PERSPECTIVES

The response of the innate immune system to viral-induced demyelination has been appreciated for a number of years, however new questions have arisen as to how neutrophils contribute to demyelination. Although the observance of neutrophils in MS patients has been elusive, likely due to their transient nature, patient samples indicate substantial evidence of neutrophil attractants and markers during disease. This is supported through evidence from several animal models of demyelination from our lab and others that have shown neutrophil recruitment into the CNS enhances demyelination. While the exact mechanisms of neutrophil contribution to demyelination remain obscure, recent studies employing autoimmune models of

neuroinflammation/demyelination argue for a role for NETs and other neutrophil host defenses as possible instigators of damage. This information has emphasized the potential for targeting these cells as a therapeutic strategy to limit white matter damage.

Author Contributions:

Y.C. and D.D.S. provided conceptual aspects related to the topics and wrote the article.

T.E.L. provided editorial assistance, wrote portions of the review and provided funding.

Funding:

This work was supported by NIH grant R01NS041249 and the the National Multiple Sclerosis Society (NMSS) Collaborative Research Center Grant CA-1607-25040 to T.E.L.

Acknowledgments: The authors gratefully acknowledge the generous support of the Ray and Tye Noorda Foundation.

Conflicts of Interest:

The authors declare no conflicts of interest.

REFERENCES

1. Steinman, L. Immunology of Relapse and Remission in Multiple Sclerosis. Annu. Rev. Immunol. 2014, 32, 257–281. [CrossRef] [PubMed]

2. Lassmann, H.; Bruck, W.; Lucchinetti, C.F. The immunopathology of multiple sclerosis: An overview. Brain Pathol. 2007, 17, 210–218. [CrossRef] [PubMed]

3. Neumann, H.; Medana, I.M.; Bauer, J.; Lassmann, H. Cytotoxic T lymphocytes in autoimmune and degenerative CNS diseases. Trends Neurosci. 2002, 25, 313–319. [CrossRef]

4. Steinman, L. Multiple sclerosis: A coordinated immunological attack against myelin in the central nervous system. Cell 1996, 85, 299–302. [CrossRef]

5. Greenfield, A.L.; Hauser, S.L. B-cell Therapy for Multiple Sclerosis: Entering an era. Ann. Neurol. 2018, 83, 13–26. [CrossRef] [PubMed]

6. Falcao, A.M.; van Bruggen, D.; Marques, S.; Meijer, M.; Jakel, S.; Agirre, E.; Samudyata; Floriddia, E.M.; Vanichkina, D.P.; Ffrench-Constant, C.; et al. Disease-specific oligodendrocyte lineage cells arise in multiple sclerosis. Nat. Med. 2018, 24, 1837–1844. [CrossRef] [PubMed]

7. Chang, A.; Nishiyama, A.; Peterson, J.; Prineas, J.; Trapp, B.D. NG2-positive oligodendrocyte progenitor cells in adult human brain and multiple sclerosis lesions. J. Neurosci. 2000, 20, 6404–6412. [CrossRef]

8. Prineas, J.W.; Kwon, E.E.; Goldenberg, P.Z.; Ilyas, A.A.; Quarles, R.H.; Benjamins, J.A.; Sprinkle, T.J. Multiple sclerosis. Oligodendrocyte proliferation and differentiation in fresh lesions. Lab. Investig. 1989, 61, 489–503.

9. Lucchinetti, C.; Bruck, W.; Parisi, J.; Scheithauer, B.; Rodriguez, M.; Lassmann, H. A quantitative analysis of oligodendrocytes in multiple sclerosis lesions. A study of 113 cases. Brain 1999, 122 Pt 12, 2279–2295. [CrossRef]

10. Roy, N.S.; Wang, S.; Harrison-Restelli, C.; Benraiss, A.; Fraser, R.A.; Gravel, M.; Braun, P.E.; Goldman, S.A. Identification, isolation, and promoter-defined separation of mitotic oligodendrocyte progenitor cells from the adult human subcortical white matter. J. Neurosci. 1999, 19, 9986–9995. [CrossRef]

11. Lassmann, H. Comparative neuropathology of chronic experimental allergic encephalomyelitis and multiple sclerosis. Schriftenr. Neurol. 1983, 25, 1–135. [PubMed]

12. Schlesinger, H. Zur Frage der akuten multiplen Sklerose und der encephalomyelitis disseminata im Kindesalter. Arb. Neurol. Inst. 1909, 17, 410–432.

13. Halfpenny, C.; Benn, T.; Scolding, N. Cell transplantation, myelin repair, and multiple sclerosis. Lancet Neurol. 2002, 1, 31–40. [CrossRef]

14. Oksenberg, J.R.; Begovich, A.B.; Erlich, H.A.; Steinman, L. Genetic factors in multiple sclerosis. Jama 1993, 270, 2362–2369. [CrossRef] [PubMed]

15. Poser, C.M. The epidemiology of multiple sclerosis: A general overview. Ann. Neurol. 1994, 36 (Suppl. 2), S180–S193. [CrossRef]

16. Raine, C.S. The Dale E. McFarlin Memorial Lecture: The immunology of the multiple sclerosis lesion. Ann. Neurol. 1994, 36 (Suppl. 1), S61–S72. [CrossRef]

17. Ebers, G.C.; Sadovnick, A.D.; Risch, N.J. A genetic basis for familial aggregation in multiple sclerosis. Canadian Collaborative Study Group. Nature 1995, 377, 150–151. [CrossRef]

18. Friedman, J.E.; Lyons, M.J.; Cu, G.; Ablashl, D.V.; Whitman, J.E.; Edgar, M.; Koskiniemi, M.; Vaheri, A.; Zabriskie, J.B. The association of the human herpesvirus-6 and MS. Mult. Scler. 1999, 5, 355–362. [CrossRef] [PubMed]

19. Johnson, R.T. The virology of demyelinating diseases. Ann. Neurol. 1994, 36 (Suppl. 1), S54–S60. [CrossRef]

20. Kennedy, P.G.; Steiner, I. On the possible viral aetiology of multiple sclerosis. QJM 1994, 87, 523–528.

21. Libbey, J.E.; Fujinami, R.S. Potential triggers of MS. Res. Probl. Cell Differ. 2010, 51, 21–42. [CrossRef]

22. Lincoln, J.A.; Hankiewicz, K.; Cook, S.D. Could Epstein-Barr virus or canine distemper virus cause multiple sclerosis? Neurol. Clin. 2008, 26, 699–715. [CrossRef] [PubMed]

23. Lipton, H.L.; Liang, Z.; Hertzler, S.; Son, K.N. A specific viral cause of multiple sclerosis: One virus, one disease. Ann. Neurol. 2007, 61, 514–523. [CrossRef]

24. McCoy, L.; Tsunoda, I.; Fujinami, R.S. Multiple sclerosis and virus induced immune responses: Autoimmunity can be primed by molecular mimicry and augmented by bystander activation. Autoimmunity 2006, 39, 9–19. [CrossRef]

25. Olson, J.K.; Ercolini, A.M.; Miller, S.D. A virus-induced molecular mimicry model of multiple sclerosis. Curr. Top. Microbiol. Immunol. 2005, 296, 39–53. [PubMed]

26. Pugliatti, M.; Harbo, H.F.; Holmoy, T.; Kampman, M.T.; Myhr, K.M.; Riise, T.; Wolfson, C. Environmental risk factors in multiple sclerosis. Acta Neurol. Scand. Suppl. 2008, 188, 34–40. [CrossRef]

27. Tao, C.; Simpson, S., Jr.; Taylor, B.V.; van der Mei, I. Association between human herpesvirus & human endogenous retrovirus and MS onset & progression. J. Neurol. Sci. 2017, 372, 239–249. [CrossRef] [PubMed]

28. Tsunoda, I.; Fujinami, R.S. Neuropathogenesis of Theiler's murine encephalomyelitis virus infection, an animal model for multiple sclerosis. J. Neuroimmune Pharmacol. 2010, 5, 355–369. [CrossRef]

29. Bergmann, C.C.; Lane, T.E.; Stohlman, S.A. Coronavirus infection of the central nervous system: Host-virus stand-off. Nat. Rev. Microbiol. 2006, 4, 121–132. [CrossRef]

30. Butchi, N.; Kapil, P.; Puntambekar, S.; Stohlman, S.A.; Hinton, D.R.; Bergmann, C.C. Myd88 Initiates Early Innate Immune Responses and Promotes CD4 T Cells during Coronavirus Encephalomyelitis. J. Virol. 2015, 89, 9299–9312. [CrossRef]

31. Lane, T.E.; Asensio, V.C.; Yu, N.; Paoletti, A.D.; Campbell, I.L.; Buchmeier, M.J. Dynamic regulation of alpha- and beta-chemokine expression in the central nervous system during mouse hepatitis virus-induced demyelinating disease. J. Immunol. 1998, 160, 970–978. [PubMed]

32. Sun, N.; Grzybicki, D.; Castro, R.F.; Murphy, S.; Perlman, S. Activation of astrocytes in the spinal cord of mice chronically infected with a neurotropic coronavirus. Virology 1995, 213, 482–493. [CrossRef] [PubMed]

33. Ryman, K.D.; Klimstra, W.B.; Nguyen, K.B.; Biron, C.A.; Johnston, R.E. Alpha/beta interferon protects adult mice from fatal Sindbis virus infection and is an important determinant of cell and tissue tropism. J. Virol. 2000, 74, 3366–3378. [CrossRef]

34. Samuel, M.A.; Diamond, M.S. Alpha/beta interferon protects against lethal West Nile virus infection by restricting cellular tropism and enhancing neuronal survival. J. Virol. 2005, 79, 13350–13361. [CrossRef] [PubMed]

35. Trottier, M.D., Jr.; Palian, B.M.; Reiss, C.S. VSV replication in neurons is inhibited by type I IFN at multiple stages of infection. Virology 2005, 333, 215–225. [CrossRef]

36. Ireland, D.D.; Stohlman, S.A.; Hinton, D.R.; Atkinson, R.; Bergmann, C.C. Type I interferons are essential in controlling neurotropic coronavirus infection irrespective of functional CD8 T cells. J. Virol. 2008, 82, 300–310. [CrossRef] [PubMed]

37. Kolumam, G.A.; Thomas, S.; Thompson, L.J.; Sprent, J.; Murali-Krishna, K. Type I interferons act directly on CD8 T cells to allow clonal expansion and memory formation in response to viral infection. J. Exp. Med. 2005, 202, 637–650. [CrossRef]

38. Vijay, R.; Fehr, A.R.; Janowski, A.M.; Athmer, J.; Wheeler, D.L.; Grunewald, M.; Sompallae, R.; Kurup, S.P.; Meyerholz, D.K.; Sutterwala, F.S.; et al. Virus-induced inflammasome activation is suppressed by prostaglandin D2/DP1 signaling. Proc. Natl. Acad. Sci. USA 2017, 114, E5444–E5453. [CrossRef]

39. Hosking, M.P.; Liu, L.; Ransohoff, R.M.; Lane, T.E. A protective role for ELR+ chemokines

during acute viral encephalomyelitis. PLoS Pathog. 2009, 5, e1000648. [CrossRef]

40. Vanguri, P.; Farber, J.M. Identification of CRG-2. An interferon-inducible mRNA predicted to encode a murine monokine. J. Biol. Chem. 1990, 265, 15049–15057.

41. Liu, M.T.; Armstrong, D.; Hamilton, T.A.; Lane, T.E. Expression of Mig (monokine induced by interferon-gamma) is important in T lymphocyte recruitment and host defense following viral infection of the central nervous system. J. Immunol. 2001, 166, 1790–1795. [CrossRef] [PubMed]

42. Trifilo, M.J.; Montalto-Morrison, C.; Stiles, L.N.; Hurst, K.R.; Hardison, J.L.; Manning, J.E.; Masters, P.S.; Lane, T.E. CXC chemokine ligand 10 controls viral infection in the central nervous system: Evidence for a role in innate immune response through recruitment and activation of natural killer cells. J. Virol. 2004, 78, 585–594. [CrossRef] [PubMed]

43. Dufour, J.H.; Dziejman, M.; Liu, M.T.; Leung, J.H.; Lane, T.E.; Luster, A.D. IFN-gamma-inducible protein 10 (IP-10; CXCL10)-deficient mice reveal a role for IP-10 in effector T cell generation and trafficking. J. Immunol. 2002, 168, 3195–3204. [CrossRef]

44. Liu, M.T.; Chen, B.P.; Oertel, P.; Buchmeier, M.J.; Armstrong, D.; Hamilton, T.A.; Lane, T.E. The T cell chemoattractant IFN-inducible protein 10 is essential in host defense against viral-induced neurologic disease. J. Immunol. 2000, 165, 2327–2330. [CrossRef]

45. Stiles, L.N.; Hosking, M.P.; Edwards, R.A.; Strieter, R.M.; Lane, T.E. Differential roles for CXCR3 in CD4+ and CD8+ T cell trafficking following viral infection of the CNS. Eur. J. Immunol. 2006, 36, 613–622. [CrossRef] [PubMed]

46. Phares, T.W.; Stohlman, S.A.; Hinton, D.R.; Bergmann, C.C. Astrocyte-derived CXCL10 drives accumulation of antibody-secreting cells in the central nervous system during viral encephalomyelitis. J. Virol. 2013, 87, 3382–3392. [CrossRef] [PubMed]

47. Bergmann, C.C.; Parra, B.; Hinton, D.R.; Ramakrishna, C.; Dowdell, K.C.; Stohlman, S.A. Perforin and gamma interferon-mediated control of coronavirus central nervous system infection by CD8 T cells in the absence of CD4 T cells. J. Virol. 2004, 78, 1739–1750. [CrossRef]

48. Parra, B.; Hinton, D.R.; Marten, N.W.; Bergmann, C.C.; Lin, M.T.; Yang, C.S.; Stohlman, S.A. IFN-gamma is required for viral clearance from central nervous system oligodendroglia. J. Immunol. 1999, 162, 1641–1647.

49. Hwang, M.; Phares, T.W.; Hinton, D.R.; Stohlman, S.A.; Bergmann, C.C.; Min, B. Distinct CD4 T-cell effects on primary versus recall CD8 T-cell responses during viral encephalomyelitis. Immunology 2015, 144, 374–386. [CrossRef]

50. Wheeler, D.L.; Sariol, A.; Meyerholz, D.K.; Perlman, S. Microglia are required for protection against lethal coronavirus encephalitis in mice. J. Clin. Investig. 2018, 128, 931–943.

[CrossRef]

51. Lane, T.E.; Buchmeier, M.J. Murine coronavirus infection: A paradigm for virus-induced demyelinating disease. Trends Microbiol. 1997, 5, 9–14. [CrossRef]

52. Hosking, M.P.; Lane, T.E. The Biology of Persistent Infection: Inflammation and Demyelination following Murine Coronavirus Infection of the Central Nervous System. Curr. Immunol. Rev. 2009, 5, 267–276. [CrossRef] [PubMed]

53. Mangale, V.; McIntyre, L.L.; Walsh, C.M.; Loring, J.F.; Lane, T.E. Promoting remyelination through cell transplantation therapies in a model of viral-induced neurodegenerative disease. Dev. Dyn. 2018. [CrossRef] [PubMed]

54. Tirotta, E.; Carbajal, K.S.; Schaumburg, C.S.; Whitman, L.; Lane, T.E. Cell replacement therapies to promote remyelination in a viral model of demyelination. J. Neuroimmunol. 2010, 224, 101–110. [CrossRef] [PubMed]

55. Elliott, R.; Li, F.; Dragomir, I.; Chua, M.M.; Gregory, B.D.; Weiss, S.R. Analysis of the host transcriptome from demyelinating spinal cord of murine coronavirus-infected mice. PLoS ONE 2013, 8, e75346. [CrossRef] [PubMed]

56. Iacono, K.T.; Kazi, L.; Weiss, S.R. Both spike and background genes contribute to murine coronavirus neurovirulence. J. Virol. 2006, 80, 6834–6843. [CrossRef] [PubMed]

57. Scott, E.P.; Branigan, P.J.; Del Vecchio, A.M.; Weiss, S.R. Chemokine expression during mouse-hepatitis-virus-induced encephalitis: Contributions of the spike and background genes. J. Neurovirol. 2008, 14, 5–16. [CrossRef]

58. Glass, W.G.; Lane, T.E. Functional analysis of the CC chemokine receptor 5 (CCR5) on virus-specific CD8+ T cells following coronavirus infection of the central nervous system. Virology 2003, 312, 407–414. [CrossRef]

59. Glass, W.G.; Lane, T.E. Functional expression of chemokine receptor CCR5 on CD4(+) T cells during virus-induced central nervous system disease. J. Virol. 2003, 77, 191–198. [CrossRef]

60. Haring, J.S.; Perlman, S. Bystander CD4 T cells do not mediate demyelination in mice infected with a neurotropic coronavirus. J. Neuroimmunol. 2003, 137, 42–50. [CrossRef]

61. Haring, J.S.; Pewe, L.L.; Perlman, S. High-magnitude, virus-specific CD4 T-cell response in the central nervous system of coronavirus-infected mice. J. Virol. 2001, 75, 3043–3047. [CrossRef] [PubMed]

62. Kim, T.S.; Perlman, S. Viral expression of CCL2 is sufficient to induce demyelination in RAG1-/- mice infected with a neurotropic coronavirus. J. Virol. 2005, 79, 7113–7120. [CrossRef] [PubMed]

63. Glass, W.G.; Hickey, M.J.; Hardison, J.L.; Liu, M.T.; Manning, J.E.; Lane, T.E. Antibody targeting of the CC chemokine ligand 5 results in diminished leukocyte infiltration into the central nervous system and reduced neurologic disease in a viral model of multiple sclerosis. J. Immunol. 2004, 172, 4018–4025. [CrossRef] [PubMed]

64. Liu, M.T.; Keirstead, H.S.; Lane, T.E. Neutralization of the chemokine CXCL10 reduces inflammatory cell invasion and demyelination and improves neurological function in a viral model of multiple sclerosis. J. Immunol. 2001, 167, 4091–4097. [CrossRef] [PubMed]

65. Das Sarma, J. Microglia-mediated neuroinflammation is an amplifier of virus-induced neuropathology. J. Neurovirol. 2014, 20, 122–136. [CrossRef] [PubMed]

66. Chatterjee, D.; Biswas, K.; Nag, S.; Ramachandra, S.G.; Das Sarma, J. Microglia play a major role in direct viral-induced demyelination. Clin. Dev. Immunol. 2013, 2013, 510396. [CrossRef] [PubMed]

67. Aube, B.; Levesque, S.A.; Pare, A.; Chamma, E.; Kebir, H.; Gorina, R.; Lecuyer, M.A.; Alvarez, J.I.; De Koninck, Y.; Engelhardt, B.; et al. Neutrophils mediate blood-spinal cord barrier disruption in demyelinating neuroinflammatory diseases. J. Immunol. 2014, 193, 2438–2454. [CrossRef] [PubMed]

68. Barthelmes, J.; de Bazo, A.M.; Pewzner-Jung, Y.; Schmitz, K.; Mayer, C.A.; Foerch, C.; Eberle, M.; Tafferner, N.; Ferreiros, N.; Henke, M.; et al. Lack of ceramide synthase 2 suppresses the development of experimental autoimmune encephalomyelitis by impairing the migratory capacity of neutrophils. Brain Behave. Immun. 2015, 46, 280–292. [CrossRef]

69. Eberle, M.; Ebel, P.; Mayer, C.A.; Barthelmes, J.; Tafferner, N.; Ferreiros, N.; Ulshofer, T.; Henke, M.; Foerch, C.; de Bazo, A.M.; et al. Exacerbation of experimental autoimmune encephalomyelitis in ceramide synthase 6 knockout mice is associated with enhanced activation/migration of neutrophils. Immunol. Cell Boil. 2015, 93, 825–836. [CrossRef] [PubMed]

70. Steinbach, K.; Piedavent, M.; Bauer, S.; Neumann, J.T.; Friese, M.A. Neutrophils amplify autoimmune central nervous system infiltrates by maturing local APCs. J. Immunol. 2013, 191, 4531–4539. [CrossRef]

71. Christy, A.L.; Walker, M.E.; Hessner, M.J.; Brown, M.A. Mast cell activation and neutrophil recruitment promotes early and robust inflammation in the meninges in EAE. J. Autoimmun. 2013, 42, 50–61. [CrossRef] [PubMed]

72. Howe, C.L.; Lafrance-Corey, R.G.; Sundsbak, R.S.; Lafrance, S.J. Inflammatory monocytes damage the hippocampus during acute picornavirus infection of the brain. J. Neuroinflamm. 2012, 9, 50. [CrossRef] [PubMed]

73. Ransohoff, R.M.; Brown, M.A. Innate immunity in the central nervous system. J. Clin.

Investig. 2012, 122, 1164–1171. [CrossRef]

74. Sayed, B.A.; Christy, A.L.; Walker, M.E.; Brown, M.A. Meningeal mast cells affect early T cell central nervous system infiltration and blood-brain barrier integrity through TNF: A role for neutrophil recruitment? J. Immunol. 2010, 184, 6891–6900. [CrossRef] [PubMed]

75. Sewell, D.L.; Nacewicz, B.; Liu, F.; Macvilay, S.; Erdei, A.; Lambris, J.D.; Sandor, M.; Fabry, Z. Complement C3 and C5 play critical roles in traumatic brain cryoinjury: Blocking effects on neutrophil extravasation by C5a receptor antagonist. J. Neuroimmunol. 2004, 155, 55–63. [CrossRef]

76. Kaplan, M.J. Role of neutrophils in systemic autoimmune diseases. Arthr. Res. Ther. 2013, 15, 219. [CrossRef]

77. Wingerchuk, D.M.; Lennon, V.A.; Lucchinetti, C.F.; Pittock, S.J.; Weinshenker, B.G. The spectrum of neuromyelitis optica. Lancet Neurol. 2007, 6, 805–815. [CrossRef]

78. Jarius, S.; Wildemann, B.; Paul, F. Neuromyelitis optica: Clinical features, immunopathogenesis and treatment. Clin. Exp. Immunol. 2014, 176, 149–164. [CrossRef]

79. Saadoun, S.; Waters, P.; Macdonald, C.; Bell, B.A.; Vincent, A.; Verkman, A.S.; Papadopoulos, M.C. Neutrophil Protease Inhibition Reduces Neuromyelitis Optica—Immunoglobulin G—Induced Damage in Mouse Brain. Ann. Neurol. 2012, 71, 323–333. [CrossRef]

80. Huber, A.K.; Wang, L.; Han, P.; Zhang, X.; Ekholm, S.; Srinivasan, A.; Irani, D.N.; Segal, B.M. Dysregulation of the IL-23/IL-17 axis and myeloid factors in secondary progressive MS. Neurology 2014, 83, 1500–1507. [CrossRef]

81. Jacob, A.; Saadoun, S.; Kitley, J.; Leite, M.; Palace, J.; Schon, F.; Papadopoulos, M.C. Detrimental role of granulocyte-colony stimulating factor in neuromyelitis optica: Clinical case and histological evidence. Mult. Scler. 2012, 18, 1801–1803. [CrossRef]

82. Kostic, M.; Dzopalic, T.; Zivanovic, S.; Zivkovic, N.; Cvetanovic, A.; Stojanovic, I.; Vojinovic, S.; Marjanovic, G.; Savic, V.; Colic, M. IL-17 and glutamate excitotoxicity in the pathogenesis of multiple sclerosis. Scand. J. Immunol. 2014, 79, 181–186. [CrossRef]

83. Naegele, M.; Tillack, K.; Reinhardt, S.; Schippling, S.; Martin, R.; Sospedra, M. Neutrophils in multiple sclerosis are characterized by a primed phenotype. J. Neuroimmunol. 2012, 242, 60–71. [CrossRef] [PubMed]

84. Openshaw, H.; Stuve, O.; Antel, J.P.; Nash, R.; Lund, B.T.; Weiner, L.P.; Kashyap, A.; McSweeney, P.; Forman, S. Multiple sclerosis flares associated with recombinant granulocyte colony-stimulating factor. Neurology 2000, 54, 2147–2150. [CrossRef] [PubMed]

85. Rumble, J.M.; Huber, A.K.; Krishnamoorthy, G.; Srinivasan, A.; Giles, D.A.; Zhang, X.;

Wang, L.; Segal, B.M. Neutrophil-related factors as biomarkers in EAE and MS. J. Exp. Med. 2015, 212, 23–35. [CrossRef]

86. Liu, L.; Belkadi, A.; Darnall, L.; Hu, T.; Drescher, C.; Cotleur, A.C.; Padovani-Claudio, D.; He, T.; Choi, K.; Lane, T.E.; et al. CXCR2-positive neutrophils are essential for cuprizone-induced demyelination: Relevance to multiple sclerosis. Nat. Neurosci. 2010, 13, 319–326. [CrossRef]

87. Simmons, S.B.; Liggitt, D.; Goverman, J.M. Cytokine-regulated neutrophil recruitment is required for brain but not spinal cord inflammation during experimental autoimmune encephalomyelitis. J. Immunol. 2014, 193, 555–563. [CrossRef] [PubMed]

88. Stoolman, J.S.; Duncker, P.C.; Huber, A.K.; Segal, B.M. Site-specific chemokine expression regulates central nervous system inflammation and determines clinical phenotype in autoimmune encephalomyelitis. J. Immunol. 2014, 193, 564–570. [CrossRef]

89. Ishizu, T.; Osoegawa, M.; Mei, F.-J.; Kikuchi, H.; Tanaka, M.; Takakura, Y.; Minohara, M.; Murai, H.; Mihara, F.; Taniwaki, T.; et al. Intrathecal activation of the IL-17/IL-8 axis in opticospinal multiple sclerosis. Brain 2005, 128, 988–1002. [CrossRef]

90. Campbell, S.J.; Meier, U.; Mardiguian, S.; Jiang, Y.; Littleton, E.T.; Bristow, A.; Relton, J.; Connor, T.J.; Anthony, D.C. Sickness behaviour is induced by a peripheral CXC-chemokine also expressed in multiple sclerosis and EAE. Brain behave. Immun. 2010, 24, 738–746. [CrossRef] [PubMed]

91. Lock, C.; Hermans, G.; Pedotti, R.; Brendolan, A.; Schadt, E.; Garren, H.; Langer-Gould, A.; Strober, S.; Cannella, B.; Allard, J.; et al. Gene-microarray analysis of multiple sclerosis lesions yields new targets validated in autoimmune encephalomyelitis. Nat. Med. 2002, 8, 500–508. [CrossRef] [PubMed]

92. Bartosik-Psujek, H.; Stelmasiak, Z. The levels of chemokines CXCL8, CCL2 and CCL5 in multiple sclerosis patients are linked to the activity of the disease. Eur. J. Neurol. 2005, 12, 49–54. [CrossRef] [PubMed]

93. Carlson, T.; Kroenke, M.; Rao, P.; Lane, T.E.; Segal, B. The Th17-ELR+ CXC chemokine pathway is essential for the development of central nervous system autoimmune disease. J. Exp. Med. 2008, 205, 811–823. [CrossRef] [PubMed]

94. Liu, Y.; Holdbrooks, A.T.; Meares, G.P.; Buckley, J.A.; Benveniste, E.N.; Qin, H. Preferential Recruitment of Neutrophils into the Cerebellum and Brainstem Contributes to the Atypical Experimental Autoimmune Encephalomyelitis Phenotype. J. Immunol. 2015, 195, 841–852. [CrossRef] [PubMed]

95. Rubio, N.; Sanz-Rodriguez, F. Induction of the CXCL1 (KC) chemokine in mouse astrocytes by infection with the murine encephalomyelitis virus of Theiler. Virology 2007, 358, 98–108. [CrossRef] [PubMed]

96. Rubio, N.; Sanz-Rodriguez, F.; Lipton, H.L. Theiler's virus induces the MIP-2 chemokine (CXCL2) in astrocytes from genetically susceptible but not from resistant mouse strains. Cell. Immunol. 2006, 239, 31–40. [CrossRef] [PubMed]

97. Hosking, M.P.; Tirotta, E.; Ransohoff, R.M.; Lane, T.E. CXCR2 signaling protects oligodendrocytes and restricts demyelination in a mouse model of viral-induced demyelination. PLoS ONE 2010, 5, e11340. [CrossRef]

98. Kang, Z.; Wang, C.; Zepp, J.; Wu, L.; Sun, K.; Zhao, J.; Chandrasekharan, U.; DiCorleto, P.E.; Trapp, B.D.; Ransohoff, R.M.; et al. Act1 mediates IL-17-induced EAE pathogenesis selectively in NG2+ glial cells. Nat. Neurosci. 2013, 16, 1401–1408. [CrossRef] [PubMed]

99. Glabinski, A.R.; Krakowski, M.; Han, Y.; Owens, T.; Ransohoff, R.M. Chemokine expression in GKO mice (lacking interferon-gamma) with experimental autoimmune encephalomyelitis. J. Neurovirol. 1999, 5, 95–101. [CrossRef] [PubMed]

100. Glabinski, A.R.; Tuohy, V.K.; Ransohoff, R.M. Expression of chemokines RANTES, MIP-1alpha and GRO-alpha correlates with inflammation in acute experimental autoimmune encephalomyelitis. Neuroimmunomodulation 1998, 5, 166–171. [CrossRef] [PubMed]

101. Marro, B.S.; Grist, J.J.; Lane, T.E. Inducible Expression of CXCL1 within the Central Nervous System Amplifies Viral-Induced Demyelination. J. Immunol. 2016, 196, 1855–1864. [CrossRef] [PubMed]

102. Grist, J.J.; Marro, B.S.; Skinner, D.D.; Syage, A.R.; Worne, C.; Doty, D.J.; Fujinami, R.S.; Lane, T.E. Induced CNS expression of CXCL1 augments neurologic disease in a murine model of multiple sclerosis via enhanced neutrophil recruitment. Eur. J. Immunol. 2018, 48, 1199–1210. [CrossRef] [PubMed]

103. Borregaard, N. Neutrophils, from marrow to microbes. Immunity 2010, 33, 657–670. [CrossRef] [PubMed]

104. Nathan, C. Neutrophils and immunity: Challenges and opportunities. Nat. Rev. Immunol. 2006, 6, 173–182. [CrossRef] [PubMed]

105. Fialkow, L.; Wang, Y.; Downey, G.P. Reactive oxygen and nitrogen species as signaling molecules regulating neutrophil function. Free Radic. Boil. Med. 2007, 42, 153–164. [CrossRef] [PubMed]

106. Mittal, M.; Siddiqui, M.R.; Tran, K.; Reddy, S.P.; Malik, A.B. Reactive oxygen species in inflammation and tissue injury. Antioxid. Redox Signal. 2014, 20, 1126–1167. [CrossRef]

107. Tecchio, C.; Micheletti, A.; Cassatella, M.A. Neutrophil-derived cytokines: Facts beyond expression. Front. Immunol. 2014, 5, 508. [CrossRef]

108. Merrill, J.E.; Ignarro, L.J.; Sherman, M.P.; Melinek, J.; Lane, T.E. Microglial cell cytotoxicity of oligodendrocytes is mediated through nitric oxide. J. Immunol. 1993, 151, 2132–2141.

109. Mitrovic, B.; Ignarro, L.J.; Montestruque, S.; Smoll, A.; Merrill, J.E. Nitric oxide as a potential pathological mechanism in demyelination: Its differential effects on primary glial cells in vitro. Neuroscience 1994, 61, 575–585. [CrossRef]

110. Delgado-Rizo, V.; Martinez-Guzman, M.A.; Iniguez-Gutierrez, L.; Garcia-Orozco, A.; Alvarado-Navarro, A.; Fafutis-Morris, M. Neutrophil Extracellular Traps and Its Implications in Inflammation: An Overview. Front. Immunol. 2017, 8, 81. [CrossRef]

111. Al-Khafaji, A.B.; Tohme, S.; Yazdani, H.O.; Miller, D.; Huang, H.; Tsung, A. Superoxide induces Neutrophil Extracellular Trap Formation in a TLR-4 and NOX-dependent mechanism. Mol. Med. 2016, 22, 621–631. [CrossRef] [PubMed]

112. Pilsczek, F.H.; Salina, D.; Poon, K.K.H.; Fahey, C.; Yipp, B.G.; Sibley, C.D.; Robbins, S.M.; Green, F.H.Y.; Surette, M.G.; Sugai, M.; et al. A novel mechanism of rapid nuclear neutrophil extracellular trap formation in response to Staphylococcus aureus. J. Immunol. 2010, 185, 7413–7425. [CrossRef] [PubMed]

113. Tillack, K.; Naegele, M.; Haueis, C.; Schippling, S.; Wandinger, K.P.; Martin, R.; Sospedra, M. Gender differences in circulating levels of neutrophil extracellular traps in serum of multiple sclerosis patients. J. Neuroimmunol. 2013, 261, 108–119. [CrossRef] [PubMed]

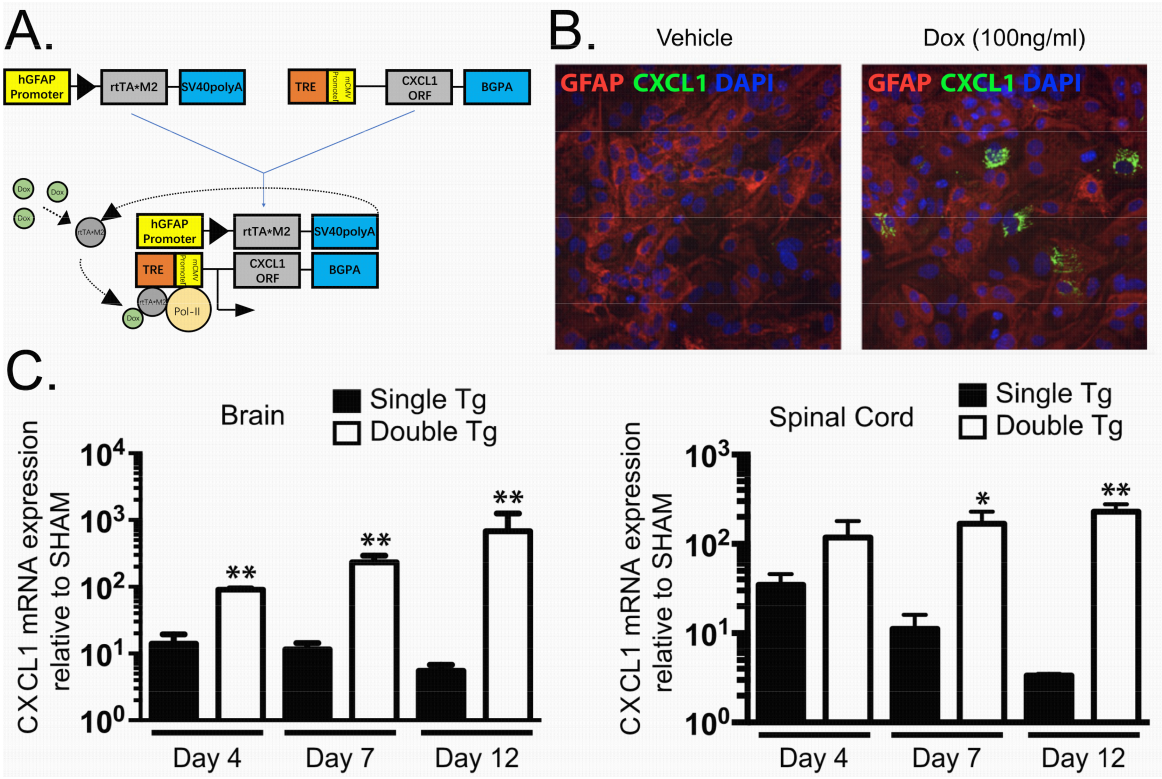

Figure 1 Derivation and characterization of a mouse model in which CXCL1 expression within the central nervous system (CNS) is under the control of a doxycycline promoter. (A) Cartoon depiction of experimental strategy to generate double (dbl) transgenic (tg) mice in which expression of mouse CXCL1 is under control of the glial fibrillary acidic protein (GFAP) promoter upon doxycycline treatment. (B) Cortex tissue from double tg and single tg postnatal day 1 (P1) mice was dissociated and enriched for astrocytes. Following 24-h of Dox (100 ng/mL) treated double tg astrocyte cultures, immunofluorescence confirmed CXCL1 expression within GFAP-positive astrocytes while vehicle treatment yielded no CXCL1 fluorescence (original magnification, ×20). (C) Within the spinal cord (SC) and brain, dox-treated double tg mice had statistically significant increases in CXCL1 mRNA expression over Dox-treated single tg mice at days 7 and 12 post-infection (p.i.) * $p < 0.05$, ** $p < 0.01$. Data derived from Marro et al., (2016) [101].

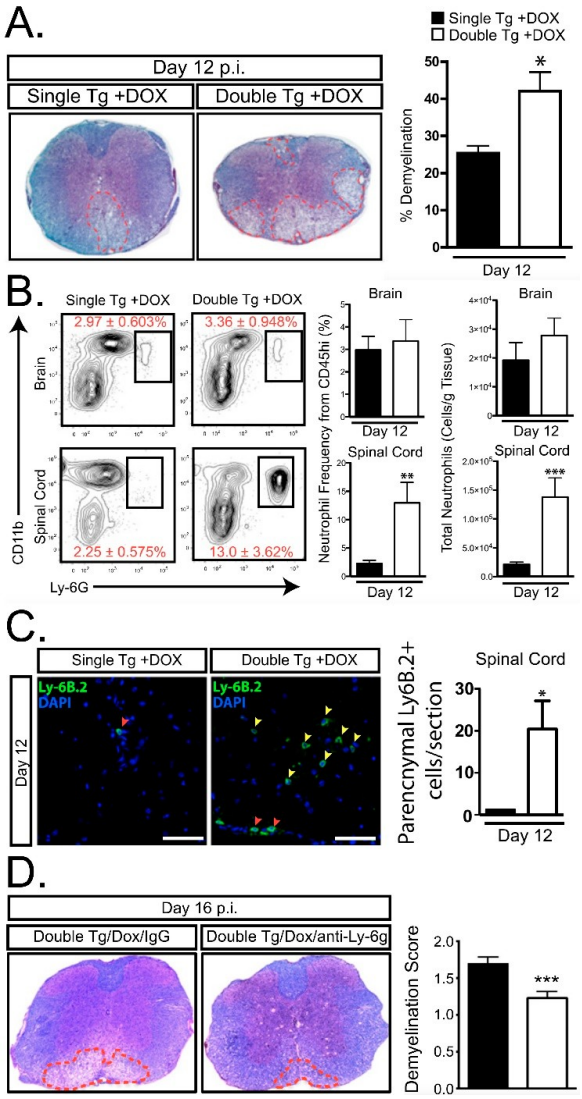

Figure 2 Elevated CNS CXCL1 expression is associated with increased neutrophil accumulation and demyelination. (A) Representative luxol fast blue (LFB)-stained spinal cords reveal increased ($p<0.05$) demyelination in mouse hepatitis virus (JHMV)-infected Dox-treated double tg mice compared to single tg controls. (B) Flow cytometric analysis revealed a significant increase in the frequency and total number of neutrophils within the spinal cord of JHMV-infected Dox-treated double tg mice compared to single tg mice. (C) Representative immune-fluorescence staining further demonstrated a significant increase in the number of Ly6B.2 positive neutrophils (yellow arrowheads) within the spinal cord parenchyma of JHMV-infected double tg compared to single tg mice; red arrowheads indicate neutrophils located within the spinal cord meninges Quantification of neutrophils within the spinal cords indicated an overall increase ($p<0.05$) in Dox-treated double tg mice compared to Dox-treated single tg mice. (D) Representative LFB-stained spinal cord sections from JHMV-infected double tg mice treated with either control IgG2a or anti-Ly6G antibody between days 3 to 15 p.i. Quantification of the severity of demyelination revealed reduced white matter damage in mice treated with anti-Ly6G antibody compared to mice treated with isogenic IgG2a control antibody. *$p<0.05$, **$p<0.01$, ***$p<0.001$. Data derived from Marro et al., (2016) [101]

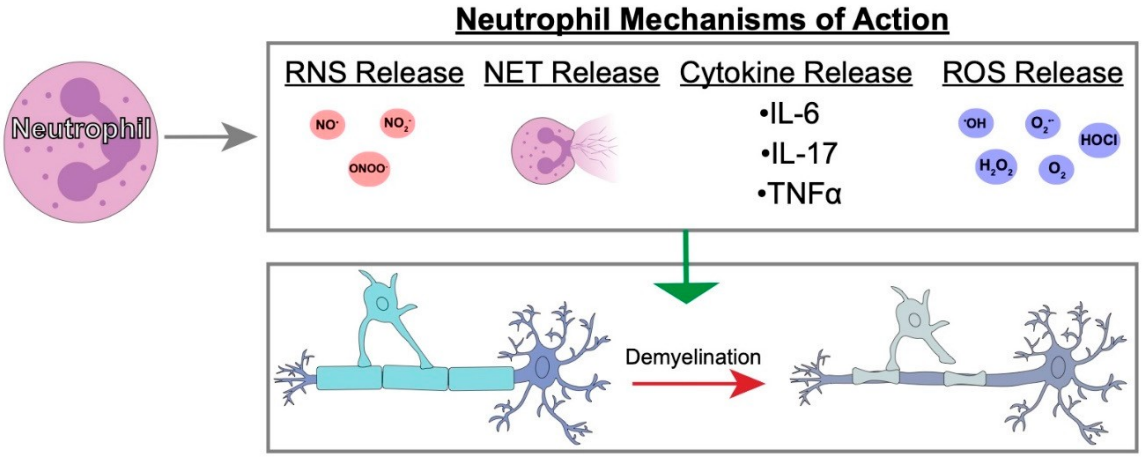

Figure 3 Characterization of possible neutrophil mechanisms of action that contribute to white matter damage. Cartoon depiction of neutrophil mechanisms of action including release of reactive nitrogen species (RNS) [105] and reactive oxygen species (ROS) [106] intermediates, neutrophil extracellular traps (NETs) [83], and select cytokines [107]. We hypothesize that these mechanisms may by responsible for the enhanced white matter damage observed following induced infiltration of neutrophils in preclinical mouse models of MS.

MICROGLIA DO NOT RESTRICT SARS-CoV-2 REPLICATION FOLLOWING INFECTION OF THE CENTRAL NERVOUS SYSTEM OF K18-hACE2 TRANSGENIC MICE

Journal of Virology

Microglia do not restrict SARS-CoV-2 replication following infection of the central nervous system of K18-hACE2 transgenic mice

Gema M. Olivarria[1*], Yuting Cheng[2*], Susana Furman[1*], Collin Pachow[2], Lindsay A. Hohsfield[1], Charlene Smith-Geater[3], Ricardo Miramontes[4], Jie Wu[5], Mara S. Burns[1], Kate I. Tsourmas[1], Jennifer Stocksdale[1], Cynthia Manlapaz[1], William H. Yong[6], John Teijaro[7], Robert Edwards[6], Kim N. Green[1], Leslie M. Thompson[1,3,5,6], and Thomas E. Lane[1,2,8 #]

[1]Department of Neurobiology & Behavior, [2]Department of Molecular Biology & Biochemistry, School of Biological Sciences, University of California, Irvine 92697

[3]Department of Psychiatry and Human Behavior, University of California, Irvine School of Medicine, Irvine 92697

[4]Institute for Memory Impairments and Neurological Disorders, School of Biological Sciences, University of California, Irvine 92697

[5]Department of Biological Chemistry, University of California, Irvine School of Medicine, Irvine 92697

[6]Department of Pathology & Laboratory Medicine, University of California, Irvine School of Medicine, Irvine 92697

[7]Department of Immunology & Microbiology, The Scripps Research Institute, La Jolla CA 92037

[8]Center for Virus Research, University of California, Irvine 92697

*These authors contributed equally to this work

#Address Correspondence

Thomas E. Lane, Ph.D.

Department of Neurobiology & Behavior

School of Biological Sciences

University of California, Irvine

(949) 824-1360

Email: tlane@uci.edu

ABSTRACT

unlike SARS-CoV-1 and MERS-CoV, infection with SARS-CoV-2, the viral pathogen responsible for COVID-19, is often associated with neurologic symptoms that range from mild to severe, yet increasing evidence argues the virus does not exhibit extensive neuroinvasive properties. We demonstrate SARS-CoV-2 can infect and replicate in human iPSC-derived neurons and that infection shows limited anti-viral and inflammatory responses but increased activation of EIF2 signaling following infection as determined by RNA sequencing. Intranasal infection of K18 human ACE2 transgenic mice (K18-hACE2) with SARS-CoV-2 resulted in lung pathology associated with viral replication and immune cell infiltration. In addition, ~50% of infected mice exhibited CNS infection characterized by wide-spread viral replication in neurons accompanied by increased expression of chemokine (*Cxcl9, Cxcl10, Ccl2, Ccl5* and *Ccl19*) and cytokine (*Ifn-λ* and *Tnf-α*) transcripts associated with microgliosis and a neuroinflammatory response consisting primarily of monocytes/macrophages. Microglia depletion via administration of colony-stimulating factor 1 receptor inhibitor, PLX5622, in SARS-CoV-2 infected mice did not affect survival or viral replication but did result in dampened expression of proinflammatory cytokine/chemokine transcripts and a reduction in monocyte/macrophage infiltration. These results argue that microglia are dispensable in terms of controlling SARS-CoV-2 replication in in the K18-hACE2 model but do contribute to an inflammatory response through expression of pro-inflammatory genes. Collectively, these findings contribute to previous work demonstrating the ability of SARS-CoV-2 to infect neurons as well as emphasizing the potential use of the K18-hACE2 model to study immunological and neuropathological aspects related to SARS-CoV-2-induced neurologic disease.

Keywords:

SARS-CoV-2, microglia, central nervous system, neuropathology

Importance

Understanding the immunological mechanisms contributing to both host defense and disease following viral infection of the CNS is of critical importance given the increasing number of viruses that are capable of infecting and replicating within the nervous system. With this in mind, the present study was undertaken to evaluate the role of microglia in aiding in host defense following experimental infection of the central nervous system (CNS) of K18-hACE2 with SARS-CoV-2, the causative agent of COVID-19. Neurologic symptoms that range in severity are common in COVID-19 patients and understanding immune responses that contribute to restricting neurologic disease can provide important insight into better understanding consequences associated with SARS-CoV-2 infection of the CNS.

INTRODUCTION

The clinical spectrum of COVID-19 is complex, and numerous risk factors and comorbidities are considered important in affecting disease severity including age, obesity, chronic respiratory disease, and cardiovascular disease [1]. In addition, neurological symptoms are common in COVID-19 patients, suggesting the virus can potentially infect and replicate in the central nervous system (CNS). Indeed, encephalitis and meningitis have been reported in COVID-19 patients, and viral RNA and protein have been detected within the CSF of infected patients [2-4]. Additionally, human brain organoids are susceptible to SARS-CoV-2 infection [2, 5], yet demonstration of extensive CNS penetrance by SARS-CoV-2 has remained elusive. It is imperative to develop pre-clinical animal models of COVID-19 that capture consistent and reproducible clinical and histologic readouts of many disease-associated symptoms following experimental infection with clinical isolates of SARS-CoV-2 [6]. Importantly, these models should be able to reliably evaluate interventional therapies to limit viral replication and mute immune-mediated pathology, as well as evaluate effectiveness of novel vaccines, all while remaining cost-effective. To date, the most common animal models employed to evaluate COVID-19 pathogenesis include mice, non-human primates (rhesus macaques, cynomolgus macaques and African green monkeys), Syrian hamsters, ferrets, and cats [6].

Human ACE2 (hACE2) transgenic mouse models have provided important insights into the pathogenesis of COVID-19. Perlman and colleagues [7] developed the K18-hACE2 mice, initially used as a mouse model of SARS-CoV-1, which has been successfully employed as a model of COVID-19 [8]. Intranasal inoculation of SARS-CoV-2 in K18-hACE2 mice results in a dose-dependent increase in weight loss and mortality with the lung being the major site of viral infection, while lower amounts of virus are detected in the heart, liver, spleen, kidney, small

intestine, and colon [8]. Examination of lungs revealed distribution of viral antigen associated with alveolar damage, interstitial lesions, edema, and inflammation. Lung infection resulted in an increase in expression of interferons as well as inflammatory cytokines and chemokines associated with neutrophil, macrophage/monocyte, and T cell infiltration. Viral RNA was also detected within the sinonasal epithelium, and viral antigen was present in sustentacular cells associated with anosmia [8].

Examination of brains of SARS-CoV-2 infected hACE2 transgenic mice has indicated that infection of the CNS is not consistent, and in some cases, virus is rarely detected [8-12]. This may reflect the SARS-CoV-2 isolate being studied as well as the dose of virus being administered. However, in those animals in which virus penetrates the brain, there can be extensive spread of the virus throughout different anatomic regions accompanied by cell death [8], and these results are consistent with early studies examining SARS-CoV-1 infection of K18-hACE2 mice [7]. High-level of CNS infection in K18-hACE2 is accompanied by meningeal inflammation associated with immune cell infiltration into the brain parenchyma and microglia activation [11]. Enhanced CNS penetrance and replication of SARS-CoV-2 within the CNS of K18-hACE2 is associated with increased mortality; although the mechanisms by which this occurs remain unclear. The present study was undertaken to i) expand on earlier studies examining SARS-CoV-2 infection of human CNS resident cells, ii) evaluate the immune response that occurs in response to SARS-CoV-2 infection of the CNS of K18-hACE2 mice and iii) assess the contributions of microglia in host defense following CNS infection by SARS-CoV-2.

RESULTS

SARS-CoV-2 infection of human neurons. Previous studies have indicated neurons are susceptible to infection by SARS-CoV-2 (2); therefore, we infected human iPSC-derived neurons with SARS-CoV-2. Similar to earlier reports, SARS-CoV-2 was able to infect and replicate within neurons as determined by staining for nucleocapsid protein (**Figure 1A and B**). By 48h p.i., viral nucleocapsid protein had spread from the neuron cell body and extended down dendritic and axonal projections (**Figure 1C and D**). Notably, we did not detect syncytia formation in neuron cultures at any time following infection with SARS-CoV-2, suggesting that virus may not spread via fusion with neighboring cells. RNA sequencing analysis revealed that expression of both anti-viral and inflammatory responses in infected neurons was limited relative to the genes within the heatmap at both 24h and 48h post-infection (**Figure 1E**). We then evaluated pathways that may progressively change between 24h and 48h post-infection comparing the Transcripts per million (TPMs) as input for Ingenuity Pathway Analysis (IPA). **Figure 1F** shows the top 12 IPA canonical pathways that are overrepresented. eIF2 signaling is the predominant pathway induced upon SARS-CoV-2 infection of neurons, followed by pathways associated with oxidative phosphorylation, eIF4, MTOR signaling and mitochondrial dysfunction, the latter with no prediction of activity. Notably, the Coronavirus Pathogenesis Pathway is also overrepresented, however is inhibited in response to neuronal infection by SARS-CoV-2 over the time frame tested with the majority of the genes represented encoding ribosomal proteins (**Figure 1F**).

SARS-CoV-2 infection of lungs of K18-hACE2 mice. K18-hACE2 mice were intranasally infected with either $1x10^4$, $5x10^4$ or $1x10^5$ plaque-forming units (PFU) of SARS-CoV-2, and

weight loss and mortality were recorded. Consistent with other reports [8-12], we observed a general trend towards dose-dependent increase in weight loss and mortality out to day 7 post-infection (p.i.) (**Figure 2A**). qPCR indicated the presence of viral RNA in lungs of infected K18-hACE2 (**Figure 2B**). *In situ* hybridization of lungs of mice infected with $5x10^4$ PFU of virus at day 7 p.i. revealed localized areas of viral infection as determined by expression of spike RNA (**Figures 2C**). Hematoxylin and eosin staining of lungs demonstrated both alveolar and interstitial lesions, with alveolar hemorrhage and edema (**Figures 2D**), interstitial congestion (**Figure 2E**) and lymphocytic infiltrates (**Figure 2F**). qPCR analysis of proinflammatory cytokines and chemokines indicated increased expression of *Ifn-λ, Cxcl10*, *Cxcr2*, and *Ccl2* yet varied expression of *Il-10*, *TNF-α, Ccl19*, *and Ccl5* and limited expression of transcripts for *Ifn-b1*(**Figure 2G**). Hematoxylin and eosin staining showed immune cell infiltrates in SARS-CoV-2-infected lungs containing inflammatory CD8+ T cells as determined by immunofluorescent staining (**Figure 3A-D**). In addition, germinal center-like structures were detected within the lungs of SARS-CoV-2-infected mice with enriched CD8+ T cell accumulation (**Figure 3E and F**). Collectively, our findings are consistent with previous studies employing SARS-CoV-2 infection of K18-hACE2 mice in terms of development of interstitial pneumonia and immune cell infiltration associated with viral RNA present within the lungs [8-12].

Neuroinvasion by SARS-CoV-2. Following intranasal infection of mice with $5x10^4$ PFU of SARS-CoV-2, virus was detected in the brain as determined by qPCR and RNAscope compared to sham-infected mice (**Figure 4A-C**). Using a Spike-specific probe, we observed wide-spread expansion of viral mRNA throughout the brain with many distinct anatomical regions infected as well as spared. By day 7 p.i., viral RNA was present within the cortex (CTX), striatum (STR),

pallidum (PAL), thalamus (TH), hypothalamus (HY), midbrain (MB), pons (P), and medulla (MD), whereas areas that were relatively spared included the olfactory bulb (OB), white matter (WM) tracts, hippocampus (HC) and cerebellum (CB) (**Figure 4B**); no viral RNA was detected in sham-infected K18-hACE2 mice (**Figure 4C**). Demyelinating lesions have been detected in post-mortem brains of COVID-19 patients [13], however we did not detect any evidence of demyelination within the brains of SARS-CoV-2-infected mice as determined by luxol-fast blue (LFB) staining (**Figure 4D and E**). The predominant cellular target for SARS-CoV-2 infection was neurons as determined by cellular morphology of cells positive for viral RNA (**Figure 5A and B**). In a small percentage of infected mice, we were able to detect viral RNA in the olfactory bulb with primary targets being mitral and glomerular neurons (**Figure 5C and D**). Prominent neuropathological changes detected included perivascular cuffing (**Figure 5E**), subventricular inflammation (**Figures 5F**) and leptomeningitis (**Figure 5G**), consistent with previous studies (2, 3).

Analysis of CNS myeloid cells showed increased IBA1 soma size and shortened/thickened processes, indicative of microglial activation in SARS-CoV-2-infected mice compared to sham-infected mice (**Figure 6A and B**). In addition, immunofluorescent co-staining for Mac2/galectin-3+ cells, a marker recently identified in peripheral cell infiltrates, and IBA1 (Hohsfield *et al. manuscript in revision*), revealed increased monocyte/macrophage infiltration within the brains of infected mice compared to sham-infected mice (**Figure 6A and B**). Mac2+ cells enter the CNS parenchyma from different anatomic areas including the ventricles, leptomeninges and vasculature (**Figure 6C and D**) when compared to uninfected control mice (**Figure 6E**).

Microglia ablation does not affect disease or control of viral replication in the CNS.

Previous studies have implicated the importance of microglia in aiding in control of neuroadapted murine beta-coronaviruses by enhancing anti-viral T cell responses through augmenting antigen presentation (11-13). Notably, microglia are dependent on signaling through the colony stimulating factor 1 receptor (CSF1R) for their survival and can be effectively eliminated with CSF1R inhibitors that cross the blood brain barrier [14]. K18-hACE2 mice were fed pre-formulated chow containing either the CSF1R inhibitor PLX5622 (1,200 ppm) [15] or control chow 7 days prior to intranasal infection with $5x10^4$ PFUs of SARS-CoV-2, and remained on drug for the duration of the experiment [6]. No notable differences were detected in weight loss between experimental groups (**Figure 7A**). SARS-CoV-2-infected mice treated with either PLX5622 or control chow were sacrificed at day 7 p.i., and viral mRNA levels in lungs and brains were determined. As shown in **Figure 7B**, we detected no significant differences in the Spike mRNA transcripts in either the lung or the brain between experimental groups. Quantification of Iba1-positive cells revealed a >95% reduction ($p<0.01$) in microglia in PLX5622-treated mice compared to control mice. Overall, PLX5622-mediated ablation of microglia resulted in a dramatic reduction in expression of proinflammatory cytokine/chemokine genes within the brains of SARS-CoV-2 infected mice when compared to infected mice fed control chow (**Figure 7D**). By day 7 p.i., SARS-CoV-2 infection resulted in increased expression of proinflammatory cytokines and chemokines in mice treated with control chow. The highest transcript levels were for the T cell chemoattractants CXCL9 and CXCL10; monocyte/macrophage chemoattractants, CCL2 and CCL5; and TNF-α (**Figure 7D**). Transcripts encoding the neutrophil chemoattractant CXCL1, and B cell chemoattractant CCL19 were also increased, as well as IFN-λ type 3 and IL-10 when compared to uninfected controls (**Figure 7D**).

Depletion of microglia resulted in a marked reduced expression of the majority chemokine/cytokines transcripts. While not significant, there was a marked reduction in Mac2/galactin3+ cells in PLX5622-treated mice when compared to control chow and this correlated with reduced expression of monocyte/macrophage chemoattractant chemokines CCL2 and CCL5 (**Figure 7E**) that have previously been shown to attract these cells into the CNS of mice infected with a neurotropic mouse coronavirus [16-21].

DISCUSSION

In the face of the ongoing COVID-19 pandemic, it is imperative to develop pre-clinical animal models of COVID-19 that capture consistent and reproducible clinical and histologic readouts of many disease-associated symptoms following experimental infection with SARS-CoV-2 [1]. For both SARS-CoV-2 and SARS-CoV-1, the surface-bound viral spike glycoprotein uses the cellular surface receptor protein, ACE2, to bind and enter cells. However, mouse ACE2 does not efficiently bind the spike glycoprotein of either SARS-CoV-1 or SARS-CoV-2, rendering wildtype mice not useful in the study of SARS or COVID-19 pathogenesis, respectively, due to an inefficient ability to infect and replicate in host cells. Human ACE2 (hACE2) transgenic mouse models have provided important insights into the pathogenesis of COVID-19 in terms of evaluating the efficacy and duration of immune responses elicited in response to infection as well as testing vaccines, anti-viral drugs and monoclonal antibody therapies to restrict viral replication and limit disease severity [8].

Intranasal inoculation of K18-hACE2 mice with SARS-CoV-2 resulted in weight loss along with viral infection and replication within the lungs that was associated with a robust inflammatory response. These findings are consistent with other reports that demonstrated the presence of neutrophils, monocytes/macrophages and T cells within the lungs of SARS-CoV-2-infected K18-hACE2 mice [8, 11]. In response to infection, expression of proinflammatory cytokines/chemokines was increased and correlated with the presence of inflammatory cells. We detected inflammatory CD8+ T cells in the lungs of infected mice and these cells are presumably responding to the T cell chemoattractant CXCL10. Our lab has previously shown that induction of CXCL10 expression following experimental infection of mice with a neuroadapted strain of murine coronavirus is critical in host defense and acts by attracting virus-specific T cells into the

CNS [22-24]. Similarly, inflammatory monocyte/macrophages are likely recruited in response to expression of CCL2 as this has been shown to attract these cells following murine coronavirus infection of mice [16-19]. The increased expression of transcripts encoding CXCR2 most likely reflects the presence of inflammatory neutrophils [25]. Therapeutic targeting of these chemokines may therefore alter immune cell trafficking into the lungs of infected mice and alleviate the severity of lung pathology. How blocking chemokine signaling would affect SARS-CoV-2-induced lung pathology in COVID-19 patients is currently under investigation.

Clinical reports of COVID-19 patients cite a dysregulated immune response characterized by elevated chemokine expression as key in the development of pathogenesis [26, 27]. Similar to our findings using the K18-hACE2 model, these reports have found upregulation of CCL2 (MCP1), CXCL8 (IL-8), and CXCL10 (IP10) to correlate with severity of disease and have suggested evaluation of these as biomarkers for disease and as targets for therapeutic intervention [28-30]. Leronlimab, a CCR5-blocking antibody, is currently in phase 2 clinical trials in the U.S. for treatment of mild, moderate, and severe COVID-19 (NCT04343651, NCT04347239). In addition, limiting neutrophil infiltration into the lungs of COVID-19 patients may help prevent disease progression and outcome. With this in mind, the monoclonal antibody BMS-986253 that blocks CXCL8 as well as Reparixin, an oral inhibitor of CXCR1/2, are both currently undergoing clinical trials in the U.S. for reducing the severity of COVID-19-related pneumonia by reducing neutrophil accumulation within the lungs of infected patients (NCT04878055, NCT04347226). A clinical trial was recently completed using measurement of CXCL10 in a Clinical Decision Support Protocol in COVID-19 patients (NCT04389645) that positively correlated CXCL10 levels with mortality suggesting that targeting CXCL10 signaling may also be beneficial in managing disease severity [31].

Examination of brains of SARS-CoV-2-infected K18-hACE2 mice, as well as brains from other hACE2 transgenic mice, has revealed that virus is able to infect, replicate and spread within the parenchyma and this is considered important in contributing to mortality [2, 5, 8, 9]. Virus can be detected in different anatomic regions of the brain and is accompanied by cell death [5] and these observations are consistent with early studies examining SARS-CoV-1 infection of K18-hACE2 mice [7]. Our results indicate that neurons are primary targets for SARS-CoV-2 infection within the brains of K18-hACE2 mice which is consistent with other studies [10, 32, 33]. Furthermore, human iPSC-derived neurons were susceptible to SARS-CoV-2 infection and virus was able to replicate in these cells. The detection of viral antigen within dendrites extending from the cell body suggests this may offer a unique mechanism of viral replication and spread in neurons and this is further emphasized by the absence of cell death and/or syncytia formation. RNA sequencing of infected neurons revealed that expression of most inflammatory and anti-viral response genes were reduced in SARS-CoV-2-infected neurons, consistent with a previously published study highlighting the muted immune response in neurons infected with SARS-CoV-2 as compared to Zika virus [2]. However, IPA analysis determined that despite the lack of induced immune and inflammatory response in infected neurons, there was a significant overrepresentation of pathways associated with eIF2, oxidative phosphorylation, regulation of eIF4 and mTOR signaling. eIF2, which mediates initiation of eukaryotic translation by binding Met-tRNA$_i^{Met}$ to the ribosomal subunit, can be activated via phosphorylation by various kinases, including protein kinase-RNA-dependent (PKR), PKR-like endoplasmic reticulum kinase (PERK), and heme regulated inhibitor (HRI) [34]. Upregulation of eIF2 phosphorylation by these can occur in response to various types of stressors including viral infection, ER stress, or oxidative stress, respectively [34]. Upregulation of eIF4, which mediates recruitment of

ribosomes to mRNA for translation, alongside overactivation of mTOR signaling, which modulates eIF4 activity, suggests infection of neurons with SARS-CoV-2 induces increased cellular activity and protein production even in the absence of inflammatory and anti-viral gene induction [35]. Whether this increase in protein production pathways corresponds to viral hijacking of cellular machinery for viral reproduction or if it corresponds to other induced mechanisms of neuronal stress/survival response remains to be determined.

Resident cells of the CNS are important in host defense following viral infection through either secretion of anti-viral cytokines like type I interferon (IFN-I) and pro-inflammatory cytokines/chemokines, and presentation of antigen to infiltration of antigen-sensitized T cells. We found the transcripts encoding the T cell chemoattractant chemokines including CXCL9 and CXCL10 were expressed along with monocyte/macrophage chemokines CCL2 and CCL5 and CXCL1 which attracts neutrophils. In addition, transcripts specific for the B cell chemoattractant CCL19 were also detected. The chemokine elicited in response to CNS infection of K18-hACE2 by SARS-CoV-2 infection is remarkably similar to the chemokine response following CNS infection of mice with the neuroadapted strains of murine coronaviruses [36, 37]. This is interesting in that murine coronavirus are primarily tropic for glial cells e.g. astrocytes, microglia and oligodendrocytes with relative sparing of neurons while neurons appear to be exclusively targeted by SARS-CoV-2. These findings argue that expression of chemokines following coronavirus infection of the CNS may not be influenced by the cellular target of infection and this may reflect a localized response to expression of interferons (IFN) expressed in response to viral infection. With this in mind, we did detect IFNl3 transcripts within the brains of SARS-CoV-2 infected mice yet IFNb1 transcripts were noticeably reduced. The inflammatory response consisted primarily of monocytes/macrophages as determined by immunofluorescent staining for

Mac2 and these cells are most likely migrating into the CNS in response to CCL2 and CCL5 expression [18-21]. We did not detect a robust T cell response and this was surprising given the expression levels of CXCL9 and CXCL10 transcripts. Whether this simply reflected that T cells had yet to migrate into the brains of infected mice at the time of sacrifice or if efficient translation of these transcripts is compromised is not known at this time.

We have recently determined that in response to JHMV infection of the CNS of immunocompetent mice, there are inflammatory monocyte/macrophage subpopulations that differentially express CD115/CSF-1R and this highlights the highly inflammatory nature of these cells in models of neurodegeneration [37]. Expression of CD115-expressing macrophages and microglia have also been detected in other models of neuroinflammation demonstrating important roles for these cells in contributing to inflammatory responses[38-40] More recently, microglia are recognized to be important in host defense in response to viral infection of the CNS [41-45]. Targeted depletion of microglia via CSF1R inhibition leads to increased mortality in mice infected with West Nile Virus (WNV) and is associated with diminished activation of antigen presenting cells (APCs) and limited reactivation of virus-specific T cells that leads to reduced viral clearance [42, 44]. Similar findings have been reported for other neurotropic viruses including Japanese encephalitis virus (JEV) [44] and Theiler's murine encephalomyelitis virus (TMEV) [43, 45]. Moreover, microglia have also been shown to enhance host defense following CNS infection by the neurotropic JHM strain of mouse hepatitis virus (JHMV, a murine coronavirus) and this was related to inefficient T cell-mediated control of viral replication [41, 46]. Additionally, the absence of microglia also results in an increase in the severity of demyelination, accompanied by a decrease in remyelination [46, 47]. In response to SARS-CoV-2 CNS infection, we did detect microgliosis indicating these cells are responding to

infection and may be involved in host defense. Ablation of microglia via PLX5622 administration did not affect clinical disease nor viral burden within the brain indicating these cells are dispensable in terms of controlling SARS-CoV-2 replication within the brain in the K18-hACE2 model. There was a marked reduction in expression of proinflammatory cytokines/chemokines including monocyte/macrophage chemoattractants CCL2 and CCL5 and this corresponded with an overall reduction in numbers of these cells in the brains of PLX5622-treated mice. These findings support the notion that microglia do contribute to the neuroinflammatory response, in part, through influencing expression of chemokines/cytokines in response to SARS-CoV-2 infection of the CNS of K18-hACE2 mice.

Very early in the COVID-19 pandemic, it became apparent that an abundant number of patients exhibited a variety of neurologic conditions that ranged in severity. Although numerous neurological symptoms have been associated with COVID-19, the most common neurologic symptoms include anosmia/dysgeusia, delirium, encephalopathy, and stroke [48-50]. The overwhelming evidence indicates that SARS-CoV-2 is not readily detected within the CNS by either PCR and/or immunohistochemical staining [2, 51] suggesting that neurologic complications associated with COVID-19 patients may occur through alternative mechanisms, including the potential development of autoreactive antibodies specific for neural antigens [52]. COVID-19 patients have anti-SARS-CoV-2 IgG antibodies in the cerebral spinal fluid (CSF) that recognized target epitopes that differ from serum antibodies. Moreover, a portion of COVID-19 patients exhibited CSF antibodies that targeted self-antigens, arguing for the possibility that neurologic disease may be associated with CNS autoimmunity [52]. Nonetheless, neurons and cells of the vasculature have been shown to be targets of infection [53-57]. Despite increasing evidence indicating extensive SARS-CoV-2 infection of the CNS does not occur, autopsy

findings indicate the presence of microglia nodules, astrocyte activation and CD8+ T cell infiltration in the brain, providing evidence for immune responses occurring within the CNS of infected patients [3, 58, 59]. Related to this, a recent study indicated microglia nodules interacting with inflammatory CD8+ T cells within distinct anatomical regions of the brains of COVID-19 patients and this correlated with alerted systemic inflammation [60]. It is incontrovertible that transgenic hACE2 models, particularly the K18-hACE2 model, have provided a better understanding of the pathogenesis of COVID-19 yet the one notable and consistent drawback of many of these models is the ability of virus to infect, efficiently replicate, and spread within the parenchyma, which contributes to increased mortality. These findings emphasize the importance of working with animal models in which SARS-CoV-2 entry into the CNS is more consistent with what has been observed in COVID-19 patients.

METHODS AND MATERIALS

Mice and viral infection: All experiments were performed in accordance with animal protocols approved by the University of California, Irvine Institutional Animal Care and Use Committee. 8-16 week-old heterozygous K18-hACE2 C57BL/6 [strain: B6.Cg-Tg(K18-ACE2)2Prlmn/J] mice were obtained from Jackson Laboratory. Animals were housed by sex in single use disposable plastic cages and provided ad-libitum water. SARS-CoV-2 isolate USA-WA1/2020 was obtained from BEI. Mice were inoculated with between 10^4-10^5 PFU of SARS-CoV-2 in 10µL of DMEM or sham inoculated. Inoculations were performed under deep anesthesia through an intraperitoneal injection of a mixture of ketamine and xylazine. Infected and uninfected mice were examined and weighed daily. Animals were euthanized early if they reached pre-determined euthanasia criteria.

iPSC-neuronal differentiation: iPSC line iCS83iCTR33n1 was previously derived, characterized [61] and maintained as described at 37ºC, 5% CO_2 - on hESC Matrigel® (Fisher Scientific cat#08774552) with daily feeding of mTeSR1™ (Stem Cell Technologies cat#85850) [62]. Neuronal differentiation was performed using the protocol as described [62] with a modification that the cells were frozen at the neural progenitor stage at day 8 in CryoStor CS10 (Stem Cell Technologies #07931). Cells were thawed into LIA medium (ADF supplemented with 2mM Glutamax, 2% B27 without vitamin A, 0.2µM LDN 193189 and 1.5µM IWR1 20ng/mL Activin A (Peprotech #120-14E)) containing 10µM Y-27632 dihydrochloride for the first day post-thaw for further neural differentiation and subsequent daily feeds with LIA without Y-27632 dihydrochloride. Differentiated neurons were plated at $1x10^6$ cells per well in 6-well

plate format or at $8x10^4$cells per chamberslide well for imaging. Cells were infected with either pseudovirus or SARS-CoV-2 at d46-50 after start of differentiation.

SARS-CoV-2 infection of iPSC-derived neurons: SARS-CoV-2 isolate USA-WA1/2020 was obtained from BEI. Media was removed from cells and replaced with virus-containing media (or non-virus media for mock-infection wells) at 500µL per well of a 6-well plate or 200µL per chamberslide well for 1hr adsorption at 37ºC, 5% CO_2, for infection of cells at MOI = 0.1. Culture plates and chamber slides were gently rocked every 15min to ensure even distribution of infection media. Following 1hr adsorption, non-virus containing media was added to all cells for final volume of 2mL per well of a 6-well plate or 700µL per chamberslide well and were allowed to incubate with virus for 24 or 48h and then fixed with 4% PFA for subsequent immunocytochemical staining. Cells in 6-well plates were allowed to incubate with virus for 24, 48, or 72h; supernatants were then collected, and cells harvested using 700µL of cold TRIzol Reagent (Ambion, 15596018) for subsequent qPCR analysis.

PLX5622 treatment: Rodent chow (AIN-76A) formulated with CSF1R inhibitor-PLX5622 at a dose of 1,200 ppm was provided by Plexxikon, Inc (Berkeley, CA). Mice were fed either PLX5622 chow or control chow 7 days prior to viral infection, and chow was continued until mice were sacrificed at defined time points post-infection.

RNA extraction: All RNA from VSV experiments with iPSC neurons, astrocytes, and microglia was extracted via the RNeasy Mini Kit (Qiagen, 74106) using the "Purification of Total RNA from Animal Cells using Spin Technology" protocol. Homogenization was performed using

QIAshredder spin columns (Qiagen, 79656). RNA from SARS-CoV-2 infected neurons was extracted via the RNeasy Mini Kit using the "Purification of Total RNA, Including Small RNAs, from Animal Cells" protocol. TRIzol was substituted for QIAzol, and Buffer RW1 was substituted for Buffer RWT. Homogenization was performed using QIAshredder spin columns. All RNA from mouse tissues was extracted via the RNeasy Mini Kit using the "Purification of Total RNA, Including Small RNAs, from Animal Tissues" protocol. TRIzol was substituted for QIAzol, and Buffer RW1 was substituted for Buffer RWT. Homogenization was performed using the Bead Ruptor 12 (Omni International) and 1.4 mm ceramic beads (Omni International, 19-627). For brain tissue, the machine was set to 2 cycles at 2.25m/s for 15 seconds with a 1 second pause between cycles. For lungs, the machine was set to 2 cycles at 2.4m/s for 20 seconds with a 1 second pause between cycles.

cDNA synthesis: All cDNA was made by following the "First Strand cDNA Synthesis" standard protocol provided by New England Biolabs with their AMV Reverse Transcriptase (New England Biolabs, M0277L). Random hexamers (Invitrogen, N8080127) were used for the reactions. RNase inhibitors were not used in the cDNA synthesis.

Gene expression analysis via quantitative PCR: All qPCRs were performed using the Bio-Rad iQ5 and iTaq™ Universal SYBR® Green Supermix (Bio-Rad, 1725120). The standard protocol by Bio-Rad for iTaq™ Universal SYBR® Green Supermix was used unless otherwise stated. Reactions were 10µL, and the machine was set to run for 1 cycle (95℃ for 3 minutes), followed by 40 cycles (95℃ for 10 seconds, then 55℃ for 30 seconds). The following primer sequences were used:

Gene Target	Forward Primer	Reverse Primer
Mouse GAPDH	AACTTTGGCATTGTGGAAGG	GGATGCAGGGATGATGTTCT
Human GAPDH	CAGCCTCAAGATCATCAGCA	TGTGGTCATGAGTCCTTCCA
SARS-CoV-2 Spike	TAGTGCGTGATCTCCCTCAG	CCAGCTGTCCAACCTGAAGA

For the brain cytokine and chemokine qPCR, Qiagen's custom qPCR arrays were employed, following the protocol, "Real-Time PCR for RT^2 Profiler PCR Arrays Formats A, C, D, E, F, G." The plates were pre-aliquoted with primers for the following murine genes: Glyceraldehyde-3-phosphate dehydrogenase (GAPDH), beta actin, chemokine ligand 10 (CXCL10), chemokine ligand 9 (CXCL9), chemokine ligand 2 (CCL2), chemokine ligand 5 (CCL5), interferon gamma (IFN-g), interferon beta-1 (IFN-B1), tumor necrosis factor (TNF-a), interleukin 10 (IL10), chemokine ligand 1 (CXCL1), interleukin 28B (IFN-L3), chemokine ligand 19 (CCL19). Reactions were 25µL (1µL cDNA, 11.5 µL UltraPure Distilled Water (Invitrogen, 10977-015), 12.5 µL iTaq™ Universal SYBR® Green Supermix). The machine was set to run for 1 cycle (95℃ for 10 minutes), followed by 40 cycles (95℃ for 15 seconds, then 60℃ for 1 minute). Ct values for each sample were normalized to an internal control (GAPDH), yielding the dCt values. dCt values of infected or PLX-treated samples were compared to appropriate control samples, as indicated, to produce ddCt values. The relative fold change between samples used in the ddCt calculation was calculated (2^{-ddCt}).

qPCR statistical analysis: Statistical analysis was performed in Prism (GraphPad Software). The Brown-Forsythe and Welch's ANOVA tests were used to compare the means between groups. Dunnett's test to correct for multiple comparisons was performed when necessary.

mRNA-Seq: Total RNA was isolated using the Qiagen RNeasy Kit and QIAshredders for cell lysis. One microgram of RNA with RNA integrity number values >9 was used for library preparation using the strand-specific Illumina TruSeq mRNA protocol. Libraries were sequenced on the NovaSeq 6000 platform using 100 cycles to obtain paired-end 100 reads at >30 million reads per sample. For RNA-seq analysis, fastq files were trimmed using a base quality score threshold of >20 and aligned to the hg38 genome with Hisat 2. Reads passing quality control were used for quantification using featureCounts and analyzed with the R package DESeq2 to identify DEGs. Genes passing an FDR of 10% were used for GO enrichment analysis using GOrilla (27) (http://cbl-gorilla.cs.technion.ac.il/). For the heatmaps, a list of genes from GO:0006955 immune response and GO:0006954 inflammatory response was used. From those lists, the genes with the top 100 most variable TPM were plotted using the R package pheatmap. For the 48h vs 24h IPA, the TPM of all genes in the 1_Infected_24h sample were subtracted from the TPM of all genes in the 2_Infected_48h sample. The list of genes were sorted by the difference and the top 400 and bottom 400 selected to use as input for IPA's core analysis.

Histology and immunohistochemical staining: Mice were euthanized at defined time points post-infection and tissues harvested according to IACUC-approved guidelines. Tissues were collected and placed in either cold TRIzol for qPCR analysis or 4% PFA for fixation and subsequent histological analysis. Following fixation, the 24-48hr brains were either

cryoprotected in 30% sucrose, embedded in O.C.T. (Fisher HealthCare), and sliced via Cryostat in 10µm sagittal sections. Alternatively, tissues were dehydrated and paraffin-embedded and subsequently use for RNAscope or hematoxylin/eosin (H&E) in combination with luxol fast blue (LFB) to assess demyelination within the brains of experimental mice. For immunohistochemical staining of O.C.T.-embedded tissues, slides were rinsed with PBS to remove residual O.C.T., and antigen retrieval (incubation with 10mM sodium Citrate at 95ºC for 15min) was performed if required for specific antigens at which point samples were incubated with 5% normal goat serum and 0.1% Triton-X, followed by overnight incubation at 4 ºC with primary antibodies. Several primary antibodies were used, including Iba1 (1:500 Wako), GFAP (1:1000 Abcam), Mac2/ Galactin-3 (1:500, CL8942AP Cedarlane), CD4 (1:200 Abcam), CD8 (1:200 Abcam), MHC I (1:200 Abcam), and MHC II (1:200 Abcam). On the second day, slides were treated with appropriate secondary antibodies (1:1000 goat anti-rat/rabbit Invitrogen, 1:1000 goat anti-chicken, Abcam) following PBS rinsing. Slides were then mounted with DAPI Fluoromount-G (SouthernBiotech). High-resolution fluorescent images were obtained using a Leica TCS SPE-II confocal microscope and LAS-X software. For whole brain stitches, automated slide scanning was performed using a Zeiss AxioScan.Z1 equipped with a Colibri camera and Zen AxioScan 2.3 software. Microglial morphology was determined using the filaments module in Bitplane Imaris 7.5, as described previously (Elmore, Lee, West, & Green, 2015). Cell quantities were determined using the spots module in Imaris.

RNAscope in situ hybridization of SARS-CoV-2 spike RNA: RNA in situ hybridization was performed via RNAscope 2.5 HD Red Assay Kit (Advanced Cell Diagnostics, Cat: 322350) in accordance with manufacturer's instructions. Fixed tissue sections were treated with the

manufacturer's Fresh Frozen Tissue Sample Preparation Protocol, fixed in chilled 4% PFA, dehydrated, and treated with H_2O_2 and Protease IV before probe hybridization. Paraffinized sections were deparaffinized and treated with H_2O_2 and Protease Plus prior to hybridization. Probes targeting SARS-CoV-2 spike (Cat: 848561), positive control Hs-PPIB (Cat: 313901), or negative control DapB (Cat: 310043) were hybridized followed by proprietary assay signal amplification and detection. Tissues were counterstained with Gill's hematoxylin. An uninfected mouse was used as a negative control and stained in parallel. Tissues were visualized using an Olympus BX60 microscope and imaged with a Nikon (Model #) camera.

Immunocytochemical staining for SARS-CoV-2: iPSC-derived neurons on glass-bottomed 4-well chamberslides were gently washed with 1X PBS and fixed for 1hr with 4% paraformaldehyde for removal from BSL-3 facility. Wells were subsequently washed 3 times with 1X PBS, permeabilized for 15min at RT in 0.1% Triton-X in PBS and blocked for 2hrs in a 2% BSA-5% NDS blocking solution. Cells were incubated overnight at 4ºC in blocking solution with primary antibodies anti-MAP2 (EnCor Biotech. Cat:NC0388389) and anti-SARS-CoV-2 nucleocapsid (Sino Bio. Cat: 40143-R019). Cells were then washed with 1X PBS and incubated in blocking solution for 2hrs at RT with secondary antibodies, Alexa Fluor 594-conjugated goat anti-chicken and Alexa Fluor 488-conjugated goat anti-rabbit. After staining, cells were imaged for presence of SARS-CoV-2 nucleocapsid staining and quantified using the Revolve D75.

Acknowledgements

This work was supported by a COVID CRAFT grant from UC Irvine Office of Research, NIH-NINDS R35 NS116835, NIH-NINDS NS041249, National Multiple Sclerosis Society grant CA-1607-25040 and support from the Ray and Tye Noorda Foundation to T.E.L. L.M.T. was supported by NIH-NINDS R35 NS116872 and K.N.G. was supported by NIH-NINDS R01NS083801. G.M.O. was supported by Immunology Research Training Grant 5T32AI060573-15 and C.S-G was supported by the Hereditary Disease Foundation. The authors wish to acknowledge the support of the Chao Family Comprehensive Cancer Center Experimental Tissue Shared Resource supported by the National Cancer Institute of the National Institutes of Health under award number P30CA062203.

REFERENCES

1. Channappanavar, R. and S. Perlman, *Age-related susceptibility to coronavirus infections: role of impaired and dysregulated host immunity.* J Clin Invest, 2020. **130**(12): p. 6204-6213.

2. Song, E., et al., *Neuroinvasion of SARS-CoV-2 in human and mouse brain.* J Exp Med, 2021. **218**(3).

3. Lou, J.J., et al., *Neuropathology of COVID-19 (neuro-COVID): clinicopathological update.* Free Neuropathol, 2021. **2**.

4. Virhammar, J., et al., *Acute necrotizing encephalopathy with SARS-CoV-2 RNA confirmed in cerebrospinal fluid.* Neurology, 2020. **95**(10): p. 445-449.

5. Pellegrini, L., et al., *SARS-CoV-2 Infects the Brain Choroid Plexus and Disrupts the Blood-CSF Barrier in Human Brain Organoids.* Cell Stem Cell, 2020. **27**(6): p. 951-961 e5.

6. Munoz-Fontela, C., et al., *Animal models for COVID-19.* Nature, 2020. **586**(7830): p. 509-515.

7. McCray, P.B., Jr., et al., *Lethal infection of K18-hACE2 mice infected with severe acute respiratory syndrome coronavirus.* J Virol, 2007. **81**(2): p. 813-21.

8. Zheng, J., et al., *COVID-19 treatments and pathogenesis including anosmia in K18-hACE2 mice.* Nature, 2021. **589**(7843): p. 603-607.

9. Bao, L., et al., *The pathogenicity of SARS-CoV-2 in hACE2 transgenic mice.* Nature, 2020. **583**(7818): p. 830-833.

10. Sun, S.H., et al., *A Mouse Model of SARS-CoV-2 Infection and Pathogenesis.* Cell Host Microbe, 2020. **28**(1): p. 124-133 e4.

11. Winkler, E.S., et al., *Publisher Correction: SARS-CoV-2 infection of human ACE2-transgenic mice causes severe lung inflammation and impaired function.* Nat Immunol, 2020. **21**(11): p. 1470.

12. Jiang, R.D., et al., *Pathogenesis of SARS-CoV-2 in Transgenic Mice Expressing Human Angiotensin-Converting Enzyme 2.* Cell, 2020. **182**(1): p. 50-58 e8.

13. Reichard, R.R., et al., *Neuropathology of COVID-19: a spectrum of vascular and acute disseminated encephalomyelitis (ADEM)-like pathology.* Acta Neuropathol, 2020. **140**(1): p. 1-6.

14. Elmore, M.R., et al., *Colony-stimulating factor 1 receptor signaling is necessary for microglia viability, unmasking a microglia progenitor cell in the adult brain.* Neuron, 2014. **82**(2): p. 380-97.

15. Spangenberg, E., et al., *Sustained microglial depletion with CSF1R inhibitor impairs parenchymal plaque development in an Alzheimer's disease model.* Nat Commun, 2019. **10**(1): p. 3758.

16. Trujillo, J.A., E.L. Fleming, and S. Perlman, *Transgenic CCL2 expression in the central nervous system results in a dysregulated immune response and enhanced lethality after coronavirus infection.* J Virol, 2013. **87**(5): p. 2376-89.

17. Kim, T.S. and S. Perlman, *Viral expression of CCL2 is sufficient to induce demyelination in RAG1-/- mice infected with a neurotropic coronavirus.* J Virol, 2005. **79**(11): p. 7113-7120.

18. Held, K.S., et al., *Differential roles of CCL2 and CCR2 in host defense to coronavirus infection.* Virology, 2004. **329**(2): p. 251-60.

19. Chen, B.P., W.A. Kuziel, and T.E. Lane, *Lack of CCR2 results in increased mortality and impaired leukocyte activation and trafficking following infection of the central nervous system with a neurotropic coronavirus.* J Immunol, 2001. **167**(8): p. 4585-92.

20. Glass, W.G., et al., *Antibody Targeting of the CC Chemokine Ligand 5 Results in Diminished Leukocyte Infiltration into the Central Nervous System and Reduced Neurologic Disease in a Viral Model of Multiple Sclerosis.* The Journal of Immunology, 2004. **172**(7): p. 4018-4025.

21. Glass, W.G., et al., *Reduced macrophage infiltration and demyelination in mice lacking the chemokine receptor CCR5 following infection with a neurotropic coronavirus.* Virology, 2001. **288**(1): p. 8-17.

22. Liu, M.T., et al., *Cutting Edge: The T Cell Chemoattractant IFN-Inducible Protein 10 Is Essential in Host Defense Against Viral-Induced Neurologic Disease.* The Journal of Immunology, 2000. **165**(5): p. 2327-2330.

23. Stiles, L.N., et al., *T cell antiviral effector function is not dependent on CXCL10 following murine coronavirus infection.* J Immunol, 2006. **177**(12): p. 8372-80.

24. Stiles, L.N., et al., *CXCL10 and trafficking of virus-specific T cells during coronavirus demyelination.* Autoimmunity, 2009. **In Press**.

25. Hosking, M.P., et al., *A protective role for ELR+ chemokines during acute viral encephalomyelitis.* PLoS Pathog, 2009. **5**(11): p. e1000648.

26. Lowery, S.A., A. Sariol, and S. Perlman, *Innate immune and inflammatory responses to SARS-CoV-2: Implications for COVID-19.* Cell Host Microbe, 2021. **29**(7): p. 1052-1062.

27. Channappanavar, R. and S. Perlman, *Pathogenic human coronavirus infections: causes and consequences of cytokine storm and immunopathology.* Semin Immunopathol, 2017. **39**(5): p. 529-539.

28. Alosaimi, B., et al., *Complement Anaphylatoxins and Inflammatory Cytokines as Prognostic Markers for COVID-19 Severity and In-Hospital Mortality.* Front Immunol, 2021. **12**: p. 668725.

29. Huang, C., et al., *Clinical features of patients infected with 2019 novel coronavirus in Wuhan, China.* Lancet, 2020. **395**(10223): p. 497-506.

30. Laudanski, K., et al., *Unbiased Analysis of Temporal Changes in Immune Serum Markers in Acute COVID-19 Infection With Emphasis on Organ Failure, Anti-Viral Treatment, and Demographic Characteristics.* Front Immunol, 2021. **12**: p. 650465.

31. Lev, S., et al., *Observational cohort study of IP-10's potential as a biomarker to aid in inflammation regulation within a clinical decision support protocol for patients with severe COVID-19.* PLoS One, 2021. **16**(1): p. e0245296.

32. Kumari, P., et al., *Neuroinvasion and Encephalitis Following Intranasal Inoculation of SARS-CoV-2 in K18-hACE2 Mice.* Viruses, 2021. **13**(1).

33. Carossino, M., et al., *Fatal neuroinvasion of SARS-CoV-2 in K18-hACE2 mice is partially dependent on hACE2 expression.* bioRxiv, 2021.

34. Schmitt, E., M. Naveau, and Y. Mechulam, *Eukaryotic and archaeal translation initiation factor 2: a heterotrimeric tRNA carrier.* FEBS Lett, 2010. **584**(2): p. 405-12.

35. Showkat, M., M.A. Beigh, and K.I. Andrabi, *mTOR Signaling in Protein Translation Regulation: Implications in Cancer Genesis and Therapeutic Interventions.* Mol Biol Int, 2014. **2014**: p. 686984.

36. Lane, T.E., et al., *Dynamic regulation of alpha- and beta-chemokine expression in the central nervous system during mouse hepatitis virus-induced demyelinating disease.* J Immunol, 1998. **160**(2): p. 970-8.

37. Syage, A.R., et al., *Single-Cell RNA Sequencing Reveals the Diversity of the Immunological Landscape following Central Nervous System Infection by a Murine Coronavirus.* J Virol, 2020. **94**(24).

38. Hagan, N., et al., *CSF1R signaling is a regulator of pathogenesis in progressive MS.* Cell Death Dis, 2020. **11**(10): p. 904.

39. Knight, A.C., et al., *Differential regulation of TREM2 and CSF1R in CNS macrophages in an SIV/macaque model of HIV CNS disease.* J Neurovirol, 2020. **26**(4): p. 511-519.

40. Zuroff, L.R., et al., *Effects of IL-34 on Macrophage Immunological Profile in Response to Alzheimer's-Related Abeta42 Assemblies.* Front Immunol, 2020. **11**: p. 1449.

41. Wheeler, D.L., et al., *Microglia are required for protection against lethal coronavirus encephalitis in mice.* J Clin Invest, 2018. **128**(3): p. 931-943.

42. Funk, K.E. and R.S. Klein, *CSF1R antagonism limits local restimulation of antiviral CD8(+) T cells during viral encephalitis.* J Neuroinflammation, 2019. **16**(1): p. 22.

43. Sanchez, J.M.S., et al., *Microglial cell depletion is fatal with low level picornavirus infection of the central nervous system.* J Neurovirol, 2019. **25**(3): p. 415-421.

44. Seitz, S., P. Clarke, and K.L. Tyler, *Pharmacologic Depletion of Microglia Increases Viral Load in the Brain and Enhances Mortality in Murine Models of Flavivirus-Induced Encephalitis.* J Virol, 2018. **92**(16).

45. Waltl, I., et al., *Microglia have a protective role in viral encephalitis-induced seizure development and hippocampal damage.* Brain Behav Immun, 2018. **74**: p. 186-204.

46. Mangale, V., et al., *Microglia influence host defense, disease, and repair following murine coronavirus infection of the central nervous system.* Glia, 2020. **68**(11): p. 2345-2360.

47. Sariol, A., et al., *Microglia depletion exacerbates demyelination and impairs remyelination in a neurotropic coronavirus infection.* Proc Natl Acad Sci U S A, 2020. **117**(39): p. 24464-24474.

48. Glatzel, M., et al., *Neuropathology associated with SARS-CoV-2 infection.* Lancet, 2021. **397**(10271): p. 276.

49. Leven, Y. and J. Bosel, *Neurological manifestations of COVID-19 - an approach to categories of pathology.* Neurol Res Pract, 2021. **3**(1): p. 39.

50. Johansson, A., et al., *Neurological manifestations of COVID-19: A comprehensive literature review and discussion of mechanisms.* J Neuroimmunol, 2021. **358**: p. 577658.

51. Matschke, J., et al., *Neuropathology of patients with COVID-19 in Germany: a post-mortem case series.* Lancet Neurol, 2020. **19**(11): p. 919-929.

52. Song, E., et al., *Divergent and self-reactive immune responses in the CNS of COVID-19 patients with neurological symptoms.* Cell Rep Med, 2021. **2**(5): p. 100288.

53. Yang, A.C., et al., *Dysregulation of brain and choroid plexus cell types in severe COVID-19.* Nature, 2021. **595**(7868): p. 565-571.

54. Karuppan, M.K.M., et al., *SARS-CoV-2 Infection in the Central and Peripheral Nervous System-Associated Morbidities and Their Potential Mechanism.* Mol Neurobiol, 2021. **58**(6): p. 2465-2480.

55. Akhter, N., et al., *Impact of COVID-19 on the cerebrovascular system and the prevention of RBC lysis.* Eur Rev Med Pharmacol Sci, 2020. **24**(19): p. 10267-10278.

56. Chia, K.X., S. Polakhare, and S.D. Bruno, *Possible affective cognitive cerebellar syndrome in a young patient with COVID-19 CNS vasculopathy and stroke.* BMJ Case Rep, 2020. **13**(10).

57. MacLean, M.A., et al., *The potential role of microvascular pathology in the neurological manifestations of coronavirus infection.* Fluids Barriers CNS, 2020. **17**(1): p. 55.

58. Thakur, K.T., et al., *COVID-19 neuropathology at Columbia University Irving Medical Center/New York Presbyterian Hospital.* Brain, 2021. **144**(9): p. 2696-2708.

59. Al-Dalahmah, O., et al., *Neuronophagia and microglial nodules in a SARS-CoV-2 patient with cerebellar hemorrhage.* Acta Neuropathol Commun, 2020. **8**(1): p. 147.

60. Schwabenland, M., et al., *Deep spatial profiling of human COVID-19 brains reveals neuroinflammation with distinct microanatomical microglia-T-cell interactions.* Immunity, 2021. **54**(7): p. 1594-1610 e11.

61. Consortium, H.D.i., *Induced pluripotent stem cells from patients with Huntington's disease show CAG-repeat-expansion-associated phenotypes.* Cell Stem Cell, 2012. **11**(2): p. 264-78.

62. Smith-Geater, C., et al., *Aberrant Development Corrected in Adult-Onset Huntington's Disease iPSC-Derived Neuronal Cultures via WNT Signaling Modulation.* Stem Cell Reports, 2020. **14**(3): p. 406-419.

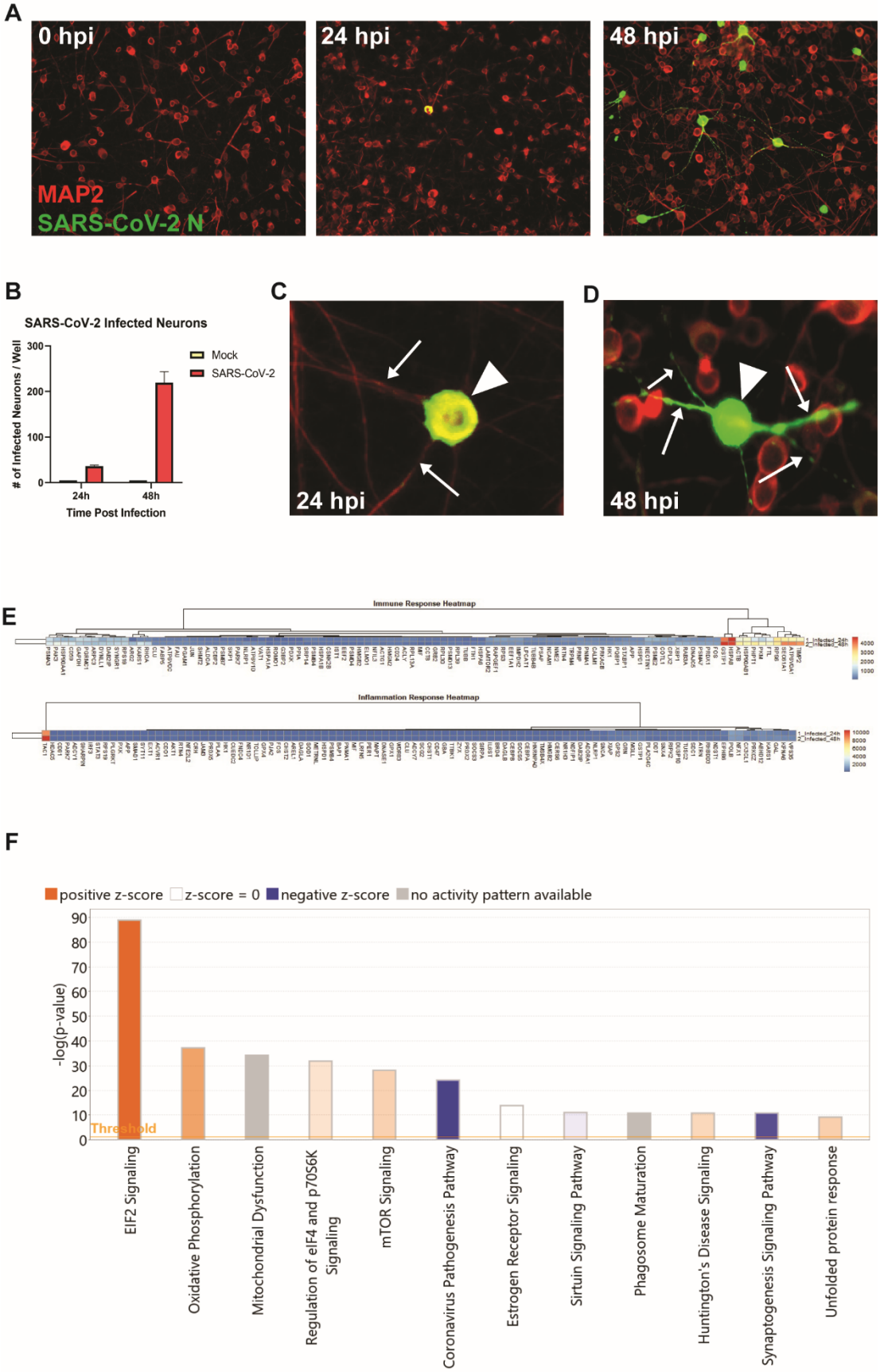
A
0 hpi
24 hpi
48 hpi
MAP2
SARS-CoV-2 N
B
SARS-CoV-2 Infected Neurons
# of Infected Neurons / Well
300
200
100
0
24h
48h
Time Post Infection
Mock
SARS-CoV-2
C
24 hpi
D
48 hpi
E
Immune Response Heatmap
Inflammation Response Heatmap
F
positive z-score
z-score = 0
negative z-score
no activity pattern available
-log(p-value)
90
80
70
60
50
40
30
20
10
0
Threshold
EIF2 Signaling
Oxidative Phosphorylation
Mitochondrial Dysfunction
Regulation of eIF4 and p70S6K Signaling
mTOR Signaling
Coronavirus Pathogenesis Pathway
Estrogen Receptor Signaling
Sirtuin Signaling Pathway
Phagosome Maturation
Huntington's Disease Signaling
Synaptogenesis Signaling Pathway
Unfolded protein response

Figure 1 SARS-CoV-2 infects human iPSC-derived neurons. (**A**) hiPSC-derived neurons were infected with SARS-CoV-2 at an MOI of 0.1, immunostained with anti-MAP2 and anti-SARS-CoV-2 N, and imaged at 0, 24, and 48 hours post-infection. (**B**) Quantification of SARS-CoV-2 GFP fluorescence of mock-infected and SARS-CoV-2-infected hiPSC-derived neurons. (**C**) Perinuclear replication of SARS-CoV-2 in neuronal soma (arrowhead) but no viral axonal (arrows) transport at 24 hours post-infection. (**D**) Perinuclear presence of SARS-CoV-2 in soma (arrowhead) and axon (arrows) at 24 hours post-infection. (**E**) Heat map of genes expressed 24 and 48h post-infection. **(F)** Top 12 canonical pathways showing progressive changes from 24 to 48 h post-infection.

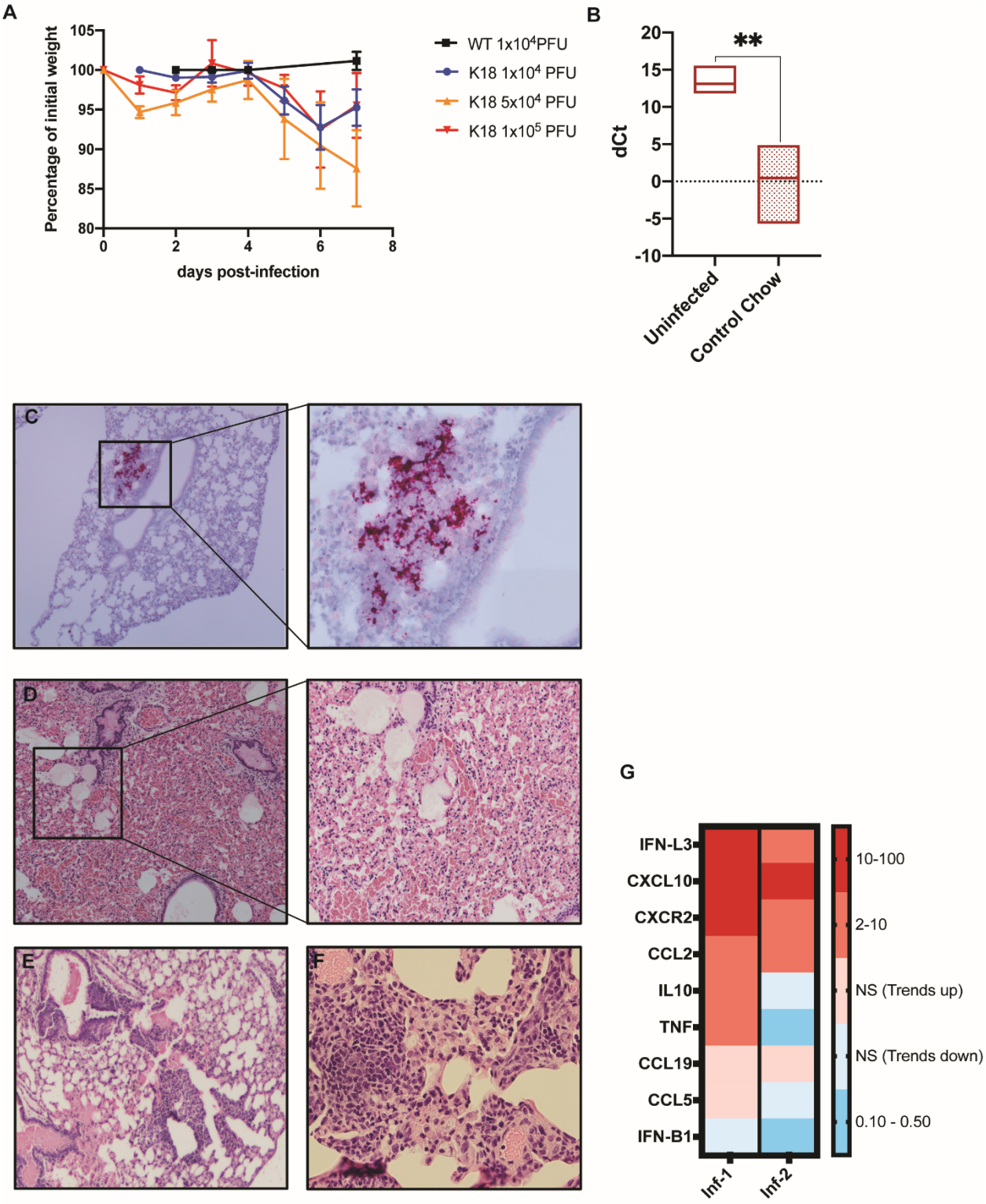
A
Percentage of initial weight
105
100
95
90
85
80
0
2
4
6
8
days post-infection
WT 1x10^4PFU
K18 1x10^4 PFU
K18 5x10^4 PFU
K18 1x10^5 PFU
B
**
dCt
20
15
10
5
0
-5
-10
Uninfected
Control Chow
C
D
E
F
G
IFN-L3
CXCL10
CXCR2
CCL2
IL10
TNF
CCL19
CCL5
IFN-B1
Inf-1
Inf-2
10-100
2-10
NS (Trends up)
NS (Trends down)
0.10 - 0.50

Figure 2 SARS-CoV-2 infection of lungs of K18-hACE2 mice. (A) Percent weight change of K18-hACE2 and WT mice infected with indicated dose of SARS-CoV-2. C57BL/6 wildtype (WT) mice (n=3) were infected with 1x104 PFU. K18-hACE2 mice were infected intranasally with SARS-CoV-2 at either $1x10^4$ PFU (n=17), $5x10^4$ PFU (n=4), or $1x10^5$PFU (n=8). (**B**) Quantitative PCR with primers for Spike mRNA on uninfected and SARS-CoV-2-infected mouse lung tissue. dCt values are derived from the difference between the Ct values of Spike mRNA and a housekeeping gene, GAPDH. Lower dCt values indicate increased viral mRNA. (**C**) K18-hACE2 mouse lung tissue at day 7 p.i. with $5x10^4$ PFU SARS-CoV-2 showing localized Spike mRNA expression as determined by RNAscope. Representative H&E images from lungs of SARS-CoV-2-infected mice ($5x10^4$ PFU) showing (**D**) airway edema, vascular congestion and intra-alveolar hemorrhage, (**E**) peri-bronchiolar lymphocytic cuffing, and (**F**) interstitial vascular congestion and lymphocytic infiltrates. (**G**) Quantitative PCR shows the fold changes of the indicated genes in two infected mouse lungs compared to uninfected mice.

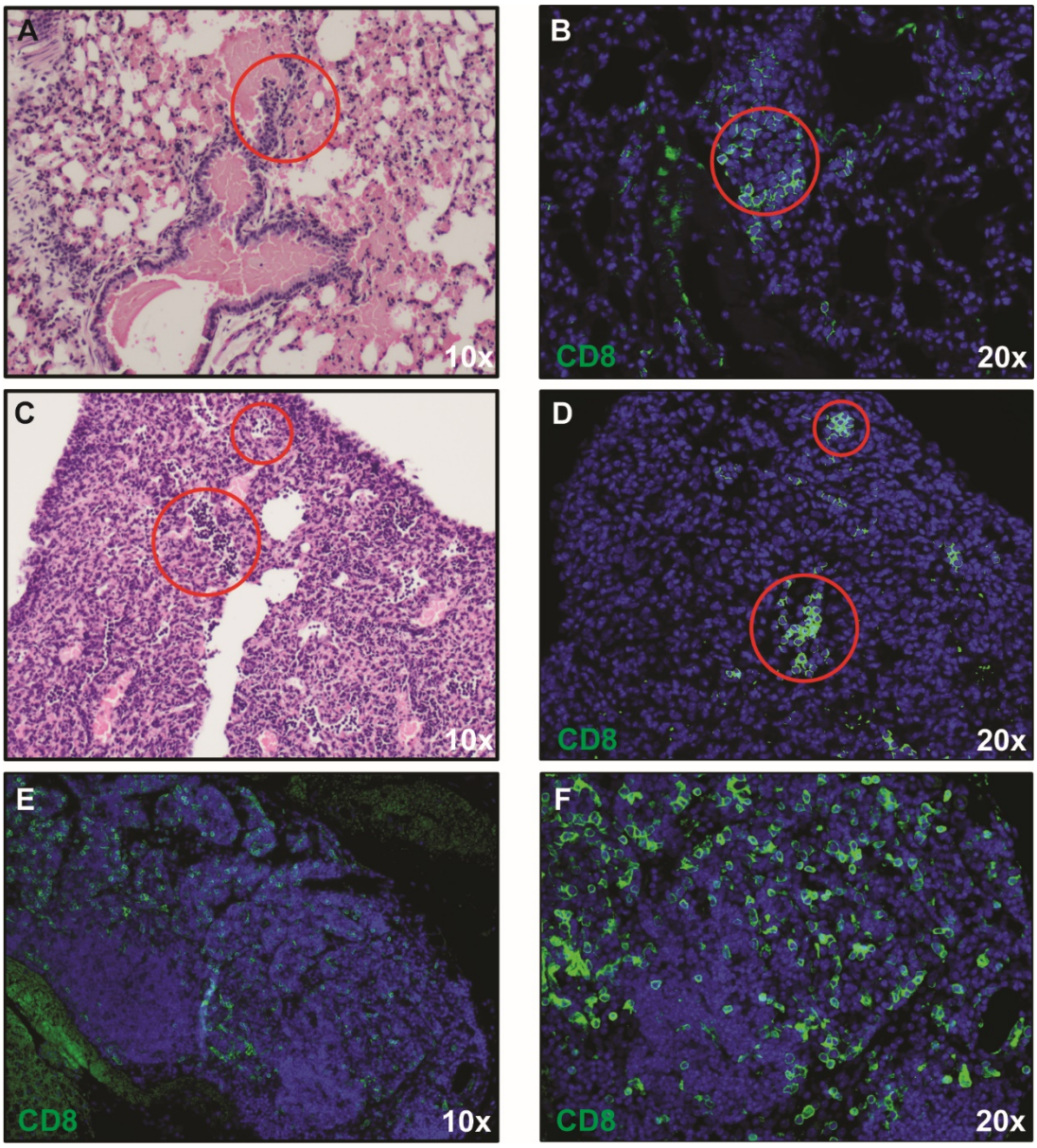

Figure 3 CD8+ T cell infiltration into lungs of SARS-CoV-2-infected mice. H&E staining of lungs of SARS-CoV-2 infected mice at day 7 post-infection reveal inflammation (**A** and **C**) associated with CD8+ T cell infiltration (**B** and **D**) as determined by immunofluorescent staining. Lymph node-like structures were also detected containing CD8+ T cells (**E** and **F**). Panels *A*, *C*, and *E* 10X magnification; panels *B*, *D*, and *F* 20X magnification.

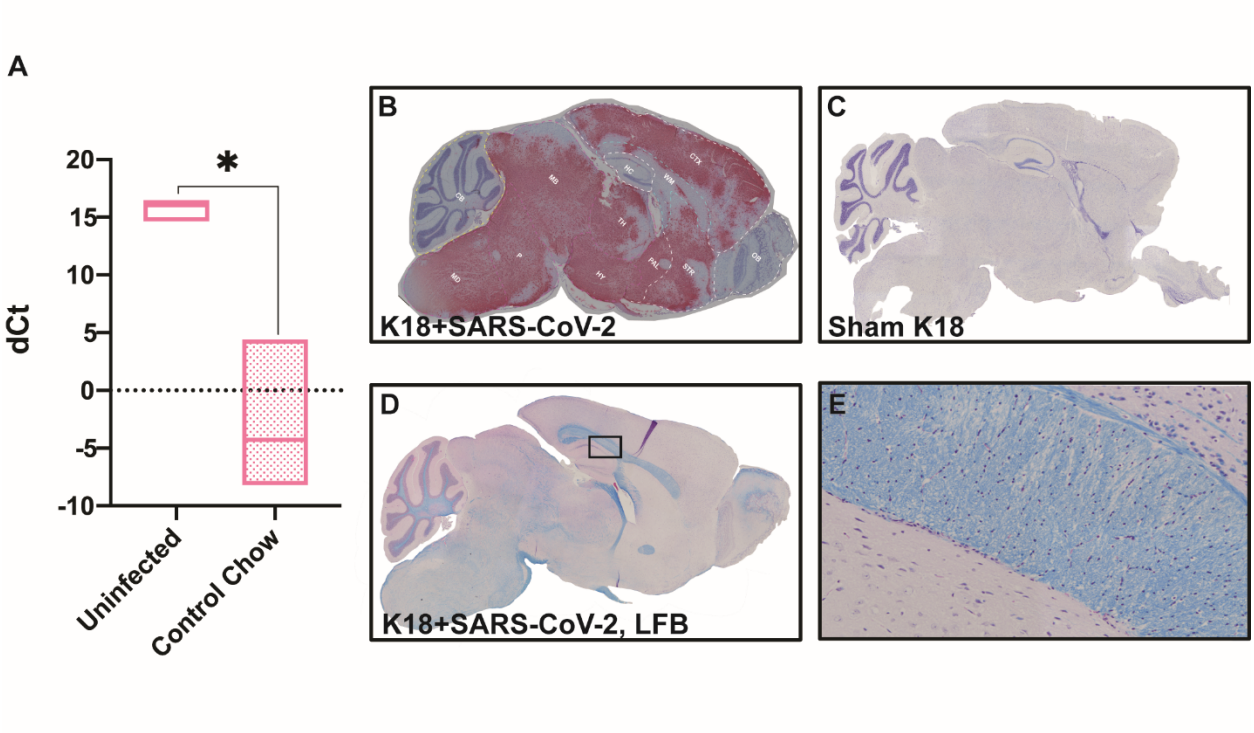

Figure 4 Widespread neuroinvasion by SARS-CoV-2 of K18 human-ACE2 mice. (A) Quantitative PCR with primers for Spike mRNA on uninfected and SARS-CoV-2-infected mouse brain tissue at day 7 p.i. dCt values are derived from the difference between the Ct values of Spike mRNA and the housekeeping gene, GAPDH. *In situ* hybridization for Spike viral mRNA in (**B**) SARS-CoV-2-infected and (**C**) sham-infected K18-hACE2 mice. Anatomical regions in which viral RNA is detected (indicated in red) are indicated: cortex (CTX), striatum (STR), pallidum (PAL), thalamus (TH), hypothalamus (HY), midbrain (MB), Pons (P), and medulla (MD), whereas areas that were relatively spared included the olfactory bulb (OB), white matter (WM) tracts and hippocampus (HC) (**D**) Representative brain from SARS-CoV-2 infected brain from panel *B* stained with LFB demonstrates lack of demyelination with (**E**) high-power image of myelin tract showing no inflammation or demyelination.

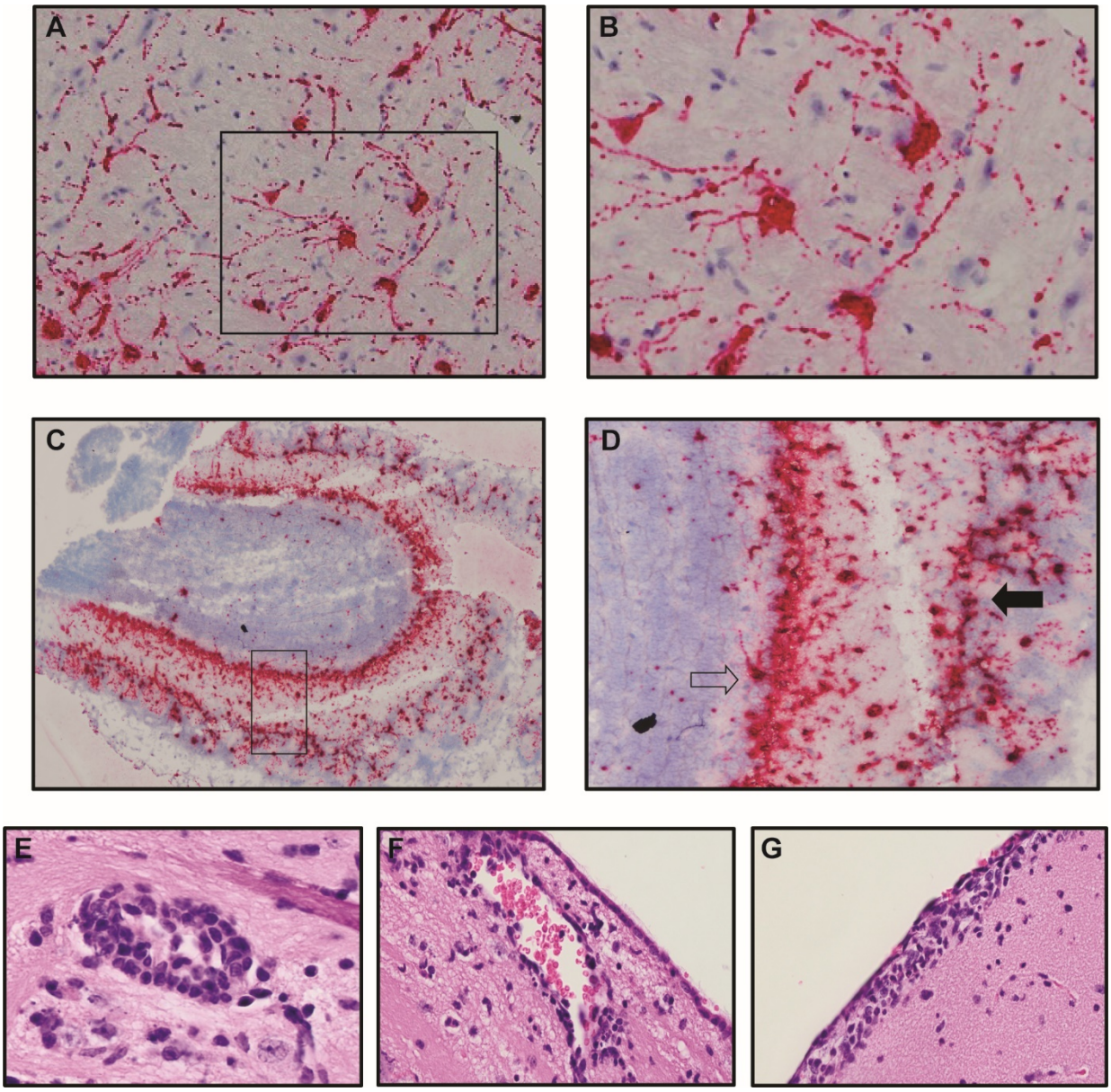

Figure 5 Neurons are targets of infection within the brains of SARS-CoV-2 infected K18-hACE2 mice. Brains of SARS-CoV-2 infected mice at day 7 p.i. were analyzed to assess cellular targets of infection through *in situ* hybridization using RNAscope *in situ* hybridization using Spike-specific probes. (**A**) Cells within the cortex with neuron morphology were primary targets of infection; (**B**) high-power image of cells boxed in panel *A* show viral RNA present within cell body as well as extending down dendrites extending from the cell body. (**C**) Viral RNA was also detected in olfactory bulbs at day 7 p.i. (**D**) high-power image cells boxed in panel *C* reveal neurons in the mitral (open arrow) and glomerular (closed arrow) are infected by virus. Representative H&E images from the brains of infected K18-hACE2 mice at day 7 p.i. depicting (**E**) perivascular cuffing, (**F**) subventricular inflammation, and (**G)** leptomeningitis.

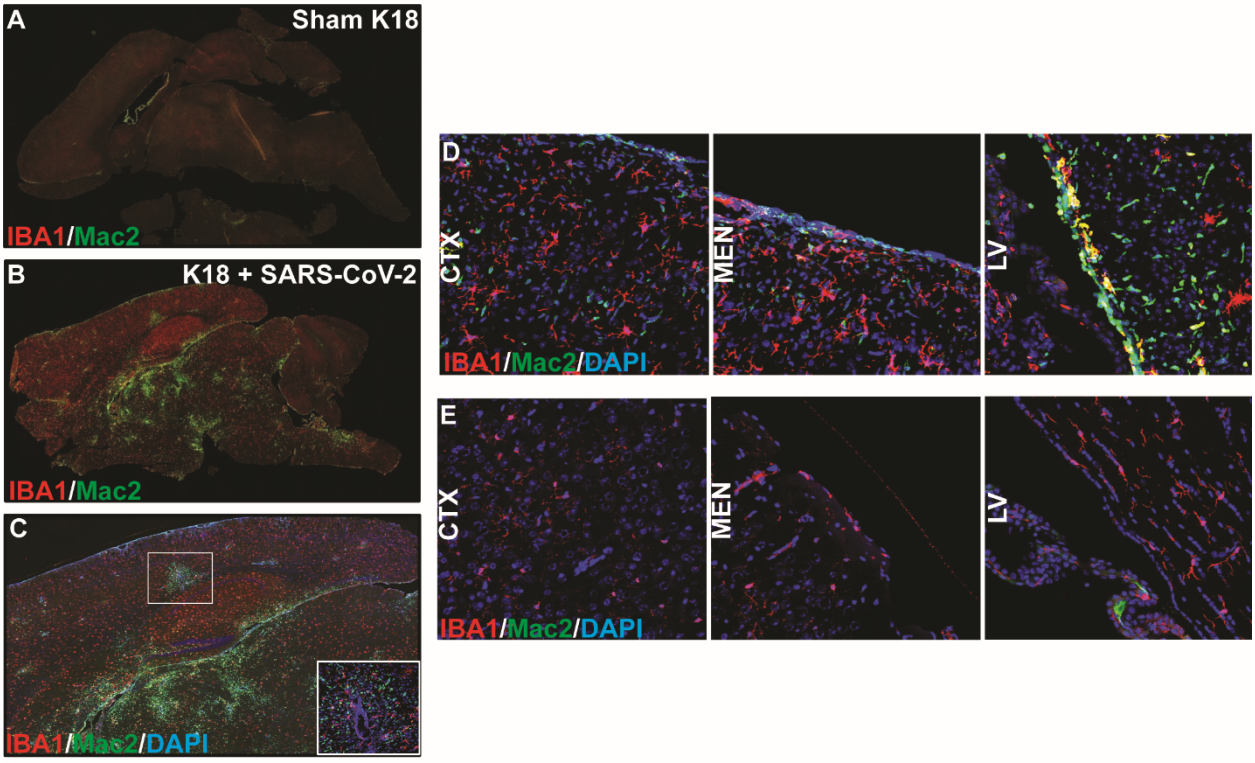

Figure 6 SARS-CoV-2 infection of K18 human-ACE2 mice results in microgliosis and myeloid cell infiltration. Brains from either SARS-CoV-2 or sham-infected mice were removed at day 7 p.i. to evaluate immune cell infiltration. Microglia activation and monocyte infiltration were determined in sham-infected mice **(A)** and SARS-CoV2 infected mice **(B)** by staining for expression of Iba1 (red) and Mac2/galectin 3 (green), respectively. Infiltration of peripheral monocytes into the SARS-CoV-2 infected brain parenchyma occurs via the vasculature (**C**) as well as ventricular and leptomeningeal spaces (**D**) compared to uninfected control mice (**E**).

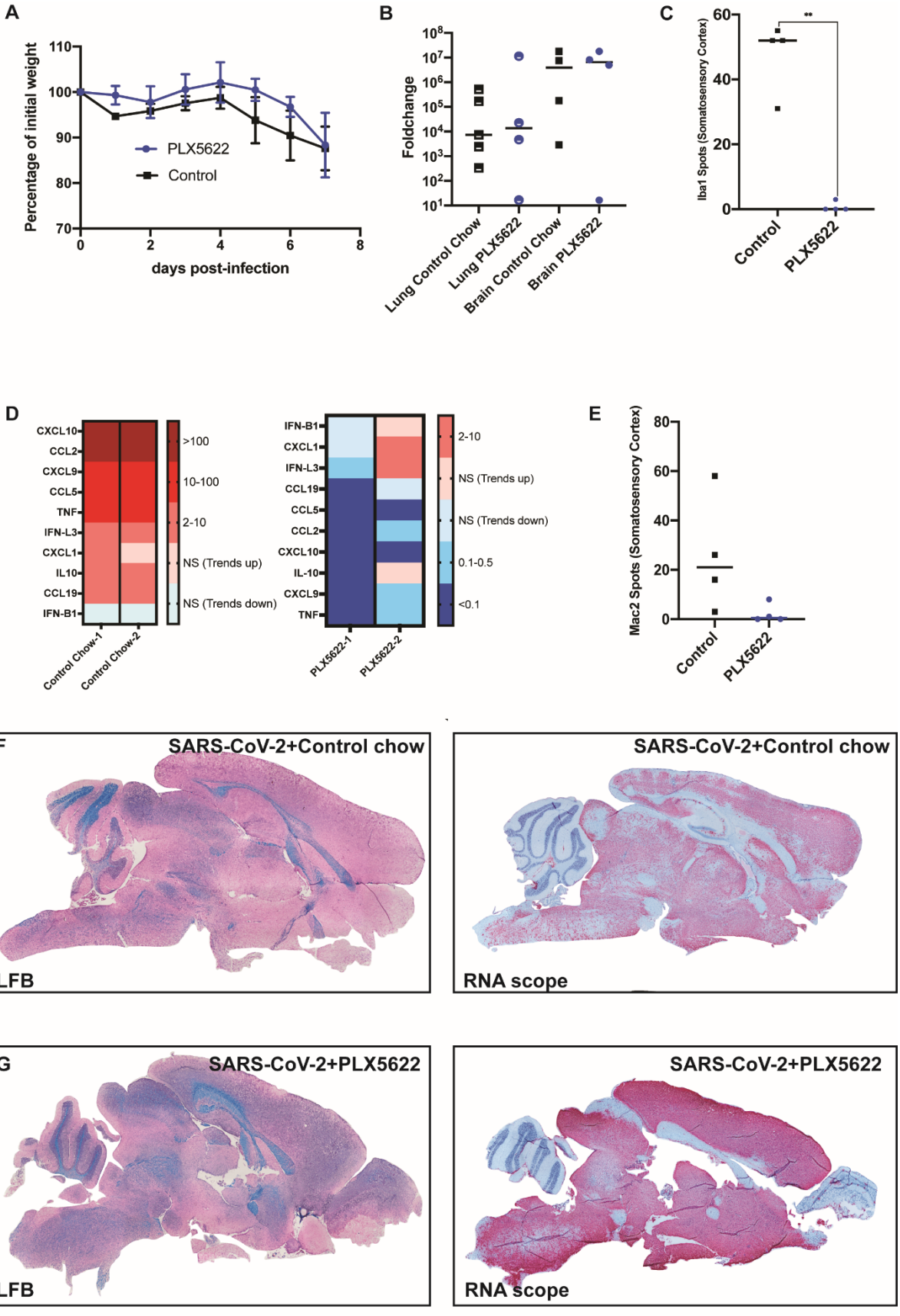
A
Percentage of initial weight
110
100
90
80
70
0
2
4
6
8
days post-infection
PLX5622
Control
B
Foldchange
10^8
10^7
10^6
10^5
10^4
10^3
10^2
10^1
Lung Control Chow
Lung PLX5622
Brain Control Chow
Brain PLX5622
C
Iba1 Spots (Somatosensory Cortex)
60
40
20
0
**
Control
PLX5622
D
CXCL10
CCL2
CXCL9
CCL5
TNF
IFN-L3
CXCL1
IL10
CCL19
IFN-B1
>100
10-100
2-10
NS (Trends up)
NS (Trends down)
Control Chow-1
Control Chow-2
IFN-B1
CXCL1
IFN-L3
CCL19
CCL5
CCL2
CXCL10
IL-10
CXCL9
TNF
2-10
NS (Trends up)
NS (Trends down)
0.1-0.5
<0.1
PLX5622-1
PLX5622-2
E
Mac2 Spots (Somatosensory Cortex)
80
60
40
20
0
Control
PLX5622
F
SARS-CoV-2+Control chow
LFB
SARS-CoV-2+Control chow
RNA scope
G
SARS-CoV-2+PLX5622
LFB
SARS-CoV-2+PLX5622
RNA scope

Figure 7 Microglia ablation does not impact control of viral replication in the CNS. (**A**) Weight loss of K18-hACE2 mice infected intranasally with $5x10^4$ PFU of SARS-CoV-2 that were fed either control chow (n=4) of PLX5622-formulated chow (n=4). (**B**) Quantitative PCR in the brains and lungs of infected PLX-treated and non-PLX-treated mice shows no significant difference in the levels of Spike mRNA in either lung or brain tissue as a result of PLX5622 treatment. **(C)** Quantification of Iba1-positive cells in the somatosensory cortex shows a significant (**$p<0.01$) depletion of microglia from PLX5622 treated mice compared to control mice. (**D**) qPCR analysis of brains of experimental mice indicated a reduction in expression of pro-inflammatory cytokines/chemokines in the brains of PLX5622-treated mice compared to control mice. **(E)** Quantification of Mac2-positive cells in the somatosensory cortex an overall trend in reduced numbers in PLX5622-treated mice compared to controls. Brains from SARS-CoV-2-infected mice treated with either (**F**) control chow or (**G**) PLX5622 were stained with LFB to assess demyelination or the presence of viral RNA determined by RNAscope. Representative brain sections are from experimental mice at day 7 p.i.

MAC2 IS A LONG-LASTING MARKER OF PERIPHERAL CELL INFILTRATES INTO THE MOUSE CNS AFTER BONE MARROW TRANSPLANTATION AND CORONAVIRUS INFECTION

GLIA

MAC2 is a long-lasting marker of peripheral cell infiltrates into the mouse CNS after bone marrow transplantation and coronavirus infection

Lindsay A. Hohsfield[1] Kate I. Tsourmas[1] Yasamine Ghorbanian[2,3] Amber R. Syage[1] Sung Jin Kim[1] Yuting Cheng[1] Susana Furman[1] Matthew A. Inlay[2,3] Thomas E. Lane[1] Kim N. Green[1]

[1]Department of Neurobiology and Behavior, University of California, Irvine, Irvine, California, USA

[2]Sue and Bill Gross Stem Cell Research Center, University of California, Irvine, Irvine, California, USA

[3]Department of Molecular Biology and Biochemistry, University of California, Irvine, Irvine, California, USA

Correspondence

Kim N. Green

3208 Biological Sciences III, University of California, Irvine, Irvine, CA 92697-4545, USA.

Email: kngreen@uci.edu

Thomas E. Lane,

Department of Neurobiology & Behavior, School of Biological Sciences, University of California, Irvine, CA, USA.

Email: tlane@uci.edu

Funding information

Alzheimer's Association, Grant/Award Number: AARF-16-442762; National Institutes of Health, Grant/Award Number: NS082174; National Institutes of Health/National Institute of Aging, Grant/Award Numbers: RF1AG056768, RF1AG065329, U54AG054349; National Institutes of Health/ National Institute of Neurological Disorders and Stroke, Grant/Award Numbers: R0NS041249, R01NS083801, R35NS116835; National Multiple Sclerosis Society, Grant/Award Number: CA-1607-25040; The Ray and Tye Noorda Foundation

ABSTRACT

Microglia are the primary resident myeloid cells of the brain responsible for maintaining homeostasis and protecting the central nervous system (CNS) from damage and infection. Monocytes and monocyte-derived macrophages arising from the periphery have also been implicated in CNS pathologies, however, distinguishing between different myeloid cell populations in the CNS has been difficult. Here, we set out to develop a reliable histological marker that can assess distinct myeloid cell heterogeneity and functional contributions, particularly in the context of disease and/or neuroinflammation. scRNAseq from brains of mice infected with the neurotropic JHM strain of the mouse hepatitis virus (JHMV), a mouse coronavirus, revealed that Lgals3 is highly upregulated in monocyte and macrophage populations, but not in microglia. Subsequent immunostaining for galectin-3 (encoded by *Lgals3*), also referred to as MAC2, highlighted the high expression levels of MAC2 protein in infiltrating myeloid cells in JHMV-infected and bone marrow (BM) chimeric mice, in stark contrast to microglia, which expressed little to no staining in these models. Expression of MAC2 was found even 6–10 months following BM-derived cell infiltration into the CNS. We also demonstrate that MAC2 is not a specific label for plaque- associated microglia in the 5xFAD mouse model, but only appears in a distinct subset of these cells in the presence of JHMV infection or during aging. Our data suggest that MAC2 can serve as a reliable and long-lasting histological marker for monocyte/ macrophages in the brain, identifying an accessible approach to distinguishing resident microglia from infiltrating cells in the CNS under certain conditions.

Keywords

Alzheimer's disease, brain, Lgals3, MAC2, microglia, monocytes, mouse coronavirus

INTRODUCTION

Myeloid cells of the innate immune system are comprised of two distinct populations: tissue-resident and monocyte-derived macrophages. In the central nervous system (CNS), the macrophage compartment consists of parenchymal macrophages, known as microglia, and non-parenchymal macrophages, known as CNS (or border)-associated macrophages (CAMs or BAMs) (Kierdorf et al., 2019; Mrdjen et al., 2018). Microglia reside in the brain parenchyma spatially arranged in discrete non-overlapping territories, while BAMs reside within specialized CNS border interfaces that separate the CNS from the periphery, including the choroid plexus, meninges, and perivascular spaces. Recent studies indicate that microglia and non-parenchymal macrophages represent ontologically, phenotypically, and functionally distinct cell populations (Jordao et al., 2019; Masuda et al., 2019; Mrdjen et al., 2018; Munro et al., 2020; Shemer et al., 2018; Utz et al., 2020; Van Hove et al., 2019); however, inflammation-induced phenotypic changes in these cells have made distinguishing and assessing different myeloid cell populations and their diverse functions during disease difficult.

In mice, studies have shown that microglia derive from erythromyeloid precursors in the yolk sac, entering the brain as primitive or pre-macrophages to colonize the CNS during embryonic development (Ginhoux et al., 2010; Kierdorf et al., 2013). Once the blood-brain barrier (BBB) is formed, myeloid cell infiltration into the CNS is restricted and microglial population maintenance relies on local self-proliferation without contributions from peripheral monocytes (Shemer et al., 2015). While studies have shown that specific BAM subsets (e.g. perivascular and leptomeningeal macrophages) also derive from the yolk sac (Gomez Perdiguero et al., 2015; Utz et al., 2020), it appears that choroid plexus and dural macrophage populations can be replenished by bone marrow (BM)-derived monocytes under steady-state conditions

(Goldmann et al., 2016; Van Hove et al., 2019). Under inflammatory or disease con- ditions (e.g., facial nerve axotomy, amyotrophic lateral sclerosis, and experimental autoimmune encephalomyelitis), studies have shown that peripheral-derived monocytes enter the brain, but do not contribute significantly to the microglial pool unless under defined experimental circumstances (e.g., irradiation, myeloablative chemotherapy, and BBB disruption) (Ajami et al., 2007; Ajami et al., 2011; Cronk et al., 2018; Ginhoux et al., 2010; Hohsfield et al., 2020; Jordao et al., 2019; Lund et al., 2018; Mildner et al., 2007; Reed-Geaghan et al., 2020).

Despite their distinct origins and functions, assessing the individual contributions of infiltrated myeloid cells and activated microglia remains one of the major challenges in neuroimmunology, particularly within the context of neuroinflammatory diseases (Herz et al., 2017; Honarpisheh et al., 2020; Prinz & Priller, 2014). Monocytes and microglia share substantial transcriptional and phenotypic overlap. Several of the genes and proteins used to separate these two populations are not exclusively expressed but instead only relatively enriched in one population (e.g., CD45, CX3CR1, and CCR2) (Haage et al., 2019; Honarpisheh et al., 2020; Ransohoff & Cardona, 2010; Shemer et al., 2015). Microglial-specific genes and proteins have been identified; however, microglia downregulate their homeostatic signature (e.g., *P2ry12, Tmem119, Sall1*, and *Siglech*) and upregulate monocyte/macrophage-associated (e.g., *Apoe, Itgax,* and *Lyz2*) markers during disease (Bennett et al., 2016; Butovsky et al., 2014; Buttgereit et al., 2016; Keren-Shaul et al., 2017; Konishi et al., 2017). Studies have also identified genes and proteins that are highly expressed in BM-derived myeloid cells, including brain engrafted macrophages (e.g., *Ms4a7, Clec12a, Ccr2, Apoe, CD38, Mrc1,* and *Cd11a*), but many of these genes are also found in other CNS myeloid subsets or fail to label cells during immunohistochemical investigations on fixed brain sections (Bennett et al., 2018; Mrdjen et al.,

2018; Shemer et al., 2018; Shukla et al., 2019). As such, there is no histological marker that can reliably identify peripheral myeloid cell infiltrates versus activated microglia in the CNS to date.

Researchers currently utilize a number of experimental approaches to identify peripheral myeloid cells in the CNS. However, many of these paradigms pose concerning caveats. The generation of GFP BM chimeras provides labeling of BM-derived cells, but this approach involves irradiation, which can induce BBB damage and non- homeostatic peripheral contributions to the microglial niche (Ajami et al., 2007; Mildner et al., 2007). Parabiosis avoids these irradiation-induced effects but can involve complicated surgery and result in host-graft rejection. Despite the usefulness of mice genetically labeled for monocyte markers (e.g., $Ccr2^{RFP}$ mice), studies have shown that these cells may downregulate CCR2 as they mature/differentiate and enter the brain (Gschwandtner et al., 2019; Saederup et al., 2010). Furthermore, these mice are haploinsufficient for CCR2, a critical factor for monocyte migration and entry into the CNS (Chu et al., 2014). Fate mapping techniques have allowed for unprecedented exploration and manipulation of monocytes, but again these techniques are not without their limitations (Chen, Sun, et al., 2020; Liu et al., 2019). The use of lineage tracing from BM-expressed drivers involves the use of tamoxifen, which has recently been identified as a neutral agonist in macrophage lineage tracing studies. A recent study has shown that tamoxifen treatment of pregnant mice induces a significant expansion of the embryonic macrophage population (Rojo et al., 2018).

Given the lack of reliable markers that can distinguish between monocyte-derived cells and activated microglia, we set out to develop a new histological tool for peripheral myeloid cell studies in the mouse CNS. To accomplish this, we employed infection of C57BL/6 mice with the neuroadapted JHM strain of mouse hepatitis virus (JHMV), a mouse coronavirus and a robust

mouse model for monocyte infiltration in the CNS. Studies indicate that JHMV-infected mice exhibit substantial infiltration by monocytes along with other peripheral immune cells (Held et al., 2004; Savarin et al., 2010). We recently employed single-cell RNA sequencing (scRNAseq) on flow-sorted CD45+ cells infiltrating into the CNS of JHMV-infected mice to better understand the immunological landscape at defined times following infection with a neurotropic virus (Syage et al., 2020). Using this approach, we identified *Lgals3* as a highly enriched gene for monocytes. We then validated the expression of this marker at the protein level via galectin-3/MAC2 staining in BM-derived myeloid cells, and its utility in distinguishing between monocyte and microglia populations in response to JHMV infection as well as in young transgenic mouse models of Alzheimer's disease (AD). This approach not only provides a reliable marker for peripheral-derived cells, but also eliminates the necessity of complex transgenic mouse lines to discern myeloid cell populations, broadening the study of myeloid cell spatial and phenotypic profiles during disease and neuroinflammation.

MATERIALS AND METHODS

Compounds. Pexidartinib (PLX3397) was provided by Plexxikon Inc. and formulated in AIN-76A standard chow at a dose of 600 ppm by Research Diets Inc.

Mice. All mice were obtained from The Jackson Laboratory. For transplant studies, bone marrow cells were isolated from CAG-EGFP mice (Stock No. 006567). Male and female 5xFAD mice were obtained from MMRRC-JAX (Stock No. 34848) and have been previously described in detail (Oakley et al., 2006). For 5xFAD genotyping, the primer sequences used were PS1 Forward 50 -AAT AGA GAA CGG CAG GAG CA-30 and PS1 Reverse 50 -GCC ATG AGG GCA CTA ATC AT-30. All other mice were male C57BL/6 (000664) mice. Animals were housed with open access to food and water under 12 h/12 h light-dark cycles.

Animal treatments. All rodent experiments were performed in accordance with animal protocols approved by the Institutional Animal Care and Use Committee at the University of California, Irvine (UCI). JHMV infection: Six-week-old C57BL/6 mice (males and females) and four-month-old 5xFAD mice (males and females) were infected intracranially (i.c.) with 200–250 PFU of JHMV in 30 μL of sterile Hanks balanced sterile solution (HBSS); control mice received an i.c. injection of HBSS. JHMV-infected C57BL/6 mice were sacrificed at 7, 14, and 21 days post-infection (d.p.i.) and brains and spinal cords isolated to assess viral titers and perform immunohistochemical staining to evaluate monocyte infiltration. JHMV-infected 5xFAD mice were sacrificed at 10 d.p.i. and brains removed to determine viral titers, evaluate β-amyloid (Aβ) burden, and perform immunohistochemical staining to assess monocyte infiltration. scRNAseq was conducted on male animals. Microglial depletion: Mice were

administered ad libitum with PLX3397 at a dosage of 600 ppm (to eliminate microglia) or vehicle (control) for 14d. Bone marrow transplant: Tissue from a previous study by Hohsfield et. al were employed for analyses performed in the present report (Hohsfield et al., 2020). In brief, C57BL/6 mice were anesthetized with isoflurane and then irradiated with 1000 cGy (whole body) and reconstituted via retroorbital injection with 2 x 106 whole BM cells from CAG-EGFP mice. Blood was measured at 4, 8, and/or 12 weeks post transplantation to track granulocyte chimerism. At time of sacrifice, mice were euthanized, and BM was harvested and analyzed by flow cytometry for HSC chimerism. This established an average percent chimerism of >95% in whole body irradiated mice as previously reported (Hohsfield et al., 2020). Tissue collection: Following treatments, adult mice were sacrificed via carbon dioxide inhalation and perfused transcardially with 1X PBS. Brains were extracted and dissected down the midline, with one half flash-frozen for subsequent RNA and protein analyses, and the other half drop-fixed in 4% paraformaldehyde. Fixed brains were cryopreserved in PBS + 0.05%
sodium azide + 30% sucrose, frozen, and sectioned at 40 μm on a Leica SM2000 R sliding microtome for subsequent immunohistochemical analyses. For brains and spinal cords from JHMV-infected mice, half brains dissected down the midline and the length of spinal cord extending from thoracic vertebrate 6–10 was cryoprotected in 30% sucrose, cut into 1-mm transverse blocks and processed to preserve the craniocaudal orientation and subsequently embedded in O.C.T. (VWR, Radnor, PA, USA). For spinal cords, 8 μm-thick coronal sections were cut and sections were stained following standard immunofluorescence protocols; for brains, 8 μm sagittal sections were cut (Blanc et al., 2015; Dickey et al., 2016; Marro et al., 2016).

Histology and confocal microscopy. Fluorescent immunolabeling followed a standard indirect technique as described previously (Elmore et al., 2014). Brain sections were stained with antibodies against the following defined antigens: ionized calcium binding adaptor molecule 1 (IBA1; 1:1000; 019-19,741, Wako and ab5076, Abcam) and MAC2/Galectin-3 (1:500; CL8942AP Cedarlane). For DAPI staining, mounted brain sections were cover- slipped using Fluoromount-G with DAPI (00-4959-52, Invitrogen). Amylo-Glo (TR-300-AG; Biosensis) staining was performed according to the manufacturer's instructions. High resolution fluorescent images were obtained using a Leica TCS SPE-II confocal microscope and LAS-X software. For confocal imaging, one field of view (FOV) per brain region was captured per mouse unless otherwise indicated. For whole brain stitches, automated slide scanning was performed using a Zeiss AxioScan.Z1 equipped with a Colibri camera and Zen AxioScan 2.3 software. Microglial morphology was determined using the Filaments module in Bitplane Imaris 7.5, as described previously (Elmore et al., 2015). Cell quantities were determined using the Spots module in Imaris. MAC1+ IBA1+ staining was quantified by using a standardized algorithm in the Surfaces module in Imaris. Total IBA1+ and MAC2+ IBA1+ surface area in the field of view was categorized as plaque-associated or non-plaque-associated based on proximity to plaques (plaque-associated ≤ 5.8 μm). Percentage of MAC2+ IBA1+ coverage was calculated by dividing MAC2+ IBA1+/total IBA1+ surface area.

Data analysis and statistics. Statistical analysis was performed with Prism Graph Pad (v.8.0.1). To compare two groups, the unpaired Student's t-test was used. To com- pare multiple groups, a one-way ANOVA with Tukey's posthoc test was performed. For all analyses, statistical significance was accepted at $p < .05$. All bar graphs are represented as means ± SEM and

significance expressed as follows: *$p < .05$, **$p < .01$, ***$p < .001$. n is given as the number of mice within each group, unless otherwise indicated.

RESULTS

Lgals3/MAC2 distinguishes infiltrating cells from microglia in the adult CNS

We and others have previously identified distinct transcriptional and phenotypic profiles of brain-engrafted peripherally derived myeloid cells from resident microglia in the adult mouse brain; however, these findings have yet to translate into reliable histological markers that distinguish peripheral infiltrates from their microglial counterparts in the CNS (Bennett et al., 2018; Cronk et al., 2018; Hohsfield et al., 2020; Anat Shemer et al., 2018). In this study, we explored a previously described scRNAseq data set to identify transcripts that distinguish between resi- dent microglia and infiltrating myeloid cells (Syage et al., 2020). scRNAseq data was obtained from the JHMV mouse model which recapitulates many characteristics of human diseases associated with encephalomyelitis and demyelination (Bergmann et al., 2006; Lampert et al., 1973; Lane & Buchmeier, 1997; Savarin et al., 2010; Weiner, 1973). In brief, intracranial inoculation of susceptible C57BL/6 mice with the neuroadapted JHMV, a member of the Coronaviridae family, results in an acute encephalomyelitis characterized by wide-spread viral replication in astrocytes, microglia, and oligodendroglia with relative sparing of neurons (Bergmann et al., 2006; Lane & Hosking, 2010). In response to JHMV infection, proinflammatory cytokines and chemokines are expressed by activated microglia and astrocytes, resulting in an orchestrated inflammatory response consisting of neutrophils, mono- cytes/macrophages, and activated virus-specific CD4+ and CD8+ T cells (Bergmann et al., 2006; Hosking & Lane, 2010; Lane & Hosking, 2010).

We recently performed a detailed analysis of immune cell infiltration into the CNS of JHMV-infected mice through scRNAseq, which highlighted the heterogeneity of the immune response following infection with a neurotropic virus, in addition to confirming that monocytes

and neutrophils are the prominent cells entering the CNS (Syage et al., 2020). Here, we employed the scRNAseq data set to identify differentially expressed genes between monocyte/macrophage cells compared to microglia. *Lgals3* transcripts were enriched in infiltrating monocytes and macrophages, and lowly expressed in microglia (specifically in MG3 and Cyc. MG clusters) even under JHMV/inflammatory conditions (**Figure 1a–d**). *Lgals3* encodes galectin-3 (also known as MAC2), which is a member of the lectin family involved in monocyte/macrophage chemo- attraction and activation (MacKinnon et al., 2008). Since low levels of *Lgals3* transcripts were detected in some microglia clusters, we next evaluated whether galectin-3/MAC2 expression was present in both monocyte/macrophage and distinct microglial populations. To assess this, we subsequently infected a separate cohort of C57BL/6 mice with JHMV and evaluated the ability of galectin-3/MAC2 to distinguish distinct myeloid cell populations. Histological analyses for MAC2 in non-infected brain sections revealed no MAC2 staining in IBA1+ cells, except in areas associated with ventricles and the choroid plexus (**Figure 1e and f**). Analysis of JHMV-infected brain and spinal cord sections showed a clear population of IBA1+/MAC2+ cells that were not present in uninfected animals. IBA1+/MAC2+ cells appear spatially and morphologically distinct from IBA1+/MAC2- cells, which resemble microglia and reside in parenchymal areas (**Figure 1e, f, and i**). In the brain, IBA1+/MAC2+ cells accumulated in the brainstem (medulla, pons, midbrain, thalamus, and hypothalamus), cerebellum (near the fourth ventricle), and in white matter tracts (corpus callosum), whereas little to no deposition was observed in the cerebrum at any timepoint (hippocampus, cortex, and striatum) with the exception of sites near the lateral ventricle and/or white matter tracts (**Figure 1e, f, and h**). Many areas of high MAC2+ cell accumulation appear to be in or near white matter areas (**Figure 1f**). IBA1+/MAC2+ cells appear less ramified with retracted/thickened processes

and enlarged cell somas compared to IBA1+/MAC2- cells **(Figure 1f**). IBA1+/MAC2+ cell infiltration in the brain appears to peak around 14 d.p.i (**Figure 1e, g, and h**); however, the brainstem still shows prominent accumulation at 21 d.p.i. In the spinal cord, IBA1+/MAC2+ cell infiltration peaked at 14 d.p.i. and declined by 21 d.p.i. with cells enriched in white matter tracts within the ventral funiculus (**Figure 1i and j**).

MAC2 is a specific and long-lasting marker for bone marrow-derived infiltrating cells

Beyond acute CNS infiltration, current monocyte markers make it difficult to distinguish between peripheral and resident myeloid cells. CCR2 and CD14 are downregulated following monocyte differentiation into macrophages (Fantuzzi et al., 1999; Steinbach & Thiele, 1994; Wong et al., 1997) and studies using CCR2RFP knock-in mice report that CCR2RFP+ cells are not detected in the CNS, even under inflammatory conditions (Saederup et al., 2010), meaning that these markers fail to label monocyte-derived cells past a few days fol- lowing engraftment in the CNS. Given these difficulties, we next sought to examine whether MAC2 could serve as (1) a marker for BM-derived cells and (2) a long-lasting marker for these cells once engrafted in the brain.

To accomplish this, we utilized BM GFP chimeric mice to assess the ability of this monocyte/macrophage marker candidate to label infiltrating BM-derived cells. CAG-GFP donor BM was administered (via retro-orbital injection) to whole body (WB, with >95% chimerism) irradiated mice and allowed to recover for ~10 months, resulting in long-term GFP chimeric mice. In this model, GFP+ expression indicates that cells derive from the BM. Following recovery, we explored co-localization of MAC2 expression in GFP+ cells in the adult mouse brains of long-term GFP BM chimeric mice and long-term GFP BM chimeric mice that

underwent colony-stimulating factor 1 receptor inhibitor (CSF1Ri)-induced myeloid cell depletion and repopulation (~6 months following CSF1Ri treatment and CNS engraftment) (**Figure 2a**). In a previous study, we demonstrated that irradiation/BM transplant followed by CSF1Ri treatment results in substantial replacement of the microglial compartment with BM-derived monocytes (Hohsfield et al., 2020), providing a model to evaluate long-term and brain-wide BM-derived monocyte/macrophage engraftment.

Ten-month WB irradiated mice exhibited ~20% infiltration of GFP+ cells, with prominent deposition observed in areas near the lateral ventri- cle/subventricular zone (SVZ), medial habenula (MHb), internal capsule (IC), and meninges (**Figure 2a and b**). In accordance with our prior data, we observed that these infiltrating GFP+ cells express little to no levels of P2RY12 and TMEM119, two canonical microglial markers (data not shown). Ten-month WB irradiated mice treated with CSF1Ri exhibited 79–96% (mean = 86%) engraftment of GFP+ cells, seen throughout the brain parenchyma (Figure 2a, d, and h–j). In aged-matched controls, no GFP+ cell deposition is visible (Figure 2b, and h–j). Notably, we found that MAC2+ staining was still apparent in GFP+/IBA1+ cells, even 6 and 10 months after CNS infiltration was stimulated, while no MAC2 expression was seen in control animals or in GFP-/IBA1+ cells (**Figure 2b–g, and h–j**). In 10 mo WB irradiated mice, an average of 89– 96% of GFP+ cells express MAC2 near the lateral ventricle/SVZ, MHb, and IC (Figure 2k–m). In 10 mo WB irradiated + CSF1Ri treated mice, an average of 85–93% of GFP+ cells express of MAC2 near the lateral ventricle/SVZ, MHb, and IC (Figure 2k–m). It should be noted that there are differential levels of MAC2+ staining in GFP+ cells in mice, which likely reflects the more recent infiltration of BM-derived cells into the parenchyma, indicating that MAC2 expression may gradually decrease over time as cells become more CNS parenchymal macrophage- or

microglia- like to fill the tissue niche. Some MAC2 expression is seen in the nuclei of resident microglia, but clearly fills the cell body and processes of GFP +/IBA+ cells. Given the high level of co-expression of MAC2 in GFP BM-derived myeloid cells, these results indicate that MAC2 can serve as a histological marker of BM-derived infiltrating cells and utilized as a potential long-lasting marker to distinguish between peripherally derived monocytes/macrophages and resident microglia.

MAC2 is not a ubiquitous marker for plaque- associated microglia during the early stages of disease in 5xFAD mice

While we identified MAC2 as a marker for peripheral infiltrates, Lgals3 has also been reported in specific myeloid cell populations under certain conditions. For example, *Lgals3* was identified as an upregulated gene in amyloid-β (Aβ) plaque-associated microglia, also known as disease-associated microglia (DAM) or microglial neurodegenerative (MGnD) phenotype (Butovsky & Weiner, 2018; Krasemann et al., 2017), and in isolated amyloid plaque-containing microglia (Grubman et al., 2021). Moreover, galectin-3/MAC2 staining has been found in microglia in close contact with Aβ plaques in both human and mice (Boza-Serrano et al., 2019). However, it is often difficult to distinguish between monocytes/macrophages and activated microglia, as they share many morphological and gene expression similarities (Bennett et al., 2016; Butovsky et al., 2014; Buttgereit et al., 2016; Keren-Shaul et al., 2017; Konishi et al., 2017). To directly test Lgals3/ Galectin-3 expression in the AD brain, we stained for MAC2 in 5xFAD mice, and then used JHMV infection to trigger peripheral infiltration, evaluating whether MAC2 expression is specific to plaque-associated microglia.

5xFAD mice, which express five human APP and PSEN1 transgenes with familial Alzheimer's disease mutations, display extensive extracellular plaque deposition and microgliosis (Oakley et al., 2006). In these mice, amyloid plaques begin to form around 3 months of age and exhibit significant plaque deposition and microglial activation in the cerebral cortex and brain stem, including the thalamus, midbrain, and hindbrain, by 4 months of age (**Figure 3a**). Here, we i.c. infected 4-month-old 5xFAD mice with JHMV to stimulate monocyte infiltration into the CNS. Brain sections of uninfected and JHMV-infected mice were stained for amyloid plaques (Amylo-Glo), myeloid cells (IBA1), and MAC2. Evaluation of whole brain sagittal sections showed profound MAC2 staining in JHMV-infected 5xFAD (**Figure 3b**), but not uninfected mice (**Figure 3a**). Similar to WT JHMV-infected mice, MAC2+ cell deposition is apparent in areas near ventricles (in the cerebellum near the fourth ventricle, in tissue near the lateral ventricle) and white matter tracts (the corpus callosum, middle longitudinal fasciculus), whereas little to no MAC2 staining is present in 5xFAD controls (**Figure 3a–e**). MAC2+ cells are seen in the choroid plexus of 5xFAD controls, but do not infiltrate into the parenchyma (**Figure 3c and e**). High resolution images show little to no MAC2+ staining in plaque-associated microglia (1.6% of MAC2 staining in plaque-associated IBA1+ cells) in uninfected 5xFAD mice (**Figure 3f–g**), and an average of 16.4% of MAC2 staining in IBA1+ cells surrounding amyloid plaques in JHMV-infected 5xFAD mice (**Figure 3h–i**). It also appears that not all plaque-associated microglia are MAC2+ nor is there an abundance of MAC2+ IBA1+ in plaque-associated regions. MAC2+ staining is also present in non-plaque-associated regions in IBA1+ cells (8.7% MAC2+ IBA1+ staining) in JHMV-infected mice (Figure 3d, and h–i). These findings provide evidence that MAC2 is not a specific marker for plaque-associated microglia

and is not expressed by microglia in the young non-infected 5xFAD mouse model, indicating that *Lgals3*/MAC2 expression may reflect peripheral infiltrates honing to plaques.

The effects of aging on MAC2 staining in WT and 5xFAD mice

Transcriptional profile analysis has revealed an upregulation of *Lgals3* in microglia isolated from mouse models of neurodegenerative disease, including Alzheimer's disease and amyotrophic lateral sclerosis as well as aging, and identified Lgals3 as a hub gene for primed microglia (Holtman et al., 2015). Safaiyan et al. recently identified white matter-associated microglia (WAM), which accumulate in white matter tracts during aging. *Lgals3* was one of 39 transcripts of the WAM signature that was identified when comparing aged white matter compared to young white matter or aged gray matter myeloid cells; and the authors report expression of galectin-3 in IBA1+ cells in old but not young white matter (Safaiyan et al., 2021).

To address whether MAC2 staining also increases with aging under steady-state and diseased conditions, we next stained brain sections from 4, 8, 12, and 18 mo WT and 5xFAD mice with MAC2, IBA1, and Amylo-Glo. Again, we observe that MAC2+ IBA1+ cells and staining is most apparent in the choroid plexus of WT and 5xFAD mice, regardless of age (**Figure 4a and b**). In line with previous studies, our data shows an age-dependent increase in MAC2+ IBA1+ cell accumulation in 5xFAD mice in the hippocampus, cortex, and in white matter areas (e.g. fimbria, corpus callosum) within close proximity to the lateral ventricle (Figure 4b, c, and e). In gray matter regions, the majority of MAC2+ cells are IBA1+ plaque-associated microglia (**Figure 4b and c**). However, there appears to be a lag in the appearance of MAC2 expression and microglial/DAM activation around plaques. For example, prominent MAC2 expression in plaque- associated IBA1+ cells appears at 18 mo of age in the cortex despite the

accumulation of these plaque-associated microglia at 4 mo of age (**Figure 4c**). Furthermore, the majority of IBA1+ plaque-associated cells do not express MAC2 (<20% of IBA1+ cells are MAC2+; **Figure 4e**), meaning MAC2 does not account for a significant proportion of plaque-associated cells. MAC2+ IBA1+ cell deposition does not occur in gray matter areas in the aged WT mice (**Figure 4a, d, and f**); however, interestingly we do observe MAC2+ IBA1+ cells present in white matter areas at 18 mo of age (Figure 4d). This is also true for 5xFAD mice (**Figure 4c**). Thus, it appears that MAC2 expression is not a specific response to plaques. Given the proximity of these brain regions to the lateral ventricles and the lack of MAC2 expression in the majority of plaque-associated microglia, we postulate two scenarios: (1) a specific subpopulation of activated microglia (subset of DAM and/or WAM) switch on Lgals3 and galectin-3/MAC2 expression over time or (2) that MAC2+ cells derive from a different cell source, such as from the periphery. Since microglia and macrophages undergo rapid morphological and transcriptional transformations upon activation, reflective of the highly plastic nature of myeloid cells, defining MAC2 expression as an indicator of cell activation or peripheral infiltration remains difficult. However, given the findings in this study, specifically the spatial and temporal expression of MAC2+ IBA1+ cells in areas that are closely associated with peripheral immune cell infiltration in CNS disorders, most prominently in white matter areas in multiple sclerosis, we hypothesize that MAC2 expression labels a subset of peripheral immune cells in the young adult brain that can infiltrate and engraft the brain.

DISCUSSION

Microglia and BM-derived monocytes are implicated in a number of neurological disorders (Herz et al., 2017). In AD, several genome-wide association studies have identified variants associated with myeloid cells that increase disease risk, highlighting the importance of myeloid cells and the growing need to decipher their phenotype and function during dis- ease (Bradshaw et al., 2013; Guerreiro et al., 2013; Jonsson et al., 2013; Lambert et al., 2013). However, myeloid cells are highly dynamic cells, which can be influenced at both the transcriptional and protein level by specific diseases during disease induction and progression, thus complicating the use of reliable and stable cell-specific markers and posing challenges to the functional exploration and contributions of these distinct cells. For instance, the presence of peripheral-derived myeloid cells around amyloid plaques and their contribution in AD pathology has been a long-standing question in the field with contrasting results (El Khoury et al., 2007; Hawkes & McLaurin, 2009; Jay et al., 2015; Reed-Geaghan et al., 2020; Simard et al., 2006).

Under steady state conditions, microglia and monocyte/ macrophages populations express several overlapping surface markers, including Cd11b, F4/80, CD115 (CSF1R), and IBA1 (Gautier et al., 2012; Prinz et al., 2011). Recent gene expression studies have identified sur- face markers and transcription factors unique to resident microglia (e.g., P2RY12, TMEM119, SIGLEC-H, and Sall1), but several of these markers lose their distinct homeostatic expression levels during disease/ cell activation (Bennett et al., 2016; Butovsky et al., 2014; Buttgereit et al., 2016; Chen & Colonna, 2021; Keren-Shaul et al., 2017; Konishi et al., 2017). Despite the utility of previous approaches (e.g., BM chimeras, parabiosis, and mouse models of fluorescent protein expression or tamoxifen-inducible Cre-recombinase under monocyte/microglia pro- moters) in providing myeloid cell-specific labeling/targeting and unprecedented opportunities to study

microglia and monocytes (Ajami et al., 2007; Jung et al., 2000; Mildner et al., 2007; Wang et al., 2016), the field has lacked a commercially available histological marker for monocyte-derived populations in the CNS.

In this study, our main goal was to identify a marker that can discern between murine microglial and monocyte-derived cell populations during inflammation and disease in the CNS. Given the plasticity of myeloid cells, we recognize that the identification of cell lineage based on a single marker is not ideal (Bennett et al., 2016; Butovsky et al., 2014); however, previous studies have identified unique single genes and markers for microglia, such as P2ry12 and Tmem119, that have aided investigations and added to the repertoire of tools utilized by CNS myeloid cell researchers (Bennett et al., 2016; Butovsky et al., 2014). These markers have been indispensable to identifying endogenous and homeostatic microglia in the CNS. Here, we show that Lgals3 is highly expressed in monocyte/macrophages in the healthy and JHMV-infected brain, and that galectin-3/MAC2 can be used as a histological marker to distinguish peripherally derived myeloid cells from microglia under both steady state and neuro- inflammatory conditions. Galectin-3/MAC2 is a β-galactoside-binding lectin that is highly expressed in and secreted by monocytes/macro- phages; it is associated with many macrophage functions, including cell adhesion, migration, proliferation, and apoptosis (MacKinnon et al., 2008). However, galectin-3 expression has also been reported in other cell populations, including fibroblasts, osteoblasts, endothelial cells, neuronal cells, and immune cells (neutrophils, eosinophils, baso- phils, mast cells) (Thomas & Pasquini, 2018). Here, we show that *Lgals3* is not highly expressed in other Cd11b+ cell populations via scRNAseq, including T cells, B cells, NK cells, neutrophils, and microglia, but is highly expressed in several monocyte and macro-phage cell clusters. Although we do not observe significant MAC2+ staining in non-IBA1+ cells

in the CNS, careful consideration here is also warranted and IBA1 (or other myeloid cell markers) should be employed in combination with MAC2 to distinguish these myeloid populations.

In line with our study, recent work by Ochocka et al. using scRNAseq and flow cytometry of CD11b+ myeloid cells in naïve and glioma-bearing mice showed that Lgals3 and galectin-3 are highly expressed by infiltrating monocyte/macrophages at RNA and protein levels, respectively (Ochocka et al., 2021). These authors propose the use of TMEM119 and galectin-3 for efficient and distinguishable separation of microglia and monocyte/macrophages in glioma models and highlighted their ability to achieve distinct spatial distribution of these cells within tumor tissue (Ochocka et al., 2021). Moreover, recent studies in mouse models of diabetes and spinal cord injury have identified unique populations of infiltrating and phagocytic macrophages, distinct from resident microglia, that express Lgals3/galectin-3/MAC2. In diabetes, galactin-3 expressing macrophages infiltrate and aggregate near injury sites, implicating these cells in the response to cerebrovascular insults (Mehina et al., 2021). In spinal cord injury, injury- activated macrophages maintain a transcriptionally distinct identify to activated microglia, expressing higher levels of Lgals3, Apoe, and Cxcr4, among other genes (Wahane et al., 2021). In the present study, we also observed distinct spatial distribution of MAC2+ cells in the JHMV-infected brain; cells were sequestered in the brain stem, white matter areas, and regions surrounding the ventricles. Further study is needed to evaluate the distinct contributions of MAC2+ myeloid cells and MAC2- myeloid cells in pathogenesis, but given the role of BM-derived myeloid cells in demyelination (Yamasaki et al., 2014), it is not surprising to find their selective recruitment in these areas. In GFP BM chimeras, MAC2+ cells were observed in the choroid plexus and perivascular spaces in whole body-irradiated mice, respectively, consistent

with their partial cell turnover from BM sources (Goldmann et al., 2016; Van Hove et al., 2019). Identifying MAC2 as a distinct histological marker for monocytes provides investigators with the ability to explore the spatial distribution and dynamics of these peripheral cells without the side effects of irradiation or other experimental caveats (e.g., tamoxifen).

In mice, monocytes express CD11b and CD45, and are divided into two main subpopulations: classical/inflammatory monocytes ($Ly6C^{hi}CCR2 + CX3CR1^{lo}$) and non-classical/patrolling monocytes ($Ly6C^{lo}CCR2^{lo}$ $CX3CR1^{hi}$) (Geissmann et al., 2003; Geissmann et al., 2010). Of interest, studies have shown that Lgals3 is enriched in a population of Ly6C+ monocytes located in the BM and blood (Mildner et al., 2017). Although transcriptional profile analyses of microglia and monocytes have generated several proposed monocyte- specific markers based off of an identified monocyte signature, including *Apoe, Ccr2, Ms4a7,* and *Clec12a* (Bennett et al., 2018; Cronk et al., 2018; Hohsfield et al., 2020; Lund et al., 2018; Anat Shemer et al., 2018) these markers have presented a number of limitations: upregulation during disease, downregulation upon macrophage differentiation, or lack of success in staining fixed adult brain tissue. For example, though Cd11a (*Itgal*) is expressed on all peripheral circulating immune cells and not microglia, it could only be detected on infiltrating cells in fixed brain sections using a tedious tyramide amplification strategy, limiting its practical use (Shukla et al., 2019). In addition, Bennett et al. identified MS4A7 as a unique marker for HSC-derived cells, but MS4A7 staining was only shown in blood, fetal brain, and primary human microglia, and RNA in situ hybridization was required to show staining in postmortem AD brain samples (Bennett et al., 2018). CD44 was a marker identified for distinguishing CNS infiltrating from CNS resident cells by Korin et al., however, later found by Mrdjen et al. to be upregulated in microglia during disease or aging (Korin et al., 2017; Mrdjen et al., 2018). Given that monocytes

and macrophages exist as heterogenous populations with varying expression profiles (reflecting functional diversity, differential origins, differentiation status, tissue of residence) and dynamic adaption of their transcription regulatory networks to changing environments (Gosselin et al., 2014; Lavin et al., 2014), it has been challenging for researchers to develop a marker for monocyte-derived cells that remains intact following differentiation and tissue engraftment. Here, we show that MAC2 staining is retained in BM-derived cells 6–10 months following CNS recruitment in the brain, indicating that MAC2 may be a marker that is conserved across several monocyte and macrophages subpopulations, or at least the subsets recruited to the CNS/sites of inflammation.

Transcriptional profile analysis of isolated microglia from mouse models of AD, amyotrophic lateral sclerosis, and aging identified Lgals3 as a central hub gene in primed microglia, along with *Apoe, Axl, Clec7a,* and *Itgax* (Holtman et al., 2015). Further comprehensive scRNAseq analysis of microglia in neurodegenerative diseases discovered a unique microglial subset, termed disease-associated microglia (DAM) or microglial neurodegenerative phenotype (MGnD) microglia. These cells exhibit a downregulation in homeostatic microglia genes (e.g., *P2ry12* and *Tmem119*) and upregulation in genes involved in phagocytic, lysosomal, and lipid metabolism pathways (e.g., *Apoe, Axl, Clec7a, Cst7, Itgax,* and *Lilrb4*) (Keren-Shaul et al., 2017), including Lgals3 (Butovsky & Weiner, 2018; Krasemann et al., 2017), which is upregulated during later stages of neurodegeneration (Chen & Colonna, 2021). However, a recent study has shown that enzymatic dissociation methods can induce aberrant gene expression signatures in microglia (Marsh et al., 2020), indicating that some scRNAseq findings may be confounded and an artifact of isolation methods, analysis, or sequencing platform. A recent investigation utilizing scRNAseq, snRNAseq and scATACseq

identified distinct microglia subpopulations in 3xTgAD and 5xFAD mice, including a DAM cluster containing *Cst7*, but lacking *Lgals3*; instead, *Lgals3* was found in a small cluster containing *Cd14* and *Itgal* (Balderrama-Gutierrez et al., 2021). Galectin-3 was also shown to be significantly elevated in human AD patients, exhibit preferential expression in microglia in contact with plaques, and serve as a ligand for TREM2 (Boza-Serrano et al., 2019). In contrast, Sobue et al. showed that gene expression levels of LGALS3, AIF1, and CD68, were unchanged in human AD precuneus samples (Sobue et al., 2021). In line with this, using bulk-tissue RNAseq analysis, our lab has shown that while *Lgals3* is upregulated in 5xFAD mice in the hippocampus and thalamus compared to wild types, expression levels do not change following sustained microglial depletion, unlike several homeostatic (e.g., *Csf1r, Cx4cr1, Hexb,* and *Siglech*) and DAM genes (e.g., *Clec7a, Cst7*, and *Itgax*) which are significantly downregulated by microglial depletion (Spangenberg et al., 2019). These data provide evidence that elevated *Lgals3* in 5xFAD brains may not be specific to microglia. Consistent with spatial transcriptomics and in situ sequencing data in $APP^{NL\text{-}G\text{-}F}$ mice, *Lgals3* was not identified in plaque-induced genes (PIGs), consisting of 57 genes that overlap with several DAM genes (Chen, Lu, et al., 2020). The current study shows that MAC2 staining is not present in plaque-associated microglia in the young 5xFAD mice, and only appears in plaque-associated IBA1+
cells during JHMV infection or in aged animals (albeit at modest numbers). A recent study—showing clonal hematopoiesis of indeterminate potential (CHIP) is associated with protection against AD—detected mutated marrow-derived cells in the brains of patients which appear indistinguishable from microglia (Bouzid et al., 2021), highlighting the potential role for peripheral infiltrates in replacing defective microglia during aging or disease. Thus, the presence of MAC2+ cells in disease and experimental models should be considered a potential sign of

peripheral infiltrates, and subsequently followed up with BM chimeric models, parabiosis, or BM lineage tracing transgenics. It is possible that microglia may upregulate Lgals3 under certain conditions, including infection or inflammatory stimulus, or that upregulated mRNA does not effectively translate to protein expression. Likewise, we can- not discount the possibility that microglia in other conditions (stroke, injury, and chronic neurodegenerative disease) may also upregulate Lgals3, or that these MAC2+ cells may derive from BM sources. Other explanations for the disparity between Lgals3 transcript levels and

MAC2 staining in plaque-associated microglia could be a result of: (1) microglia and infiltrating peripheral myeloid cells expressing different isoforms of *Lgals3*/galectin-3, in which one isoform is detectible by the MAC2 antibody while the other is not, or (2) different secretion and/or cellular retention rates of *Lgals3*/galectin-3 within these two myeloid cell populations. Moreover, *Lgals3* may also be expressed by discrete microglial populations in the brain–for example, in specialized axon tract-associated microglia (ATM) or P7/early postnatal microglia (termed proliferative region-associated microglia (PAM), which appear as amoeboid cells that transiently reside in axon tracts of the corpus callosum and cerebellum (Hammond et al., 2019; Li et al., 2019), as well as in white matter-associated microglia (WAM), found specifically in white matter areas that increase with aging (Safaiyan et al., 2021). Furthermore, surviving microglia following CSF1Ri-induced depletion have been described as MAC2+ (Zhan et al., 2020). Given these findings and the data from this current study, we would implore

researchers to consider *Lgals3*/MAC2 expression as a potential indicator of peripheral origins, but encourage further validation with other important tools, such as fate-mapping techniques. For example, lineage tracing from *Ms4a3* or *Cxcr4* could be utilized, as it has recently been shown as a specific gene expressed by BM-derived granulocyte- monocyte progenitors (GMPs) or HSC-

derived monocytes, respectively, to efficiently trace monocyte-derived cells (Liu et al., 2019; Werner et al., 2020). Other markers include Cd49d, also expressed by T cells and DCs, and Cd49e, which were identified in peripheral monocyte populations, but not in CNS resident myeloid cell populations utilizing CyTOF (Bahareh Ajami et al., 2018).

In sum, we identify galectin-3/MAC2 as a potential monocyte marker that can be utilized in inflamed CNS tissue. Unlike other markers, BM-derived myeloid cells retain MAC2 expression even as they leave perivascular areas and occupy the parenchymal niche for prolonged periods of time. The ability to discern peripherally derived cells from resident microglia is critical to exploring their distinct roles in health and disease. Growing attention has been placed on understanding CNS myeloid cells and the environmental cues that sculpt their transcriptional and phenotypic profiles, particularly during disease. Detailed knowledge of these distinct myeloid cell populations and our ability to distinguish microglia and monocytes will prove essential in targeting these cells for improved therapeutic strategies.

Acknowledgments

We thank Edna Hingco for her excellent technical assistance. WT and 5xFAD time course tissue was provided by U54 AG054349 (NIA Model Organism Development and Evaluation for Late onset Alzheimer's Disease [MODEL-AD]). K.N.G was supported by the National Institutes of Health (NIH) under awards: R01NS083801 (NINDS), RF1AG056768 (NIA), and RF1AG065329 (NIA). L.A.H. was supported by the Alzheimer's Association Research Fellowship (AARF-16-442762). T.E.L. was supported by the National Institutes of Health (NIH) under awards: R01NS041249 (NINDS) and R35NS116835 (NINDS), the National Mul-

tiple Sclerosis Society (NMSS) Collaborative Research Center grant CA- 1607-25040 and The Ray and Tye Noorda Foundation. Y.G. was supported by NIH T32 training grant (NS082174).

Conflict of interest

The authors declare that they have no conflicts of interest.

Author contributions

L.A.H. developed experimental protocols, designed, performed, and analyzed experiments and wrote the manuscript. K.I.T., Y.G., A.R.S., S.J.K., Y.C. and S.F. performed, and analyzed experiments. M.A.I. and T.E.L. contributed to project design. K.N.G directed the project, designed the experiments, interpreted the results and wrote the manuscript.

Data availability statement

The data that support the findings of this study are available from TEL and KNG upon reasonable request.

ORCID

Matthew A. Inlay https://orcid.org/0000-0002-0451-2076

Thomas E. Lane https://orcid.org/0000-0003-0392-0825

Kim N. Green https://orcid.org/0000-0002-6049-6744

REFERENCES

1. Ajami, B., Bennett, J. L., Krieger, C., McNagny, K. M., & Rossi, F. M. (2011). Infiltrating monocytes trigger EAE progression, but do not contribute to the resident microglia pool. Nature Neuroscience, 14(9), 1142–1149. https://doi.org/10.1038/nn.2887

2. Ajami, B., Bennett, J. L., Krieger, C., Tetzlaff, W., & Rossi, F. M. (2007). Local self-renewal can sustain CNS microglia maintenance and function throughout adult life. Nature Neuroscience, 10(12), 1538–1543. https://doi.org/10.1038/nn2014

3. Ajami, B., Samusik, N., Wieghofer, P., Ho, P. P., Crotti, A., Bjornson, Z., Prinz, M., Fantl, W. J., Nolan, G. P., & Steinman, L. (2018). Single-cell mass cytometry reveals distinct populations of brain myeloid cells in mouse neuroinflammation and neurodegeneration models. Nature Neuroscience, 21(4), 541–551. https://doi.org/10.1038/s41593-018- 0100-x

4. Balderrama-Gutierrez, G., Liang, H., Rezaie, N., Carvalho, K., Forner, S., Matheos, D., Rebboah, E., Green, K. N., Tenner, A. J., LaFerla, F., & Mortazavi, A. (2021). Single-cell and nucleus RNA-seq in a mouse model of AD reveal activation of distinct glial subpopulations in the presence of plaques and tangles. bioRxiv. https://doi.org/10.1101/ 2021.09.29.462436

5. Bennett, F. C., Bennett, M. L., Yaqoob, F., Mulinyawe, S. B., Grant, G. A., Hayden Gephart, M., Plowey, E. D., & Barres, B. A. (2018). A combination of ontogeny and CNS environment establishes microglial identity. Neuron, 98(6), 1170–1183. https://doi.org/10.1016/j.neuron.2018.05.014

6. Bennett, M. L., Bennett, F. C., Liddelow, S. A., Ajami, B., Zamanian, J. L., Fernhoff, N. B., Mulinyawe, S. B., Bohlen, C. J., Adil, A., Tucker, A., Weissman, I. L., Chang, E. F., Li, G., Grant, G. A., Hayden Gephart, M. G., & Barres, B. A. (2016). New tools for studying microglia in the mouse and human CNS. Proceedings of the National Academy of Sciences of the United States of America, 113(12), E1738– E1746. https://doi.org/10.1073/pnas.1525528113

7. Bergmann, C. C., Lane, T. E., & Stohlman, S. A. (2006). Coronavirus infec- tion of the central nervous system: Host-virus stand-off. Nature Reviews. Microbiology, 4(2), 121–132. https://doi.org/10.1038/ nrmicro1343

8. Blanc, C. A., Grist, J. J., Rosen, H., Sears-Kraxberger, I., Steward, O., & Lane, T. E. (2015). Sphingosine-1-phosphate receptor antagonism enhances proliferation and migration of engrafted neural progenitor cells in a model of viral-induced demyelination. The American Journal of Pathology, 185(10), 2819–2832. https://doi.org/10.1016/j.ajpath.2015.06.009

9. Bouzid, H., Belk, J. A., Jan, M., Qi, Y., Sarnowski, C., Wirth, S., Ma, L., Chrostek, M., Ahmad, H., Nachun, D., Yao, W., Beiser, A., Bick, A. G., Bis, J., Fornage, M., Longstreth, W. T., Lopez, O., Nataranjan, P., & Jaiswal, S. (2021). Clonal hematopoiesis is associated with protection from Alzheimer's disease. Blood, 138, 5. https://doi.org/10.1101/ 2021.12.10.21267552

10. Boza-Serrano, A., Ruiz, R., Sanchez-Varo, R., García-Revilla, J., Yang, Y., Jimenez-Ferrer, I., Paulus, A., Wennström, M., Vilalta, A., Allendorf, D., Davila, J. C., Stegmayr, J., Jiménez, S., Roca-Ceballos, M. A., Navarro- Garrido, V., Swanberg, M., Hsieh, C. L., Real, L. M., Englund, E., … Deierborg, T. (2019). Galectin-3, a novel endogenous TREM2 ligand, detrimentally regulates inflammatory response in Alzheimer's disease. Acta Neuropathologica, 138(2), 251–273. https://doi.org/10.1007/ s00401-019-02013-z

11. Bradshaw, E. M., Chibnik, L. B., Keenan, B. T., Ottoboni, L., Raj, T., Tang, A., Rosenkrantz, L. L., Imboywa, S., Lee, M., Von Korff, A., Alzheimer Dis- ease Neuroimaging Initiative, Morris, M. C., Evans, D. A., Johnson, K., Sperling, R. A., Schneider, J. A., Bennett, D. A., & De Jager, P. L. (2013). CD33 Alzheimer's disease locus: Altered monocyte function and amyloid biology. Nature Neuroscience, 16(7), 848–850. https://doi.org/10. 1038/nn.3435

12. Butovsky, O., Jedrychowski, M. P., Moore, C. S., Cialic, R., Lanser, A. J., Gabriely, G., Koeglsperger, T., Dake, B., Wu, P. M., Doykan, C. E., Fanek, Z., Liu, L., Chen, Z., Rothstein, J. D., Ransohoff, R. M., Gygi, S. P., Antel, J. P., & Weiner, H. L. (2014). Identification of a unique TGF-beta-dependent molecular and functional signature in microglia. Nature Neuroscience, 17(1), 131–143. https://doi.org/10. 1038/nn.3599

13. Butovsky, O., & Weiner, H. L. (2018). Microglial signatures and their role in health and disease. Nature Reviews. Neuroscience, 19(10), 622–635. https://doi.org/10.1038/s41583-018-0057-5

14. Buttgereit, A., Lelios, I., Yu, X., Vrohlings, M., Krakoski, N. R., Gautier, E. L., Nishinakamura, R., Becher, B., & Greter, M. (2016). Sall1 is a transcriptional regulator defining microglia identity and function. Nature Immunology, 17(12), 1397–1406. https://doi.org/10.1038/ni.3585

15. Chen, H.-R., Sun, Y.-Y., Chen, C.-W., Kuo, Y.-M., Kuan, I. S., Tiger Li, Z.-R., Short-Miller, J. C., Smucker, M. R., & Kuan, C.-Y. (2020). Fate mapping via CCR2-CreER mice reveals monocyte-to-microglia transition in development and neonatal stroke. Science Advances, 6(35), eabb2119. https://doi.org/10.1126/sciadv.abb2119

16. Chen, W. T., Lu, A., Craessaerts, K., Pavie, B., Sala Frigerio, C., Corthout, N., Qian, X., Laláková, J., Kühnemund, M., Voytyuk, I., Wolfs, L., Mancuso, R., Salta, E., Balusu, S., Snellinx, A., Munck, S., Jurek, A., Fernandez Navarro, J., Saido, T. C., … de Strooper, B. (2020). Spatial transcriptomics and in situ sequencing to study Alzheimer's dis- ease. Cell, 182(4), 976–991.e919. https://doi.org/10.1016/j.cell.2020. 06.038

17. Chen, Y., & Colonna, M. (2021). Microglia in Alzheimer's disease at single- cell level. Are there common patterns in humans and mice? Journal of Experimental Medicine, 218(9), e20202717. https://doi.org/10.1084/ jem.20202717

18. Chu, H. X., Arumugam, T. V., Gelderblom, M., Magnus, T., Drummond, G. R., & Sobey, C. G. (2014). Role of CCR2 in inflammatory conditions of the central nervous system. Journal of Cerebral Blood Flow and Metabolism, 34(9), 1425–1429. https://doi.org/10.1038/

jcbfm.2014.120

19. Cronk, J. C., Filiano, A. J., Louveau, A., Marin, I., Marsh, R., Ji, E., Goldman, D. H., Smirnov, I., Geraci, N., Acton, S., Overall, C. C., & Kipnis, J. (2018). Peripherally derived macrophages can engraft the brain independent of irradiation and maintain an identity distinct from microglia. The Journal of Experimental Medicine, 215(6), 1627–1647. https://doi.org/10.1084/jem.20180247

20. Dickey, L. L., Worne, C. L., Glover, J. L., Lane, T. E., & O'Connell, R. M. (2016). MicroRNA-155 enhances T cell trafficking and antiviral effector function in a model of coronavirus-induced neurologic disease. Journal of Neuroinflammation, 13(1), 240. https://doi.org/10.1186/ s12974-016-0699-z

21. El Khoury, J., Toft, M., Hickman, S. E., Means, T. K., Terada, K., Geula, C., & Luster, A. D. (2007). Ccr2 deficiency impairs microglial accumulation and accelerates progression of Alzheimer-like disease. Nature Medi- cine, 13(4), 432–438. https://doi.org/10.1038/nm1555

22. Elmore, M. R., Lee, R. J., West, B. L., & Green, K. N. (2015). Characterizing newly repopulated microglia in the adult mouse: Impacts on animal behavior, cell morphology, and neuroinflammation. PLoS One, 10(4), e0122912. https://doi.org/10.1371/journal.pone.0122912

23. Elmore, M. R., Najafi, A. R., Koike, M. A., Dagher, N. N., Spangenberg, E. E., Rice, R. A., Kitazawa, M., Matusow, B., Nguyen, H., West, B. L., & Green, K. N. (2014). Colony-stimulating factor 1 receptor signaling is necessary for microglia viability, unmasking a microglia progenitor cell in the adult brain. Neuron, 82(2), 380–397. https://doi.org/10.1016/j. neuron.2014.02.040

24. Fantuzzi, L., Borghi, P., Ciolli, V., Pavlakis, G., Belardelli, F., & Gessani, S. (1999). Loss of CCR2 expression and functional response to monocyte chemotactic protein (MCP-1) during the differentiation of human monocytes: Role of secreted MCP-1 in the regulation of the chemo- tactic response. Blood, 94(3), 875–883.

25. Gautier, E. L., Shay, T., Miller, J., Greter, M., Jakubzick, C., Ivanov, S., Helft, J., Chow, A., Elpek, K. G., Gordonov, S., Mazloom, A. R., Ma'ayan, A., Chua, W. J., Hansen, T. H., Turley, S. J., Merad, M., & Randolph, G. J. (2012). Gene-expression profiles and transcriptional regulatory pathways that underlie the identity and diversity of mouse tissue macrophages. Nature Immunology, 13(11), 1118–1128. https:// doi.org/10.1038/ni.2419

26. Geissmann, F., Jung, S., & Littman, D. R. (2003). Blood monocytes consist of two principal subsets with distinct migratory properties. Immunity, 19(1), 71–82. https://doi.org/10.1016/s1074-7613(03)00174-2

27. Geissmann, F., Manz, M. G., Jung, S., Sieweke, M. H., Merad, M., & Ley, K. (2010). Development of monocytes, macrophages, and dendritic cells. Science, 327(5966), 656–661. https://doi.org/10.1126/science.1178331

28. Ginhoux, F., Greter, M., Leboeuf, M., Nandi, S., See, P., Gokhan, S., Mehler, M. F., Conway, S. J., Ng, L. G., Stanley, E. R., Samokhvalov, I. M., & Merad, M. (2010). Fate mapping analysis reveals that adult microglia derive from primitive macrophages. Science, 330(6005), 841–845. https://doi.org/10.1126/science.1194637

29. Goldmann, T., Wieghofer, P., Jord~ao, M. J. C., Prutek, F., Hagemeyer, N., Frenzel, K., Amann, L., Staszewski, O., Kierdorf, K., Krueger, M., Locatelli, G., Hochgerner, H., Zeiser, R., Epelman, S., Geissmann, F., Priller, J., Rossi, F. M. V., Bechmann, I., Kerschensteiner, M., … Prinz, M. (2016). Origin, fate and dynamics of macrophages at central nervous system interfaces. Nature Immunology, 17(7), 797–805. https://doi.org/10.1038/ni.3423

30. Gomez Perdiguero, E., Klapproth, K., Schulz, C., Busch, K., Azzoni, E., Crozet, L., Garner, H., Trouillet, C., de Bruijn, M. F., Geissmann, F., & Rodewald, H.-R. (2015). Tissue-resident macrophages originate from yolk-sac-derived erythro-myeloid progenitors. Nature, 518(7540), 547–551. https://doi.org/10.1038/nature13989

31. Gosselin, D., Link, V. M., Romanoski, C. E., Fonseca, G. J., Eichenfield, D. Z., Spann, N. J., Stender, J. D., Chun, H. B., Garner, H., Geissmann, F., & Glass, C. K. (2014). Environment drives selection and function of enhancers controlling tissue-specific macrophage identities. Cell, 159(6), 1327–1340. https://doi.org/10.1016/j.cell.2014.11.023

32. Grubman, A., Choo, X. Y., Chew, G., Ouyang, J. F., Sun, G., Croft, N. P., Rossello, F. J., Simmons, R., Buckberry, S., Landin, D. V., Pflueger, J., Vandekolk, T. H., Abay, Z., Zhou, Y., Liu, X., Chen, J., Larcombe, M., Haynes, J. M., McLean, C., … Polo, J. M. (2021). Transcriptional signa- ture in microglia associated with Aβ plaque phagocytosis. Nature Communications, 12(1), 3015. https://doi.org/10.1038/s41467-021-23111-1

33. Gschwandtner, M., Derler, R., & Midwood, K. S. (2019). More than just attractive: How CCL2 influences myeloid cell behavior beyond chemo- taxis. Frontiers in Immunology, 10, 2759. https://doi.org/10.3389/ fimmu.2019.02759

34. Guerreiro, R., Wojtas, A., Bras, J., Carrasquillo, M., Rogaeva, E., Majounie, E., Cruchaga, C., Sassi, C., Kauwe, J. S., Younkin, S., Hazrati, L., Collinge, J., Pocock, J., Lashley, T., Williams, J., Lambert, J. C., Amouyel, P., Goate, A., Rademakers, R., … Hardy, J. (2013). TREM2 variants in Alzheimer's disease. The New England Journal of Medicine, 368(2), 117–127. https://doi.org/10.1056/ NEJMoa1211851

35. Haage, V., Semtner, M., Vidal, R. O., Hernandez, D. P., Pong, W. W., Chen, Z., Hambardzumyan, D., Magrini, V., Ly, A., Walker, J., Mardis, E., Mertins, P., Sauer, S., Kettenmann, H., & Gutmann, D. H. (2019). Comprehensive gene expression meta-analysis identifies signature genes that distinguish microglia from peripheral monocytes/macrophages in health and glioma. Acta Neuropathologica Communications, 7(1), 20. https://doi.org/10.1186/s40478-019- 0665-y

36. Hammond, T. R., Dufort, C., Dissing-Olesen, L., Giera, S., Young, A., Wysoker, A., Walker,

A. J., Gergits, F., Segel, M., Nemesh, J., Marsh, S. E., Saunders, A., Macosko, E., Ginhoux, F., Chen, J., Franklin, R. J. M., Piao, X., McCarroll, S. A., & Stevens, B. (2019). Single-cell RNA sequencing of microglia throughout the mouse lifespan and in the injured brain reveals complex cell-state changes. Immunity, 50(1), 253–271.e256. https://doi.org/10.1016/j.immuni.2018.11.004

37. Hawkes, C. A., & McLaurin, J. (2009). Selective targeting of perivascular macrophages for clearance of beta-amyloid in cerebral amyloid angiopathy. Proceedings of the National Academy of Sciences of the United States of America, 106(4), 1261–1266. https://doi.org/10.1073/pnas.0805453106

38. Held, K. S., Chen, B. P., Kuziel, W. A., Rollins, B. J., & Lane, T. E. (2004). Differential roles of CCL2 and CCR2 in host defense to coronavirus infection. Virology, 329(2), 251–260. https://doi.org/10.1016/j.virol.2004.09.006

39. Herz, J., Filiano, A. J., Smith, A., Yogev, N., & Kipnis, J. (2017). Myeloid cells in the central nervous system. Immunity, 46(6), 943–956. https://doi. org/10.1016/j.immuni.2017.06.007

40. Hohsfield, L. A., Najafi, A. R., Ghorbanian, Y., Soni, N., Hingco, E. E., Kim, S. J., Jue, A. D., Swarup, V., Inlay, M. A., & Green, K. N. (2020). Effects of long-term and brain-wide colonization of peripheral bone marrow-derived myeloid cells in the CNS. Journal of Neuroinflammation, 17(1), 279. https://doi.org/10.1186/s12974-020-01931-0

41. Holtman, I. R., Raj, D. D., Miller, J. A., Schaafsma, W., Yin, Z., Brouwer, N., Wes, P. D., Möller, T., Orre, M., Kamphuis, W., Hol, E. M., Boddeke, E. W. G. M., & Eggen, B. J. (2015). Induction of a common microglia gene expression signature by aging and neurodegenerative conditions: A co-expression meta-analysis. Acta Neuropathologica Communications, 3, 31. https://doi.org/10.1186/s40478-015-0203-5

42. Honarpisheh, P., Lee, J., Banerjee, A., Blasco-Conesa, M. P., Honarpisheh, P., d'Aigle, J., Mamun, A. A., Ritzel, R. M., Chauhan, A., Ganesh, B. P., & McCullough, L. D. (2020). Potential caveats of putative microglia-specific markers for assessment of age-related cerebrovascular neuroinflammation. Journal of Neuroinflammation, 17(1), 366. https://doi.org/10.1186/s12974-020-02019-5

43. Hosking, M. P., & Lane, T. E. (2010). The role of chemokines during viral infection of the CNS. PLoS Pathogens, 6(7), e1000937. https://doi.org/ 10.1371/journal.ppat.1000937

44. Jay, T. R., Miller, C. M., Cheng, P. J., Graham, L. C., Bemiller, S., Broihier, M. L., Xu, G., Margevicius, D., Karlo, J. C., Sousa, G. L., Cotleur, A. C., Butovsky, O., Bekris, L., Staugaitis, S. M., Leverenz, J. B., Pimplikar, S. W., Landreth, G. E., Howell, G. R., Ransohoff, R. M., & Lamb, B. T. (2015). TREM2 deficiency eliminates TREM2+ inflammatory macrophages and ameliorates pathology in Alzheimer's disease mouse models. The Journal of Experimental Medicine, 212(3), 287–295. https://doi.org/10.1084/jem.20142322

45. Jonsson, T., Stefansson, H., Steinberg, S., Jonsdottir, I., Jonsson, P. V., Snaedal, J., Bjornsson,

S., Huttenlocher, J., Levey, A. I., Lah, J. J., Rujescu, D., Hampel, H., Giegling, I., Andreassen, O. A., Engedal, K., Ulstein, I., Djurovic, S., Ibrahim-Verbaas, C., Hofman, A., … Stefansson, K. (2013). Variant of TREM2 associated with the risk of Alzheimer's disease. The New England Journal of Medicine, 368(2), 107–116. https://doi.org/ 10.1056/NEJMoa1211103

46. Jordao, M. J. C., Sankowski, R., Brendecke, S. M., Sagar, Locatelli, G., Tai, Y. H., Tay, T. L., Schramm, E., Armbruster, S., Hagemeyer, N., Groß, O., Mai, D., Çiçek, Ö., Falk, T., Kerschensteiner, M., Grün, D., & Prinz, M. (2019). Single-cell profiling identifies myeloid cell subsets with distinct fates during neuroinflammation. Science, 363(6425), eaat7554. https://doi.org/10.1126/science.aat7554

47. Jung, S., Aliberti, J., Graemmel, P., Sunshine, M. J., Kreutzberg, G. W., Sher, A., & Littman, D. R. (2000). Analysis of fractalkine receptor CX(3) CR1 function by targeted deletion and green fluorescent protein reporter gene insertion. Molecular and Cellular Biology, 20(11), 4106– 4114. https://doi.org/10.1128/mcb.20.11.4106-4114.2000

48. Keren-Shaul, H., Spinrad, A., Weiner, A., Matcovitch-Natan, O., Dvir- Szternfeld, R., Ulland, T. K., David, E., Baruch, K., Lara-Astaiso, D., Toth, B., Itzkovitz, S., Colonna, M., Schwartz, M., & Amit, I. (2017). A unique microglia type associated with restricting development of Alzheimer's disease. Cell, 169(7), 1276–1290.e1217. https://doi.org/ 10.1016/j.cell.2017.05.018

49. Kierdorf, K., Erny, D., Goldmann, T., Sander, V., Schulz, C., Perdiguero, E. G., Wieghofer, P., Heinrich, A., Riemke, P., Hölscher, C., Müller, D. N., Luckow, B., Brocker, T., Debowski, K., Fritz, G., Opdenakker, G., Diefenbach, A., Biber, K., Heikenwalder, M., … Prinz, M. (2013). Microglia emerge from erythromyeloid precursors via Pu.1- and Irf8-dependent pathways. Nature Neuroscience, 16(3), 273– 280. https://doi.org/10.1038/nn.3318

50. Kierdorf, K., Masuda, T., Jord~ao, M. J. C., & Prinz, M. (2019). Macrophages at CNS interfaces: Ontogeny and function in health and disease. Nature Reviews Neuroscience, 20(9), 547–562. https://doi.org/10. 1038/s41583-019-0201-x

51. Konishi, H., Kobayashi, M., Kunisawa, T., Imai, K., Sayo, A., Malissen, B., Crocker, P. R., Sato, K., & Kiyama, H. (2017). Siglec-H is a microglia- specific marker that discriminates microglia from CNS-associated macrophages and CNS-infiltrating monocytes. Glia, 65(12), 1927–1943. https://doi.org/10.1002/glia.23204

52. Korin, B., Ben-Shaanan, T. L., Schiller, M., Dubovik, T., Azulay-Debby, H., Boshnak, N. T., Koren, T., & Rolls, A. (2017). High-dimensional, single- cell characterization of the brain's immune compartment. Nature Neu- roscience, 20(9), 1300–1309. https://doi.org/10.1038/nn.4610

53. Krasemann, S., Madore, C., Cialic, R., Baufeld, C., Calcagno, N., el Fatimy, R., Beckers, L., O'Loughlin, E., Xu, Y., Fanek, Z., Greco, D. J., Smith, S. T., Tweet, G., Humulock, Z., Zrzavy, T., Conde-Sanroman, P., Gacias, M., Weng, Z., Chen, H., … Butovsky, O. (2017). The TREM2-APOE pathway drives the transcriptional phenotype of dysfunctional microglia

in neurodegenerative diseases. Immunity, 47(3), 566–581.e569. https://doi.org/10.1016/j.immuni.2017.08.008

54. Lambert, J. C., Ibrahim-Verbaas, C. A., Harold, D., Naj, A. C., Sims, R., Bellenguez, C., Jun, G., DeStefano, A. L., Bis, J. C., Beecham, G. W., Grenier-Boley, B., Russo, G., Thornton-Wells, T. A., Jones, N., Smith, A. V., Chouraki, V., Thomas, C., Ikram, M. A., Zelenika, D., … Amouyel, P. (2013). Meta-analysis of 74,046 individuals identifies 11 new susceptibility loci for Alzheimer's disease. Nature Genetics, 45(12), 1452–1458. https://doi.org/10.1038/ng.2802

55. Lampert, P. W., Sims, J. K.,& Kniazeff, A. J. (1973). Mechanism of demyelination in JHM virus encephalomyelitis. Electron microscopic studies. Acta neuropathologica, 24(1), 76–85. https://doi.org/10.1007/bf00691421

56. Lane, T. E., & Buchmeier, M. J. (1997). Murine coronavirus infection: A paradigm for virus-induced demyelinating disease. Trends in Microbiology, 5(1), 9–14. https://doi.org/10.1016/s0966-842x(97)81768-4

57. Lane, T. E., & Hosking, M. P. (2010). The pathogenesis of murine coronavirus infection of the central nervous system. Critical Reviews in Immunology, 30(2), 119–130. https://doi.org/10.1615/critrevimmunol.v30. i2.20

58. Lavin, Y., Winter, D., Blecher-Gonen, R., David, E., Keren-Shaul, H., Merad, M., Jung, S., & Amit, I. (2014). Tissue-resident macrophage enhancer landscapes are shaped by the local microenvironment. Cell, 159(6), 1312–1326. https://doi.org/10.1016/j.cell.2014.11.018

59. Li, Q., Cheng, Z., Zhou, L., Darmanis, S., Neff, N. F., Okamoto, J., Gulati, G., Bennett, M. L., Sun, L. O., Clarke, L. E., Marschallinger, J., Yu, G., Quake, S. R., Wyss-Coray, T., & Barres, B. A. (2019). Developmental heterogeneity of microglia and brain myeloid cells revealed by deep single-cell RNA sequencing. Neuron, 101(2), 207–223.e210. https:// doi.org/10.1016/j.neuron.2018.12.006

60. Liu, Z., Gu, Y., Chakarov, S., Bleriot, C., Kwok, I., Chen, X., Shin, A., Huang, W., Dress, R. J., Dutertre, C. A., Schlitzer, A., Chen, J., Ng, L. G., Wang, H., Liu, Z., Su, B., & Ginhoux, F. (2019). Fate mapping via Ms4a3-expression history traces monocyte-derived cells. Cell, 178(6), 1509–1525.e1519. https://doi.org/10.1016/j.cell.2019.08.009

61. Lund, H., Pieber, M., Parsa, R., Han, J., Grommisch, D., Ewing, E., Kular, L., Needhamsen, M., Espinosa, A., Nilsson, E., Överby, A. K., Butovsky, O., Jagodic, M., Zhang, X. M., & Harris, R. A. (2018). Competitive repopulation of an empty microglial niche yields functionally distinct subsets of microglia-like cells. Nature Communications, 9(1), 4845. https://doi.org/10.1038/s41467-018-07295-7

62. MacKinnon, A. C., Farnworth, S. L., Hodkinson, P. S., Henderson, N. C., Atkinson, K. M., Leffler, H., Nilsson, U. J., Haslett, C., Forbes, S. J., & Sethi, T. (2008). Regulation of alternative macrophage activation by galectin-3. Journal of immunology (Baltimore, Md.:

1950), 180(4), 2650–2658. https://doi.org/10.4049/jimmunol.180.4.2650

63. Marro, B. S., Grist, J. J., & Lane, T. E. (2016). Inducible expression of CXCL1 within the central nervous system amplifies viral-induced demyelination. Journal of Immunology, 196(4), 1855–1864. https://doi.org/10. 4049/jimmunol.1501802

64. Marsh, S. E., Kamath, T., Walker, A. J., Dissing-Olesen, L., Hammond, T. R., Young, A. M. H., Abdulraouf, A., Nadaf, N., Dufort, C., Murphy, S., Kozareva, V., Vanderburg, C., Hong, S., Bulstrode, H., Hutchinson, P. J., Gaffney, D. J., Franklin, R. J. M., Macosko, E. Z., & Stevens, B. (2020). Single cell sequencing reveals glial specific responses to tissue processing & enzymatic dissociation in mice and humans. BioRvix. https://doi.org/10.1101/2020.12.03.408542

65. Masuda, T., Sankowski, R., Staszewski, O., Bottcher, C., Amann, L., Scheiwe, C., Nessler, S., Kunz, P., van Loo, G., Coenen, V. A., Reinacher, P. C., Michel, A., Sure, U., Gold, R., Grün, D., Priller, J., Stadelmann, C., & Prinz, M. (2019). Spatial and temporal heterogeneity of mouse and human microglia at single-cell resolution. Nature, 566(7744), 388–392. https://doi.org/10.1038/s41586-019-0924-x

66. Mehina, E. M. F., Taylor, S., Boghozian, R., White, E., Choi, S. E., Cheema, M. S., Korbelin, J., & Brown, C. E. (2021). Invasion of phago- cytic galectin 3 expressing macrophages in the diabetic brain disrupts vascular repair. Science Advances, 7(34), eabg2712. https://doi.org/10. 1126/sciadv. abg2712

67. Mildner, A., Schmidt, H., Nitsche, M., Merkler, D., Hanisch, U. K., Mack, M., Heikenwalder, M., Brück, W., Priller, J., & Prinz, M. (2007). Microglia in the adult brain arise from Ly-6ChiCCR2+ monocytes only under defined host conditions. Nature Neuroscience, 10(12), 1544–1553. https://doi.org/10.1038/nn2015

68. Mildner, A., Schönheit, J., Giladi, A., David, E., Lara-Astiaso, D., Lorenzo- Vivas, E., Paul, F., Chappell-Maor, L., Priller, J., Leutz, A., Amit, I., & Jung, S. (2017). Genomic characterization of murine monocytes reveals C/EBPβ transcription factor dependence of Ly6C(-) cells. Immunity, 46(5), 849–862.e847. https://doi.org/10.1016/j.immuni. 2017.04.018

69. Mrdjen, D., Pavlovic, A., Hartmann, F. J., Schreiner, B., Utz, S. G., Leung, B. P., Lelios, I., Heppner, F. L., Kipnis, J., Merkler, D., Greter, M., & Becher, B. (2018). High-dimensional single-cell mapping of central nervous system immune cells reveals distinct myeloid sub- sets in health, aging, and disease. Immunity, 48(2), 380–395.e386. https://doi.org/10.1016/j.immuni.2018.01.011

70. Munro, D. A. D., Bradford, B. M., Mariani, S. A., Hampton, D. W., Vink, C. S., Chandran, S., Hume, D. A., Pridans, C., & Priller, J. (2020). CNS macrophages differentially rely on an intronic Csf1r enhancer for their development. Development, 147(23), dev194449. https://doi. org/10.1242/dev.194449

71. Oakley, H., Cole, S. L., Logan, S., Maus, E., Shao, P., Craft, J., Guillozet- Bongaarts, A., Ohno, M., Disterhoft, J., van 2Eldik, L., Berry, R., & Vassar, R. (2006). Intraneuronal beta-amyloid aggregates, neurodegeneration, and neuron loss in transgenic mice with five familial Alzheimer's disease mutations: Potential factors in amyloid plaque formation. The Journal of Neuroscience, 26(40), 10129–10140. https:// doi.org/10.1523/jneurosci.1202-06.2006

72. Ochocka, N., Segit, P., Walentynowicz, K. A., Wojnicki, K., Cyranowski, S., Swatler, J., Mieczkowski, J., & Kaminska, B. (2021). Single-cell RNA sequencing reveals functional heterogeneity of glioma-associated brain macrophages. Nature Communications, 12(1), 1151. https://doi. org/10.1038/s41467-021-21407-w

73. Prinz, M., & Priller, J. (2014). Microglia and brain macrophages in the molecular age: From origin to neuropsychiatric disease. Nature Reviews. Neuroscience, 15(5), 300–312. https://doi.org/10.1038/ nrn3722

74. Prinz, M., Priller, J., Sisodia, S. S., & Ransohoff, R. M. (2011). Heterogeneity of CNS myeloid cells and their roles in neurodegeneration. Nature Neuroscience, 14(10), 1227–1235. https://doi.org/10.1038/nn.2923

75. Ransohoff, R. M., & Cardona, A. E. (2010). The myeloid cells of the central nervous system parenchyma. Nature, 468(7321), 253–262. https:// doi.org/10.1038/nature09615

76. Reed-Geaghan, E. G., Croxford, A. L., Becher, B., & Landreth, G. E. (2020). Plaque-associated myeloid cells derive from resident microglia in an Alzheimer's disease model. The Journal of Experimental Medicine, 217 (4), e20191374. https://doi.org/10.1084/jem.20191374

77. Rojo, R., Sauter, K. A., Lefevre, L., Hume, D. A., & Pridans, C. (2018). Maternal tamoxifen treatment expands the macrophage population of early mouse embryos. bioRxiv, 296749. https://doi.org/10.1101/296749

78. Saederup, N., Cardona, A. E., Croft, K., Mizutani, M., Cotleur, A. C., Tsou, C. L., Ransohoff, R. M., & Charo, I. F. (2010). Selective chemokine receptor usage by central nervous system myeloid cells in CCR2-red fluorescent protein knock-in mice. PLoS One, 5(10), e13693. https://doi.org/10.1371/journal.pone.0013693

79. Safaiyan, S., Besson-Girard, S., Kaya, T., Cantuti-Castelvetri, L., Liu, L., Ji, H., Schifferer, M., Gouna, G., Usifo, F., Kannaiyan, N., Fitzner, D., Xiang, X., Rossner, M. J., Brendel, M., Gokce, O., & Simons, M. (2021). White matter aging drives microglial diversity. Neuron, 109(7), 1100– 1117.e1110. https://doi.org/10.1016/j.neuron.2021.01.027

80. Savarin, C., Stohlman, S. A., Atkinson, R., Ransohoff, R. M., & Bergmann, C. C. (2010). Monocytes regulate T cell migration through the glia limitans during acute viral encephalitis. Journal of Virology, 84(10), 4878–4888. https://doi.org/10.1128/jvi.00051-10

81. Shemer, A., Erny, D., Jung, S., & Prinz, M. (2015). Microglia plasticity during health and

disease: An immunological perspective. Trends in Immunology, 36(10), 614–624. https://doi.org/10.1016/j.it.2015.08.003

82. Shemer, A., Grozovski, J., Tay, T. L., Tao, J., Volaski, A., Süß, P., Ardura- Fabregat, A., Gross-Vered, M., Kim, J. S., David, E., Chappell-Maor, L., Thielecke, L., Glass, C. K., Cornils, K., Prinz, M., & Jung, S. (2018). Engrafted parenchymal brain macrophages differ from microglia in transcriptome, chromatin landscape and response to challenge. Nature Communications, 9(1), 5206. https://doi.org/10.1038/s41467-018-07548-5

83. Shukla, A. K., McIntyre, L. L., Marsh, S. E., Schneider, C. A., Hoover, E. M., Walsh, C. M., Lodoen, M. B., Blurton-Jones, M., & Inlay, M. A. (2019). CD11a expression distinguishes infiltrating myeloid cells from plaque- associated microglia in Alzheimer's disease. Glia, 67(5), 844–856. https://doi.org/10.1002/glia.23575

84. Simard, A. R., Soulet, D., Gowing, G., Julien, J. P., & Rivest, S. (2006). Bone marrow-derived microglia play a critical role in restricting senile plaque formation in Alzheimer's disease. Neuron, 49(4), 489–502. https://doi. org/10.1016/j.neuron.2006.01.022

85. Sobue, A., Komine, O., Hara, Y., Endo, F., Mizoguchi, H., Watanabe, S., Murayama, S., Saito, T., Saido, T. C., Sahara, N., Higuchi, M., Ogi, T., & Yamanaka, K. (2021). Microglial gene signature reveals loss of homeostatic microglia associated with neurodegeneration of Alzheimer's disease. Acta Neuropathologica Communications, 9(1), 1. https://doi.org/ 10.1186/s40478-020-01099-x

86. Spangenberg, E., Severson, P. L., Hohsfield, L. A., Crapser, J., Zhang, J., Burton, E. A., Zhang, Y., Spevak, W., Lin, J., Phan, N. Y., Habets, G., Rymar, A., Tsang, G., Walters, J., Nespi, M., Singh, P., Broome, S., Ibrahim, P., Zhang, C., … Green, K. N. (2019). Sustained microglial depletion with CSF1R inhibitor impairs parenchymal plaque development in an Alzheimer's disease model. Nature Communications, 10(1), 3758. https:// doi.org/10.1038/s41467-019-11674-z

87. Steinbach, F., & Thiele, B. (1994). Phenotypic investigation of mononuclear phagocytes by flow cytometry. Journal of Immunological Methods, 174(1–2), 109–122. https://doi.org/10.1016/0022-1759 (94)90015-9

88. Syage, A. R., Ekiz, H. A., Skinner, D. D., Stone, C., O'Connell, R. M., & Lane, T. E. (2020). Single-cell RNA sequencing reveals the diversity of the immunological landscape following central nervous system infection by a murine coronavirus. Journal of Virology, 94(24), e01295. https://doi.org/10.1128/jvi.01295-20

89. Thomas, L., & Pasquini, L. A. (2018). Galectin-3-mediated glial crosstalk drives oligodendrocyte differentiation and (re)myelination. Frontiers in Cellular Neuroscience, 12, 297. https://doi.org/10.3389/fncel.2018.00297

90. Utz, S. G., See, P., Mildenberger, W., Thion, M. S., Silvin, A., Lutz, M., Ingelfinger, F., Rayan, N. A., Lelios, I., Buttgereit, A., Asano, K., Prabhakar, S., Garel, S., Becher, B.,

Ginhoux, F., & Greter, M. (2020). Early fate defines microglia and non-parenchymal brain macrophage development. Cell, 181(3), 557–573.e518. https://doi.org/10.1016/j.cell.2020.03.021

91. van Hove, H., Martens, L., Scheyltjens, I., de Vlaminck, K., Pombo Antunes, A. R., de Prijck, S., Vandamme, N., de Schepper, S., van Isterdael, G., Scott, C. L., Aerts, J., Berx, G., Boeckxstaens, G. E., Vandenbroucke, R. E., Vereecke, L., Moechars, D., Guilliams, M., van Ginderachter, J. A., Saeys, Y., & Movahedi, K. (2019). A single-cell atlas of mouse brain macrophages reveals unique transcriptional identities shaped by ontogeny and tissue environment. Nature Neuro- science, 22(6), 1021–1035. https://doi.org/10.1038/s41593-019-0393-4

92. Wahane, S., Zhou, X., Zhou, X., Guo, L., Friedl, M.-S., Kluge, M., Ramakrishnan, A., Shen, L., Friedel, C. C., Zhang, B., Friedel, R. H., & Zou, H. (2021). Diversified transcriptional responses of myeloid and glial cells in spinal cord injury shaped by HDAC3 activity. Science. Advances, 7(9), eabd8811. https://doi.org/10.1126/sciadv.abd8811

93. Wang, Y., Ulland, T. K., Ulrich, J. D., Song, W., Tzaferis, J. A., Hole, J. T., Yuan, P., Mahan, T. E., Shi, Y., Gilfillan, S., Cella, M., Grutzendler, J., DeMattos, R. B., Cirrito, J. R., Holtzman, D. M., & Colonna, M. (2016). TREM2-mediated early microglial response limits diffusion and toxicity of amyloid plaques. The Journal of Experimental Medicine, 213(5), 667– 675. https://doi.org/10.1084/jem.20151948

94. Weiner, L. P. (1973). Pathogenesis of demyelination induced by a mouse hepatitis. Archives of Neurology, 28(5), 298–303. https://doi.org/10. 1001/archneur.1973.00490230034003

95. Werner, Y., Mass, E., Ashok Kumar, P., Ulas, T., Händler, K., Horne, A., Klee, K., Lupp, A., Schütz, D., Saaber, F., Redecker, C., Schultze, J. L., Geissmann, F., & Stumm, R. (2020). Cxcr4 distinguishes HSC-derived monocytes from microglia and reveals monocyte immune responses to experimental stroke. Nature Neuroscience, 23(3), 351–362. https://doi.org/10.1038/s41593-020-0585-y

96. Wong, L. M., Myers, S. J., Tsou, C. L., Gosling, J., Arai, H., & Charo, I. F. (1997). Organization and differential expression of the human mono- cyte chemoattractant protein 1 receptor gene. Evidence for the role of the carboxyl-terminal tail in receptor trafficking. The Journal of Biological Chemistry, 272(2), 1038–1045. https://doi.org/10.1074/jbc.272.2.1038

97. Yamasaki, R., Lu, H., Butovsky, O., Ohno, N., Rietsch, A. M., Cialic, R., Wu, P. M., Doykan, C. E., Lin, J., Cotleur, A. C., Kidd, G., Zorlu, M. M., Sun, N., Hu, W., Liu, L. P., Lee, J. C., Taylor, S. E., Uehlein, L., Dixon, D., … Ransohoff, R. M. (2014). Differential roles of microglia and monocytes in the inflamed central nervous system. The Journal of Experimental Medicine, 211(8), 1533–1549. https://doi.org/10.1084/jem.20132477

98. Zhan, L., Fan, L., Kodama, L., Sohn, P. D., Wong, M. Y., Mousa, G. A., Zhou, Y., Li, Y., & Gan, L. (2020). A MAC2-positive progenitor-like microglial population is resistant to CSF1R inhibition in adult mouse brain. eLife, 9, e51796. https://doi.org/10.7554/eLife.51796

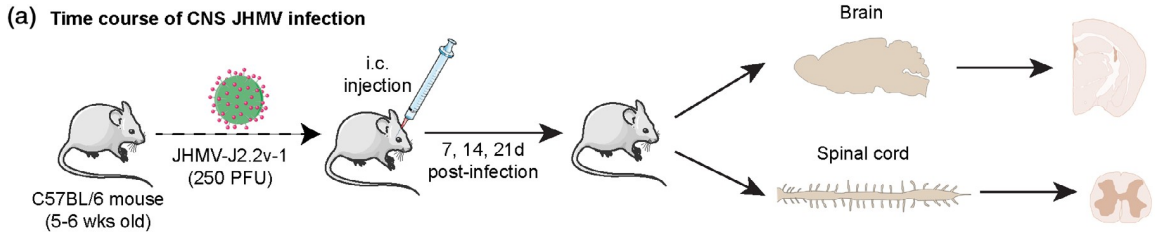

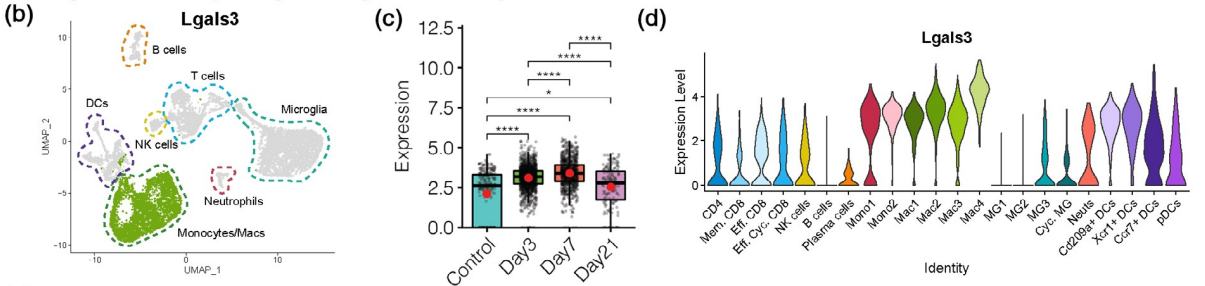

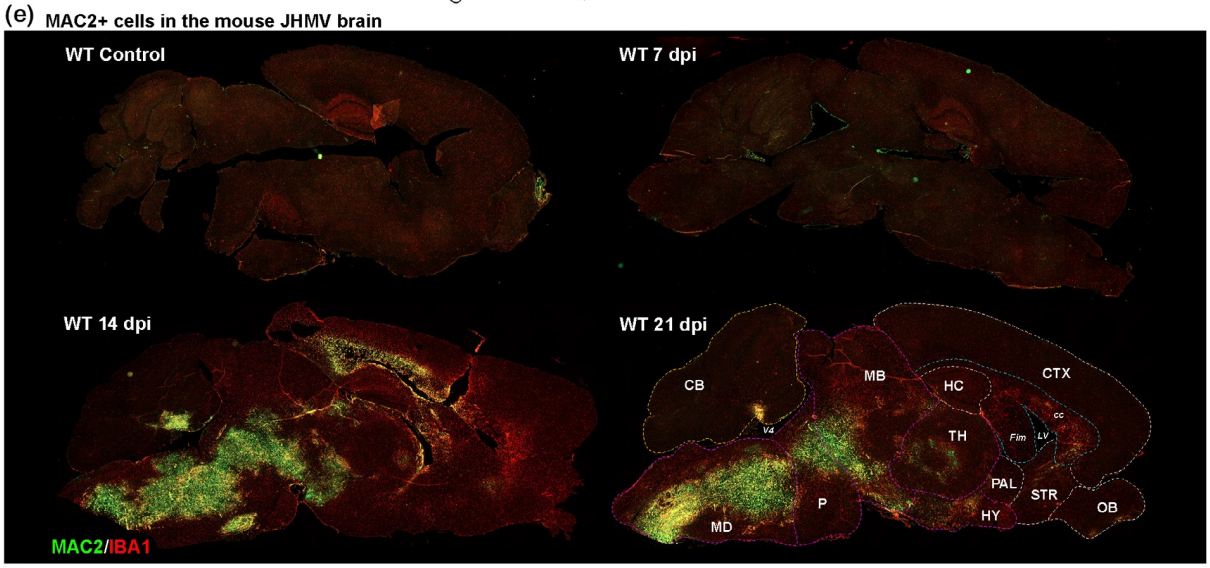

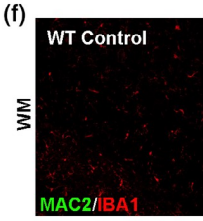

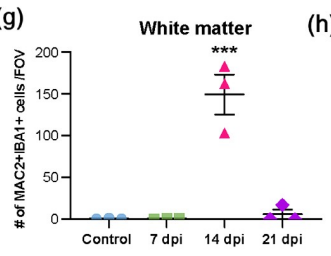

(h) MAC2+ distribution in JHMV mouse brain

	Animal group			
Brain region	Control	7 dpi	14 dpi	21 dpi
Brainstem	-	-	+++	+++
Cerebellum	-	-	++	+
White matter	-	-	+++	+
Cerebrum	-	-	-	-

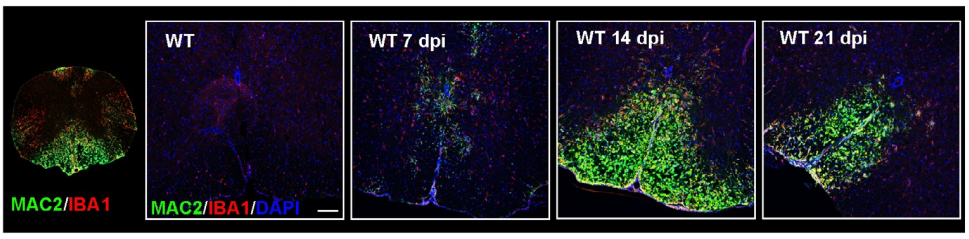

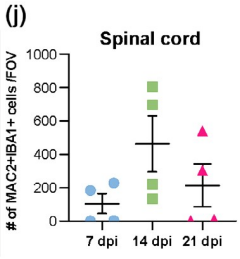

Figure 1 Lgals3/MAC2 distinguishes infiltrating cells from microglia in the adult CNS. (a) Schematic of experimental design of intracranial (i.c.) infection of five to six-week-old C57BL/6 wild type (WT) mice with 250 PFU of the neurotropic JHM-J2.2v-1 strain of mouse hepatitis virus (JHMV). Brains and spinal cords were collected at 7, 14, 21 days post infection (d.p.i.). (b) UMAP plot displays aggregate data of CD45+ cells and shows scaled expression of transcripts encoding *Lgals3* in monocyte/macrophage (Monocytes/Macs) clusters (Syage et al., 2020). (c) Temporal analysis of expression of transcripts encoding Lgals3. Transcript levels were elevated at defined timepoints during JHMV infection. Data is presented as normalized expression values, and random noise was added to show data point distribution. Box plots show interquartile range and median value (bold horizontal bar). Red dots indicate the average expression value per sample. Wilcoxon's test was used for statistical analysis. (d) Violin plot shows gene expression of Lgals3 in all CD45+ cells on the single-cell level and that Lgals3 is upregulated in monocytes and macrophage clusters. (e) Representative whole sagittal brain sections of MAC2 (green) and IBA1 (red) staining in WT non-infected and JHMV- infected mice at 7, 14, and 21 d.p.i. (f) High resolution 20x confocal images of MAC2+ (green) and IBA1+ (red) cells in the white matter tracts of WT non-infected and JHMV-infected at 14 d.p.i. (g) Quantification of MAC + IBA1+ cells per field of view (FOV) in white matter tracts of brains in WT control and JHMV-infected mice. (h) Table of the relative MAC2+ cell distribution in distinct brain regions. - indicates no accumulation. + indicates low accumulation. ++ indicates moderate accumulation. +++ indicates extensive accumulation. (i) Representative confocal images of MAC2+ (green) and IBA1+ (red) cells in the spinal cords of WT control and JHMV-infected mice at various timepoints post infection. (j) Quantification of (i). Mouse, syringe and virus illustrations were obtained from Servier Medical Art at smart.servier.com. IBA1, ionized calcium adapter molecule 1; CB, cerebellum; cc, corpus callosum; CTX, cortex; Fim, fimbria; HC, hippocampus; HY, hypothalamus; LV, lateral ventricle; MB, midbrain; MD, medulla; OB, olfactory bulb; P, pons; PAL, pallidum; STR, striatum; TH, thalamus; V4, fourth ventricle. Data are represented as mean ± SEM (n = 3–4 mice/timepoint). * $p < .05$, *** $p < .001$, **** $p < .0001$, compared to control unless otherwise indicated. Scale bar in (f) ~100 μm; in (i) inserts ~160 μm

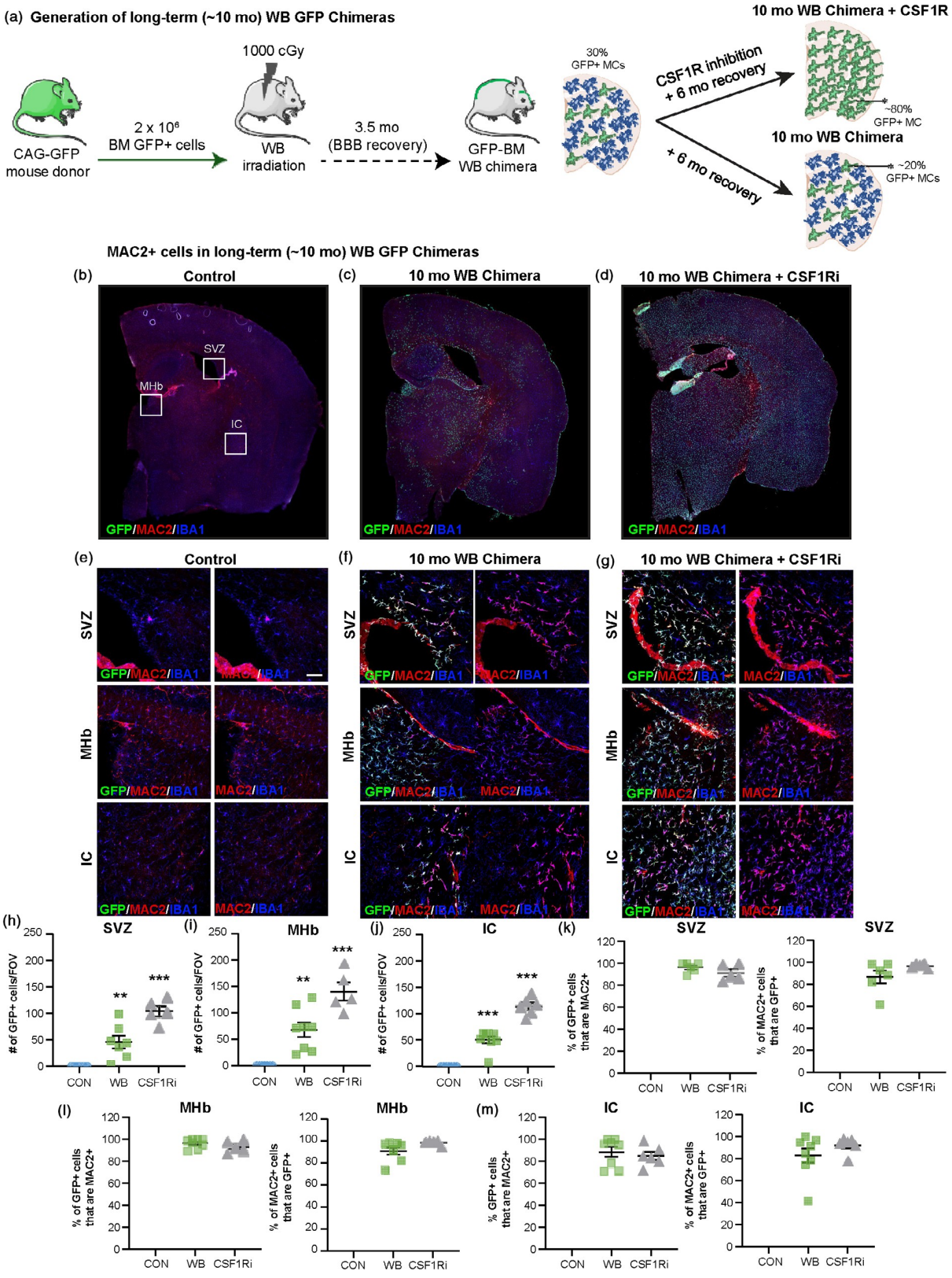
(a) Generation of long-term (~10 mo) WB GFP Chimeras
10 mo WB Chimera + CSF1R
CAG-GFP mouse donor
2 x 10⁶ BM GFP+ cells
1000 cGy
WB irradiation
3.5 mo (BBB recovery)
GFP-BM WB chimera
30% GFP+ MCs
CSF1R inhibition + 6 mo recovery
+ 6 mo recovery
~80% GFP+ MC
10 mo WB Chimera
~20% GFP+ MCs
MAC2+ cells in long-term (~10 mo) WB GFP Chimeras
(b) Control
(c) 10 mo WB Chimera
(d) 10 mo WB Chimera + CSF1Ri
SVZ
MHb
IC
GFP/MAC2/IBA1
(e) Control
(f) 10 mo WB Chimera
(g) 10 mo WB Chimera + CSF1Ri
MAC2/IBA1
(h) SVZ
(i) MHb
(j) IC
(k) SVZ
# of GFP+ cells/FOV
% of GFP+ cells that are MAC2+
% of MAC2+ cells that are GFP+
CON
WB
CSF1Ri
(l) MHb
(m) IC

Figure 2 MAC2 is a specific and long-lasting marker for bone marrow-derived infiltrating cells. (a) Schematic of experimental design for the generation of long-term green fluorescent protein (GFP) bone marrow (BM) chimeras. Treatment of BM chimeras with colony-stimulating factor 1 receptor (CSF1R) inhibitor results in extensive parenchymal engraftment of BM-derived peripheral myeloid cells in the brain (Hohsfield et al., 2020). Four-month-old wild type (WT) mice underwent whole body (WB) irradiation (1000 cGy) and BM transplant via retro-orbital injection of 2 x 106 BM cells from age- and sex- matched CAG-GFP mice. Following a 3.5 mo recovery, mice were treated with CSF1R inhibitor PLX3397 (600 ppm) for 14d, and then placed on control diet for 6 mo. (b–g) Representative images of whole coronal brain sections (b–d) and high resolution 20x confocal (e–g) images of GFP+ (green), MAC2+ (red) and IBA1+ (red) cells in control (b, e), ~10 mo WB chimeras (c, f), and ~ 10 mo WB chimeric mice treated with a CSF1R inhibitor (d, g). White boxes in (b) indicate brain regions of interest shown in (e–g). Images show that MAC2+ cells co-localize with GFP BM-derived cells in the brain parenchyma. (h–j) Quantification of the number of GFP+ cells per field of view (FOV) in the subventricular zone (SVZ) (h), medial habenula (MHb) (i), and internal capsule (IC) (j) in control, ~10 mo WB chimeras, and ~ 10 mo WB chimeric mice treated with a CSF1R inhibitor. (k–m) Percentage of GFP+ cells that express MAC or MAC2+ cells that express GFP in the subventricular zone (SVZ) (k), medial habenula (MHb) (l), and internal capsule (IC) (m) in control, ~10 mo WB chimeras, and ~10 mo WB chimeric mice treated with a CSF1R inhibitor. Data are represented as mean ± SEM (n = 5–9). ** $p < .01$, ***
$p < .001$, compared to control. Scale bar ~60 μm

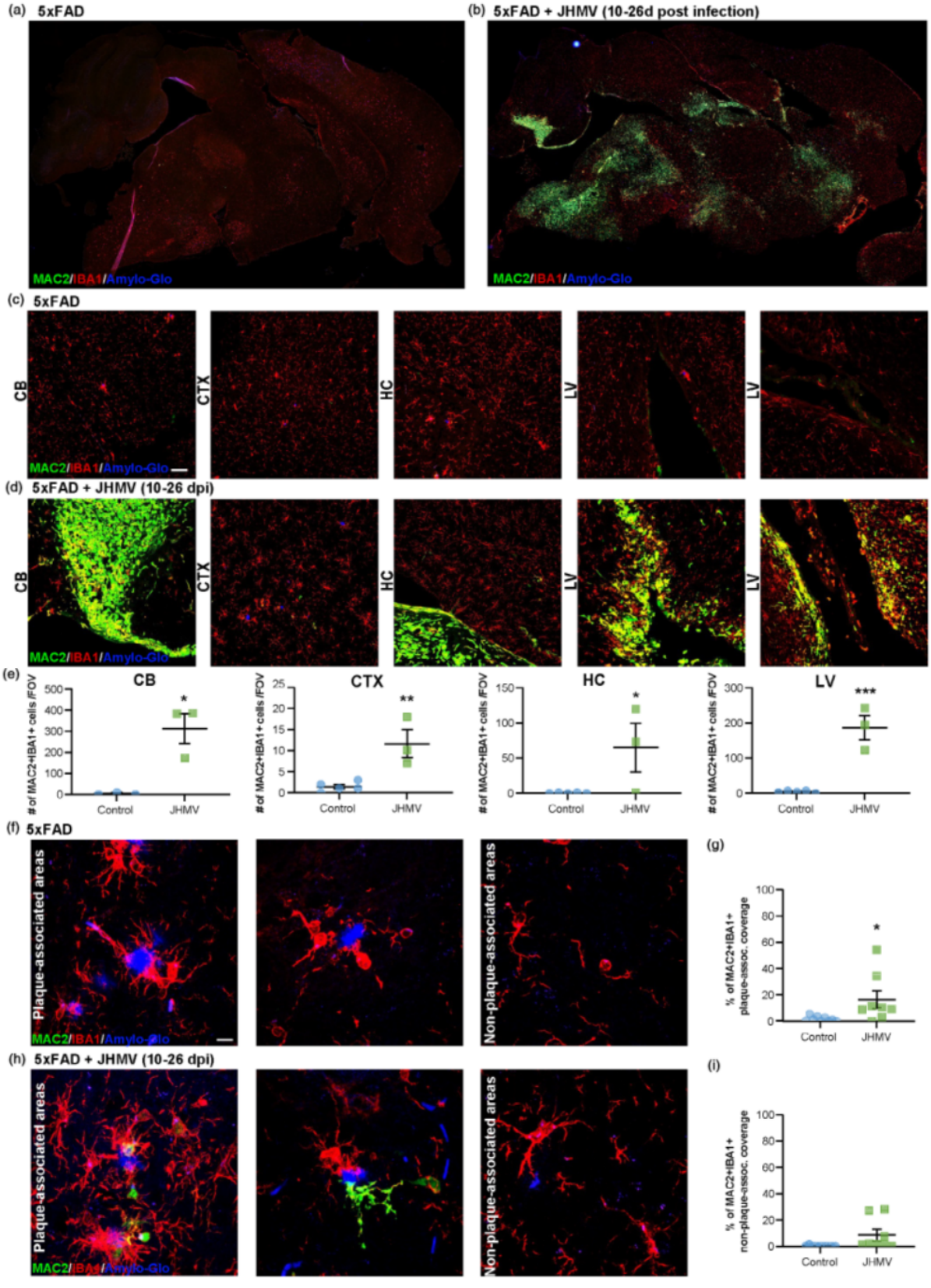
(a) 5xFAD
(b) 5xFAD + JHMV (10-26d post infection)
MAC2/IBA1/Amylo-Glo
(c) 5xFAD
CB
CTX
HC
LV
(d) 5xFAD + JHMV (10-26 dpi)
(e)
# of MAC2+IBA1+ cells /FOV
Control
JHMV
(f) 5xFAD
Plaque-associated areas
Non-plaque-associated areas
(g)
% of MAC2+IBA1+ plaque-assoc. coverage
(h) 5xFAD + JHMV (10-26 dpi)
(i)
% of MAC2+IBA1+ non-plaque-assoc. coverage

Figure 3 MAC2 is not a ubiquitous marker for plaque-associated microglia during the early stages of disease in 5xFAD mice. Four-month- old 5xFAD mice were infected intracranially with 200 PFU of JHMV strain and brains evaluated at 10–25 d.p.i. (a–d) Representative whole sagittal brain section (a–b) and 20x confocal (c–d) images of Amylo-Glo (amyloid, blue), MAC2 (green), and IBA1 (red) staining in control (a, c) and JHMV-infected (b, d) 5xFAD mice. (e) Quantification of the number of MAC2+ IBA1+ cells per field of view (FOV) in the cerebellum (CB), cortex (CTX), hippocampus (HC), and lateral ventricle (LV). (f, h) Representative high resolution 100x confocal images of Amylo-Glo + plaques (amyloid, blue), MAC2+ (green) cells, and IBA1+ (red) cells in plaque-associated and non-plaque-associated areas in the brains of control (f) and JHMV- infected (h) 5xFAD mice. Images show that MAC2+ cells do not label plaque-associated microglia in non-infected 5xFAD mice. (g,i) Quantification of % MAC2+ IBA1+ staining in IBA1+ cells and in plaque-associated (g) and non-plaque-associated (i) areas of the cortex and hippocampus. Multiple field of views in these brain regions were quantified across three animals from each group. Data are represented as mean ± SEM (n = 8–9). * $p < .05$. Scale bar in (c) ~60 μm; in (e) ~10 μm

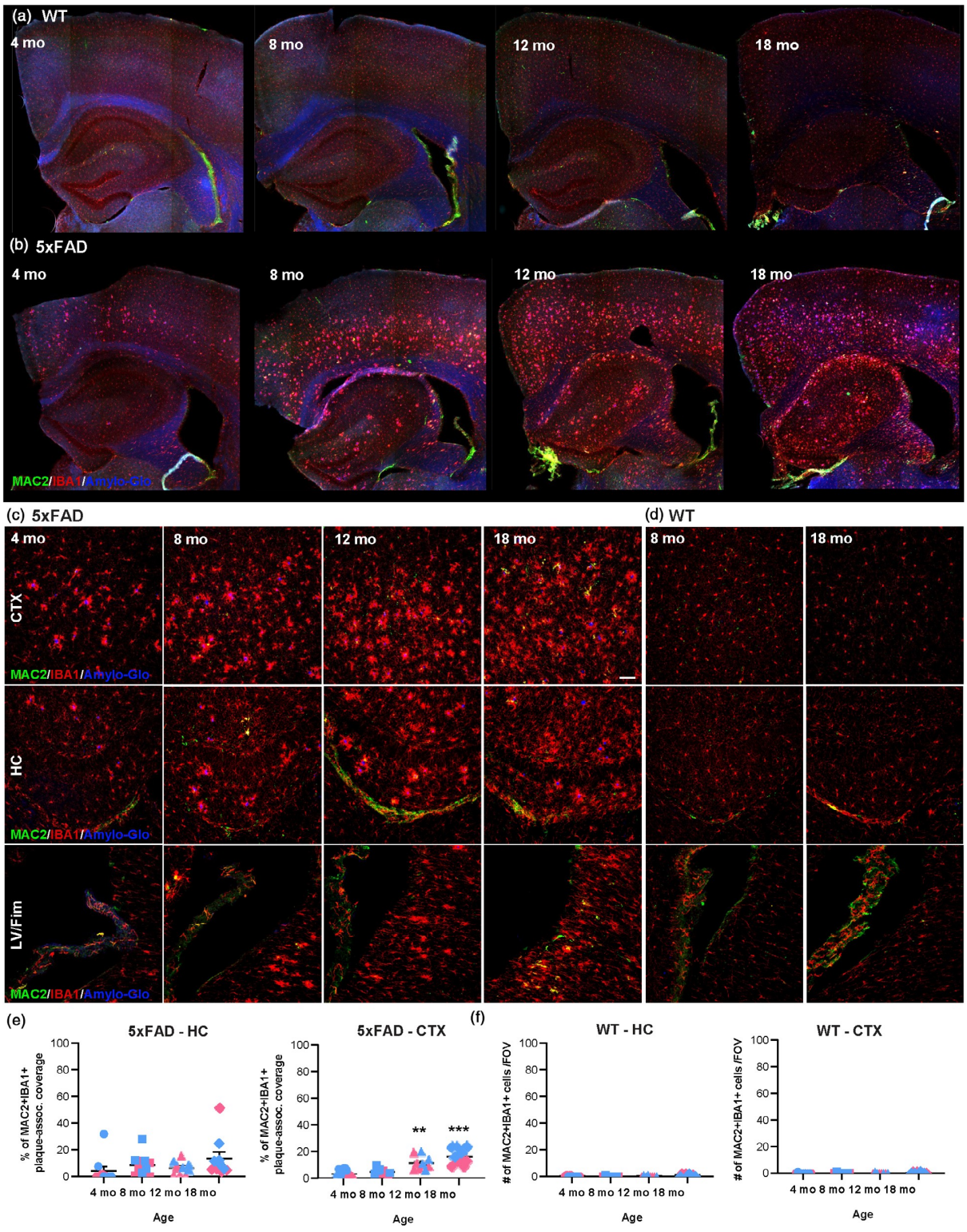
(a) WT
4 mo
8 mo
12 mo
18 mo
(b) 5xFAD
4 mo
8 mo
12 mo
18 mo
MAC2/IBA1/Amylo-Glo
(c) 5xFAD
(d) WT
4 mo
8 mo
12 mo
18 mo
8 mo
18 mo
CTX
HC
LV/Fim
MAC2/IBA1/Amylo-Glo
(e)
5xFAD - HC
5xFAD - CTX
% of MAC2+IBA1+ plaque-assoc. coverage
4 mo 8 mo 12 mo 18 mo
Age
**
***
(f)
WT - HC
WT - CTX
# of MAC2+IBA1+ cells /FOV
4 mo 8 mo 12 mo 18 mo
Age

Figure 4 The effects of aging on MAC2 staining in WT and 5xFAD mice. Brains of wild type (WT) and 5xFAD mice at 4, 8, 12, and 18 months (mo) of age were evaluated for MAC2 staining in plaque-associated microglia. (a–b) Representative images of MAC2 (green), IBA1 (red, myeloid cells), and Amylo-Glo (blue, amyloid plaques) staining in brain sections of WT (a) and 5xFAD (b) mice. (c–d) Representative 20x confocal images of MAC2, IBA1, and Amylo-Glo staining in the cortex (CTX), hippocampus (HC), and lateral ventricle (LV)/fimbria (Fim) of WT (d) and 5xFAD (c) mice shows the age-dependent increase in MAC2 staining in 5xFAD mice. (e–f) Quantification of plaque-associated MAC2+ IBA1+ staining and MAC2+ IBA1+ cells in 5xFAD and WT mice, respectively. Female (pink) and male (blue) mice are indicated by color scheme. Data are represented as mean ± SEM (n = 3–5). ** $p < .01$, *** $p < .001$, compared to 4 mo. Scale bar in (c) ~60 μm